Cardiff University

School Of Chemistry

Catalytic Dechlorination of Chloroalkenes by Multimetallic Cobaloximes- Synthesis, Chemistry and Catalysis.

Thesis submitted for the degree of Doctor of Philosophy by:

Richard John Arthur

Supervisor: Dr. M. P. Coogan

School of Chemistry

Cardiff University

March 2010

ProQuest LLC
789 East Eisenhower Parkway
P.O. Box 1346
Ann Arbor, MI 48106-1346

Declaration.

This work has not previously been accepted in substance for any degree and is not concurrently submitted in candidature for any degree.

Signed.....(candidate) Date.5/3/10.....

STATEMENT 1

This thesis is being submitted in partial fulfilment of the requirements for the degree of Doctor of Philosophy.

Signed.....(candidate) Date.5/3/10.....

STATEMENT 2

This thesis is the result of my own independent work/investigation, except where otherwise stated. Other sources are acknowledged by explicit references.

Signed.....(candidate) Date.5/3/10.....

STATEMENT 3

I hereby give consent for my thesis, if accepted, to be available for photocopying and for interlibrary loan, and for the title and summary to be made available to outside organisations.

Signed.....(candidate) Date.5/3/10.....

Acknowledgments.

Firstly, I would like to thank my supervisor Dr. Mike Coogan for all of his advice, his ideas, guidance and for correcting the "wenglish" that plagued earlier versions of this thesis. I would also like to thank Dr. Sarah Oakley for teaching me the dark arts of schlenkery and for her advice when I needed it the most. Finally, a big thank you to Mr. Robin Hicks and Dr. Robert Jenkins for their efforts with gas chromatography, especially when it came to its lighting, and mass spectrometry.

Inside lab 1.86, and later 2.84, I would like to thank all the workers, especially Txell, Leni, Stephane, Soraya, Dirk, Tracy, Flo and Jen for making it a fun place to work, and for the coffee breaks when they were much needed. Outside of the lab, there are too many people to mention who have offered advice and general support when needed, but Andrew, Jenn, Laura, Andy, Rhys, Frenchie and Vincenzo have always been around when needed the most. A massive, massive thanks is reserved for Manu & Vane and Lino & Grazia for their friendship, and inviting me to go away with them to many new places, I don't feel I can thank you guys enough.

Out in the real world, I would like to take this moment to thank my brothers-in-arms, whom I have known and lived with since moving to Cardiff many, many moons ago. Taking me under their wing and offering a unique insight into rugby and music, and making the City Arms a second home: Steve, Davo, Daz, Tom M, Dan, Andy, Ian, Matt, Dewi, Tom F and Yoz, it's been emotional.

Finally I would like to thank my parents, Maurice and Barbara, Ellie and my sister, Bethan, all of whom I am eternally grateful to; for standing by me, putting up with my sense of humour and looking after me whilst I have been writing up, especially Ellie, who has proof read this thesis as many times as I have.

Abbreviations.

3-Bromopyr	3-Bromopyridine
4-Bromopyr	4-Bromopyridine
Å	Angstrom
ATP	Adenosine triphosphate
B_{12}	Vitamin B_{12}
Bipy	Bipyridine
BPA	Bis(4-pyridyl)acetylene
ca	*Circa*
CHGH	Cyclohexanedioneglyoxime
cm	Centimetre
Cob	Generic Cobaloxime
Conc	Concentrated
Cp	η^5 -C_5H_5
CV	Cyclic voltammetry
δ	Chemical shift
D.F.T.	Density Function Theory
DCE	Dichloroethylene
DCM	Dichloromethane
dd	Doublet of doublets
DDD	Dichlorodiphenyldichloroethane
DDT	1,1,1-trichloro-2,2-bis(4-chlorophenyl)ethane
deg	Degree
diphos	Bis(diphenylphosphino)ethane
DMF	N,N -Dimethylformamide
DMGH	Dimethylglyoxime
DNAPL	Dense non-aqueous phase liquid
DPGH	Diphenylglyoxime
dppf	1,19- Bis(diphenylphosphino) ferrocene
dppm	μ_2-Diphenylphosphinomethane
dq	Doublet of quartets
dt	Doublet of triplets

e.g.	*Exempli gratia (for example)*
Eq	Equation
Equiv	Equivalents
ESI	Electrospray Ionisation
Et	Ethyl
et al	*Et alii (and others)*
EtOH	Ethanol
Fc	Ferrocene
Flu	η^5-$C_{13}H_{10}$
Flu*	η^5-$C_{13}Me_9H$
g	Gram
GC	Gas Chromatography
GC-MS	Gas Chromatography-Mass spectrometry
GH	Glyoxime
HMPA	Hexamethylphosphoramide
Hrs	Hours
HRMS	High Resolution Mass Spectrometry
Hz	Hertz
i.e.	*id est (that is)*
IPA	Propan-2-ol
IR	Infra-Red Spectroscopy
kcal	Kilocalories
kDa	Kilodaltons
kg	Kilogram
L	Ligand
m	meta
m	Multiplet
M	Molar
Me	Methyl
MeOH	Methanol
mg	Milligram
MHz	Megahertz
ml	Millilitre
mmol	Millimole

mV	Millivolt
ν	Wavenumber
NMR	Nuclear Magnetic Resonance
o	Ortho
°	Degree
°C	Degrees Celsius
ORTEP	Oak-Ridge thermal ellipsoid plot
Oxid	Oxidation
p	Para
PBB	Polybrominated biphenyl
PCB	Polychlorinated biphenyl
PCE	Tetrachloroethylene/Perchloroethylene
Ph	Phenyl
ppm	Parts per million
Pyr	Pyridine
Pyz	Pyrazine
q	Quartet
Red	Reduction
s	Singlet
SHE	Standard hydrogen electrode
t	Triplet
TBAP	Tetrabutylammonium hexafluorophosphate
TCE	Trichloroethylene
TLC	Thin Layer Chromatography
TON	Turnover number
tt	Triplet of triplets
UV	Ultra-Violet
V	Volts
VC	Vinyl chloride

Abstract.

The work presented in this thesis is primarily concerned with the synthesis and applications of cobaloximes towards reductive dechlorination of organohalides, such as perchloroethylene. The toxicity and relevance of these organohalides is discussed in chapter one, which also describes the current industrial methods for their removal from the environment.

An insight into the mechanism of dechlorination of perchloroethylene has been offered in chapter three, which describes the mechanism of dechlorination of PCE. This reaction proceeds via electron transfer from the catalytic cobaloxime to the PCE for the removal of the first chloride, but the subsequent dechlorination steps proceed via organocobalt intermediates. The role of the axial ligands and the coordination chemistry of the cobaloxime intermediate during reduction from Co(III) to Co(I) is then studied by means of a cross over experiment.

Chapters four and five describe more complex, novel multimetallic cobaloximes, which have been designed and synthesised for their use as dechlorination catalysts. The structure and electrochemical behaviour of these multimetallic cobaloximes has been discussed and their catalytic ability towards dechlorination of PCE has been studied. The work in chapter four looks at cobaloximes with a μ^2-dicobaltcarbonyl bridged ligand, whilst chapter five describes a series of nitrogen heterocycle bridged dinuclear cobaloximes. As a result of the findings of chapter three, the final section of chapter five investigates the incorporation of the secondary metal centre into an equatorial ligand.

Table of Contents.

Chapter 1.

Introduction.

1.1. Organohalides.

1.1.1. Occurrence and Uses of Organohalides.

Organohalides are defined as organic molecules containing covalent bonds between a carbon atom and one or more Group VII atoms, with 6,6'-dibromoindigo, **1.1**, the main component of the dye *Tyrian purple*, being one of the earliest commercially used organohalides, dated back to pre-Roman times.[1] One of the earliest man-made organohalides was trichloroacetaldehyde, **1.2**, which Liebig first synthesised in 1832.[2] Ever since, considerable attention has been given to organohalides, due to their vast array of chemical and commercial applications. It is this range of properties that makes them such a versatile class of organic compounds.

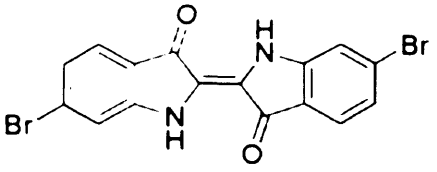

1.1

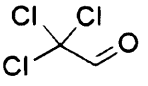

1.2

Figure 1.1. Historical organohalides; 6,6'-dibromoindigo and trichloroacetaldehyde.

In synthetic chemistry, short-chained organohalides such as dichloromethane and chloroform are often used as solvents, due to their relatively low boiling points and polarity. Many organic transformations, such as the Sonogashira coupling shown in **Scheme 1.1** and nucleophilic substitution reactions, depicted in **Scheme 1.2**,[3] begin with, or proceed via a halogenated species.

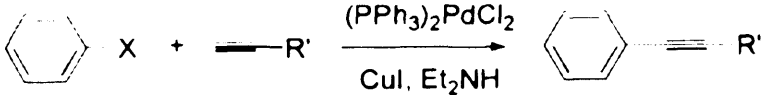

Scheme 1.1. Sonogashira coupling reaction, where X is a halide.

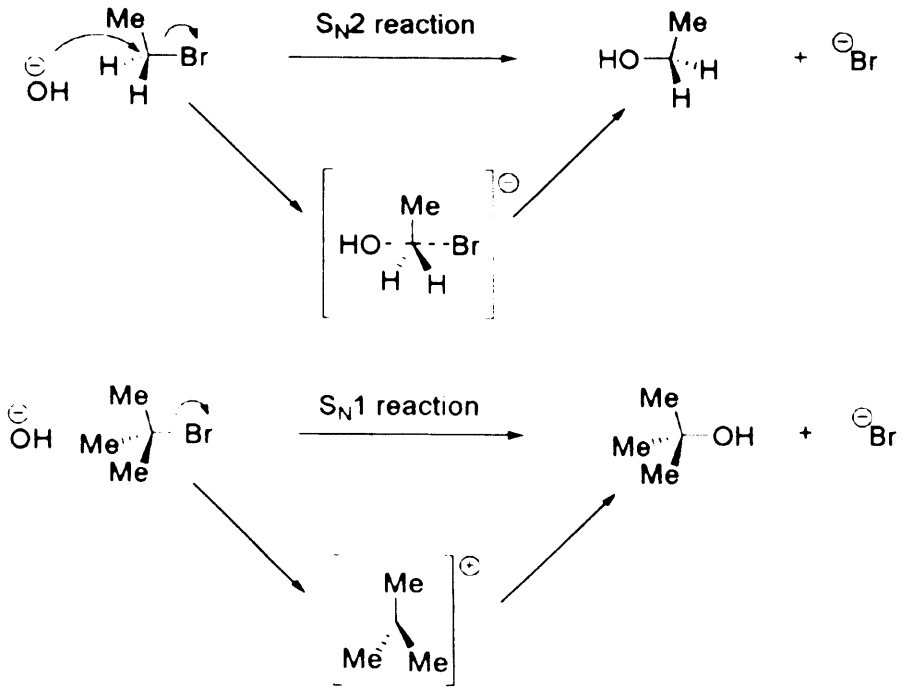

Scheme 1.2. Nucleophilic substitution reactions.

Commercially, organohalides can be found in everyday life, with chlorofluorocarbons (CFCs), such as Freon (CCl_2F_2), used as propellants in aerosols and urethane foam blowing.[4] Polychlorinated biphenyls (PCBs) consist of a mixture of different congeners and isomers, and are used as fire suppressants in furniture, due to their flame retardance; tetrachloroethylene (PCE) is used in dry and metal cleaning,[5] and trichloroethylene (TCE) is used in adhesive surface treatment, paint removers and strippers.[6]

Polymers of the organohalide monomers depicted in **Figure 1.2**, are also very common in modern life, poly(vinyl chloride), "PVC", has applications ranging from the plastic used in food packaging and keyboards, to fabric and childrens' toys, due to its fire and water resistance; poly(tetrafluoroethene), "PTFE" or "Teflon", is used as non-stick plastic coating and poly(chloroprene), "neoprene", is a synthetic rubber used in clothing.

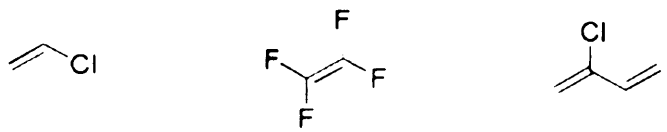

Vinylchloride Tetrafluoroethene Chloroprene

Figure 1.2. Organohalide monomers of common polymers.

There are many halogenated compounds, such as those depicted in **Figure 1.3**, used in the pharmaceutical industry. Possibly the best known is the anti-depressant fluoxetine, **1.3**, commercially known as "Prozac", as well as the anti-fungal fluconazole, **1.4**, anti-histaminic chloropheniramine, **1.5** and anti-microbial chlorhexidine, **1.6**.

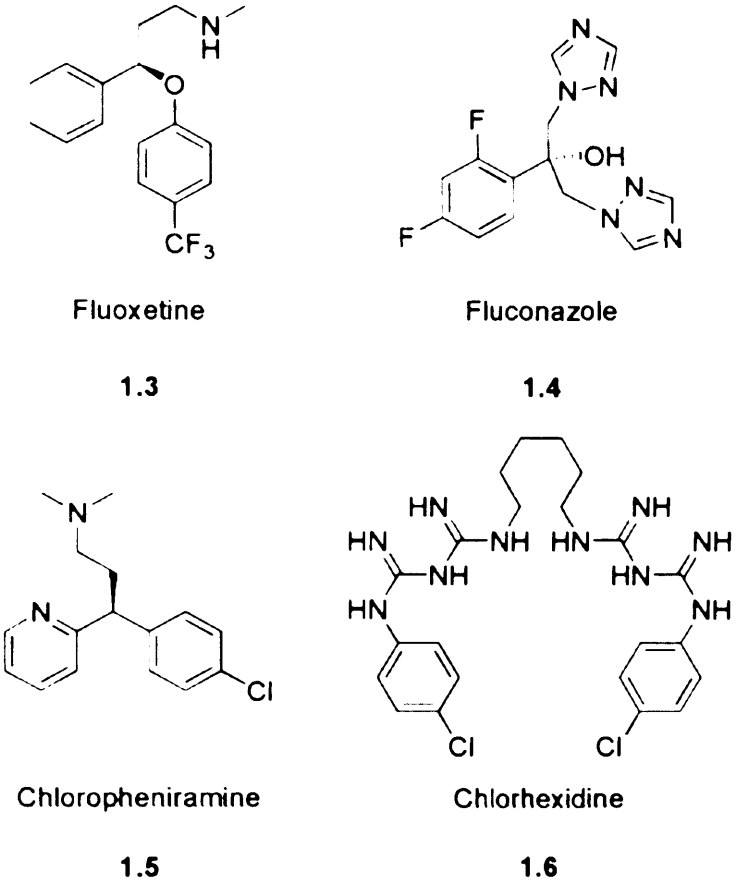

Figure 1.3. Pharmaceutical organohalides.

Organohalides also occur naturally, with more than 1500 chlorine-containing natural products known alone, and are produced by plants, fungi, marine organisms, amphibians, insects, and even mammals. These natural organohalides show diverse biological activities and some offer medicinal properties. For example, chloramphenicol, **1.7**,[7] and vancomycin, **1.8**,[8] isolated from bacteria cultures *Estreptomyces venezuelae* and *Estreptomyces orientalis* respectively, are both antibacterial agents and are very effective in treating diseases such as typhus, meningitis, urinal infections, brucellosis, and some viruses. Halogenated secondary metabolites are also common in red algae,[9,10] lichens[11] and marine sponges.[12,13]

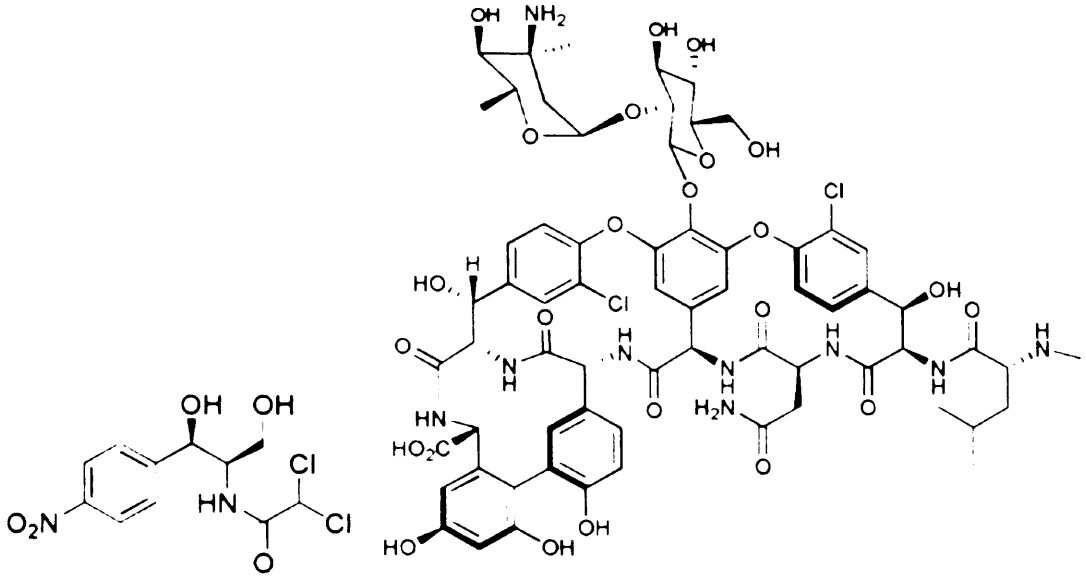

Chloramphenicol
1.7

Vancomycin
1.8

Figure 1.4. Bioactive organohalides.

One of the few natural molecules in the human body containing a halogen is the thyroid hormone thyroxine, **1.9**, with four carbon-iodine bonds.[14] Many of these halogenated natural products such as chloramphenicol, **1.7**, and vancomycin, **1.8**, have represented important challenges as targets for synthetic organic chemists,[15,16] and thus have been instrumental in developing new reactions in synthetic chemistry.

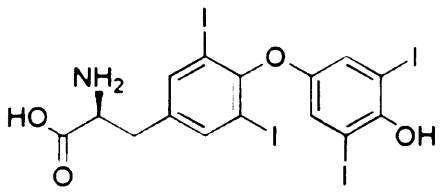

Thyroxine
1.9

Figure 1.5. Thyroid hormone.

1.1.2. Deleterious Effects of Organohalides on the Environment.

In addition to the positive, therapeutic qualities of some organohalides, there are some that have negative effects on living organisms and the environment. During the First World War many of the toxic gases used were chlorine-based compounds, including asphyxiating gases such as chlorine, Cl_2, chloropicrine ($Cl_3CCH_2NO_2$), **1.10**, diphosgene ($Cl_3COOCCl_3$), **1.11**, and phosgene ($COCl_2$), **1.12**, lachrymatory agents such as chloroacetone ($ClCH_2C(O)CH_3$), **1.13**, and chloroacetophenone ($ClCH_2C(O)Ph$), **1.15**, or vesicant gases such as 1,5-dichloro-3-thiapentane (also referred to as mustard gas) [$(ClCH_2CH_2)_2S$], **1.14**, and Lewisite ($ClCH{=}CHAsCl_2$), **1.16**.

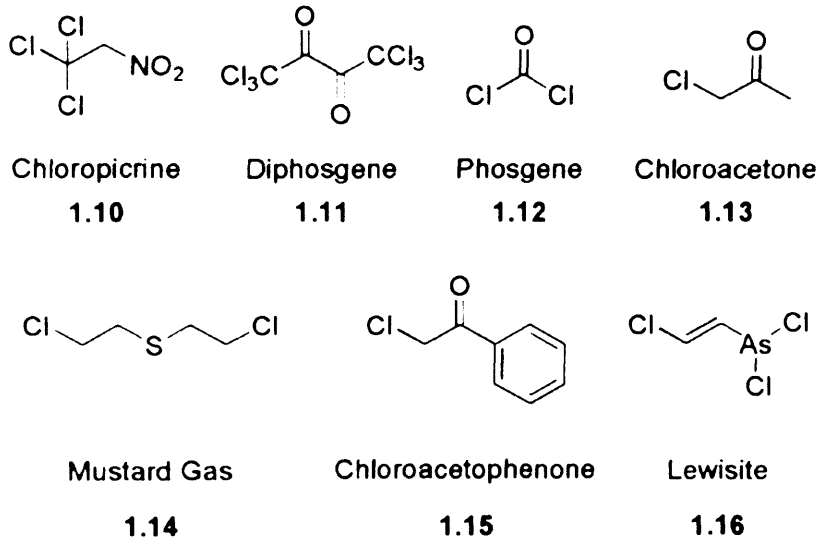

Figure 1.6. Organohalides used in chemical warfare.

In 1974, Rowland and Molina[17] showed that the UV photolytic decomposition of CFCs could be a major source of inorganic chlorine in the stratosphere, affecting the ozone layer. The chlorine reacts catalytically with the ozone, with a turnover number greater than 100,000. A loss of stratospheric ozone results in more of the harmful UV-B radiation reaching the Earth's surface, which can cause biological damage to plants, animals and human beings. The Antarctic ozone hole[18] is perhaps the most famous example of stratospheric ozone depletion, and was described by Farman and his colleagues in 1985.[19] In 1987, 27 nations signed a global environmental treaty, the "Montreal Protocol to Reduce Substances that Deplete the Ozone Layer",[20] which had a

provision to reduce 1986 production levels of these compounds by 50 % before the year 2000.

Chlorinated dioxins, and the structurally similar bis-furans, are probably the environmental contaminants with the worst reputation,[21] and are generated during combustion of municipal and chemical wastes. Running vehicle engines and wood burning are also sources of dioxins.[22] 2,3,7,8- tetrachlorodibenzo-*p*-dioxin (2,3,7,8-TCDD), **1.17**, is considered to be "the most toxic man-made chemical",[23] and is lethal at very low concentrations (LD_{50}[a] = 0.02 mg/kg)[24] making it 800 times more toxic than strychnine and 300 times more toxic than sodium cyanide, whose LD_{50} values are 16 mg/kg[25] and 6.4 mg/kg[26] respectively. 2,3,7,8-TCDD is the most potent cancer promoter known, hence is a class I carcinogen. The following effects have been associated with exposure to 2,3,7,8-TCDD: damage to organs including the liver, kidneys and the immune system; reproductive effects (miscarriage, sterility); chloracne[b] and birth defects.[27]

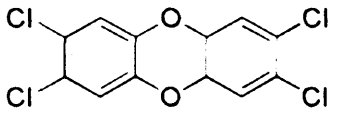

2,3,7,8- tetrachlorodibenzo-*p*-dioxin
1.17

Figure 1.7. 2,3,7,8-TCDD, the most toxic man-made chemical.

Due to their thermal stability and chemical inertness, polychlorinated biphenyls tend to be resistant to degradation and so, tend to accumulate in animals higher in the food chain. High exposure to PCBs during pregnancy has been linked to miscarriages and low scores on the psychomotor scale. It is believed that they may cause toxemia by affecting the immune system. Polybrominated biphenyls (PBBs) are also serious environmental contaminants,[28] with documented cyto- and genotoxicity[29] as well as long-term health effects.[30] Recent studies have estimated their half-life in the body to be about eleven years and showed their possible association with breast cancer.[31] These

[a] The lethal dose required to kill 50 % of a test population.

[b] An acne-like eruption of cysts on the skin, which afflicted Viktor Yushchenko, incumbent Ukrainian President at time of writing.

factors have seen the popularity of PCBs decrease; their use banned, and so, they are no longer produced.

1.1.3. Organohalides as Pesticides and Insecticides.

The hydrated form of trichloroacetaldehyde **1.2** is known as "choral", which is a key reagent in the synthesis of 1,1,1-trichloro-2,2-bis(4-chlorophenyl)ethane (DDT), **1.18**, a powerful insecticide and pesticide used in agriculture.[32] In the 1940s, the production and use of chlorinated insecticides was at its greatest, with further research developing lindane, and the "drin" family (aldrin, endrin and dieldrin, **1.19**) as supplementary options to DDT.

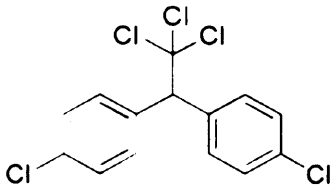

1,1,1-trichloro-2,2-bis(4-chlorophenyl)ethane
1.18

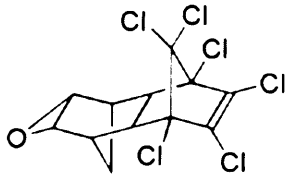

Dieldrin
1.19

Figure 1.8. Organohalides previously used as pesticides and insecticides.

The use of DDT throughout the early decades of the twentieth century eliminated the *Anopheles mosquito*, a carrier of the malaria-causing parasite, saving many millions of lives. Whilst the toxicity of DDT towards mammals is relatively low (the fatal dose for humans is approximately 500 mg per kg of body weight), it is very resistant to biodegradation, causing it to bioaccumulate in the food chain, making it hazardous to species at the top of the food chain, such as fish and mammals. Consequently, DDT has been banned from use by the US Environmental Protection Agency, but it is still used in less affluent counties, due to its low cost and high effectiveness.

1.1.4. Environmental Contamination.

The improper use and storage of obsolete pesticide stockpiles is a problem in many developing countries. The elimination of such chemicals by conventional means is expensive and difficult given the lack of suitable facilities in many locations.

Organohalides, including per- or tetra- chloroethylene (PCE), trichloroethylene (TCE), carbon tetrachloride and polychlorinated biphenyls, as well as their derivatives, comprise 17 of the 25 organic pollutants most commonly found in the waters of the United States of America,[33] and over half of the United States Environmental Protection Agency's priority organic pollutant list.[34] Halogenated compounds that contain either one or two carbon atoms are the principal pollutants, as the movement of ground water easily transports them[35] and they do not break down easily under aerobic conditions.[36] However, it has been reported that organohalides, such as PCE, will break down under anaerobic conditions,[33-36] where the stepwise dechlorination of the chlorinated compound is shown in **Scheme 1.3**.

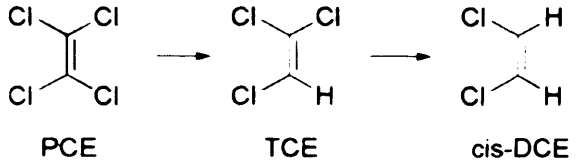

Scheme 1.3. Dechlorination pathway for PCE, mediated by Vitamin B_{12} containing enzymes in anaerobic bacteria.[41]

Without the presence of certain anaerobic bacteria, tetrachloroethylene, trichloroethylene, and 1,1,1-trichloroethane are degraded with half-lives of 300 days,[42] and, perhaps even more worrying, 1,2-dichloroethane has a half-life of greater than 50 years and is a class II carcinogen.[43]

The major concern with regards to organohalides is that they were believed to be carcinogens and mutagens for many years,[44] and it is possible for some to react in the environment photochemically, yielding cytotoxins such as hydroxyl radicals.[45] The carcinogenic effects of PCE, TCE and vinyl chloride (VC) were confirmed in 1985 when a study by the World Health Organisation found that organohalides were capable of causing liver tumours in rodents. The same was found for humans who have been under constant, heavy exposure, with damage occurring to the Central Nervous System, in addition to the carcinogenic effects.[46]

Due to their density and immiscibility with water, organohalides tend to aggregate as a layer below the water, which will lay dormant until disturbed. This will then release a

plume of the pollutants, which can enter drinking water supplies. Most remediation attempts aim at treating the plumes, however source remediation is almost unknown.[47]

1.2. Remediation of Sources Polluted with Organohalides.

In the US alone the cost associated with chlorinated solvent clean up is expected to be in the billions. Despite considerable efforts and progress in a variety of remediation techniques, a recent US report concluded that "as far as the panel is aware, there is no documented, peer reviewed case study of DNAPL[c] source zone depletion beneath the water table where US drinking water standards or maximum contaminant levels have been achieved and sustained throughout the affect subsurface volume regardless of the *in situ* technology applied".[47]

Recently, the preservation of the environment has become a major concern for governments and hence the need for a safe method for the disposal of chlorinated alkenes has become a challenge for research institutions. A series of policies have come into action to control production, emission and disposal of these halogenated materials, based on international laws established by the Montreal Protocol and the Stockholm Convention. In addition to this, efforts are also focused on risk assessment of the thousands of halogenated compounds in use today. Emphasis is focused on the effects of three of the most environmentally deleterious classes: chlorofluorocarbons (CFCs), chlorinated dibenzo-*p*-dioxins (dioxins), and polyhalogenated biphenyls (PCBs and PBBs).

There are no natural sources of PCE[48] and so, one can say that this is entirely a man made problem, which has been found to affect ground water, soil near rivers, and the animals which inhabit these areas,[5] hence dechlorination of perchloroethylene and trichloroethylene is presently being applied as an important remediation technique.

[c] Dense non-aqueous phase liquid - a liquid that is denser than water and forms a separate, immiscible layer in water

1.2.1. Current Technologies for the Destruction of Organohalides.

The most widespread method for the destruction of organohalides is high temperature incineration. Although this process is effective for both liquid and soil-based organohalide waste, the cost is based on weight; hence this remains an expensive option for contaminated soils. Public concerns about waste discharge from incinerators are also forcing a move towards alternative strategies. In general, an effective technology for the destruction of organic pollutants needs to have the following qualities;

- High destructive efficiency, i.e. a high turnover rate.
- The method should release non-toxic, environmentally benign substances.
- Ideally, the process needs to be as "green" as possible, carried out at standard temperature and pressures, with the reagents used also being non-toxic and environmentally benign.

Current technologies presently being applied to this problem include:

a) Base catalysed decomposition/Glycolate dehalogenation. Contaminated crushed soil is initially treated with sodium carbonate. Glycolate (alkaline polyethylene glycol or "APEG") is then used to form water-soluble by-products from dehalogenation. These methods require large amounts of both sodium carbonate and APEG. The soil is removed to an oven or a furnace where it is heated to 300 ^{0}C. The by-products from APEG decomposition (glycolate ethers, decomposed polyethylene glycol) may also be toxic, and the heat drives off volatile halides (PCE, TCE), rather than destroying them. The unreacted APEG is removed by washing the soil with water and can then be reused in further remediation of soil.[4]

b) Metal-mediated reduction *in situ*. In recent years, zero valent iron based permeable reactive barriers have been used *in situ* for the remediation of redox active groundwater contaminants, such as PCE and TCE. The contaminated water flows through trenches containing cassettes charged with zero valent iron, where electrons are transferred from the iron medium to the organohalides, which are then reductively dehalogenated. The chlorine moieties are removed stepwise, as depicted in **Scheme 1.4**,

forming the less chlorinated species.[6,49] Palladium catalysed hydrogenation has also been shown effective in field trials of contaminated groundwater.

$$C_2HCl_3 + Fe^0 + H_2O \rightarrow C_2H_2Cl_2 + Cl^- + OH^- + Fe^{2+}$$

Scheme 1.4. Dechlorination of trichloroethylene by zero valent iron.

However, these technologies all raise potential problems, i.e. the loss of toxic palladium to the environment, the large quantities of a complicated preparation of iron required and the fact that these processes are extremely expensive, instead of harnessing or mimicking an environmentally benign natural process.

c) Oxidative Routes. Chloroalkenes can be detoxified with suitable oxidising agents including Fenton's reagent, ozone or hydrogen peroxide, with the advantage that the reactions are carried out at room temperature. These processes result in the chloride moiety being replaced with a hydroxy group. It is the hydroxy radical that is the active species in the reaction. Fenton's reagent is a solution of hydrogen peroxide and typically, an iron (II) sulfate catalyst, where the iron (II) species is oxidised by the hydrogen peroxide to iron (III), a hydroxyl radical and a hydroxyl anion (1). Iron (III) is then reduced back to iron (II), a peroxide radical and a proton, again by hydrogen peroxide (2).

$$(1)\ Fe^{2+} + H_2O_2 \rightarrow Fe^{3+} + OH\cdot + OH$$
$$(2)\ Fe^{3+} + H_2O_2 \rightarrow Fe^{2+} + OOH\cdot + H^+$$

Scheme 1.5. Formation of hydroxyl radical in Fenton's reagent.

d) Electrochemical Reduction. On a laboratory scale, it has been shown that reductive dechlorination of carbon tetrachloride occurs in a liquid-phase electrochemical reactor, when a -0.4 V (vs. SHE) potential is applied to a copper cathode with a carbon anode. The dechlorination reaction at the cathode is shown in **Scheme 1.6**.

$$CCl_4 + 4H^+ + 8e^- \rightarrow CH_4 + 4Cl$$

Scheme 1.6. Dechlorination of carbon tetrachloride by electrolysis.

Additionally, a vitamin B_{12} derivative has covalently immobilised onto a platinum electrode surface,[50] which then exhibits Co(II)/Co(I) redox activity, where the Co(I) species can react with the organohalide. For example, irradiation of 1-(2-bromoethyl) benzene with visible light in the presence of a B_{12}/platinum electrode yields styrene, with a turnover greater than 6,000 after one hour.[51] Electrochemical elimination of PCE and TCE, with vitamin B_{12} immobilised onto a platinum catalyst in the presence of a polypyrrole film, yields chloride ions and the corresponding alkene with one less chlorine moiety.[36,52,53] However, this has only been shown effective on a research scale, and has yet to be applied on an industrial scale. These electrochemical systems are highly versatile, but this is offset by the expense of the electrodes and the power consumption needed for the process.

1.2.2. Bacterial Dehalogenation.

The methods described in **Section 1.2.1** are slow at dechlorination, and can be expensive. However, over the last 20 years, bioremediation has been reported as an alternative method for the dechlorination of PCE. There are several strains of bacteria, including *Dehalobacter restrictus*, and *Dehalospirillum multivorans*,[54] which reductively dechlorinate PCE and TCE.[55] In these systems, the chlorinated alkene acts as a terminal electron acceptor in the respiratory cycle, producing energy. PCE is dechlorinated stepwise, as shown in **Scheme 1.3**. During this cycle, the toxic chlorinated alkenes are progressively reduced to less toxic chlorinated alkenes, and under methanogenic conditions it is possible to yield ethene, ethane and carbon dioxide.[37,56]

The *tetrachloroethylene reductase* enzyme crucial for this process has been isolated from these bacteria, and was found to be dependent on a cobalamin species, requiring reduction from Co(III) to Co(I) for the dehalogenation.[55] Following the purification of the enzyme, its reaction chemistry has been studied and its genetic sequence determined.[36] The active single subunit of the enzyme has a molecular mass of 60 kDa and contains a corrinoid system with a standard redox potential of -0.35 V, as determined by EPR spectroscopy, which also showed that the cobalt of the corrinoid is present in the base-off form. The presence of two FeS clusters of the type $[4Fe\text{-}4S]^{(2+,1+)}$ in the subunit was also reported, with redox potentials of -0.48 V; these are believed to

initiate the electron transfer process. The requirement for a low potential electron donor (less than -0.36 V) provided the first indication of the involvement of a corrinoid cofactor in reductive dechlorination. In laboratory studies, it has been shown that, in the presence of a sacrificial reducing agent, cyanocobalamin (vitamin B_{12}) can carry out the dehalogenation reaction without the presence of this enzyme.

The loss of the chloride ion from the chlorinated alkene, **Scheme 1.7**, is a result of the respiration cycle of the bacteria. The energy that is released in the dechlorination reaction is used to synthesise adenosine triphosphate (ATP); hence this process is called dehalorespiration, as described in **Scheme 1.8**.[36]

$$R\text{-}Cl + 2H^+ + 2e^- \longrightarrow R\text{-}H + HCl$$

Scheme 1.7. Reductive dechlorination of organohalide.

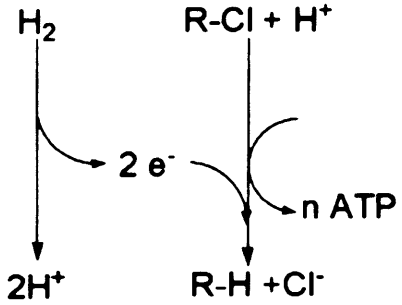

Scheme 1.8. Relationship between dechlorination and ATP synthesis.

For the coupling of ATP synthesis to reductive dechlorination, and therefore energy conservation, to occur, the reaction depicted in **Scheme 1.7** must be thermodynamically favourable.[36] It was demonstrated that the loss of the first chloride ion from PCE, **Scheme 1.9**, is exergonic[d], with $\Delta G^{o'}$ -192 $kJmol^{-1}$ and so is favourable for dehalorespiration.

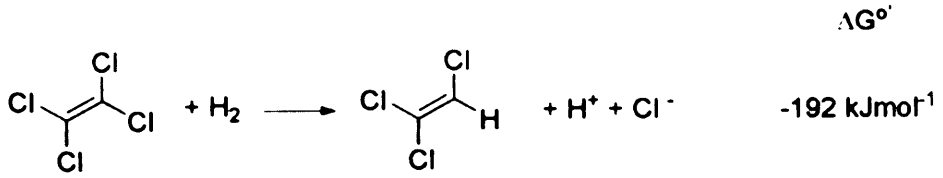

Scheme 1.9. Dehalorespiration of PCE.

[d] Energy released as heat alone.

1.3. Cobalamins.

1.3.1. The Structure of Cobalamins.

Cobalamins are bulky, tetrapyrrolic species with four equatorial nitrogen donors provided by the pyrrole moieties of the corrin ring coordinated to the central cobalt atom. The fifth nitrogen comes from a pendant axial benzimidazole ligand, which is appended from one of pyrrole rings. The base at the terminus of the propanolamine, which tethers this to the tetrapyrrole, varies between organisms, and in cobalamins, is the unusual ribonucleoside dimethylbenzimidazole.

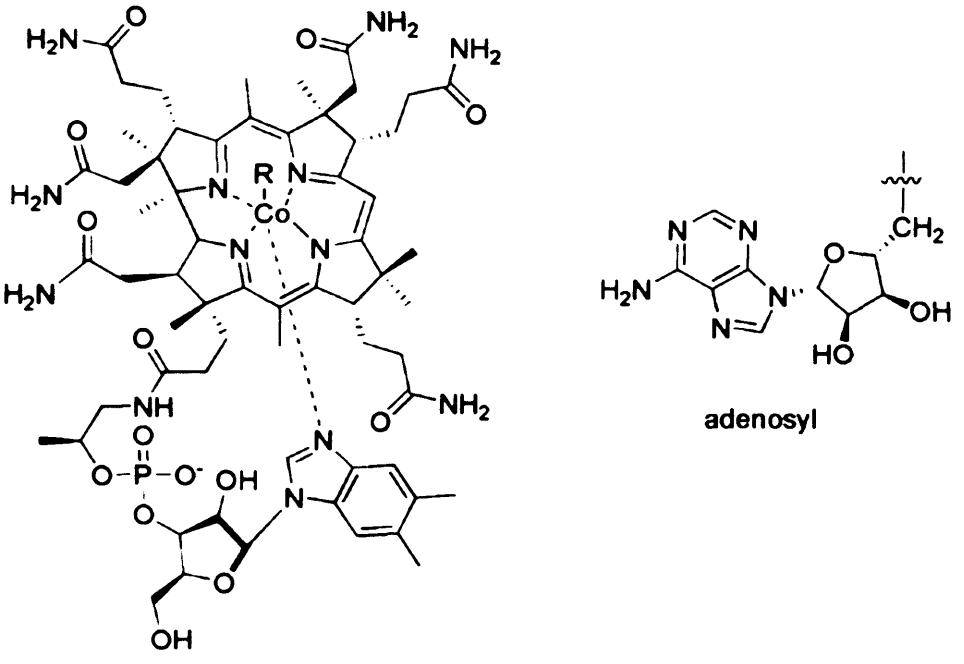

Figure 1.9. Cobalamin and its derivatives.

Diversity is also observed in the ligand *trans* to the pendant ligand, where the ligand can be either a hydroxy, adenosyl or methyl groups. The three forms of cobalamin, depicted in **Figure 1.9**, are found in plants and animals and are referred to as hydroxocobalamin (OHCbl), adenosylcobalamin (AdoCbl) and methylcobalamin (MeCbl). A fourth form, cyanocobalamin (CNCbl), where the ligand *trans* to the benzimidazole is a cyano group, is found only in bacteria. Cyanocobalamin can be synthesised from its analogues and is used in pharmaceuticals and supplements, due to its stability and low cost. In the body, cyanocobalamin is then converted to the active physiological forms,

methylcobalamin and adenosylcobalamin. Cyanocobalamin is the most commonly used cobalamin and is often referred to as vitamin B_{12}. The cobalamin family offers the only biological instance of a stable metal-alkyl bond.

1.3.2. History of Vitamin B_{12}.

Vitamin B_{12} was first described simultaneously by both Whipple, and Minot & Murphy in 1925, as an anti-pernicious anaemia factor,[57,58] and was first isolated in 1948 by both Smith and Folkers from several grams of uncooked liver, as a red crystalline compound.[59,60] The total synthesis was completed in 1965 by a transatlantic partnership between the Woodward and Eschenmoser laboratories,[61] owing much to Hodgkin's solution of the crystal structure in 1956.[62]

Vitamin B_{12} is a complex organometallic molecule, and is found in three subfamilies of enzymes: the adenosylcobalamin-dependent isomerases, the methylcobalamin-dependent methyltransferases, and the most recently discovered class; the cyanocobalamin-dependant reductive dehalogenases. It is this third class that carries out dehalogenation. Vitamin B_{12} is the name attributed to the class of cobalt-corrin based chemicals, known as cobalamins, and are the only example of naturally occurring cobalt-based systems.

1.3.3. The Function of Cobalamin Dependant Enzymes.

Cyanocobalamin was first described as a substrate vital in the prevention of the onset of pernicious anaemia in humans.[63] Adenosylcobalamin-dependent isomerases are the largest subfamily of vitamin B_{12} dependant enzymes; those found in bacteria play an important role in fermentation.[64] In some organisms they aid the conversion of ribonucleotides to deoxyribonucleotides, the process fundamental to DNA replication and repair.[65] Methylcobalamin-dependent methyltransferases catalyse the movement of methyl groups from methyl donors to methyl acceptors, playing an important role in amino acid metabolism in humans,[66] as well as one-carbon and CO_2 fixing in anaerobic bacteria.[67]

The most relevant class of vitamin B_{12} containing enzymes to this study are the reductive dehalogenase family. The vitamin B_{12} unit in the *tetrachloroethylene reductase* enzyme is in close proximity to two ferrodoxin clusters of the $[4Fe\text{-}4S]^{(2+,1+)}$ type, their role to shuttle electrons to and from the Co centre, initiating the redox cycle between Co(II) and Co(I), which is essential to the process. **Scheme 1.10** depicts a simplified form of this. Both aerobic and anaerobic bacteria have the enzyme required for the dehalorespiration, however anaerobic bacteria are more efficient.[65]

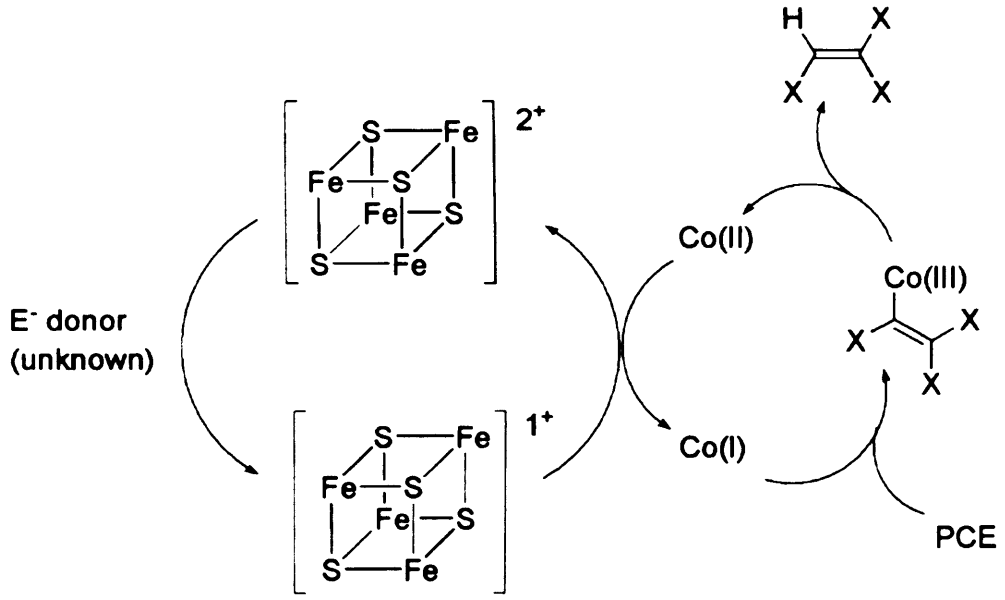

Scheme 1.10. The electron transfer cycle between the ferrodoxin cluster and the Co centre in the stepwise dechlorination.

There are two proposed reaction mechanisms for the enzyme based cob(I)alamin catalysed dechlorination in bacteria:

a) Scheme 1.11 shows the mechanism proposed by Wohlfarth, where the addition of cob(I)alamin to one of the alkene carbons is followed by the β-elimination of the chlorine substituent.[68] The cobalamin is reduced to Co(I), which oxidatively adds to the PCE, forming an organometallic species, where the cobalt centre has been oxidised to Co(III). This is then followed by β-elimination of the dechlorinated organohalides, in this case TCE, leaving the cobalamin to be reduced from Co(III) to Co(II), regenerating the starting cobalamin. However, there is only computational evidence for this proposal, although chlorovinyl cobalamin has been isolated from enzymatic reactions with PCE.

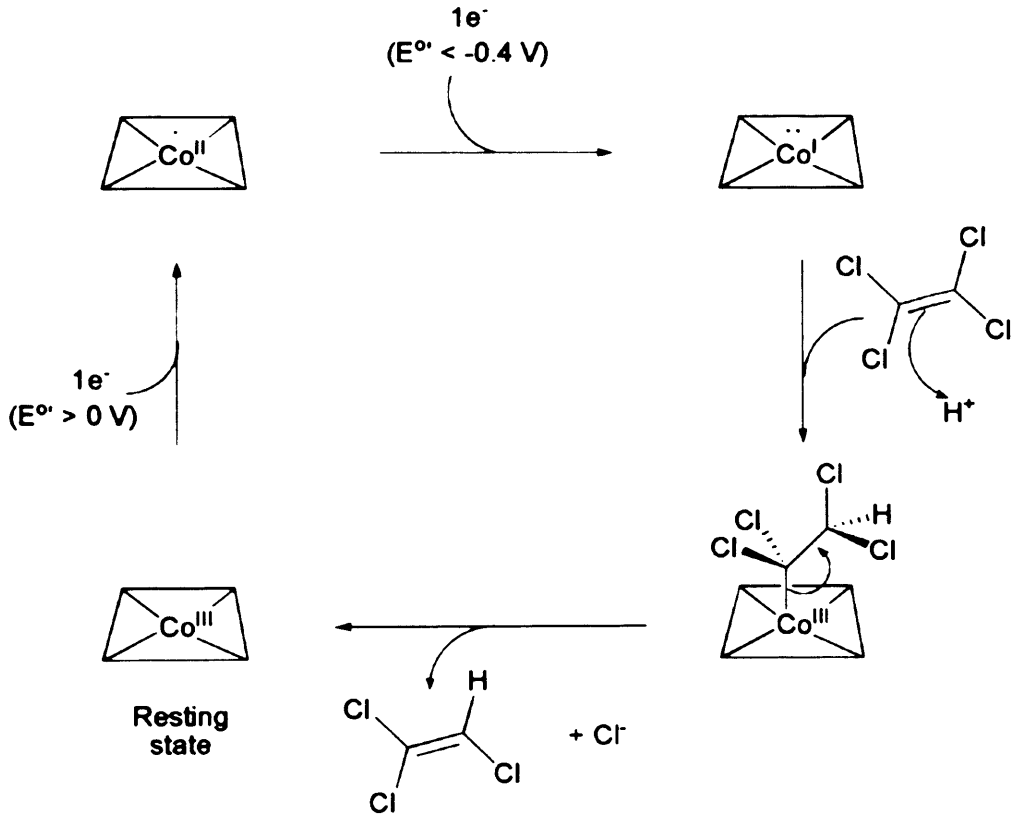

Scheme 1.11. The Wohlfarth mechanism for the cobalamin mediatedbdechlorination. (Co within the rhombus represents the corrinoid centre)

b) Scheme 1.12 shows an alternative mechanism, proposed by Glod, for the loss of the first chloride moiety, involving electron transfer from the cob(I)alamin moiety to the chlorinated alkene, followed by elimination of the anion.[69] In this reaction, there is no organometallic species formed initially, but instead the reaction proceeds via a radical mechanism, where a single electron is transferred from the Co(I) species to the PCE giving a radical anion. This then loses a chloride ion, leaving a trichloroethenyl radical, which then coordinates to the Co(II) species formed earlier. Elimination of this TCE species then occurs, and again, the starting cobalamin is regenerated.

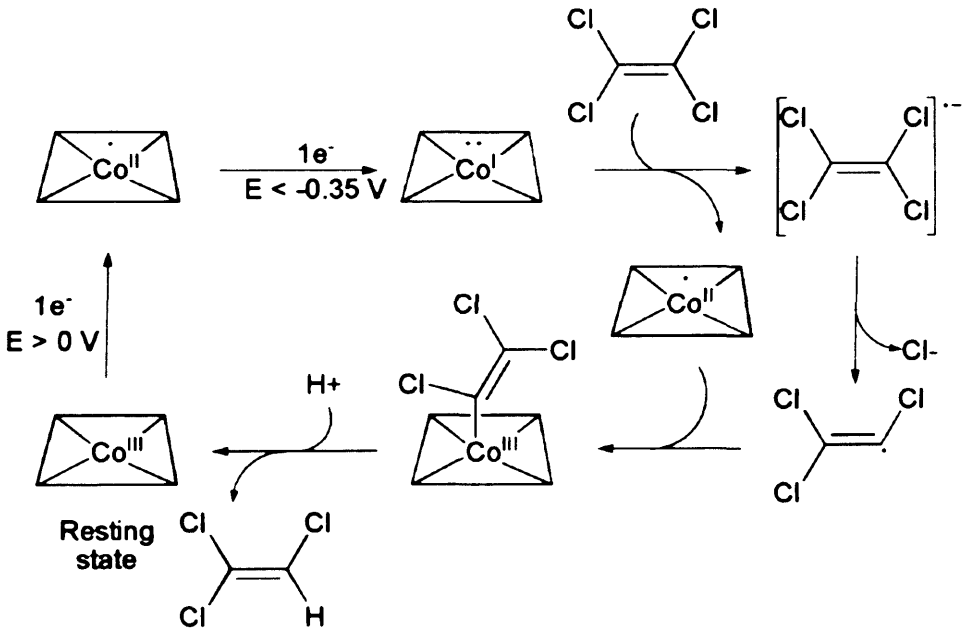

Scheme 1.12. The alternative mechanism proposed by Glod[69] for dechlorination. (Co within the rhombus represents the corrinoid centre)

Other natural complexes are capable of catalytic dehalogenation without the presence of an enzyme, and instead require an external reducing agent.[52] Such species include heme and F_{430}, both of which are structurally similar to vitamin B_{12}.[70,71,72] For example, heme has been found to be a useful cofactor in the reductive dechlorination of DDT to DDD,[73] and F_{430}, which is the active centre of the methyl coenzyme M reductase, will catalyse the reductive dehalogenation of alkyl halides.[74]

1.3.4. Cobaloximes as Models for Vitamin B_{12}.

Since vitamin B_{12} is an extremely complicated molecule, any attempt at a total synthesis or an adaptation of the species is an unrealistic route to large quantities of catalyst. Fortunately, cobaloximes have been shown to be useful models for cobalamins.[75] Cobaloximes generally take the form $[RCo^{(III)}B(L)_2]$, where R is a halide or an alkyl moiety σ-bonded to the cobalt centre, B is an axial ligand *trans* to the R group, often a Lewis base and L_2 represents two monoanionic dioxime ligands. **Figure 1.10** depicts such a cobaloxime, with pyridine *trans* to the chloride, and two dimethylglyoxime moieties making up the macrocycle completed by O-H-O hydrogen bonding between the hydroxyl and the oxide moiety, analogous to the corrinoid ring of vitamin B_{12}.

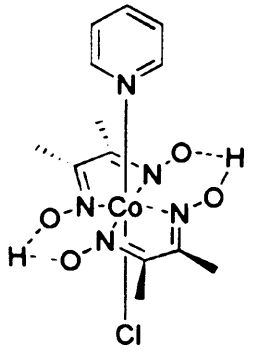

Figure 1.10. Chloropyridylcobaloxime

1.3.5. The Chemistry and Applications of Cobaloximes.

In addition to their use as models for vitamin B_{12}, cobaloximes are used in catalytic reactions and have rich coordination chemistry; there are almost unlimited possibilities for substituents in the axial positions, and variation of the equatorial ligands. Their use as models for vitamin B_{12} stemmed from the need to understand the mechanism of homo- or heterolytic cleavage of the organocobalt bond in vitamin B_{12} dependant enzymatic reactions. This is due, in the case of organocobaloximes, to the inherently weak cobalt-sp^3 carbon bond. Due to this labile cobalt-carbon bond, organocobaloximes are known to catalyse a variety of chemical processes, and have also been utilised in organic synthesis and in polymer chemistry.

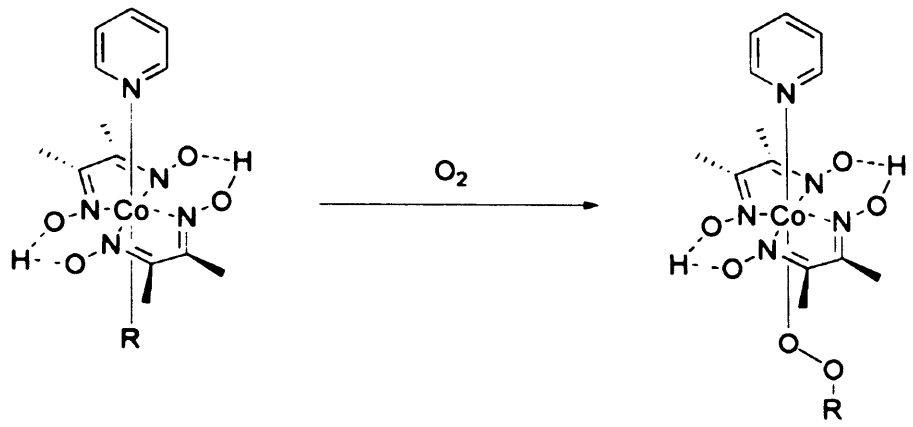

Scheme 1.13. O_2 insertion into Co-C bond.

Cobaloximes themselves have developed a rich, independent field of research, and whilst the research into their spectral and structural properties is discussed in later chapters, the applications of cobaloximes are highlighted here. Cleavage of the weak Co-C bond is a key step in vitamin B_{12} dependant enzymatic reactions, and so, cobaloximes have been utilised to understand this. Following from this reactivity, the insertion of small di- and triatomic species, such as O_2 and SO_2, into this bond has been documented, as demonstrated in **Scheme 1.13**. Insertion reactions have been used to test the reactivity of organometallic bonds, and occur with a wide range of organometallic compounds.

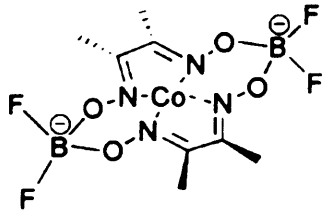

Figure 1.11. [Bis[μ-[(2,3-butanedione dioximato)-O,O']tetrafluorodiborato-N,N, N',N'']] cobalt (COBF).

Catalytic chain transfer polymerisation (CCTP) of methacrylates and styrene using cobalt complexes is a well-established synthetic route to functionalised oligomers. Low-spin Co(II) complexes, such as COBF, depicted in **Figure 1.11**, catalyse the chain transfer to monomer reaction, via the mechanism shown below. First, a growing polymeric radical, shown in **Scheme 1.14**, undergoes a hydrogen transfer reaction with the Co(II) complex to form a growing polymer chain, and a Co(III)H complex. This

Co(III)H complex subsequently reacts with a monomer molecule, to produce the original Co(II) complex and a monomeric radical, which then proceeds to polymerise.

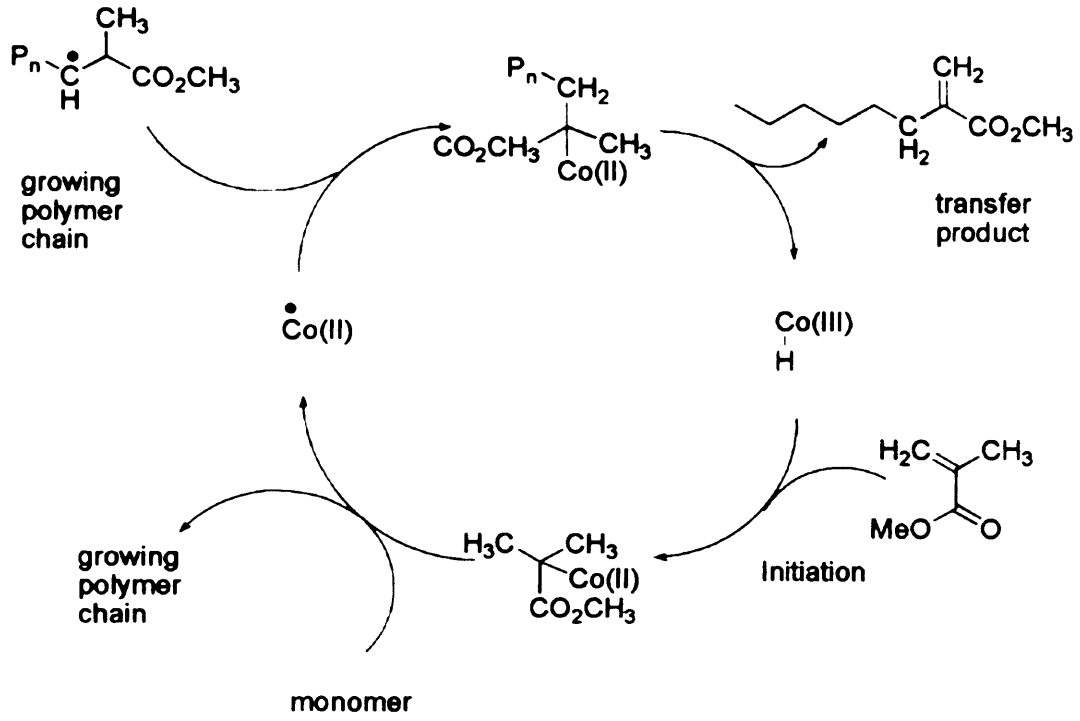

Scheme 1.14. Catalytic steps of COBF mediated polymerisation of methylmethacrylate.

Whilst cobaloximes are good structural and functional mimics for vitamin B_{12}, they do not reproduce the exact chemical properties, such as standard electrode potentials.[76] An isolated cobaloxime is a poor model for the overall redox chemistry of vitamin B_{12}. For instance, the Co(I)/(II) and Co(II)/(III) redox potentials for cobalamins and cobaloximes each differ with the latter being about 0.4 V more negative, i.e. there is less electron density on the cobalt centre.[77] This could be due to the fact that vitamin B_{12} contains a rigid corrinoid ring, whilst cobaloximes contain a less rigid glyoxime ring, which is held together by two O-H-O hydrogen bonds, so the equatorial ligands of the cobaloxime system force some differences from cobalamin chemistry.[78,79]

Van der Donk,[41] and others,[80] have shown that cobaloximes are good mimics for B_{12} in the dehalogenation reactions of interest here, although low turnover number have been recorded. This is believed to be a result of the slow cleavage of the final cobalt-sp^2 carbon bond formed between the final ethene and the cobaloxime. In order to achieve complete dechlorination of PCE to free ethene, the stability of the final ethene-cobaloxime complex needs to be overcome. It is this reductive cleavage of the Co-C

bond represented in **Scheme 1.10**, which is thought to be missing from model systems, and essential for catalysis.

1.4. The Carbon-Halogen Bond.

The reactivity of organohalides generally follows the order I > Br > Cl > F. This order is due to the selective strengths of the carbon-halogen bonds, and can be observed in the dissociation energy of the appropriate bonds (C-I, 53 kcal mol^{-1}; C-Br, 67 kcal mol^{-1}; C-Cl, 81 kcal mol^{-1}; C-F, 109 kcal mol^{-1}).[81] Due to the strength of the C-F bond, organofluorides are somewhat resistant to reduction, though many efforts have been made to overcome this chemical inertness by appropriate activation. Concerning the structure of the substrate, the cleavage of the carbon-halogen bond is favoured in the order benzylic > allylic > vinylic > aromatic > aliphatic.

The reactivity of primary, secondary, and tertiary halides is dependent on the reagent employed, with the steric environment affecting the rate of the reduction. Generally, primary halides are the most easily reduced when the process involves an S_N2 mechanism or in catalytic hydrogenation. The trend is just the opposite when the reaction proceeds through an S_N1 mechanism, or with the participation of free radicals as intermediates, the reduction following the sequence tertiary > secondary > primary.

The strength of the carbon-halogen bond will have a major influence on how the effective the catalyst is and on the mechanism of dechlorination. As the substrate is dechlorinated, the chemistry of the alkene changes as with each substituent loss, the electronegativity of the C=C bond is altered. As a result, the loss of the first halide is believed to proceed via an electron transfer mechanism, whilst subsequent halide loss proceeds via an organocobalt species. The mechanism of dechlorination by vitamin B_{12} species is discussed in detail in **Chapter 3**.

1.5. Aims and Objectives.

The main aims of this work is to synthesise and test a series of cobaloximes that mimic the dehalogenation reactions of *tetrachloroethylene reductase* enzymes found in nature. As discussed previously, isolated cobaloximes, whilst good models for vitamin B_{12} reactivity, are poor models for the overall redox chemistry of vitamin B_{12}, which is shown in **Figure 1.10**. To mimic the redox shuttle effect of the FeS cluster, cobaloximes will be synthesised which include a secondary redox active metallic moiety, demonstrated in **Figure 1.12**.

It is believed that the incorporation of this metal centre will mimic the electron transfer effect of the FeS cluster present in the enzyme, reducing the Co(III) centre to the catalytically active Co(I) species required for the dechlorination cycle. Reduction to this active species will be achieved using laboratory reagents (Ti(III) citrate, borohydrides, vitamin C, H_2) as the bulk reductants. The redox centre will be attached via an axial *N* ligand, as this should not significantly affect the reactivity of the systems as the nature of the axial *N* ligand has been shown to have only minor influence on cobalamin reactivity.[82] The R and X moieties offer an opportunity to introduce electron donating or withdrawing groups to fine-tune the catalytic ability of the multimetallic cobaloxime. Further fine tune catalytic ability by to this motif, dicobaloximes species that have a bidentate ligand coordinated to two cobaloxime centres have been presented by Gupta *et al*,[83] which fit the scope of this work, but their catalytic activity towards dechlorination has yet to be analysed.

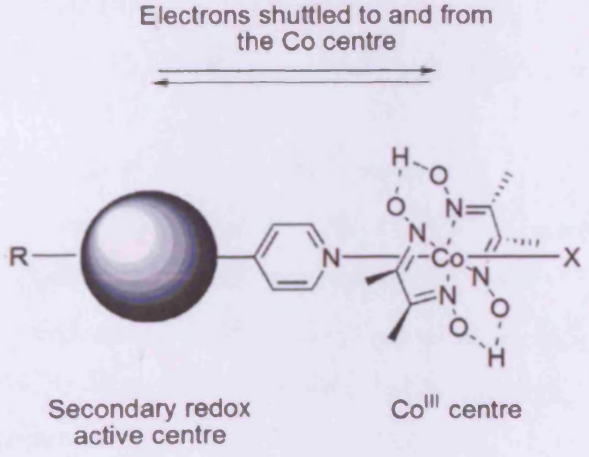

Figure 1.12. Target cobaloxime.

It is generally believed, though no evidence has been provided either way, that in cobalamin chemistry, reduction of a Co(III) species to Co(I) proceeds via a four-coordinate intermediate, where both the axial ligands are lost, then the favoured six-coordinate geometry is regained by oxidation of the Co(I) species.[84] By analogy, it would be expected that the ligand bearing the secondary metal centre would also dissociate following reduction. This loss then re-association would have a detrimental affect on the catalytic ability, as the turnover frequency and stability of the catalysts would be affected, thus cobaloximes with secondary metal centres contained in equatorial ligand also need to be studied. Evidence in favour of or disproving the four-coordinate intermediate will also be sought via a series of ligand exchange reactions.

Each of the potential catalysts will be screened for catalytic ability in dechlorination of pollutants, principally perchlorothylene, with a variety of reducing agents. The product ratios from these reactions will be examined as complete dechlorination is required, since the intermediates of the dechlorination process, e.g. vinyl chloride, are often more toxic than the starting substrate.

1.6. References.

1 C. J. Cooksey, *Molecules*. **2001**, 6, 736.

2 The Merck Index, 11th ed.; Merck & Co: Rahway, NJ, 1989; p 317

3 B. M. Trost, I. Fleming, Comprehensive Organic Chemistry; Eds.; Pergamon Press: Oxford, 1991

4 Dry cleaning, some chlorinated solvents and other industrial chemicals. Lyon, international Agency for Research on Cancer, 1995 (IARC Monographs on the Evaluation of Carcinogenic Risks to Humans, Vol.63)

5 Trichloroethylene. Geneva, World Health Organization, 1985 (Environmental Health Criteria, No. 50)

6 Toxicological profile for trichloroethylene. Atlanta, GA, Agency for Toxic Substances and Disease Registry, 1993 (US Public Health Service Report, No. TP-92/19).

7 (a) K. C. Nicholau, E. J. Sorenson, Classics in Total Synthesis I, Wiley-WCH; (b) K. C. Nicholau, S. Snyder, Classics in Total Synthesis II, Wiley-WCH.

8 K. C. Nicolaou, *Angew. Chim. Int. ed.* **1999**, 38, 240.

9 C. S. Vairappan, M. Suzuki, T. Abe, M. Masuda, *Phytochemistry*. **2001**, 58, 517.

10 T. Rezanka, V. M. Dembitsky, *Phytochemistry*. **2001**, 57, 607.

11 T. Rezanka, V. M. Dembitsky, *Phytochemistry*. **2001**, 57, 869.

12 G. M. Cameron, B. L. Stapleton, S. M. Simonsen, D. J. Brecknell, M. J. Garson, *Tetrahedron*. **2000**, 56, 5247.

13 B. L. Stapleton, G. M. Cameron, M.J. Garson, *Tetrahedron*. **2001**, 57, 4603.

14 E. C. Kendall, *J. Am. Med. Assoc.* **1915**, 16, 2042

15 E. J. Corey, X-M, Cheng, The Logic of Chemical Synthesis; Wiley-Interscience: New York, 1989; pp 362-423.

16 R. Matsumara, T. Suzuki, H. Hagiwara, T. Hoshi, M. Ando, *Tet. Lett.* **2001**, 42, 1543.

17 M. J. Molina, F. S. Rowland, *Nature*. **1974**, 249, 810

18 S. Cagin, P. Dray, Between Earth and Sky: How CFCs Changed Our World and Threatened the Ozone Layer; Pantheon Press: New York, 1993.

19 J. C. Farman, B. G. Gardiner, J. D. Shanklin, *Nature*. **1985**, 315, 207.

20 Montreal Protocol on Substances that Deplete the Ozone Layer; United Nations Environmental Programme (UNEP): New York, 1987.

21 Report on Carcinogens, Eleventh Edition; U.S. Department of Health and Human Services, Public Health Service, National Toxicology Program

22 C. Rappe, *Pure. Appl. Chem.* **1996**, 68, 1781.

23 R. Eisler, Eisler's encyclopedia of environmentally hazardous priority chemicals

24 U.S. National Toxicology Program acute toxicity studies for Dioxin (2,3,7,8-TCDD) http://www.pesticideinfo.org/List_NTPStudies.jsp?Rec_Id=PC35857

25 Material Safety Data Sheet- Strychnine, available from http://msds.chem.ox.ac.uk/ST/strychnine.html

26 Material Safety Data Sheet- Sodium Cyanide, available from http://msds.chem.ox.ac.uk/SO/sodium_cyanide.html

27 P. A. Bertazzi, *Sci. Total Environ.* **1991**, 106, 5.

28 N. Krieger, M. S. Wolff, R. A. Hiatt, M. Rivera, J. Vogelman, N. J. Orentreich, *Natl. Cancer Inst.* **1994**, 86, 589.

29 M. R. Mclean, L. W. Robertson, R. C. Gupta, *Chem. Res. Toxicol.* **1996**, 9, 165.

30 G. F. Fries, *Sci. Total Environ.* **1996**, 185, 93.

31 K. S. Kang, M. R. Wilson, T. Hayashi, C. C. Chang, J. E. Trosko, *Environ. Health Perspect.* **1996**, 104, 192.

32 J, Leuschner. Arzneim.-Forsch. **1998**, 48, 961.

33 P. J. Squillace, *Environ. Sci. Technol.* **1999**, 33 4176.

34 USEPA, 40 CFR Part 131, 42159—42208, 1997

35 P. V. Roberts, *J. Environ. Eng. Div. (Am. Soc. Civ. Eng.).* **1978**, 104, 933.

36 E. J. Bouwer, *Environ. Sci. Technol.* **1981**, 15, 596.

37 E. J. Bouwer, *Appl. Environ. Microbiol.* **1983**, 45, 1286.

38 T. D. DiStefano, *Appl. Environ. Microbiol.* **1991**, 57, 2287.

39 B. Z. Fathepure, *Appl. Environ. Microbiol.* **1987**, 53, 2671.

40 C. Holliger, *FEMS Microbiol. Revs.* **1999**, 22, 383.

41 W. A. van der Donk, *J. Am. Chem. Soc.* **2000**, 122, 12403.

42 P. V. Roberts, *Water Res.* **1982**, 16, 1025.

43 S. Premaratne, M. Mandel, H. F. Mower, *J. Biochem. Cell Biol.* **1995**. 27, 789.

44 R. L. Jolley, H. Gorchev, D. H. Hamilton Jr. (ed.). 1978. Water chlorination environmental impact and health effects, vol. 2. Ann Arbor Science Publishers, Inc., Ann Arbor, Mich

45 T. Goswami, A. Rolfs, M. A. Hediger, *Biochem Cell Biol.* **2002**, 80, 679.

46 Trichloroethylene. Geneva, World Health Organization, 1985 (Environmental Health Criteria, No. 50).

47 "DNAPL Remediation: Selected Projects Approaching Regulatory Closure" EPA 542-R-04-016 Dec. 2004

48 Air quality Guidelines — Second edition. © WHO Regional Office for Europe, Copenhagen, Denmark 2000. Chapter 5.15, pg 1

49 S. Fetzner, F. Lingens, *Microbiol. Rev.* **1994**, 58, 641.

50 C. Costentin, M. Robert, J. M. Saveant, *J. Am. Chem. Soc.* **2003**, 125, 10729.

51 H. Shimakoshi, M. Tokunaga, K. Kuroiwa, N. Kimizuka, Y. Hisaeda, *Chem. Comm.* **2004**, 50.

52 C. J. Gantzer, L. P. Wackett, *Environ. Sci. Technol.* **1991**, 25, 715.

53 C. Holliger, *Curr. Opin. Biotechnol.* **1995**, 6, 47.

54 W. W. Mohn, J. M. Tiedje, *Microbiol. Rev.* **1992**, 56, 482.

55 N. Assaf-Anid, K. F. Hayes, T. M.Vogel, *Environ. Sci. Technol.* **1994**, 28, 246.

56 T. M. Vogel, P. L. McCarty, *Appl. Environ. Microbiol.* **1985**, 49, 1080.

57 G. H. Whipple, F.S. Robscheit-Robbins, *Am. J. Physiol.* **1926**, 72, 408.

58 G. R. Minot, W. P. Murphy, *JAMA*, **1926**, 87, 470.

59 E. L. Smith, *Nature*. **1948**, 161, 638.

60 E. L. Rickes, N. G. Brink, F. R. Konivszy, T. R. Wood, K. Folkers, *Science*, **1948**, 107, 396.

61 R. Stevens, In B12, Vol. 1, **1982**. ed. D. Dolphin, pp. 169. New York: Wiley

62 D. C. Hodgkin, J. Kamper, M. Mackay, J. W. Pickworth, K. N. Trueblood, J. G. White, *Nature*, **1956**, 178, 64.

63 H. A. Barker, H. Weissbach, R. D. Smyth, *Proc. Natl. Acad. Sci. USA*, **1958**, 44, 1093.

64 R. Banerjee, *Chem. Biol.* **1997**, 4, 175.

65 R. Banerjee, S. W. Ragsdale, *Annu. Rev. Biochem.* **2003**, 72, 209.

66 R. G. Matthews, *Acc. Chem. Res.* **2001**, 34, 681.

67 S. W. Ragsdale, 1998. In Vitamin B_{12} and B_{12}-Proteins, ed. B Krautler, pp. 167. Weinheim, Ger.: Wiley-VCH

68 U. Wohlfarth, G. Diekert, *Curr. Opin. Biotechnol.* **1997**, 8, 290.

69 G. Glod, W. Angst, C. Holliger, R. P. Schwarzenbach, *Environ. Sci. Technol.* **1997**, 31, 253.

70 C. A. Schanke, L. Wackett, *Environ. Sci. Technol.* **1992**, 26, 830.

71 C. Holliger, G. Schraa, *J. Bacteriol.* **1992**, 174, 4427.

72 U. E. Kronem, K. Laufer, R. K., Thauer, *Biochemistry.* **1989**, 28, 10061.

73 K. Sugihara, S. Kritamura, S. Ohta, *Biochem. and Molec. Biol. Int.* **1998**, 45, 85.

74 T. Arai, K. Kashitani, H. Kondo, S. Sakaki, *Bull. of the Chem. Soc. of Japan.* **1994**, 67, 705.

75 G. N. Schrauzer, *Acc. Chem. Res.* **1968**, 1, 97.

76 K. L. Brown, H. B. Brooks, *Inorg. Chem.* **1991**, 30, 3420.

77 M. C. Elliott, E. Hershenhart, R. G. Finke, B. L. Smith, *J. Am. Chem. Soc.* **1981**, 103, 5558.

78 G. N. Schrauzer, R. J. Windgassen, *J. Am. Chem. Soc.* **1966**, 88, 3738.

79 M. K.Geno, J. Halpern, *J. Am. Chem. Soc.* **1987**, 109, 1238.

80 S. Lesage, S. Brown, K. Millar, *Environ. Sci. Tech.* **1998**, 32, 2264.

81 J. D. Lee Concise Inorganic Chemistry; 5th edition, Blackwell Science. 932

82 K. P. Jensen, U. Ryde, *J. Mol. Struct., Theochem*, **2002**, 585, 239.

83 a) B.D. Gupta, K. Qanungo, *J. Organomet.. Chem.* **1997**, 534, 213, b) B. D. Gupta, K. Qanungo, *J. Organomet.. Chem.* **1997**, 534, 213

84 G. N. Schrauzer, R. J. Windgassen, *J. Am. Chem. Soc.* **1966**, 88, 3738.

Chapter 2.

Experimental Methods.

2.1. General Methods.

All starting materials, reagents and solvents were purchased from commercial suppliers and used as supplied unless otherwise stated. All ^{1}H and ^{13}C nuclear magnetic resonance spectra were recorded on a Bruker DPX-250, Bruker DPX-400 or Bruker Avance 500 spectrometer, with ^{1}H spectra being recorded at 250, 400 or 500 MHz and ^{13}C spectra being recorded at 62.5, 100 or 125 MHz respectively. ^{31}P spectra were recorded on a Jeol Eclipse 300 spectrometer at 121 MHz. Unless otherwise stated, all spectra were recorded in deuterated chloroform at ambient temperature, and all chemical shifts are reported in δ (ppm) and coupling constants (*J*) are reported in Hertz (Hz). ^{1}H NMR spectra were referenced to the residual proton impurity in the solvent ($CHCl_3$, 7.26 ppm). ^{13}C spectra were referenced against the solvent resonance ($CDCl_3$, 77.0 ppm). A program incorporated in Jeol was used to externally reference ^{31}P-NMR spectra. ^{13}C-NMR and ^{31}P-NMR spectra were recorded proton decoupled.

Ligand synthesis, their coordination and subsequent work up were carried out under air, unless otherwise stated, when standard Schlenk techniques were employed. Solvents were used as received, apart from when pre-dried or degassed solvents were required, in which case, they were dried over the relevant molecular sieves or if needed they were taken from a MB SPS-800 solvent purification system.

When appropriate, reactions were conducted in oven-dried apparatus under an atmosphere of dry nitrogen using standard Schlenk techniques. All organic solutions from aqueous work-ups were dried by brief exposure to dried sodium sulfate, followed by gravity filtration. The resulting dried solutions were evaporated using a Büchi rotary evaporator under reduced pressure using a Büchi vacuum pump, at an appropriate temperature unless otherwise stated. Column chromatography was carried out using Merck Silica Gel 60 (230–400 mesh). TLC analyses were carried out using Merck silica gel 60 F_{254} pre-coated, aluminium-backed plates, which were observed using ultraviolet.

Low-resolution mass spectrometry data was obtained using a Waters LCT Premier XE mass spectrometer, whilst high-resolution mass spectrometry data was obtained from the EPSRC mass spectrometry service at Swansea. Warwick Analytical Services, the

University of Warwick, UK, carried out elemental analyses. Infrared spectra were recorded on a JASCO FT/IR-660 Plus instrument as nujol mulls between sodium chloride plates or in solution cell bearing sodium chloride windows. Gas Chromatography was carried out on a Perkin Elmer gas chromatograph 8700, and Gas chromatography-mass spectra was carried out on a Waters LCT Premier XE mass spectrometer.

2.2. Cyclic Voltammetry.

Cyclic voltammetry studies the electrochemical behaviour of redox species over a wide potential range. It is a potentiodynamic method for measuring the formal potential of a half reaction when both the oxidised and reduced forms are stable during the time required to obtain the voltammogram. The potential of a small stationary working electrode is changed linearly with time, starting from a potential where no electrode reaction occurs, and moving to potentials where reduction or oxidation of the material studied occurs. Cyclic voltammetry is characterised by a smooth increase of a working electrode potential from one potential limit to the other and back. Both the potential limits and the potential sweep rate are adjustable parameters. The current at the working electrode is then plotted versus the applied voltage to give the cyclic voltammogram trace, as shown in **Figure 2.1**.

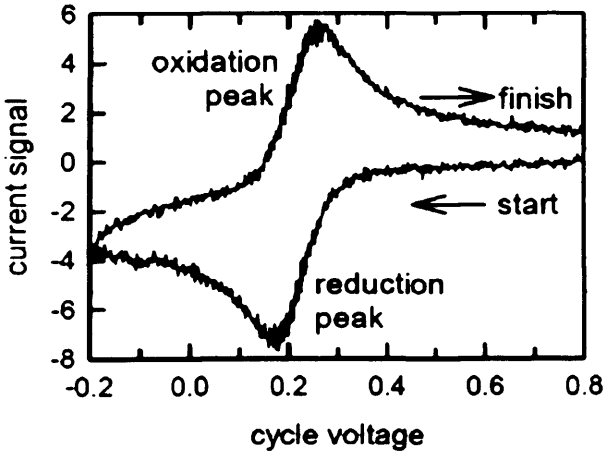

Figure 2.1. Typical cyclic voltammogram.

The method consists of cycling the potential between two electrodes, which are immersed in a degassed and unstirred acetonitrile solution of the analyte and an

electrolyte (often tetrabutylammonium hexafluorophosphate), and the resultant current measured. **Figure 2.2** shows a cartoon representation of an electrochemical cell for voltammetry.

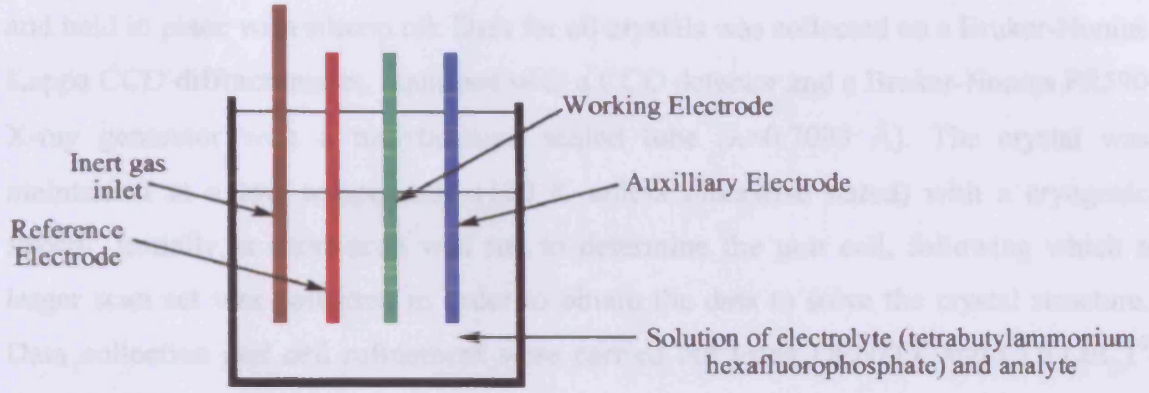

Figure 2.2. Cell for voltammetry.

- **Inert gas inlet**: inert gas to degas the solvent between each measurement.
- **Reference electrode**: provides a known reference potential which is insensitive to small variations of temperature or the passage of a small current within solution, e.g. Saturated Calomel Electrode (SCE).
- **Working electrode**: the electrode on which the investigated process takes place.
- **Auxiliary electrode or counter electrode**: completes the circuit with the working electrode.

Generally there are two limiting cases for all systems, either a reversible electrode process or an irreversible electrode process. The potential difference between the reduction and oxidation peaks is theoretically 60/n mV (n: number of electron associated with the process) for a reversible reaction. In practice, the difference is typically 70-100 mV. Larger differences, or non-symmetric reduction and oxidation peaks are an indication of a non-reversible reaction.

2.3. X-Ray Crystallography.

A single, crack free crystal of correct size (0.2 mm^3) was mounted upon a glass fibre and held in place with silicon oil. Data for all crystals was collected on a Bruker-Nonius Kappa CCD diffractometer, equipped with a CCD detector and a Bruker-Nonius FR590 X-ray generator with a molybdenum sealed tube (λ=0.7093 Å). The crystal was maintained at a low temperature (150 K unless otherwise stated) with a cryogenic stream. Initially, a short scan was run to determine the unit cell, following which a larger scan set was collected in order to obtain the data to solve the crystal structure. Data collection and cell refinement were carried out using DENZO[1] and COLLECT[2] through Nonius SUPERGUI. Structure solution and refinement was achieved using DIRDIF-99[3] (Patterson method), SIR-92,[4] SIR-97[5] SIR-2002[6] (direct methods) and SHEXL-97[7] through MAXUS[8] and WinGX32[9] graphical interfaces; absorption corrections were performed using SORTAV, and resolved using a "least squares model" on the SHELX suite of programs.[10] Non-hydrogen atoms were refined in anisotropic approximation (with exception to disordered atoms) and hydrogen atoms were placed in calculated positions using the riding model. Structure visualisation was achieved using Xseed[11] and POV-ray.

The candidate solved the following crystal structures during the course of the project, and the data can be found on the appendix CD.

- The following bis(imino)aryl iridium(III) and bis(imino)aryl rhodium(III) pincer complexes were prepared by addition of 2-bromoisophthalaldimines to $[IrCl(COD)]_2$ or $[RhCl(COE)]_2$. These species were found to act as precursors to active catalytic species for use in base-catalysed hydrogen transfer reactions, converting ketones to alcohols.[12]

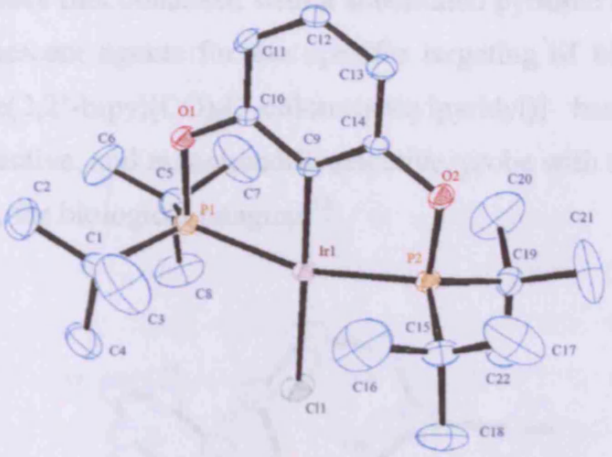

Figure 2.3. ORTEP representations of the structure of Bis(dimethylphosphino)aryl Iridium(I) Chloride with thermal ellipsoids drawn at the 30 % level.

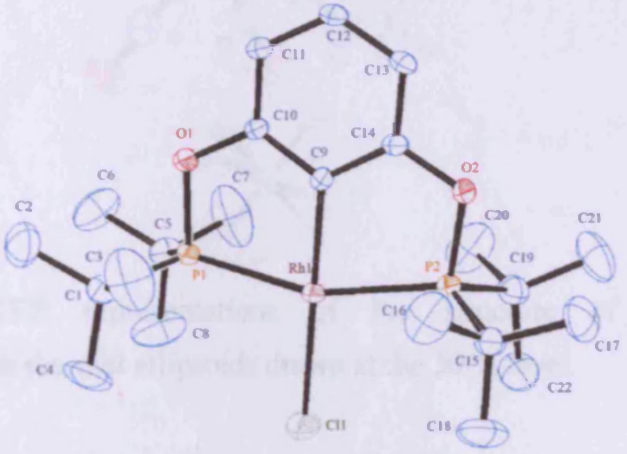

Figure 2.4. ORTEP representations of the structure of Bis(dimethylphosphino)aryl Rhodium(I)Chloride with thermal ellipsoids drawn at the 30 % level.

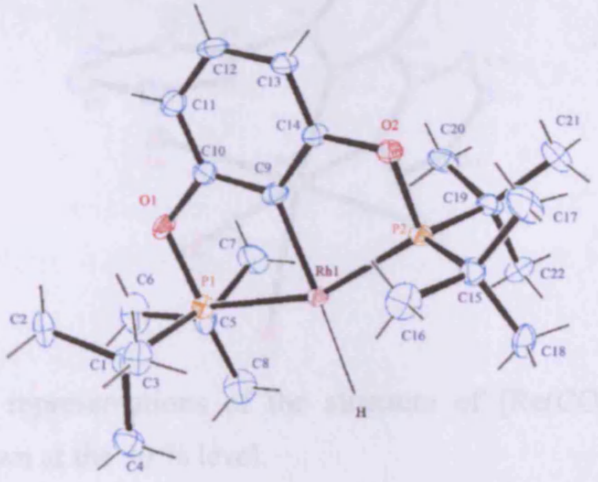

Figure 2.5. ORTEP representations of the structure of Bis(dimethylphosphino)aryl Rhodium(I)hyrdride with thermal ellipsoids drawn at the 30 % level.

- Rhenium complexes functionalised with a substituted pyridine unit have been used as ^{3}MLCT luminescent agents for the specific targeting of biological entities in imaging. [*fac*-Re(2,2'-bipy)$(CO)_3$(3-chloromethylpyridyl)] has the potential to provide a thiol-reactive, and mitochondria-selective, probe with a long lifetime and a large Stokes shift, for biological imaging.[13]

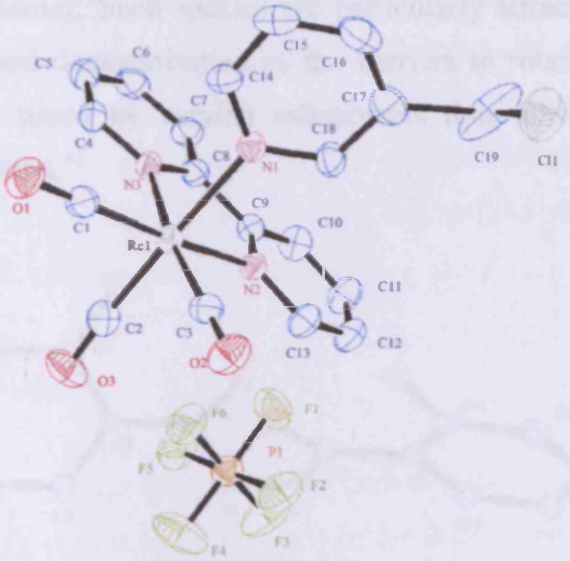

Figure 2.6. ORTEP representations of the structure of $[Re(CO)_3(bpy)(3\text{-chloropyr})][PF_6]$ with thermal ellipsoids drawn at the 30 % level.

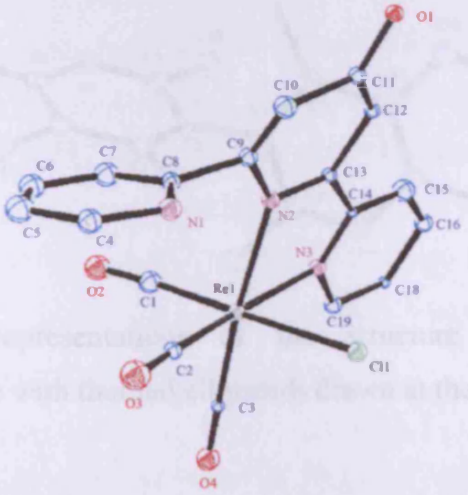

Figure 2.7. ORTEP representations of the structure of $[Re(CO)_3(terpy)(Cl)]$. with thermal ellipsoids drawn at the 30 % level.

- Cyclic acyl hydrazines, such as 3,3'-dimethyl-2,2'-biquinazoline-4'-thio-4-one, are examples of N–N atropisomeric materials, where the chirality is derived from hindered rotation around an N–N bond. These compounds can undergo a phenomenon known as "conglomerate crystallisation" whereby a sample in solution that consists of a mixture of two enantiomers spontaneously separates during the crystallisation process to form a physical mixture of crystals each of which contains only a single enantiomer. Such species are particularly attractive for the study of crystallization-induced deracemisation as the barriers to rotation around the N–N chiral axis can be tuned by varying substituents thus allowing a pathway for racemisation in solution.[14]

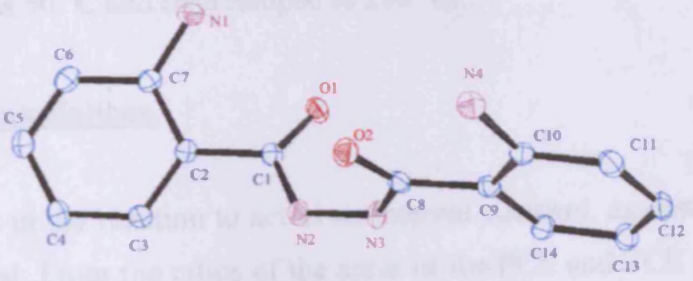

Figure 2.8. ORTEP representations of the structure of 1,2-bis-(2-aminobenzoyl)hydrazine with thermal ellipsoids drawn at the 30 % level.

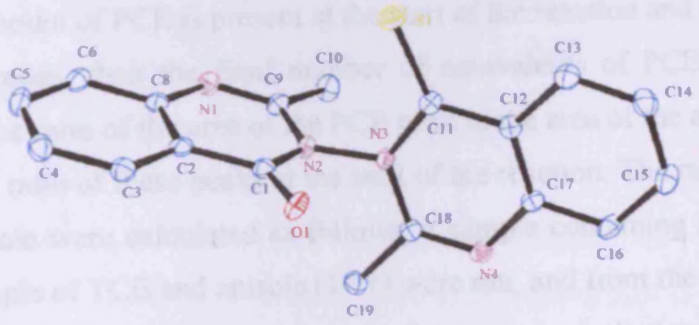

Figure 2.9. ORTEP representations of the structure of 2,2'-dimethyl-3,3'-biquinazoline-4-thio-4'one with thermal ellipsoids drawn at the 30 % level.

5.4. Catalysis Procedure.

5.4.1. General Protocol for Catalytic Dechlorination.

A solution of the catalyst (0.1 mmol), anisole (0.1 mmol) and perchloroethylene (1 mmol) in methanol (5 ml) was prepared and a solution of sodium borohydride (0.2 mmol) and sodium hydroxide (0.3 mmol) in water (1 ml) was added. The reaction vessel was sealed and allowed to stir for one hour at which point, 1 ml of the solution was removed, filtered through a plug of both celite and silica to remove inorganics and submitted for GC analysis. On the Perkin Elmer gas chromatograph used, the retention times of PCE, TCE, DCE and anisole are 3.3, 1.8, 1.3 and 7.4 minutes respectively, where the oven was 50 °C and then ramped to 200 °C.

5.4.2. Catalysis Calculations.

Anisole is present in the reaction to act as an internal standard, against which the peak areas are compared. From the ratios of the areas of the PCE and TCE peaks relative to the area of the anisole peak the amount of PCE and TCE present within the reaction mixture can be determined.

Since a known amount of PCE is present at the start of the reaction and this decreases as the reaction proceeds, then the final number of equivalents of PCE present can be calculated from the ratio of the area of the PCE peak to the area of the anisole peak, as a percentage of the ratio of these peaks at the start of the reaction. The ratios of both PCE and TCE to anisole were calculated as follows; a sample containing PCE and anisole (10:1), and a sample of TCE and anisole (10:1) were run, and from the resultant graphs, shown in **Figure 2.10**, the ratio of the equivalents to area was calculated by dividing the initial concentration by the area of the resultant peak.

From these values, the ratio of 1 equivalent of PCE per unit area, to 1 equivalent of anisole per unit area was calculated as 0.904/0.214 = 4.22, and the ratio 1 equivalent of TCE per unit area to 1 equivalent of anisole per unit area was calculated as 0.742/0.225 = 3.30. Hence, the number of equivalents of both PCE and TCE remaining after a

dechlorination experiment can be found by taking the ratio of the area of the peak attributed to PCE or TCE, to the area of the peak due to anisole, and multiplying it by 4.22 and 3.30 respectively.

Area (PCE) = 11.065

Area (Anisole) = 4.672

$$\frac{[PCE]}{P_{Area}} = \frac{10}{11.065} = 0.904$$

Area (TCE) = 13.445

Area (Anisole) = 4.448

$$\frac{[TCE]}{T_{Area}} = \frac{10}{13.445} = 0.743$$

$$\frac{[Anisole]}{A_{Area}} = \frac{1}{4.672} = 0.214$$

$$\frac{[Anisole]}{A_{Area}} = \frac{1}{4.448} = 0.225$$

Figure 2.10. Analysis of the PCE:anisole (10:1) and TCE:anisole (10:1) mixtures.

	Area of Peak			
Catalyst	DCE	TCE	PCE	Anisole
$Co_2(CO)_8$	0.0556	0.1792	6.5868	3.097

Table 2.1. GC peak areas from catalysis test of $Co_2(CO)_8$.

From **Table 2.1**, The ratio of the PCE:anisole peaks is 6.5868/3.097 = 2.13. Therefore, the number of equivalents of PCE remaining after the experiment is found by 2.13 x 4.22 = 8.98, whilst the ratio of TCE:anisole peaks is 0.1792/3.097 = 0.06, and the number of equivalents of TCE present after the reaction is 0.06 x 3.30 = 0.198. From these values it can be deduced that $Co_2(CO)_8$ is a stoichiometric dechlorinator of PCE as only 1.02 equivalents of PCE is reduced of which 1.02 – 0.198 = 0.822 equivalents are reduced further.

2.5. References.

1 Z. Otwinowski, W. Minor, in 'DENZO', ed. C. W. Carter and R. M. Sweet, New York, **1996**.

2 Nonius, in 'COLLECT', **1999**.

3 P. T. Beurskens, G. Beurskens, R. d. Gelder, S. Garcia-Granda, R. O. Gould, R. Israel, J. M. M. Smits, in 'DIRDIFF-99', University of Nijmegen, Nijmegan, The Netherlands, **1999.**

4 A. Altomare, G. Cascarano, C. Giacovazzo, and A. Guagliardi, *J. Appl. Cryst.* **1993**, 26, 343.

5 A. Altomare, M. C. Burla, M. Camalli, G. L. Cascarano, C. Giacovazzo, A. Guagliardi, A. G. G. Moliterni, G. Polidori, R. Spagna, *J. Appl. Cryst.* **1999**, 32, 115.

6 M. C. Burla, M. Camalli, B. Carrozzini, G. L. Cascarano, C. Giacovazzo, G. Polidori, R. Spagna, *J. Appl. Cryst.* , **2003**, 36, 1103.

7 G. M. Sheldrick, in 'SHELXL-97', University of Gottingen, Gottengen, Germany, **1998**.

8 BrukerAXS, in 'MaXus', 1999.

9 L. J. Fallugia, *J. Appl. Cryst.* **1997**, 32, 837.

10 R. H. Blessing, *Acta Cryst.* **1995**, A51, 33.

11 L. J. Barbour, *J. Supramol. Chem*, **2001**, 1, 189.

12 S. H. Oakley, M. P. Coogan, R. J. Arthur, *Organometallics*, **2007**, 9, 2285.

13 A. J. Amoroso, R. J. Arthur, M. P. Coogan, J. B. Court, V. Fernandez-Moreira, A. J. Hayes, D. Lloyd, C. Millet, S. J. A. Pope, *New J. Chem.*, **2008**, 32, 1097.

14 R. J. Arthur, M. P. Coogan, M. Casadesus, R. Haigh, D. A. Headspith, M. Grazia Francesconi, R. H. Laye, *Cryst. Eng. Comm.*, **2009**, 11, 610.

Chapter 3.

Dechlorination Studies of PCE with Cobaloximes.

3.0. Compound List.

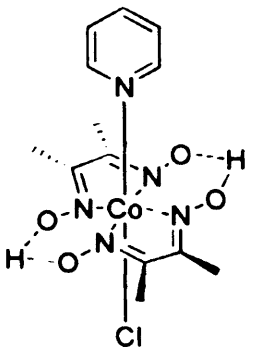

3.1

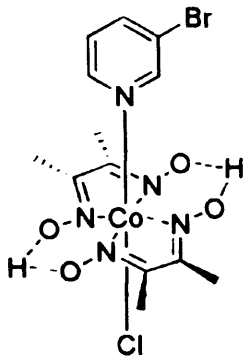

3.2

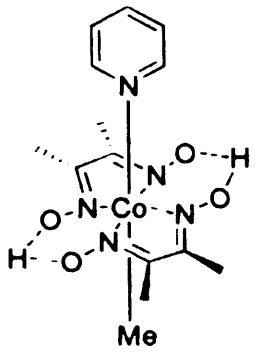

3.3

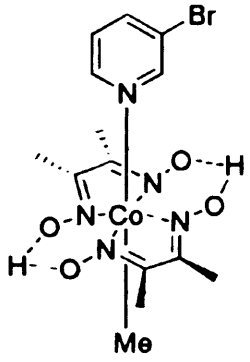

3.4

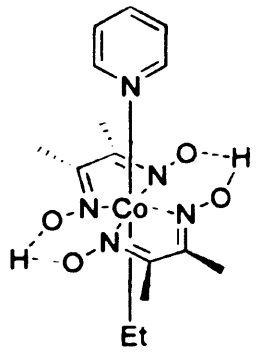

3.5

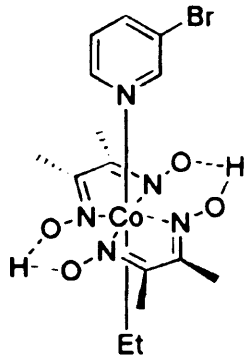

3.6

3.1 Introduction.

3.1.1. The Use of Simple Cobaloximes in the Elucidation of the Dechlorination Mechanism for PCE.

3.1.1.1. The Conversion from PCE to TCE.

Much research has gone into understanding the mechanism of the vitamin B_{12}-mediated dechlorination of PCE observed during dehalorespiration, using cobaloximes as models for the *tetrachloro reductase* enzyme. Based on the literature, there are at least five viable mechanisms for the conversion of PCE to TCE. Mechanisms **A-D**, shown in **Scheme 3.1**, proceed via the formation of an organocobalt species, by means of nucleophilic attack of the cob(I)alamin on the olefin, and only differ in the manner by which the chloride is lost, and the Co-C bond is cleaved. Due to the high nucleophilicity of the cob(I)alamins, nucleophilic attack of the cob(I)alamin species on the electron deficient olefin appears a good suggestion for the first step. The final proposed mechanism **E**, however, proceeds via electron transfer from the cob(I)alamin to PCE, and does not involve an organocobalt species.

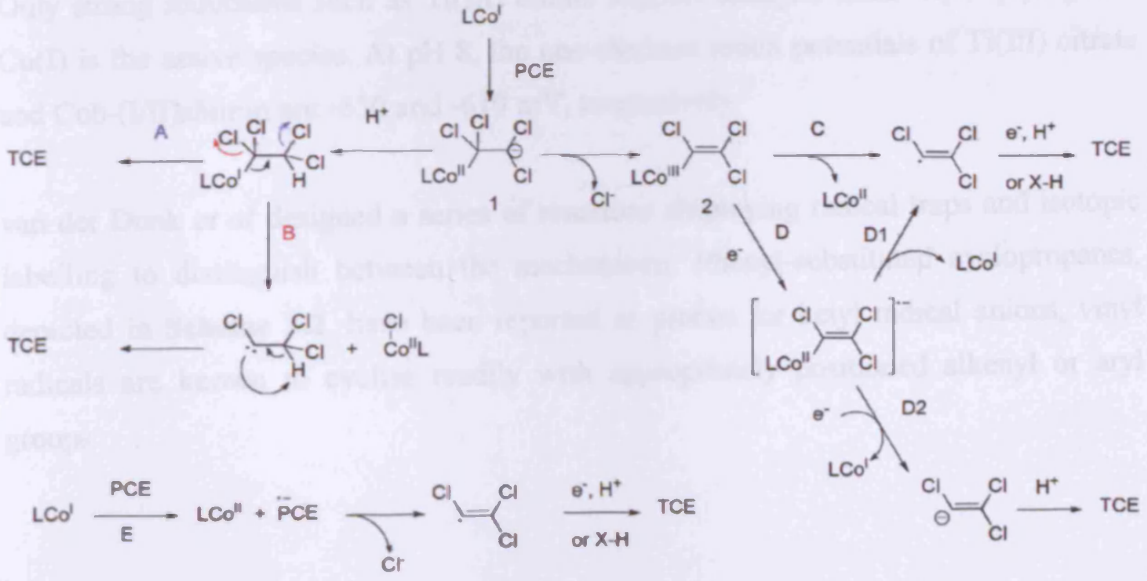

Scheme 3.1. Possible mechanisms for the reductive dechlorination of PCE to TCE. [1,2,3]

In pathway **A**, Co-C cleavage occurs via β-elimination of the chloride from the tetrachloroethylcobalamin species. This electrofugal Co-C cleavage has precedent in organocobalamins with good leaving groups in the β-position. The α-elimination of the chloride from the tetrachloroethylcobalamin species would generate a carbene, which could undergo either C-H or C-Cl bond insertion, to give TCE as the product (pathway **B**).

The dehydrochlorination of the initial addition intermediate **1** yields trichloroethenylcobalamin **2**. The homolytic cleavage of the Co-C bond, followed by the reduction of the resultant trichloroethenyl radical is shown in pathway **C**. Pathway **D** proceeds via a one-electron reduction of the trichlorovinylcobaloxime, yielding the radical anion. There are two routes this can then undertake; **D1** shows the homolytic cleavage of the Co-C bond, similar to **C**, whilst in **D2** the Co-C bond is cleaved when a second electron reduces the species further, leaving the trichloroethenyl anion to abstract a hydrogen.

The non-nucleophilic mechanism **E** proceeds via a one electron transfer from cob(I)alamin to PCE, giving the trichloroethenyl radical which could then be reduced, protonated or act as a hydrogen abstractor, if a suitable donor is present, to yield TCE. Only strong reductants such as Ti(III) citrate support catalytic turnover, implying that Co(I) is the active species. At pH 8, the one-electron redox potentials of Ti(III) citrate and Cob-(I/II)alamin are -630 and -610 mV, respectively.[1]

van der Donk *et al* designed a series of reactions employing radical traps and isotopic labelling to distinguish between the mechanisms. Phenyl-substituted cyclopropanes, depicted in **Scheme 3.2**, have been reported as probes for ketyl radical anions, vinyl radicals are known to cyclise readily with appropriately positioned alkenyl or aryl groups.

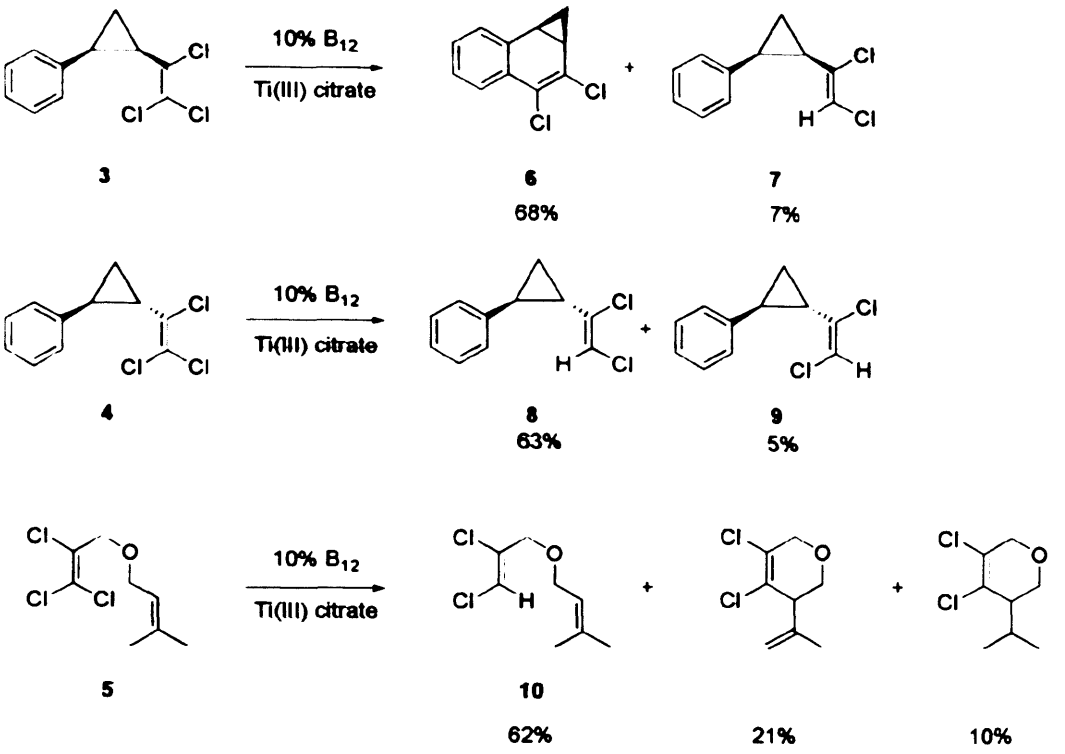

Scheme 3.2. Cyclisation reactions in the presence of vitamin B_{12}.

Based upon these considerations, compounds **3-5** were designed, with a view to probe the involvement of the radical anions or vinyl radical intermediates. Compounds **3-5** were reacted with a catalytic amount of vitamin B_{12} in the presence of excess Ti(III) citrate. From the chlorinated species **3**, the major product observed was **6**. Compounds **3-5** also provided the reduced compounds **7-10** respectively. Due to the almost exclusive 6-(π-endo)exo mode of cyclisation, van der Donk deduced that the evidence supports mechanism **E**, a one electron transfer from cob(I)alamin to PCE, as the first step in the catalytic dechlorination.[2] No cyclisation of **4** is observed, only reduction, as the phenyl ring and the vinyl group are not on the same face of the cyclopropane ring. Further studies of the reduction product run in deuterated IPA/H_2O showed that the hydrogen was abstracted from the C-2 of the IPA solvent.[a]

[a] The observance of a greater amount of the hydrogenated product than the deuterated product is attributed to the primary kinetic isotope effect in the abstraction step.

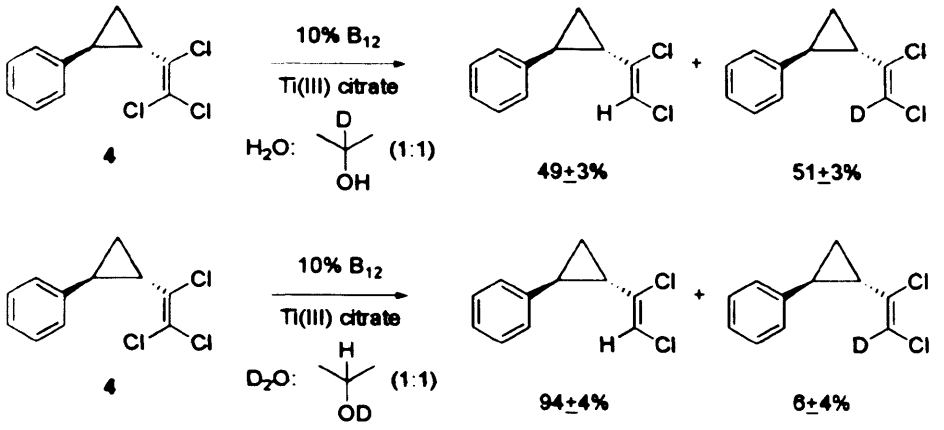

Scheme 3.3. Reactions showing the origin of the vinylic hydrogen.

3.1.1.2. The conversion from TCE to DCE.

Unlike the developing consensus on the mechanism for the conversion of PCE to TCE, the mechanism of B_{12}-catalysed reductive dechlorination of TCE and the various resultant isomers of DCE is less clear. Simple cobaloximes of the type [RCo(glyoxime)$_2$X] have been used as models for vitamin B_{12} to study their role in the dechlorination of chloroethenes under reductive conditions.

The reductive dechlorination of TCE almost exclusively gives *cis*-DCE, with trace amounts of both *trans*- and *geminal* DCE observed, where the ratio of the *cis* isomer to the sum of both *trans* and *geminal* isomers was found to be approximately 23:1,[3] whilst mass spectrometry confirmed the presence of organocobalt species. Computational studies based on D.F.T. and coupled-cluster theory,[b] have shown that the expected ratios based on thermodynamic stability and the likely radical intermediates are 3:1, and 5:1, respectively, each in favour of the *cis* isomer.[4]

[b] A computational technique where the interactions of many-body systems is modelled by *ab initio* quantum chemistry methods.

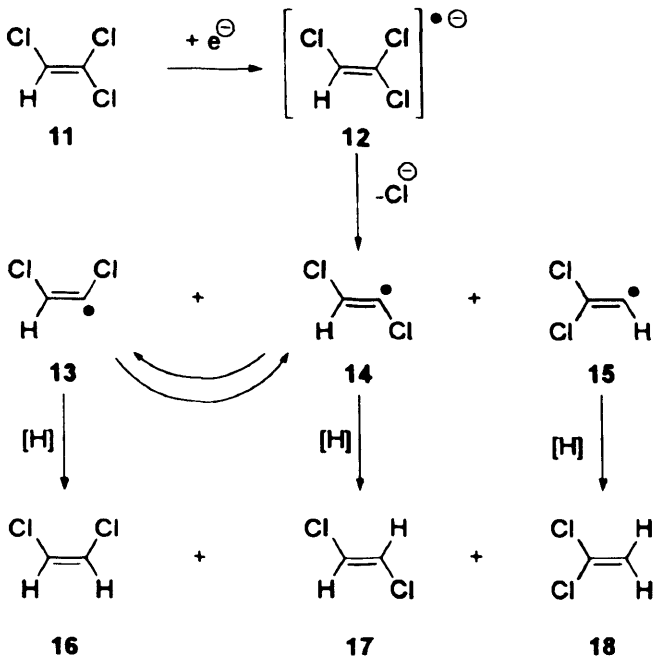

Scheme 3.4. Factors affecting the ratios of DCE isomer formation.

The distribution of products in **Scheme 3.4** depends on two factors; the interconversion between **13** and **14**, and the rate of hydrogen abstraction of each. If the interconversion between **13** and **14** is slow, then the initial concentrations of **13** and **14**, and thus the kinetics of their formation from **12**, will be the major factor, and the difference in rate of hydrogen abstraction from **13** to **16**, or **14** to **17** will play no part in the distribution of products. However, if the interconversion is fast, then the difference in rate of hydrogen abstraction will be the major factor.

Studies showed that of the three isomeric radicals investigated, the *cis*-1,2-dichloroethylene-1-yl radical **13** is predicted at all computational levels to be most stable. The corresponding *trans*- isomer **14** is less stable by about 6 $kJmol^{-1}$, and the 1,1-dichloroethen-2-yl radical **15** is significantly less stable than **13** by 21 $kJmol^{-1}$. The calculated relative energies can be rationalised by considering the difference in the ability of the unpaired electron to delocalise over the nonbonding orbitals of the α-substituents. Isomers **13** and **14** are of similar energy as both have the nonbonding orbitals of the α-chloride for the electron to be delocalised into. However, the less stable geminal isomer, **15**, has no α-chlorine and, therefore, cannot delocalise the unpaired electron, which is then localised on the carbon alone.

The same relative order of stability is also predicted for closed shell products **16-18.** The calculated barrier for interconversion of the two 1,2-dichlorinated vinyl radicals lies between approximately 30-40 $kJmol^{-1}$, depending on the level of theory. Since the energy needed for interconversion between the radicals **13** and **14** is higher than that required for hydrogen abstraction, the mechanism of formation of the radicals will be the key factor in product distribution, as once formed, the radical is more likely, based on energy considerations, to abstract a hydrogen than to convert to the other radical isomer.

Computational stereochemical analysis shows that organocobalt intermediate **B** is more stable than **A** due to the sterics of addition, where the cobaloxime species adds to the least hindered carbon, giving **B** as the anti-Markovnikov product. For this reason, very little geminal DCE is observed.

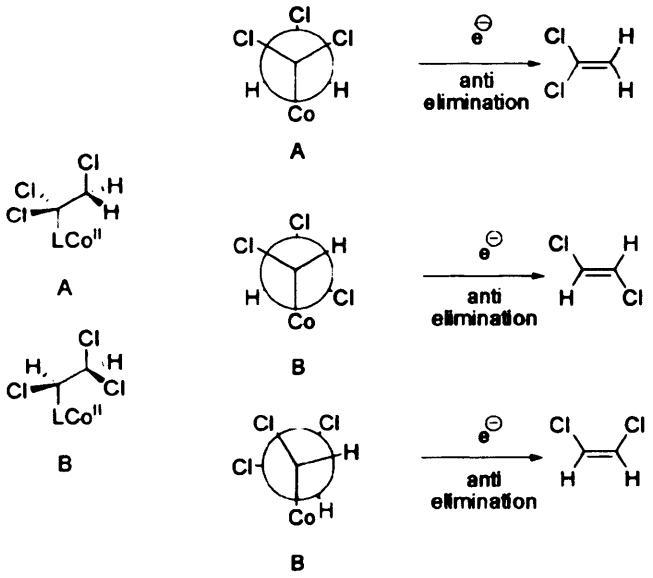

Figure 3.1. Elimination of chloride from trichloroethylcobalamin intermediates.

The Newman projections depicted in **Figure 3.1** show the arrangements needed for the anti-periplanar eliminations of a β-chloride. Calculations showed[3] that the staggered conformation has the largest interaction between the corrin ring and the chloride, whereas the eclipsed conformation, where the Cl-Cl are syn-periplanar overlapping, was calculated to be of lower energy, and so the favoured conformation for the elimination. For this reason, *cis*-DCE is the favoured isomer from the reduction of TCE to DCE.

3.1.1.3. The conversion from DCE to VC.

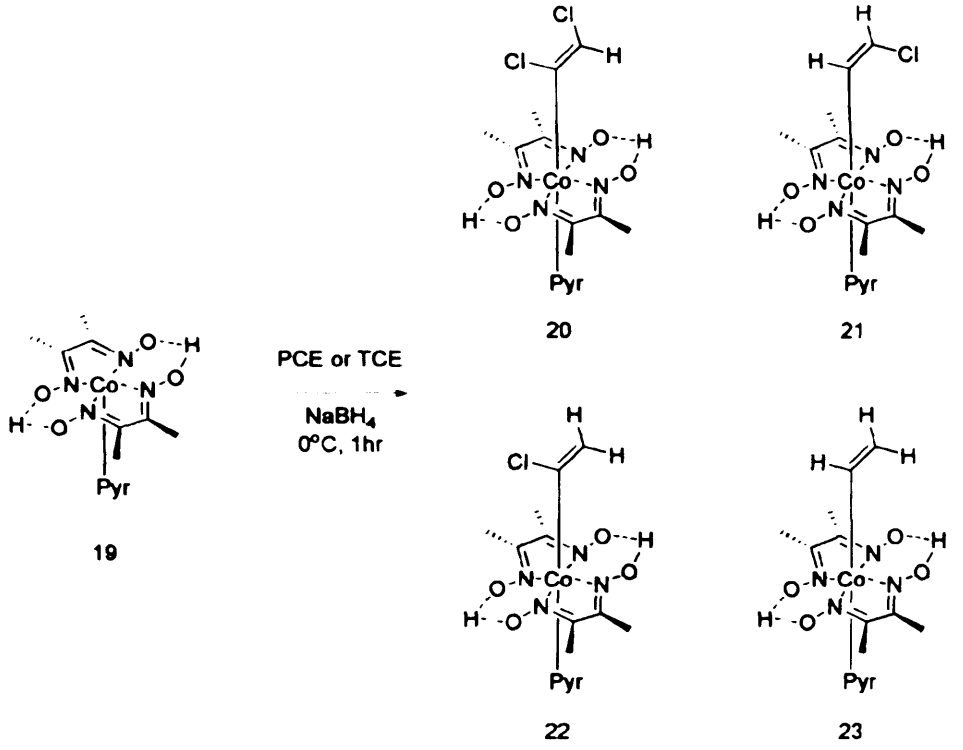

Scheme 3.5. Organocobaloxime species observed upon reduction of PCE and TCE.

Addition of $[Co^{I}(DMGH)_2Pyr]$ **19**, reduced in situ, with PCE or TCE generated the various chlorinated cobaloximes depicted in **Scheme 3.5**. Further studies showed that in the presence of the Co(I) catalyst, **19**, and a sacrificial reductant $NaBH_4$, dichlorovinylcobaloxime **20** could be converted into monochlorovinyl cobaloximes **21** and **22**, which is in turn reduced to vinylcobaloxime **23**. Based on UV-visible absorbance data,[5,6] mass spectrometry data[7] and kinetic data,[8] organometallic intermediates have also been proposed in the dechlorination of *cis*- and *trans*-dichloroethylenes. The reaction of low-valent metal complexes with halogenated ethylenes results in the formation of chlorovinyl complexes.[9] As it was unknown whether they are the final products of the reaction or potentially active intermediates, van der Donk synthesised several chlorinated alkenylcobalamins to study this, **20-23**.

To test whether the dichlorovinylcobaloximes could be converted into the monochlorovinylcobaloxime, **20** was treated with both sodium borohydride and H_2. In each case, no reduction was observed, and so it was deduced that the dichlorovinylcobaloximes are inert to these conditions. However, in the presence of a

reducing agent and a catalytic amount of dimeric $[Co^{II}(DMGH)_2Pyr]_2$ (**24**), **20** was consumed, generating **21** and **22**. When a stoichiometric amount of **24** was added, **20** was dechlorinated to give **21** and **22**, eventually yielding **23** alone, showing that these organocobalt species are active intermediates in the dechlorination reaction, and not inert end products.

The conversion from **20** to **21** can occur via either cleavage of Co-C, or with chloride elimination taking place on the cobaloxime, without the cleavage. To study this, van der Donk employed a series of ligand exchange experiments, depicted in **Scheme 3.6**, to determine whether the Co-C bond undergoes cleavage. Cobaloxime **25** was reacted with one equivalent of the reducing agent **24** under H_2, and produced **21**. The analogous reaction of **20** with the alternative reducing agent **26** gave the crossed over product **27**. In both cases, the observed transfer of the chloroethene moiety from the starting material, **25** and **20,** to the cobaloxime acting as a reducing agent, **24** and **26**, is consistent with Co-C cleavage.

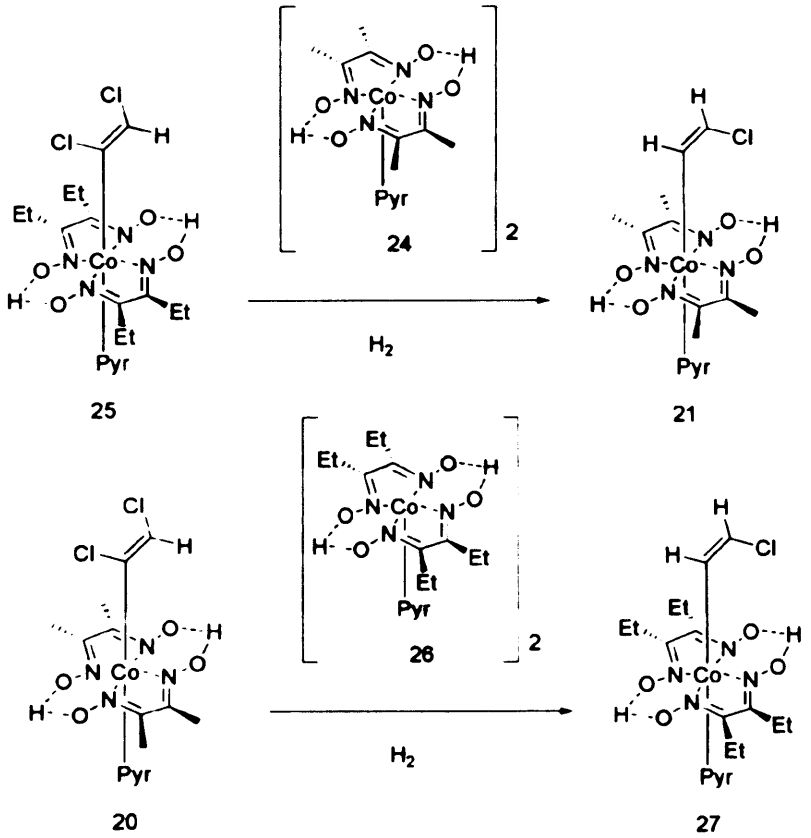

Scheme 3.6. Ligand exchange experiments demonstrating the Co-C cleavage upon reduction.

The two possible routes for Co-C bond cleavage are depicted in **Scheme 3.7**. The homo- or heterolytic scission of Co-C bond followed by hydrogen or proton transfer would result in *cis*-dichloroethenylcobaloxime (pathway **F**). The subsequent reaction of *cis*-DCE with cob(I)aloxime via addition-elimination, with stereochemistry retained, would give **21**. However, studies showed that **F** is unfeasible, as the reaction between 1,2-*cis* DCE and cob(I)aloxime did not yield any detectable monochlorinated ethynylcobaloximes.

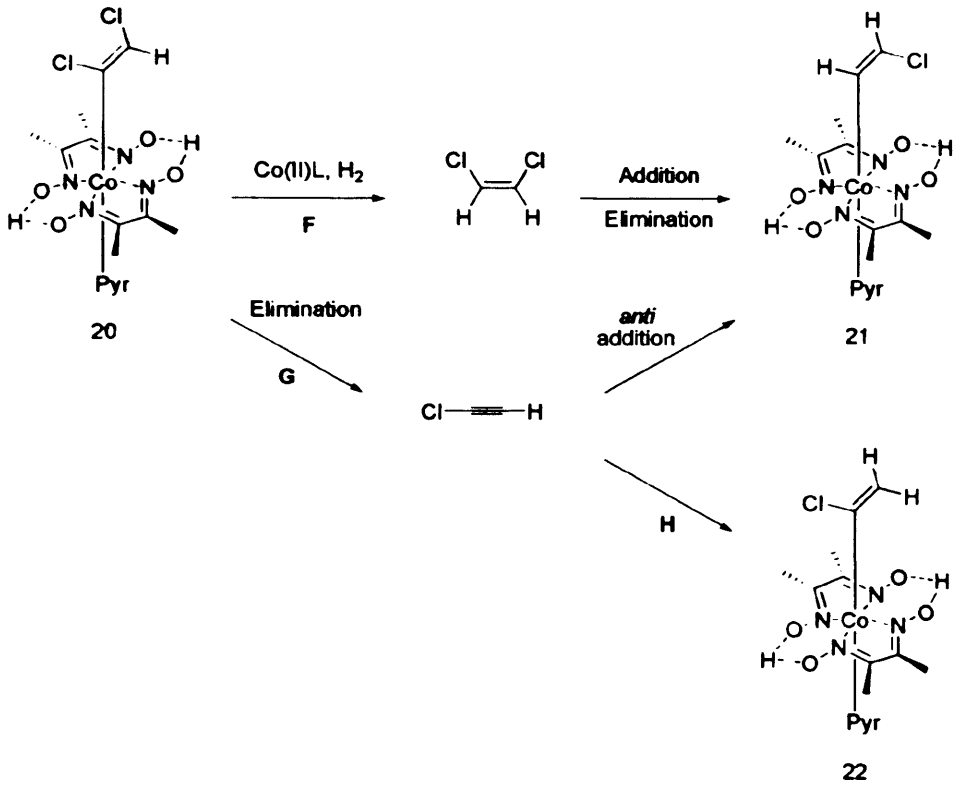

Scheme 3.7. Mechanisms for the reduction of dichlorovinylcobaloxime to chlorovinylcobaloxime.

Burris[10] and Semadeni[11] both indicated that the acetylene produced in the dechlorination of TCE is derived from chloroacetylene, suggesting that the organometallic (*cis*-dichlorovinyl)cobaloxime may be the precursor to chloroacetylene. Mechanism **G** involves the elimination of chloroacetylene, followed by its addition to the cobaloxime. For this to be viable for the generation of **21** from **20**, the addition must occur with regio- and anti-stereoselectivity. The feasibility of pathway **G** was examined by reaction of cob(I)aloxime with chloroacetylene generated *in situ*, which produced **21** as the minor product and **22** as the major (1:3). Pathway **G** is the most likely route to convert

20 to **21**, and chloroacetylene can also account for the observation of **22** (pathway **H**). The formation of ethynylcobaloxime was not observed in these experiments, similarly to the absence of ethynylcobalamin formation in B_{12}-catalysed dechlorination of PCE and TCE.[7]

There are two possible mechanisms for the Co-C cleavage of chlorovinyl organometallic intermediates, both involving a one-electron reduction. **Scheme 3.8** depicts the two routes for loss of cobaloxime; Pathway **I** shows production of a radical,[7] and pathway **J** shows the anion.[12] That chloroacetylene is detected during the experiment, provides evidence of the anion, as chlorine elimination from the radical species has been calculated as unfavourable.[13] When radical traps were introduced to the system, no effect on product distribution was observed, but on addition of anion traps, *cis*-DCE observed as a product of reduction, hence indicating the presence of a chlorovinyl anion. However, it is unknown whether the anion is produced directly or indirectly through the further reduction of the chloroalkenyl radical, due to the kinetic constraints of the experiment.

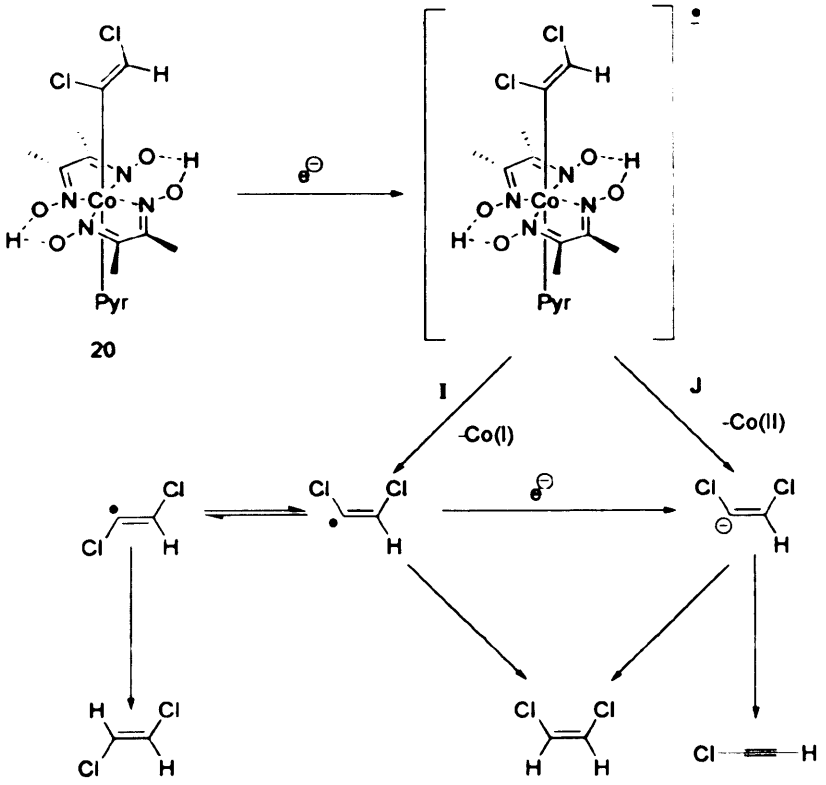

Scheme 3.8. Mechanisms for the loss of DCE.

3.1.1.4. The conversion from Chlorovinylcobaloxime to Vinylcobaloxime.

With regards to the formation of **23**, submitting either **21** or **22** to the reductive conditions induced slow consumption of the starting complexes and formation of vinylcobaloxime **23**.

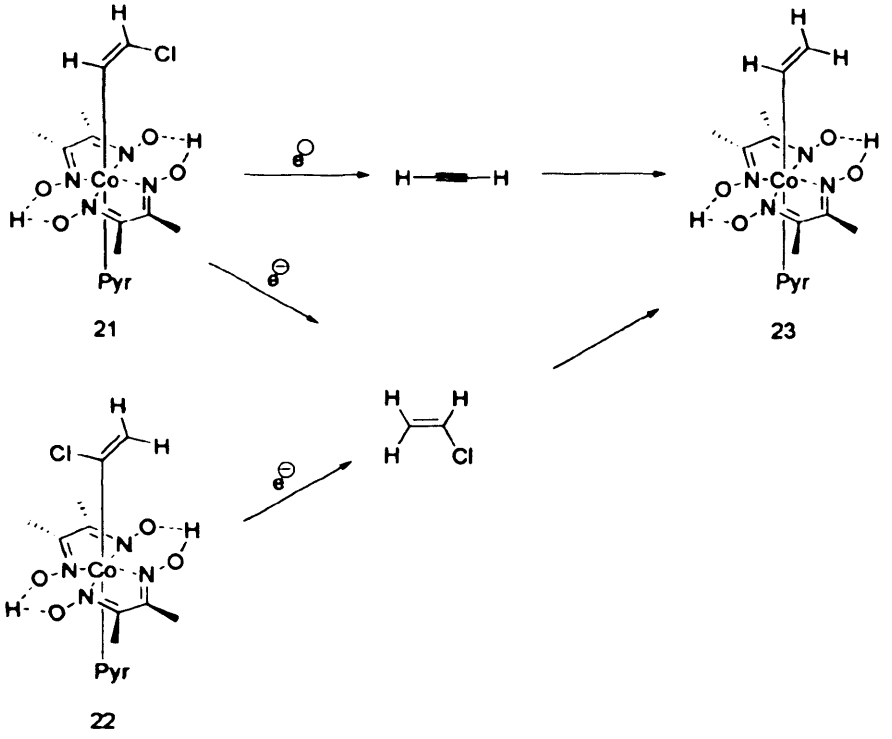

Scheme 3.9. The reduction of Chlorovinylcobaloxime to vinylcobaloxime.

The mechanism of the reductive dechlorination of *cis*-chlorovinylcobalamin involves the formation of acetylene, by elimination of the β-chloride upon reduction of the organocobaloxime. This reductive dealkylation is particularly facile for multichlorinated vinylcobaloximes, but not for vinylcobaloxime, as the olefin becomes less electron deficient with each chloride removed.

Reduction of vinylcobalamin cannot follow such a mechanism, and as a result, the one-electron reduced intermediate is remarkably stable due to the strong Co-C bond. If the system is to be truly catalytic, then it is necessary for the vinylcobalamin to be returned to the catalytically active cob(I)alamin state. The resistance of vinyl cobaloxime toward reductive dealkylation prevents the rapid regeneration of the active catalyst, and this presents an obstacle for efficient B_{12}-catalysed reductive dechlorination of chlorinated ethylenes.

3.1.1.5. Summary.

The reductive dechlorination of PCE to vinylcobaloxime proceeds with the stepwise loss of chloride, via TCE, DCE and VC. Electron transfer to the chlorinated olefin initiates the reduction of PCE, but each subsequent step proceeds via an organocobalt species, as the olefin becomes less electron deficient with each chloride removed, and thus electron-transfer pathways become less favourable in the order PCE > TCE > DCE > VC. Upon loss of the final chloride, to potentially give ethene, the vinylcobaloxime produced has been shown to be resistant towards reductive dealkylation, and thus preventing the rapid regeneration of the active catalyst, whereas in *tetrachloroethylene reductase*, reduction to ethene is observed. This vinylcobaloxime stops the catalytic cycle, as the cobaloxime catalyst is now inactive, and will provide an obstacle for efficient vitamin B_{12} inspired catalytic reductive dechlorination of chlorinated ethylenes.

3.1.2 The Role of the Axial Ligand Upon Reduction of Cobaloximes from Co(III) to Co (I).

The role of the axial ligands in cobaloxime and B_{12} mediated reductive dechlorination has been discussed, but not experimentally studied. In a communication by Schrauzer *et al* concerning alkylcobaloximes and their relation to alkylcobalamins such as vitamin B_{12},[14] it was postulated that, upon reduction of alkylcobaloximes, the initial six-coordinate covalency of the octahedral Co(III) centre is lost, with the dissociation of the axial ligands, leaving a square planar four-coordinate Co(I) species. Upon oxidation to a Co(III) species, the cobaloxime returns to the initial six coordinate octahedral geometry, as shown in **Scheme 3.10**.

This loss, followed by re-association of the axial ligands, may not be ideal if high turnover frequency and stable catalysts are to be achieved, particularly if the secondary metal centre is contained in an axial ligand. As no experimental evidence has been found in support of, or against, the reduction step proceeding via a four-coordinate intermediate, a series of ligand exchange experiments were designed to study the covalency of the intermediate. Alkylation of pyridyl (chloro)cobaloximes

[ClCo(DMGH)$_2$(Pyr)], is a known reaction, where the cobaloxime is reduced from Co(III) to Co(I), to form the reactive cobaloxime nucleophile, which then reacts with halogenoalkane, for example iodoethane, forming the pyridyl (alkyl)cobaloxime [EtCo(DMGH)$_2$(Pyr)]. To determine whether the reaction intermediate is four- or six-coordinate, a secondary distinct pyridine species, such as 3-bromopyridine, can be introduced to the reaction.

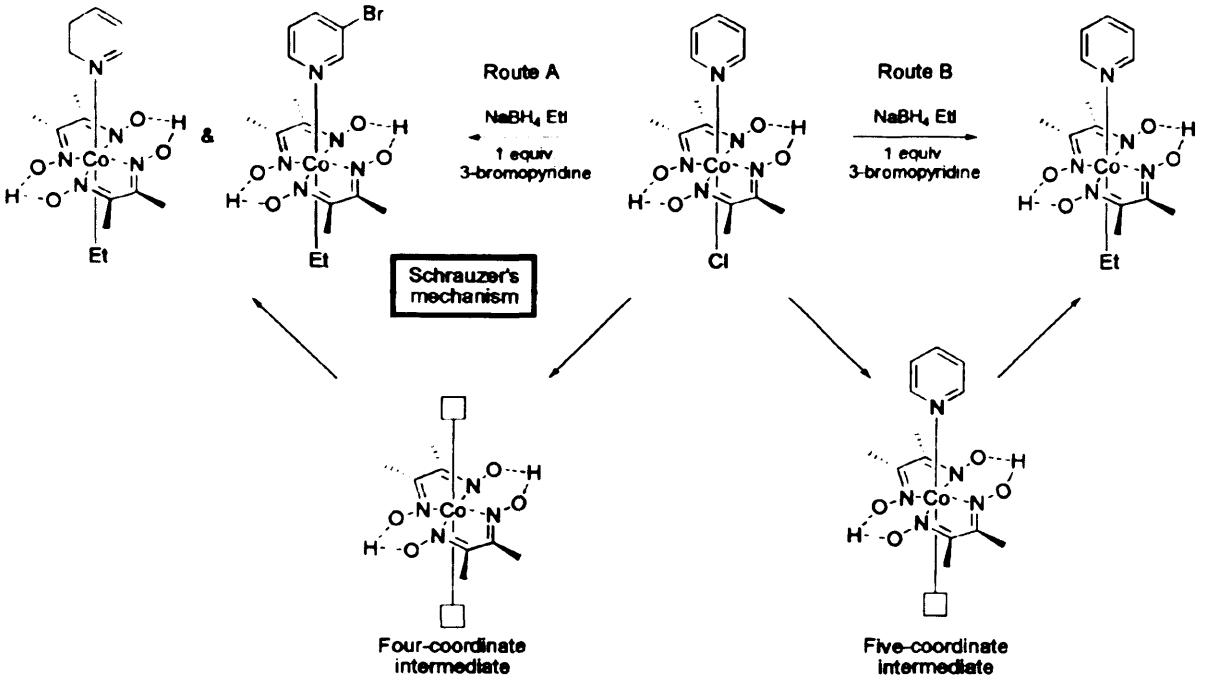

Scheme 3.10. Two possible intermediates from the ligand exchange experiments.

If Schrauzer is correct, route A, and the reaction does proceed via a four-coordinate intermediate [Co(DMGH)$_2$(vacant)$_2$], the organocobaloxime resulting from alkylation [EtCo(DMGH)$_2$(vacant)] will react to complete its coordination sphere with a pyridine. As there are two pyridyl species- the dissociated pyridine and the free 3-bromopyridine-competing in solution, there will be two products observed, one being the alkylated analogue of the starting material [EtCo(DMGH)$_2$(Pyr)], and the other being the crossed-over product [EtCo(DMGH)$_2$(3-bromopyr)] where the Co(III) species has completed its coordination sphere with the free 3-bromopyridine ligand, i.e. the ligands have exchanged. However, if Schrauzer is incorrect, and the intermediate does not proceed via a four coordinate species, as is shown in Route B, then only one product will be observed, which is the alkylated analogue of the starting material [EtCo(DMGH)$_2$(Pyr)].

The coordination number of the reactive Co(I) intermediate will be a major factor in the catalyst design and activity. High turnover numbers and general catalyst stability may be compromised if the axial ligand bearing the secondary, redox active metal centre is continually dissociating from, and re-coordinating to the cobalt centre during the catalytic cycle. The work undertaken in this chapter examines the covalency of the Co^{I} intermediate by means of a series of ligand exchange experiments.

3.2 Results and discussion.

3.2.1 Synthesis, Physical and Structural Properties.

In order to investigate the coordination number of the reduced Co(I) intermediate, a series of simple pyridyl cobaloximes were first synthesised following the preparation by Schrauzer. Upon addition of a solution of cobalt(II) dichloride to a warmed solution of dimethylglyoxime (DMGH), the magenta Co(II) species is oxidised by air to the green Co(III) species, dichloride (dimethylglyoximato-κ^2N,N`)-(dimethylglyoxime-$\kappa^2$N,N`) cobalt(III), $[Cl_2Co(DMGH)(DMGH_2)]$, which precipitated out as a crystalline solid in a near quantitative yield, 99 %. The addition of aqueous sodium bicarbonate to a dichloromethane suspension of $[Cl_2Co(DMGH)(DMGH_2)]$ and the desired pyridine in a three phase system, as demonstrated in **Scheme 3.11**, yielded the crude cobaloximes. These were then purified by washing the cobaloxime products into the organic phase, drying *in vacuo*, resulting in brown crystalline solids of **3.1** and **3.2** in good yields; 89 % and 93 % respectively.

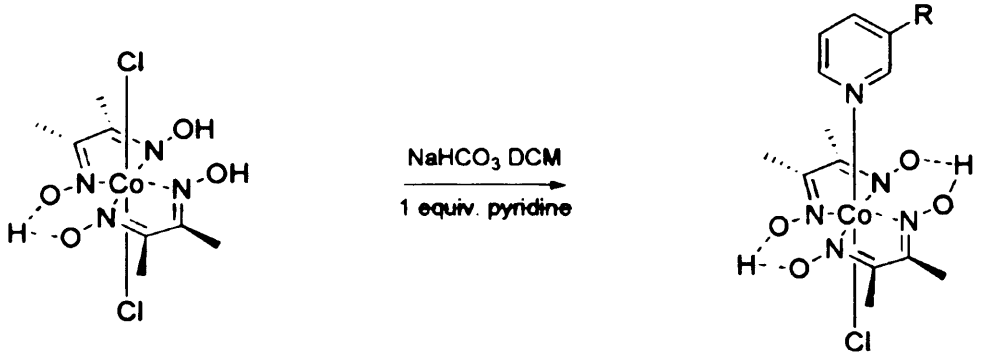

R = H (**3.1**), Br (**3.2**)

Scheme 3.11. Synthesis of chloropyridylcobaloximes.

The alkylation of these cobaloximes, **Scheme 3.12**, was carried out in a manner similar to that described by Gupta,[15] by reduction of a methanolic solution of either [ClCo(DMGH)$_2$(Pyr)], **3.1**, or [ClCo(DMGH)$_2$(3-Bromopyr)], **3.2**, in the presence of the desired alkyliodide. On addition of sodium borohydride to these methanolic solutions, the dark brown colour gave way to the blue-green colour associated with Co(I) species, followed by effervescence (H_2), before the solution returned to a red-brown colour of a Co(III) cobaloxime. These alkylated cobaloximes were then easily separated from the sodium iodide by-product, by extracting the cobaloxime into an organic solvent, typically dichloromethane, which yielded the methylated species [MeCo(DMGH)$_2$(Pyr)], **3.3**, and [MeCo(DMGH)$_2$(3-Bromopyr)], **3.4**, and the ethylated species [EtCo(DMGH)$_2$(Pyr)], **3.5**, and [EtCo(DMGH)$_2$(3-Bromopyr)], **3.6**, as brown crystalline solids in good yields, 93 %, 95 %, 89 % and 91 % respectively.

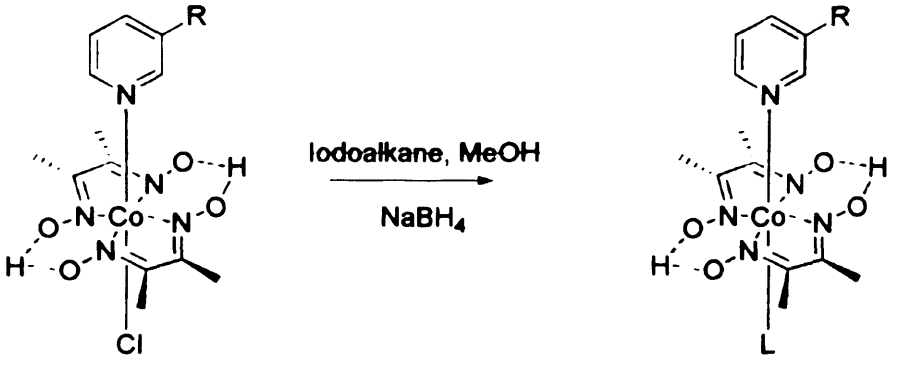

R = H, L = Me (**3.3**)
R = Br, L = Me (**3.4**)
R = H, L = Et (**3.5**)
R = Br, L = Et (**3.6**)

Scheme 3.12. Alkylation of chloropyridylcobaloximes.

The presence of a coordinated ethyl group was confirmed by the observation of a triplet resonance corresponding to the CH_3 moeity *ca.* 0.38 ppm. This unusually high field shifting is due to the highly delocalised π–electron system of the equatorial ligands creating a ring current, which shields the methyl group, causing the resonance to occur at a frequency lower than is typical for a methyl moiety in an ethyl group.

	NMR Shift		
Cobaloxime	DMGH	α-CH_x	β-CH_x
3.1	2.45	N/A	N/A
3.3	2.12	0.78	N/A
3.5	2.13	1.74	0.30

Table 3.1. Relative positions of aliphatic resonances.

The aromatic regions of the ^{1}H-NMR spectra are of greater interest in the ligand exchange experiments than the aliphatic region, depicted in **Figure 3.2**, as the methyl and ethyl resonances overlap, whereas the aromatic resonances, shown in **Figures 3.3** and **3.4**, are distinct, and characteristic of the observed products.

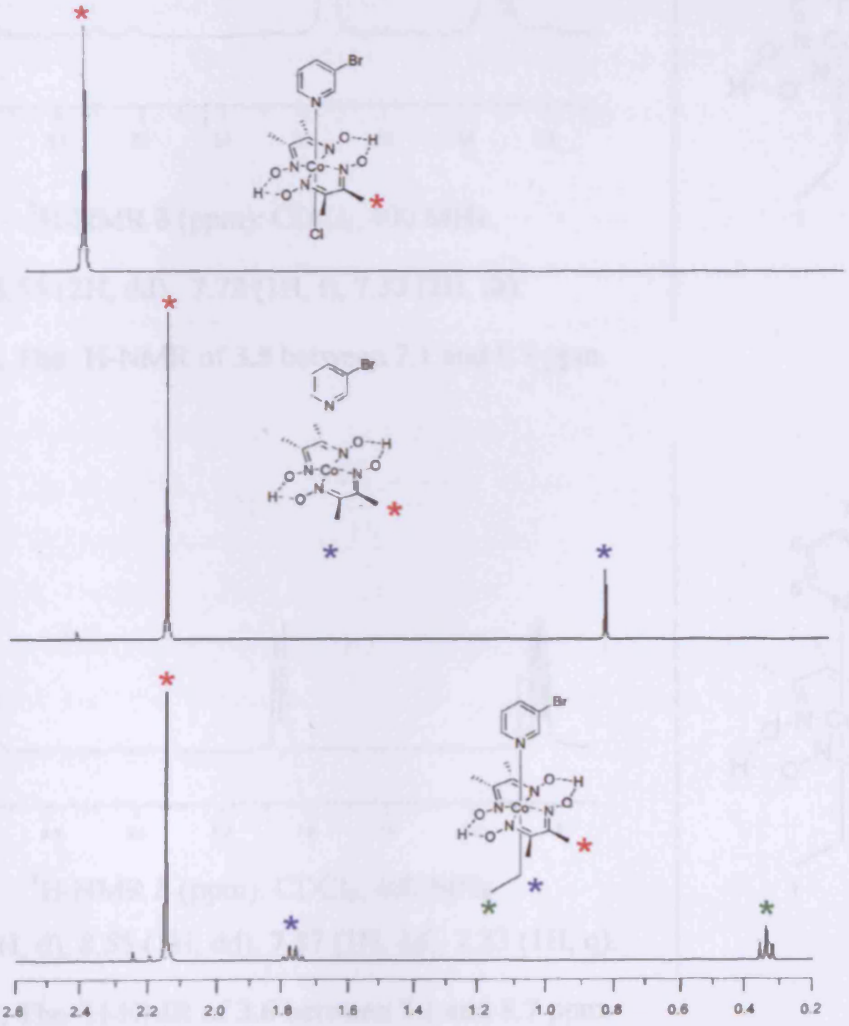

Figure 3.2. Characteristic resonances of Co coordinated alkyl groups, recorded at 400 MHz in $CDCl_3$.

The change in the moiety *trans* to the pyridine species has an effect on the equatorial DMGH ligands. The chloride species is considered to be electron withdrawing, which results in electron density being removed from the macrocycle. However, the alkyl groups are more electron donating, hence there is more electron density in the macrocycle ring, resulting in the methyl group of the DMGH ligands being more shielded and so the resonance is observed at a lower frequency.

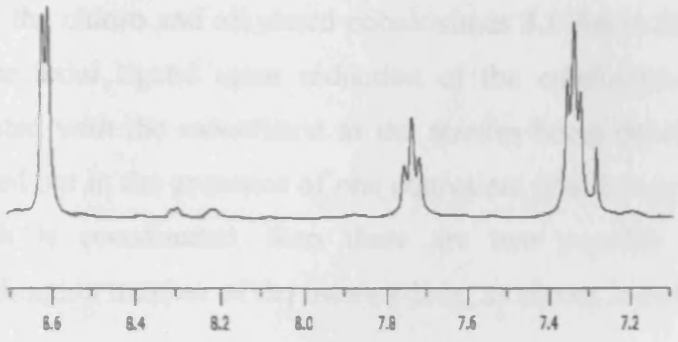

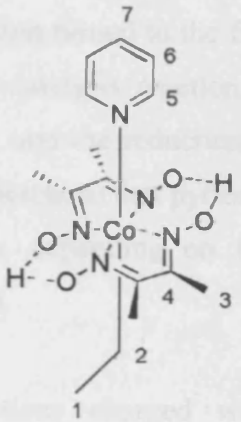

^{1}H-NMR δ (ppm): $CDCl_3$, 400 MHz

8.55 (2H, dd), 7.72 (1H, t), 7.33 (2H, dt).

Figure 3.3. The ^{1}H-NMR of **3.5** between 7.1 and 8.7 ppm.

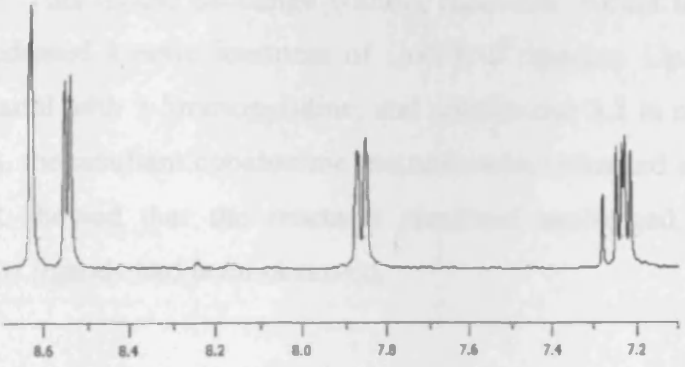

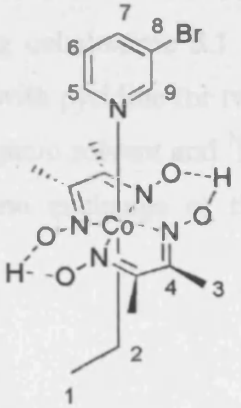

^{1}H-NMR δ (ppm): $CDCl_3$, 400 MHz

8.64 (1H, d), 8.55 (1H, dd), 7.87 (1H, dd), 7.23 (1H, q).

Figure 3.4. The ^{1}H-NMR of **3.6** between 7.1 and 8.7 ppm.

The distinct triplet of triplets at 7.72 ppm corresponding to the C-7 hydrogen of the $[EtCo(DMGH)_2(Pyr)]$ and the doublet of doublets at 7.87 ppm corresponding to the C-7

hydrogen of the [EtCo(DMGH)$_2$(3-Bromopyr)] are both resonances indicative of single hydrogens. The presence of either or both of these resonances in the ^{1}H-NMR of the ligand exchange experiments will unequivocally show whether crossover of the pyridyl ligands has occurred. The integrations of these resonances will give the ratio of the products.

3.2.2. Ligand Exchange Experiments with Simple Cobaloximes.

With the chloro and alkylated cobaloximes **3.1-3.6** in hand, attention turned to the fate of the axial ligand upon reduction of the cobaloximes. If the catalysis reaction is imitated with the iodoalkane as the species being dehalogenated, and the reduction is carried out in the presence of one equivalent of a free pyridine different to that pyridine which is coordinated, then there are two possible outcomes, depending on the coordination number of the intermediate, as shown in **Scheme 3.10**.

Initially blank reactions, **Scheme 3.13**, in methanolic solutions charged with [ClCo(DMGH)$_2$(3-Bromopyr)], one equivalent of both pyridine and iodoethane, in the absence of the reducing agent, sodium borohydride, were undertaken. This was to show that no displacement of the pyridyl ligands occurred when the cobaloxime was in solution and hence any exchange of ligands will be due to the reduction of Co(III) to Co(I). This ligand exchange without reduction, would be unexpected due to the well precedented kinetic inertness of Co(III) d^6 species. Upon stirring cobaloxime **3.1** in methanol with 3-bromopyridine, and cobaloxime **3.2** in methanol with pyridine for two hours, the resultant cobaloxime mixtures were extracted into an organic solvent and ^{1}H-NMR showed that the reactants remained unchanged. Hence, no exchange of the pyridyl ligands had been observed.

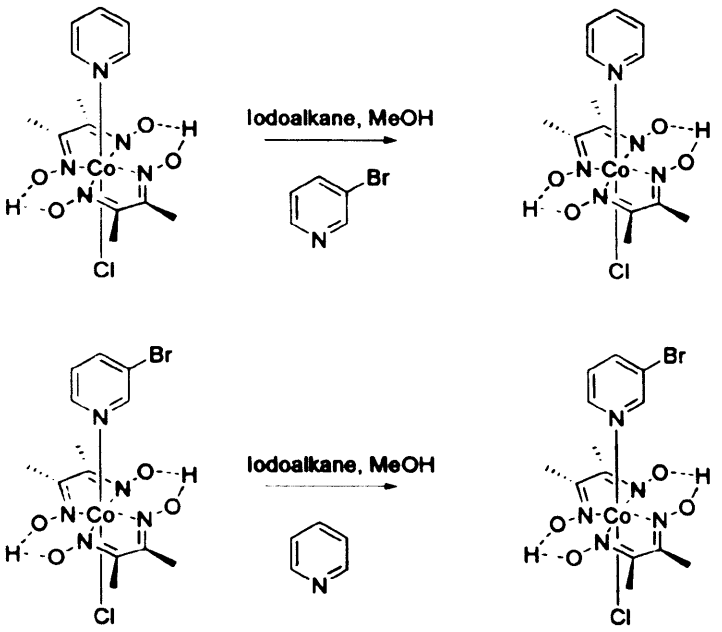

Scheme 3.13. No ligand exchange or alkylation observed without reduction.

On repeating these reactions with sodium borohydride (1 mol equivalent) added, the red-brown solution of the cobaloxime turned the blue-grey colour associated with the presence of Co(I), followed by effervescence. The reactions were stirred for one hour, at which point the solvent was removed *in vacuo*, and the resultant cobaloxime extracted into an organic solvent. The solvent was then removed *in vacuo*, yielding a brown crystalline powder; ^{1}H-NMR studies of which showed ethylation had occurred, due to the resonance observed *ca.* 0.38 ppm, corresponding to the CH_3 group of an ethyl moiety coordinated to the cobalt centre. The results of the ligand exchange experiments carried out on [ClCo(DMGH)$_2$(Pyr)] and [ClCo(DMGH)$_2$(3-Bromopyr)] are shown in **Table 3.2**, and the ^{1}H-NMR spectra are shown in **Figures 3.5** and **3.6** respectively.

Entry	Starting Cobaloxime	Free pyridine	Ethylated Product	Ligand exchange Product	Ratio
1	**3.1**	3-Bromopyridine	**3.3**	**3.6**	38 : 62
2	**3.4**	Pyridine	**3.6**	**3.3**	37 : 63

Table 3.2. The degree of ligand exchange observed. Ratio is the average from 3 runs.

Further examination of the spectra showed both a doublet of triplets at 7.72 ppm, and a doublet of doublets at 7.87 ppm corresponding to C*H* (7) of [EtCo(DMGH)$_2$(Pyr)] and C*H* (7) of [EtCo(DMGH)$_2$(3-Bromopyr)] respectively, indicating exchange of the pyridyl ligands had occurred in each reaction. Consequently, it can be deduced that

upon reduction from Co(III) to Co(I), cobaloximes go through a four-coordinate intermediate, as both axial ligands are exchanged, and only the DMGH ligands remain the same. It is possible for some of the reaction to proceed via a five-coordinate intermediate as well, but this is unlikely, as the reduced intermediate, $[Co(I)(DMGH)_2(vacant)_2]$, is an example of a low spin, 16 electron, d^8 species, which, in accordance with Ligand Field Theory,[c] adopts a square planar geometry. This is due to the loss of the two axial ligands, which results in the stabilisation of the d_z^2 and (to a lesser extent) d_{zx} and d_{zy} orbitals. Conversely $d_{x^2-y^2}$ is destabilised as it now takes the majority of the metal-ligand bonding. The $[Co(I)(DMGH)_2(vacant)_2]$ intermediate is comparable to the electronically and structurally similar Wilkinson's catalyst $[ClRh(PPh_3)_3]$.[16]

Interestingly, there is a greater amount of the alkylated cobaloxime corresponding to the free pyridine than there is of the alkylated starting material, approximately 3:2 in each case. Since both reactions favour product from the coordination of the free pyridine from solution, then there is no selectivity of one pyridine over the other, based on their chemistry, as this would result in the same ethylcobaloxime product favoured in each experiment.

Statistically, since the cobaloxime ($Co\text{-}Pyr_{coord}$) and the free pyridine (Pyr_{free}) are equimolar in the reaction, prior to the addition of the sodium borohydride, $[Co\text{-}Pyr_{coord}]$ is equal to $[Pyr_{free}]$. On addition of the reducing agent, initially there will be a far greater concentration of the free Pyr_{free} present in solution, than there is of the Pyr_{coord} that has been lost from the cobaloxime, hence the four-coordinate cobaloxime will preferentially be trapped by the coordination of Pyr_{free}. As the reaction proceeds, however, the ratio of the concentrations of the displaced Pyr_{coord} to Pyr_{free} in solution begins to equilibrate, hence the probability of coordination of Pyr_{coord} increases, whilst the probability of Pyr_{free} coordinating decreases. At some point in the reaction, the probabilities of coordination will be equal, and from then on each will coordinate at similar rates. However by this point, the excess concentration of Pyr_{free} at the start of the reaction will have been sufficient to provide an excess of the product where the ligands have been

[c] A model that describes the bonding, orbital arrangement and electronic structure of transition metal compounds.

exchanged over the ethylated starting material. For this reason, more $[EtCo(DMGH)_2(Pyr_{free})]$ is yielded than $[EtCo(DMGH)_2(Pyr_{coord})]$ and ultimately, a preference of coordination of Pyr_{free} over the dissociated Pyr_{coord}, is observed.

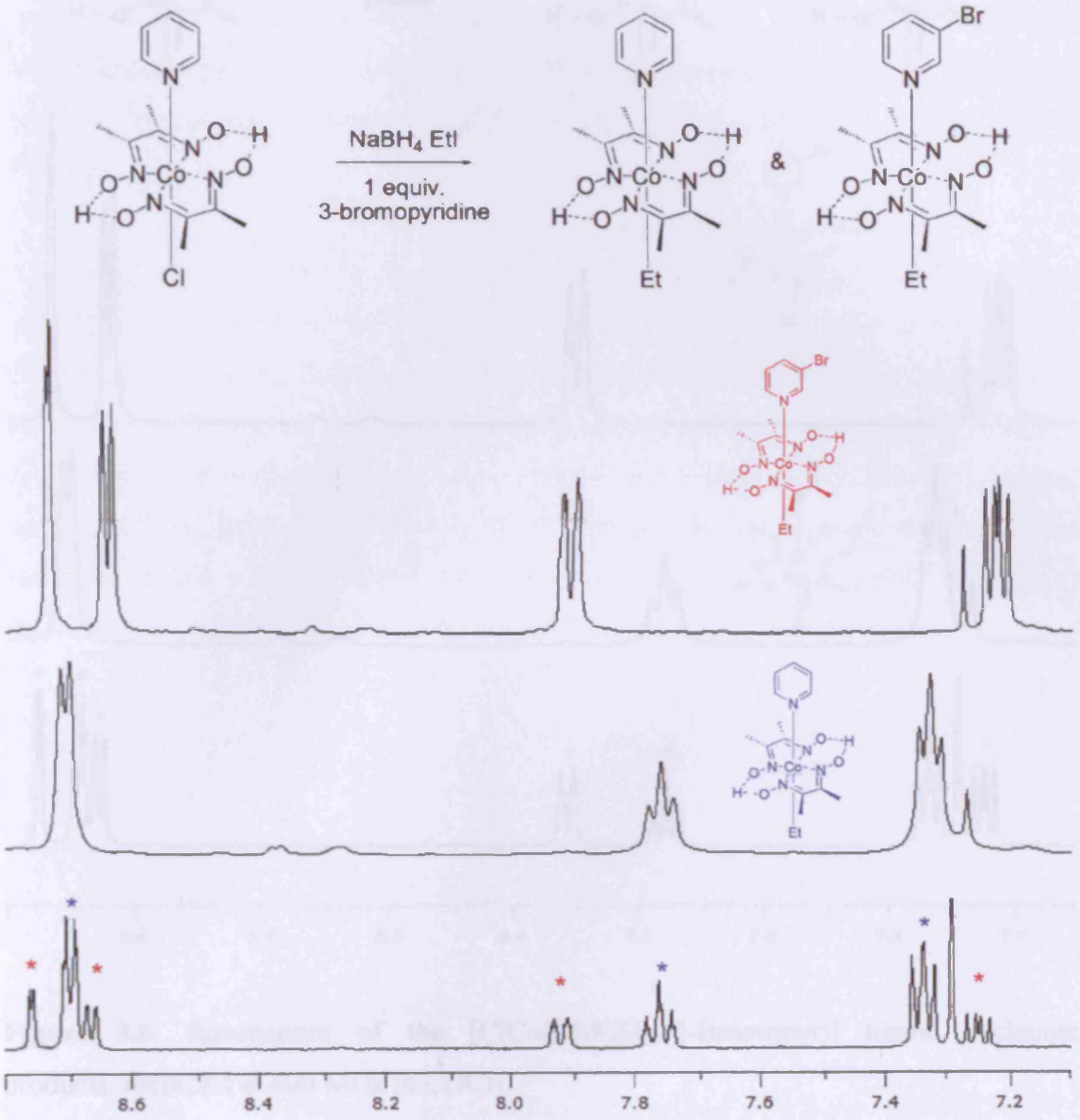

Figure 3.5. Resonances of the $[ClCo(DMGH)_2(Pyr)]$ ligand exchange products, recorded at 400 MHz in $CDCl_3$.

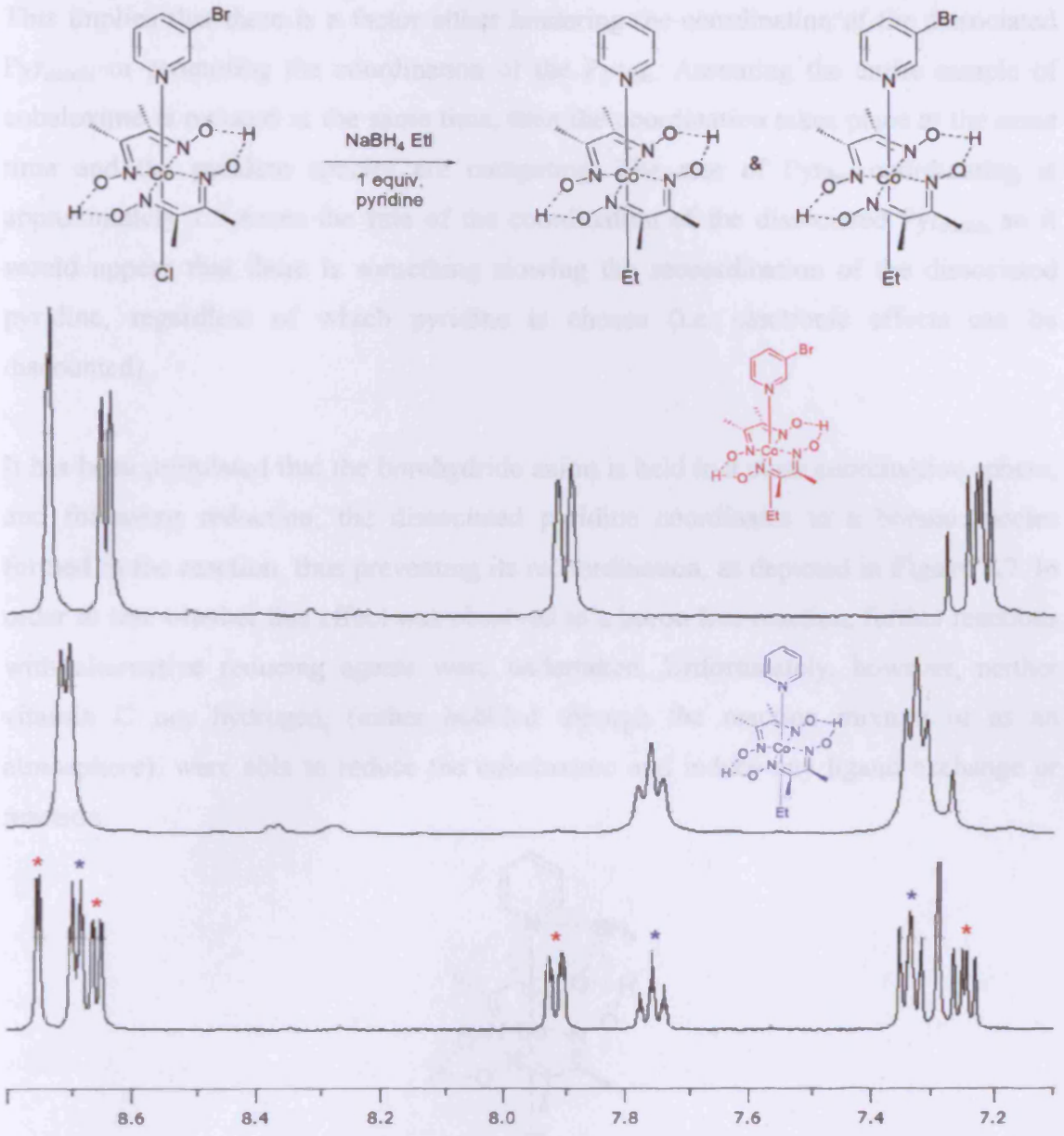

Figure 3.6. Resonances of the [ClCo(DMGH)$_2$(3-Bromopyr)] ligand exchange products, recorded at 400 MHz in $CDCl_3$.

However, this assumes that all the reaction steps are simultaneously occurring in the mixture, whereas it is likely that the initial addition of borohydride reduces all the cobaloxime to Co(I) in a single step, followed by subsequent alkylation. If all the cobaloxime is reduced simultaneously, then according to the model, all the cobaloxime will be four-coordinate (as there is no chlorocobaloxime observed in the ^{1}H-NMR, therefore all of the cobaloxime is reduced).

This implies that there is a factor either hindering the coordination of the dissociated Pyr_{coord}, or promoting the coordination of the Pyr_{free}. Assuming the entire sample of cobaloxime is reduced at the same time, then the coordination takes place at the same time and the pyridine species are competing. The rate of Pyr_{free} coordinating is approximately 1.5 times the rate of the coordination of the dissociated Pyr_{coord}, so it would appear that there is something slowing the recoordination of the dissociated pyridine, regardless of which pyridine is chosen (i.e. electronic effects can be discounted).

It has been postulated that the borohydride anion is held in a close coordination sphere, and following reduction, the dissociated pyridine coordinates to a borane species formed in the reaction, thus preventing its recoordination, as depicted in **Figure 3.7**. In order to test whether this effect was observed in a boron free reaction, further reactions with alternative reducing agents were undertaken. Unfortunately, however, neither vitamin C nor hydrogen, (either bubbled through the reaction mixture or as an atmosphere), were able to reduce the cobaloxime and induce any ligand exchange or reaction.

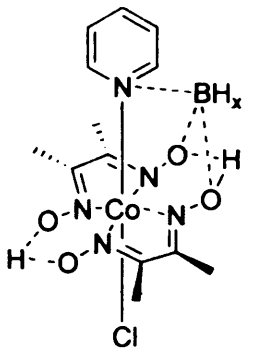

Figure 3.7. Postulated borane coordinated cobaloxime intermediate.

The reduction of methanolic solutions of $[ClCo(DMGH)_2(3\text{-Bromopyr})]$ and of $[ClCo(DMGH)_2(Pyr)]$, each in the presence of one equivalent of both iodomethane and iodoethane, gave almost exclusively the methylated products **3.3** and **3.4**, as shown in **Scheme 3.14**. A triplet resonance *ca.* 0.38 ppm corresponding to the ethylated products was observed in both spectra, indicating that less than 10 % of the starting material had been ethylated in each reactions. Hence, there is a preference for methylation over ethylation, which can be rationalised by the fact that the halocarbon of iodoethane is much less electrophillic than that of iodomethane, due to the inductive effects of the

methyl group. There is also a second factor, that of steric hindrance, which impedes the approach of the nucleophilic cobaloxime, whereas the iodomethane is more susceptible to nucleophilic attack. Hence, the chemistry of the pyridine species *trans-* to the chloride causes little or no effect on alkyl selection and so confirming that the chemistry of the pyridine ligand has no influence on the outcome of the ligand exchange experiments.

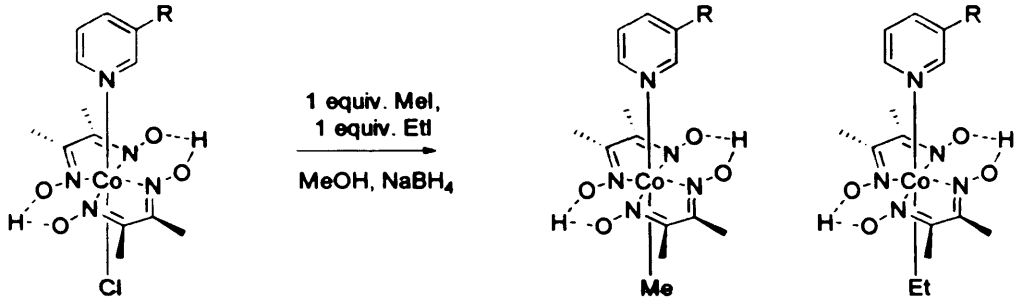

R = H (3.1)
R = Br (3.2)

R = H (3.3)
R = Br (3.4)

R = H (3.5)
R = Br (3.6)

Scheme 3.14. Reduction of cobaloximes **3.1** and **3.2** in the presence of EtI and MeI.

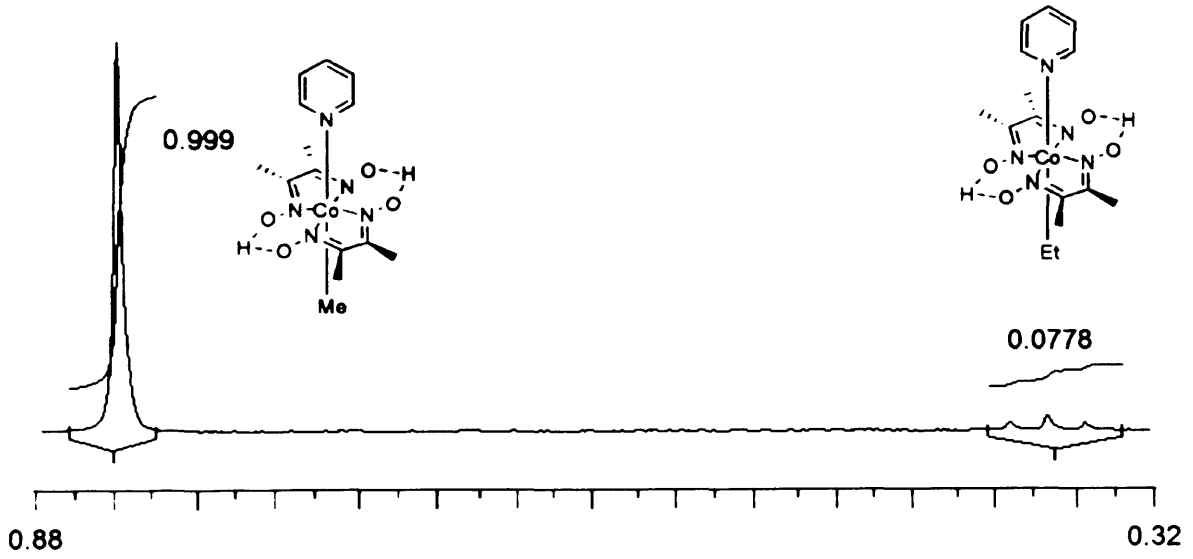

Figure 3.8. The selectivity of methylation over ethylation.

CH_3 Resonance	Relative Integration	% of product
3.5	0.078	**7%**
3.3	0.999	93%

Table 3.3. Results of the alkylation experiment on $[ClCo(DMGH)_2(Pyr)]$.

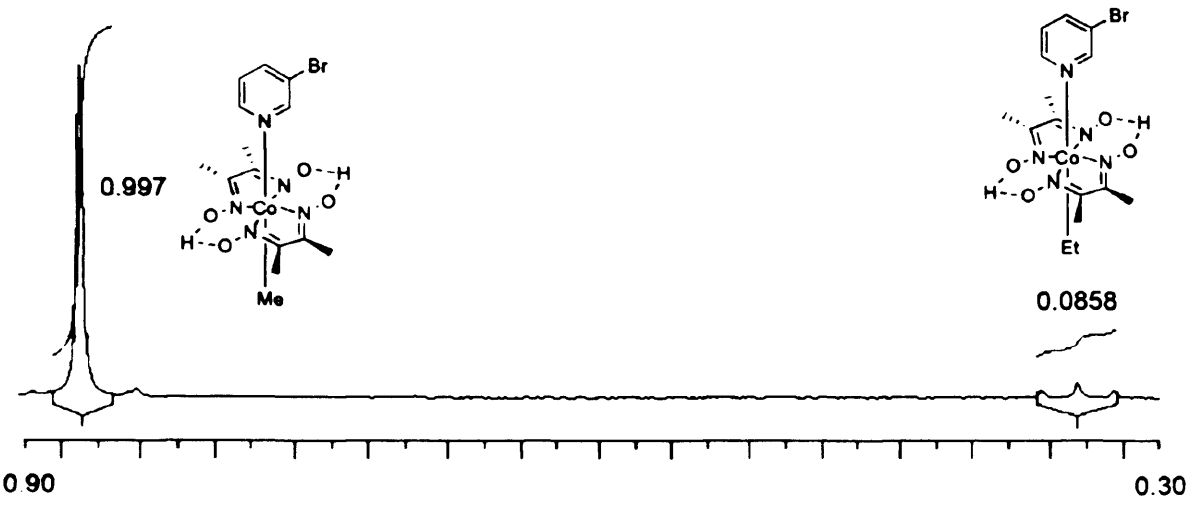

Figure 3.9. The selectivity of methylation over ethylation.

CH_3 Resonance	Relative Integration	% of product
3.6	0.086	8%
3.4	0.997	92%

Table 3.4. Results of the alkylation experiment on [ClCo(DMGH)$_2$(3-Bromopyr)].

3.2.3. Ligand Exchange Experiment with Vitamin B_{12}.

A brief investigation of crossover reactions was conducted with vitamin B_{12}, using triphenylphosphine as the free ligand, to see whether the ligand exchange observed upon reduction of cobaloximes was also observed when vitamin B_{12} was reduced. Triphenylphosphine was added in a five-fold excess, as the axial benzimidazole ligand is part of a chelate system, and so the re-coordination of this is entropically favoured. The phosphate ester of the vitamin B_{12} system resonates at 0.27 ppm in the ^{31}P-NMR spectrum. The free triphenylphosphine resonance is observed at approximately -5 ppm, whilst Co coordinated triphenylphosphine resonances are observed between 20 and 30 ppm.[17]

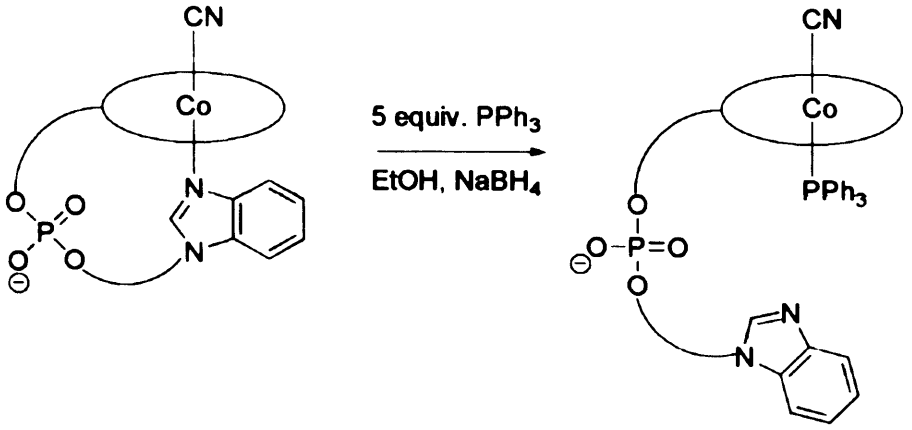

Scheme 3.15. Ligand exchange reaction with cyanocobalamin. (The ellipse represents the corrin ring.)

The control reaction was first undertaken to test whether the benzimidazole ligand disassociated in solution, thus allowing addition of triphenylphosphine, in the absence of a reducing agent. ^{31}P-NMR showed only two peaks present, at 0.27 ppm and -4.53 ppm, attributed to the phosphate ester and the free triphenylphosphine, therefore no exchange of ligand had occurred in solution.

Upon the reduction of a methanolic solution of vitamin B_{12} in the presence of triphenylphosphine with $NaBH_4$, the magenta solution was converted to a dark brown solution, indicative of reduction of the cobalt centre. After 30 minutes, the ^{31}P-NMR spectrum showed resonances at 33.02 ppm, attributed to a cobalt-coordinated triphenylphosphine, whilst the phosphate ester had shifted to 0.95 ppm and the uncoordinated triphenylphosphine resonance was observed at -4.53 ppm. The shift of the resonance due to the phosphate ester from 0.27 ppm to 0.95 ppm indicates that the benzimidazole ligand is no longer coordinated, and it is this ligand that has been replaced by the triphenylphosphine.

In accordance with the evidence from the ligand exchange experiments undertaken on the cobaloximes, it can be deduced that exchange of the ligands has occurred, due to the presence of the coordinated triphenylphosphine peak, and the shifting of the phosphate ester resonance as the benzimidazole moiety is now uncoordinated. Therefore, cyanocobalamin also proceeds with loss of axial ligands when reduced from Co(III) to Co(I).

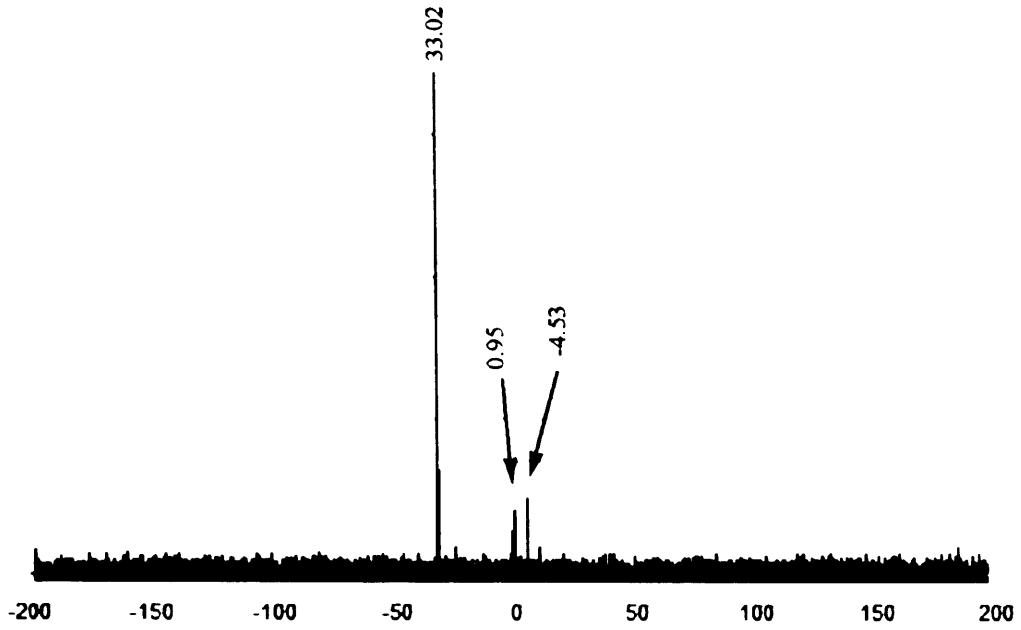

Figure 3.10. $^{31}P\{H\}$-NMR spectrum confirming ligand exchange had occurred when vitamin B_{12} was reduced, recorded at 400 MHz in $CDCl_3$.

3.3 Conclusions.

The observation of exchange of the pyridyl ligands in solution and those coordinated to the cobaloxime demonstrates that, upon reduction of cobaloximes from Co(III) to Co(I), the reduced intermediate is four-coordinate, with both axial ligands lost. This is in accordance with Schrauzer's hypothesis. This process of the axial ligands continually dissociating and re-coordinating will have a major bearing on the catalysis; if the secondary metal centre needed to initiate the reaction is situated in the axial ligand, the turn over number may be affected.

3.4 Experimental.

Dichlorido(dimethylglyoximato-κ^2N,N`)-(dimethylglyoxime-$\kappa^2$N,N`)cobalt(III).[18]

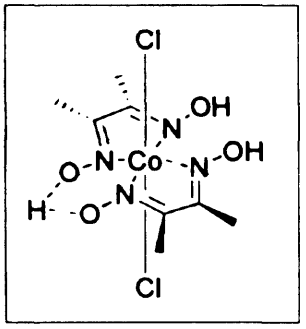

To a solution of $CoCl_2.6H_2O$ (5 g, 21.0 mmol) in acetone (100 ml) was added a warmed solution of dimethylglyoxime (5 g, 43.1 mmol. 2.1 equiv.) in acetone (150 ml). Air was bubbled through the resultant blue mixture and stirred for 20 minutes and then left to stand for 2 hours, yielding green crystals of $[Cl_2Co(DMGH)(DMGH_2)]$, which were filtered off and dried in a desiccator (7.51 g, 99 %). δH ($CDCl_3$) (ppm) 2.11 (12H, s, C*H*$_3$, DMGH)

Pyridylchlorocobaloxime 3.1[19]

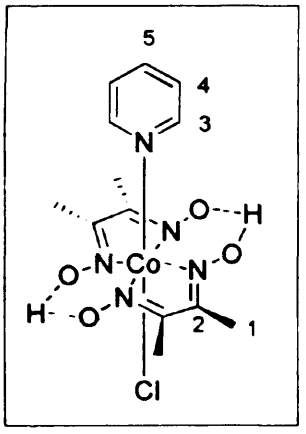

To a stirred suspension of $[Cl_2Co(DMGH)(DMGH_2)]$ (1 g, 2.8 mmol) and pyridine (0.25 ml, 1 equiv., 3.0 mmol) in dichloromethane (10 ml) was added $NaHCO_3$ (10 ml), and allowed to stir at room temperature for 1 hour at which point, the solution was diluted further with dichloromethane (20 ml) and washed with water (2 x 20 ml). The organic fractions were combined, dried over Na_2SO_4, filtered and evaporated to dryness, yielding $[ClCo(DMGH)_2(Pyr)]$ as a brown crystalline solid (0.994 g, 89 %). δH ($CDCl_3$) (ppm) 8.29 (2H, dd, *J* = 5.2, 1.2 Hz, C*H*(3) Pyr), 7.72 (1H, tt, *J* = 7.6, 1.3 Hz, C*H*(5) Pyr), 7.25 (2H, dt, *J* = 7.6, 1.4 Hz, C*H*(4) Pyr), 2.41 (12H, s, C*H*$_3$(1) DMGH). δC 152.6 (*C*' (3), Pyr), 151.1 (*C*' (2) DMGH), 137.4 (*C*' (5) Pyr), 125.7 (*C*' (4) Pyr), 13.1 (*C*H$_3$ (1) DMGH). *m/z* (ESI) 404.2 $[MH]^+$. HRMS (ESI) calculated $[M]^+$ = 404.0536; measured $[M]^+$ = 404.0539.

3-Bromopyridinechlorocobaloxime 3.2

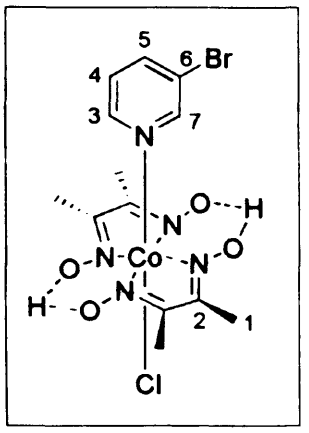

To a stirred suspension of $[Cl_2Co(DMGH)(DMGH_2)]$ (1 g, 2.8 mmol) and 3-bromopyridine (0.29 ml, 3.0 mmol, 1.1 equivs.) in dichloromethane (10 ml) was added $NaHCO_3$ (10 ml), and the mixture was allowed to stir at room temperature for 1 hour at which point, the solution was diluted further with dichloromethane (20 ml) and washed with water (2 x 20 ml). The organic fractions were combined, dried over Na_2SO_4, filtered and evaporated to dryness, yielding $[ClCo(DMGH)_2(3\text{-Bromopyr})]$ as a brown solid (1.24 g, 93 %) δH ($CDCl_3$) (ppm) 8.37 (1H, d, *J* = 1.9 Hz, C*H*(7) Pyr), 8.28 (1H, d, *J* = 5.6 Hz, C*H*(3) Pyr), 7.85 (1H, dd, *J* = 8.1, 1.1 Hz, C*H*(5) Pyr), 7.15 (1H, dq, *J* = 5.8, 1.1 Hz, C*H*(4) Pyr), 2.45 (12H, s, CH_3(1) DMGH). δC 152.9 (*C* (3), Pyr), 152.6 (*C* (7), Pyr), 149.4 (*C* (2), DMGH), 136.9 (*C* (5), Pyr), 126.7 (*C* (4) Pyr), 121.5 (*C* (6), Pyr), 13.2 (CH_3 (1) DMGH), *m/z* (ESI) 492.1 $[MH]^+$. HRMS (ESI) calculated $[MH]^+$ = 481.9641; measured $[MH]^+$ = 481.9637.

Pyridinemethylcobaloxime 3.3[20]

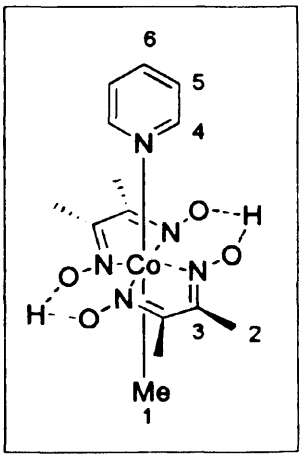

Under an atmosphere of nitrogen, $[ClCo(DMGH)_2(Pyr)]$ (500 mg, 1.24 mmol) was dissolved in methanol (10 ml). To this solution, methyl iodide (0.085 ml, 1.36 mmol, 1.1 equivs.) and $NaBH_4$ (50 mg) were added. The reaction was left to stir for 2 hours, and left to crystallise. The brown solid was filtered off, dissolved in dichloromethane (20 ml) and extracted with distilled water (3 x 20ml). The organic phase was dried and then filtered, evaporated to dryness and $[MeCo(DMGH)_2(Pyr)]$ was isolated as a brown solid (441 mg, 93 %) δH ($CDCl_3$) (ppm) 8.62 (2H, dd, *J* = 6.4, 1.5 Hz, C*H*(4) Pyr), 7.73 (1H, tt, 7.7, 1.5 Hz, C*H*(6) Pyr), 7.34 (2H, dt, J = 6.4, 1.5 Hz, C*H*(5) Pyr), 2.14 (12H, s, CH_3(2) DMGH), 0.83 (3H, s, CH_3 (1), Co-Me), δC ($CDCl_3$) (ppm) 150.0 (*C* (4), Pyr), 149.0 (*C* (3), DMGH), 137.5 (*C* (6), Pyr), 125.2 (*C* (5) Pyr), 40.8 (*C* (1) Co-CH_3), 12.0 (CH_3 (2) DMGH). *m/z* (ESI) 384.1 $[MH]^+$. HRMS (ESI) calculated $[MH]^+$ = 384.1082; measured $[MH]^+$ = 384.1079.

3-Bromopyridinemethylcobaloxime 3.4

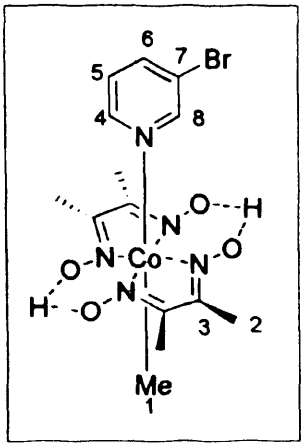

Under an atmosphere of nitrogen, [ClCo(DMGH)$_2$(3-Bromopyr)] (500 mg, 1.04 mmol) was dissolved in methanol (10 ml). To this solution, methyl iodide (0.07 ml, 1.14 mmol, 1.1 equivs.) and $NaBH_4$ (50 mg) were added. The reaction was left to stir for 2 hours, and left to crystallise. The brown solid was filtered off, dissolved in dichloromethane (20 ml) and extracted with distilled water (3 x 20 ml). The organic phase was dried and then filtered, evaporated to dryness and [MeCo(DMGH)$_2$(3-Bromopyr)] was isolated as a brown solid (455 mg, 95 %) δH ($CDCl_3$) (ppm) 8.59 (1H, d, *J* = 1.9 Hz, C*H*(8) Pyr), 8.53 (1H, d, *J* = 5.6 Hz, C*H*(4) Pyr), 7.85 (1H, dd, *J* = 8.1, 1.1 Hz, C*H*(6) Pyr), 7.19 (1H, dq, *J* = 5.8, 1.1 Hz, C*H*(5) Pyr), 2.12 (12H, s, CH_3(2) DMGH), 0.78 (3H, s, CH_3 (1), Co-Me). δC ($CDCl_3$) (ppm) 151.1 (*C* (3), DMGH), 149.3 (*C* (4), Pyr), 148.5 (*C* (8), Pyr), 136.4 (*C* (6), Pyr), 126.1 (*C* (5) Pyr), 121.4 (*C* (7), Pyr), 41.1 (*C* (1) Co-CH_3), 12.1 (CH_3 (2) DMGH). *m/z* (ESI) 462.0 $[MH]^+$. HRMS (ESI) calculated $[MH]^+$ = 462.0187; measured $[MH]^+$ = 462.0189.

Pyridylethylcobaloxime 3.5[20]

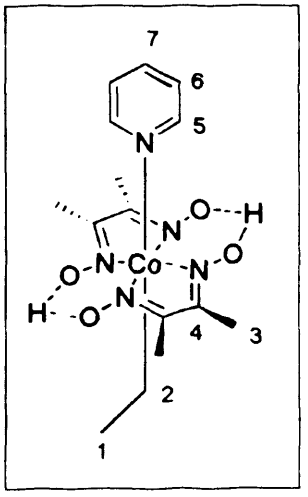

Under an atmosphere of nitrogen, [ClCo(DMGH)$_2$(Pyr)] (500 mg, 1.24 mmol) was dissolved in methanol (10 ml). To this solution, ethyl iodide (0.11 ml, 1.36 mmol, 1.1 equivs.) and $NaBH_4$ (50 mg) were added. The reaction was left to stir for 2 hours, and left to crystallise. The brown solid was filtered off, dissolved in dichloromethane (20 ml) and extracted with distilled water (3 x 20ml). The organic phase was dried and then filtered, evaporated to dryness and [EtCo(DMGH)$_2$(Pyr)] was isolated as a brown solid (217 mg, 89 %) Found: δ_H 8.55 (2 H, dd, J = 4.9, 1.4 Hz C*H* (5) Pyr), 7.72 (1 H, tt, J = 7.6, 1.5 Hz C*H* (7) Pyr), 7.33 (2 H, dt, J = 6.5, 1.4 Hz C*H* (6) Pyr), 2.14 (12 H, s, CH_3 (3), DMGH), 1.75 (2 H, q, J = 7.7 Hz, CH_2 (2), Co-CH_2-CH_3), 0.38 (3 H, t, J = 7.7 Hz, CH_3 (1), Co-CH_2-CH_3). δC ($CDCl_3$) (ppm) 150.0 (*C* (5), Pyr), 149.0 (*C* (4), DMGH), 137.5 (*C* (7), Pyr), 125.2 (*C* (6) Pyr), 40.8 (*C* (2) Co-CH_2-CH_3),

16.1 (*C* (1) Co-CH_2-CH_3), 12.0 (CH_3 (3) DMGH). *m/z* (ESI) 399.0 $[MH]^+$. HRMS (ESI) calculated $[MH]^+$ = 398.1239; measured $[MH]^+$ = 398.1243.

3-Bromopyridineethylcobaloxime 3.6

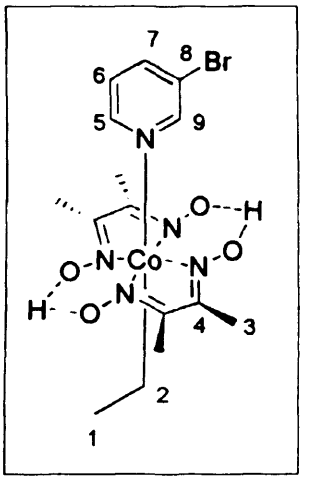

Under an atmosphere of nitrogen, [ClCo(DMGH)$_2$(3-Bromopyr)] (500 mg, 1.04 mmol) was dissolved in methanol (10 ml). To this solution, ethyl iodide (0.09 ml, 1.14 mmol, 1.1 equivs.) and $NaBH_4$ (50 mg) were added. The reaction was left to stir for 2 hours, and left to crystallise. The brown solid was filtered off, dissolved in dichloromethane (20 ml) and extracted with distilled water (3 x 20ml). The organic phase was dried and then filtered, evaporated to dryness and [EtCo(DMGH)$_2$(3-Bromopyr)] was isolated as a brown solid (458 mg, 93 %) δH ($CDCl_3$) (ppm) 8.64 (1H, d, *J* = 1.9 Hz, C*H*(9) Pyr), 8.55 (1H, d, *J* = 5.4 Hz, C*H*(5) Pyr), 7.87 (1H, dd, *J* = 8.1, 1.1 Hz, C*H*(7) Pyr), 7.23 (1H, dq, *J* = 5.3, 1.1 Hz, C*H*(6) Pyr), 2.13 (12 H, s, CH_3 (3), DMGH), 1.74 (2H, q, *J* = 7.6 Hz. CH_2 (2), Co-CH_2-CH_3), 0.36 (3H, t, *J* = 7.6 Hz, CH_3 (1), Co-CH_2-CH_3), δC ($CDCl_3$) (ppm) 151.1 (*C* (4), DMGH), 149.3 (*C* (5), Pyr), 148.5 (*C* (9), Pyr), 137.0 (*C* (7), Pyr), 126.0 (*C* (6) Pyr), 121.5 (*C* (8), Pyr), 40.8 (*C* (2) Co-CH_2-CH_3), 16.1 (*C* (1) Co-CH_2-CH_3), 12.1(CH_3 (3) DMGH). *m/z* (ESI) 476.1 $[MH]^+$. HRMS (ESI) calculated $[MH]^+$ = 476.0344; measured $[MH]^+$ = 476.0352.

General procedure for the ligand exchange experiments.

To a stirred solution of [ClCo(DMGH)$_2$(3-Bromopyr)] (100 mg, 0.25 mmol) in methanol (5 ml), iodoethane (0.017 ml, 0.25 mmol) and pyridine (0.012 ml, 0.25 mmol) were added. To this solution, $NaBH_4$ (15 mg) was added, and left to stir for two hours, and the reaction was monitored using TLC. The resulting brown solid was filtered off, pumped down and analysed. The ^{1}H-NMR showed the presence of both [EtCo(DMGH)$_2$(3-Bromopyr)] and [EtCo(DMGH)$_2$(Pyr)].

To a stirred solution of [ClCo(DMGH)$_2$(Pyr)] (100 mg, 0.2 mmol) in methanol (10 ml), iodoethane (0.15 ml, 0.2 mmol) and 3-bromopyridine (0.15 ml, 0.2 mmol) were added. To this solution, $NaBH_4$ (15 mg) was added, and left to stir for two hours, and the

reaction was monitored using TLC. The resulting brown solid was filtered off, pumped down and analysed. The ^{1}H-NMR showed the presence of both [EtCo(DMGH)$_2$(3-Bromopyr)] and [EtCo(DMGH)$_2$(Pyr)].

The ligand exchange experiment on B_{12}.

To a stirred solution of cyanocobalamin (50 mg, 0.04 mmol) in ethanol (5 ml) was added triphenylphosphine (48 mg, 5 equivs., 0.185 mmol) and $NaBH_4$ (5 mg). The reaction was left to stir for 30 minutes, when a sample was removed for ^{31}P-NMR.

The Alkyl ligand exchange experiments.

To a stirred solution of [ClCo(DMGH)$_2$(Pyr)] (250 mg, 0.62 mmol) in methanol (5 ml), were added iodoethane (0.039 ml, 0.62 mmol), and iodomethane (0.050 ml, 0.62 mmol). To this solution, $NaBH_4$ (30 mg) was added, and left to stir for two hours, and the reaction was monitored using TLC. The resulting brown solid was filtered off, pumped down and analysed. The ^{1}H-NMR revealed a mixture of [MeCo(DMGH)$_2$(Pyr)] and [EtCo(DMGH)$_2$(Pyr)].

To a stirred solution of [ClCo(DMGH)$_2$(3-Bromopyr)] (250 mg, 0.52 mmol) in methanol (5 ml), were added iodoethane (0.041 ml, 0.52 mmol), and iodomethane (0.032 ml, 0.52 mmol). To this solution, $NaBH_4$ (25 mg) was added, and left to stir for two hours, and the reaction was monitored using TLC. The resulting brown solid was filtered off, pumped down and analysed. The ^{1}H-NMR revealed a mixture of both [MeCo(DMGH)$_2$(Pyr)] and [EtCo(DMGH)$_2$(Pyr)].

3.5 References.

1 A. J. B. Zehnder, K. Wuhrmann, *Science.* **1976**, 194, 1165.

2 W. A. van der Donk, J. Shey, *J. Am. Chem. Soc.* **2000**, 122, 12403.

3 G. Glod, U. Brodmann, W. Angst, C. Holliger, R. P. Schwarzenbach, *Environ. Sci. Technol.* **1997**, 31, 3154.

4 C. Nonnenberg, W. A. van der Donk, H. Zipse, *J. Phys. Chem. A.* **2002**, 106, 8708.

5 C. J. Gantzer, L. P. Wackett, *Environ. Sci. Technol.* **1991**, 25, 715.

6 G. Glod, W. Angst, C. Holliger, R. P. Schwarzenbach, *Environ. Sci. Technol.* **1997**, 31, 253.

7 S. Lesage, S. Brown, K. Millar, *Environ. Sci. Technol.* **1998**, 32, 2264.

8 J. K. Gotpagar, E. A. Grulke, D. Bhattacharyya, *J. Hazard. Mater.* **1998**, 62, 243.

9 M. J. Hacker, G. W. Littlecott, R. D. W. Kemmitt, *J. Organomet. Chem.* **1973**, 47, 189.

10 D. R. Burris, C. A. Delcomyn, B. Deng, L. E. Buck, K. Hatfield, *Environ. Toxicol. Chem.*, **1998**, 17, 1681.

11 M. Semadeni, P. C. Chiu, M. Reinhard, *Environ. Sci. Technol.* **1998**, 32, 1207.

12 K. M. McCauley, S. R. Wilson, W.A . van der Donk, *Inorg. Chem.* **2002**, 41, 393.

13 P. N. Balasubramanian, E. S. Gould, *Inorg. Chem.* **1984**, 23, 825.

14 G. N. Schrauzer, R. J. Windgassen, *J. Am. Chem. Soc.* **1966**, 88, 3738.

15 B. Gupta, *Organometallics.* **2003**, 22, 2670.

16 J. A. Osborn, F. H. Jardine, J. F. Young, G. Wilkinson, *J. Chem. Soc. A*, **1966**, 1711.

17 J. Galinkina, E. Rusanov, C. Wagner, H. Schmidt, D. Strhl, S. Tobisch, D. Steinborn *Organometallics*, **2003**, 22, 4873.

18 P. Ramesh, A. Subbiah Pandi, P. Jothi, C. Revathib A. Dayalan, *Acta Cryst.* **2008** E64, m300.

19 B.D. Gupta, U. Tiwari, T. Barclay, W. Cordes, *J. Organomet. Chem.* **2001**, 629, 83,

20 B. D. Gupta, Veena Singh, R. Yamuna, T. Barclay, W. Cordes *Organometallics* **2003,** 22, 2670.

Chapter 4.

μ^2-Dicobaltcarbonyl Bridged Alkynylpyridines as Ligands for Cobaloximes.

4.0. Compound List.

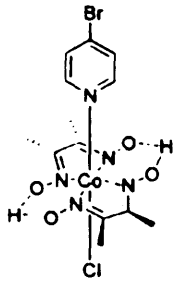

4.1

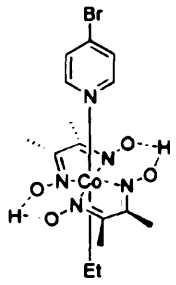

4.2

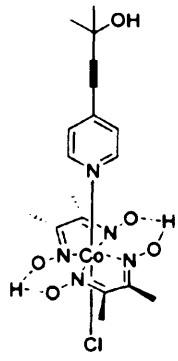

4.3

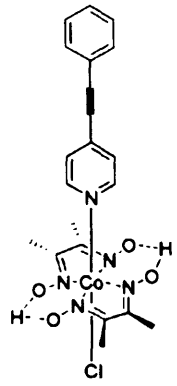

4.4

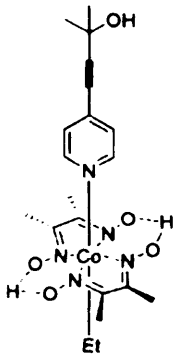

4.5

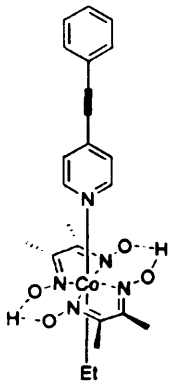

4.6

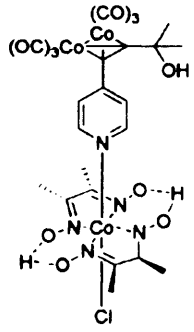

4.7

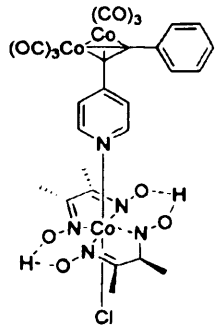

4.8

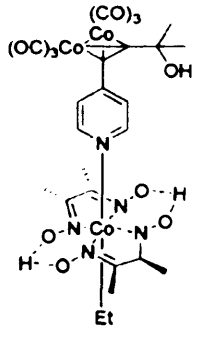

4.9

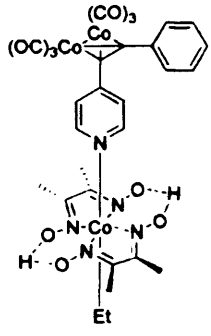

4.10

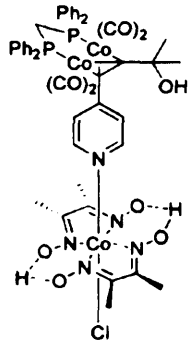

4.11

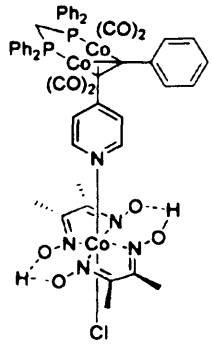

4.12

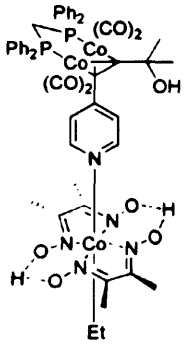

4.13

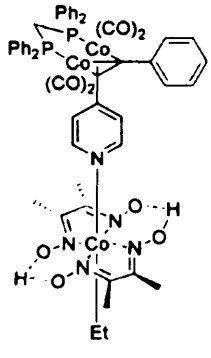

4.14

4.1. Introduction.

4.1.1. Design of Ligands Bearing a Secondary Coordination Site.

As demonstrated in **Chapter 3**, cobaloximes are useful mimics for vitamin B_{12} in the reductive dechlorination of chlorinated olefins such as PCE, as they show similar chemical properties. Whilst the vitamin B_{12}-containing *tetrachloroethylene reductase* enzyme found in dehalogenating bacteria has the ability to remove all chlorides stepwise, isolated cobaloximes are poor models for the overall redox system, where the catalytic cycle finishes with the vinylcobaloxime species. In addition to the B_{12} centre, the *tetrachloroethylene reductase* enzyme also contains a Fe-S cluster, which is believed to initiate and maintain the redox cycle. It is this external reductant that is missing from the isolated cobaloximes, and so the incorporation of a secondary, redox active metal centre into a cobaloxime species to give a multimetallic system, could enhance the catalytic ability of cobaloximes. This would be one of very few examples of cobaloximes containing a secondary-metal unit; cobaloximes bearing ferrocenylphosphine and azaferrocene ligands have previously been synthesised,[1,2] as has a cobaloxime bearing a dicobaltcarbonyl bridged alkyne moiety. [3]

This Chapter describes the incorporation of the metal centre into an axial ligand. Ligands will be synthesised with a view to incorporating a secondary centre to facilitate the movement of electrons to and from the cobalt centre, and mimic the Fe_4S_4 cluster present in the enzyme. It is believed that this will enable the cobaloxime to complete the final reduction step from vinyl chloride to ethylene, and reductive cleavage of the Co-alkene bond, the bottleneck in the catalytic process.

4.1.2. Dicobaltoctacarbonyl Clusters and Related Compounds.

$Co_2(CO)_8$ and its derivative, $Co_2(CO)_6(\mu$-dppm), are good candidates for the redox active secondary metal centre, as they have a rich coordination chemistry with alkynes,[4, 5] and the resultant species are easily reduced.[6, 7]

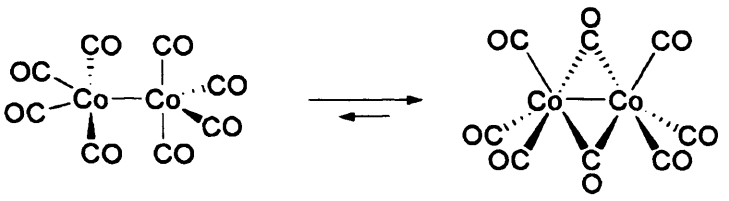

Scheme 4.1. Isomerisation of dicobaltoctacarbonyl.

The two isomers depicted in **Scheme 4.1** rapidly interconvert. The minor isomer has no bridging CO ligands, and is described as $[(CO)_4Co\text{-}Co(CO)_4]$. The major isomer contains two bridging CO ligands, and two octahedral cobalt and is described as $[(CO)_3Co(\mu\text{-}CO)_2Co(CO)_3]$.[8] Reaction of dicobaltoctacarbonyl with one equivalent of bis(diphenylphosphino)methane yields μ^2-diphenylphosphinomethane dicobalt hexacarbonyl, $[Co_2(CO)_6(\mu\text{-dppm})]$, **Figure 4.1**, which, due to the bridging bis(diphenylphosphino)methane backbone, should be more stable and resilient to oxidative decomposition than dicobaltoctacarbonyl.

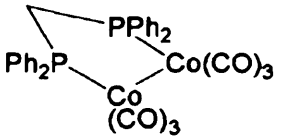

Figure 4.1. $Co_2(CO)_6(\mu\text{-dppm})$.

4.1.3. Organodicobaltcarbonyl Chemistry.

Dicobaltcarbonyl alkyne species are of interest in synthetic chemistry, as they are intermediates in carbon-carbon bond-forming reactions, such as the Pauson-Khand (PK) and the Nicholas reactions. These reactions proceed via an organocobalt species with a mutually bridged bond between the two π-bonds of acetylene and the cobalt-cobalt bond of dicobalthexacarbonyl. There are numerous examples of organodicobaltcarbonyl compounds found in organic synthesis, due to the high affinity of cobalt for carbon-carbon and carbon-nitrogen π bonds, particularly those that react readily with alkynes to give organocobalt heteronuclear complexes. As shown in **Figure 4.2**, the alkyne uses both sets of filled π orbitals to bond with the dicobalt fragment, and, in accordance with the Dewar-Chatt-Duncanson model,[9] the substituents on the bridged alkyne bend away from the metal centre due to the metal to ligand π electron back-bonding mechanism.

The reduction of the dicobaltcarbonyl cluster would involve the addition of one electron to an anti-bonding orbital; it is hoped that the destabilisation of the centre will result in transfer of the electron to the cobaloxime cluster, resulting in the reduction of the cobaloxime, which is necessary for the catalytic process.

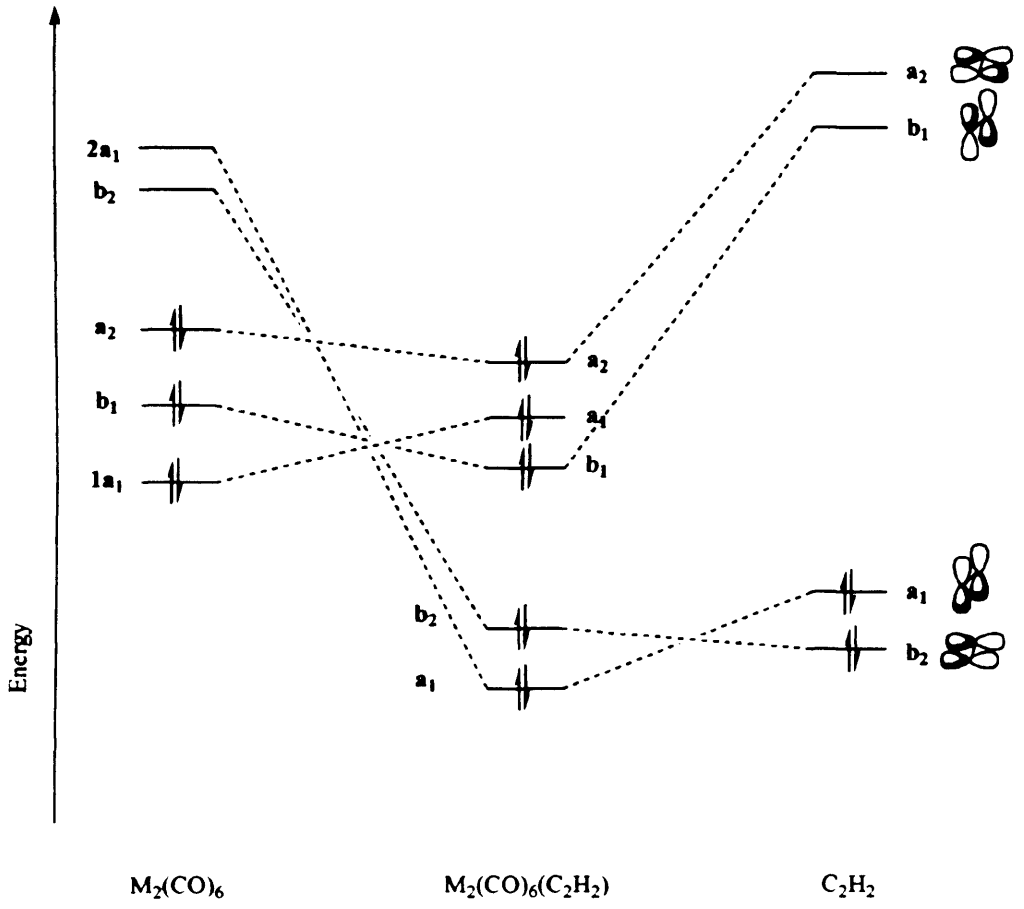

Figure 4.2. Frontier orbitals formed from addition of C_2H_2 to $Co_2(CO)_6$ (anti-bonding orbitals not shown).[10]

4.1.3.1. The Pauson-Khand Reaction.

The Pauson-Khand reaction, **Scheme 4.2**, is a dicobaltoctacarbonyl mediated organic transformation in which three carbon-carbon bonds are formed. It consists of a one-pot [2+2+1] cycloaddition of an acetylene species, an olefin and a cobalt carbonyl, which gives a α,β-cyclopentenone ring. Due the high regio- and stereo- selectivity afforded by the reaction, which arises from the alkene insertion step, the PK reaction is viewed as a useful reaction in synthetic chemistry.

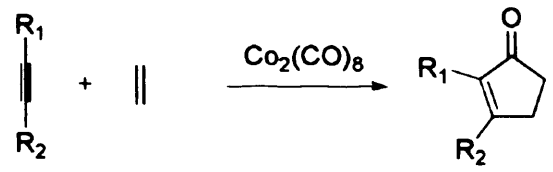

Scheme 4.2. The Pauson-Khand reaction.

The two π-bonds of the acetylene interact with the dicobaltoctacarbonyl species, to form the bridged organodicobaltcarbonyl species. From this species, the dissociation of a carbonyl results in a vacant site on the cobalt, to which the olefin coordinates. The insertion of this cobalt coordinated alkene into the cobalt-carbon bond occurs at the least hindered end of the alkene, and is followed by insertion of a carbonyl into this new cobalt-carbon bond, forming the second new carbon-carbon bond. Reductive elimination of one cobalt carbonyl forms the final carbon-carbon single bond. The double bond is formed by dissociation of the dicobaltcarbonyl fragment to yield the cyclopentenone product. The reaction is catalytic in Co in the presence of excess CO.

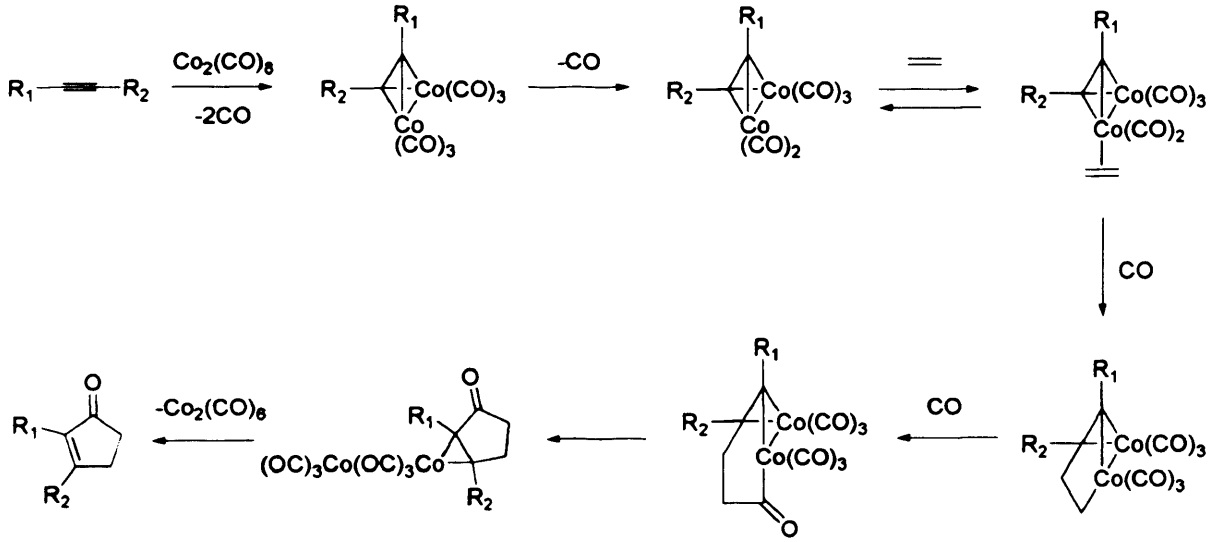

Scheme 4.3. The intermediates of the PK reaction.

4.1.3.2. The Nicholas Reaction.

The Nicholas reaction, depicted in **Scheme 4.4**, is another organic reaction utilising an organodicobaltcarbonyl species. The organodicobaltcarbonyl intermediate allows nucleophilic substitution of moieties that are poor leaving groups and not readily displaced by nucleophiles.

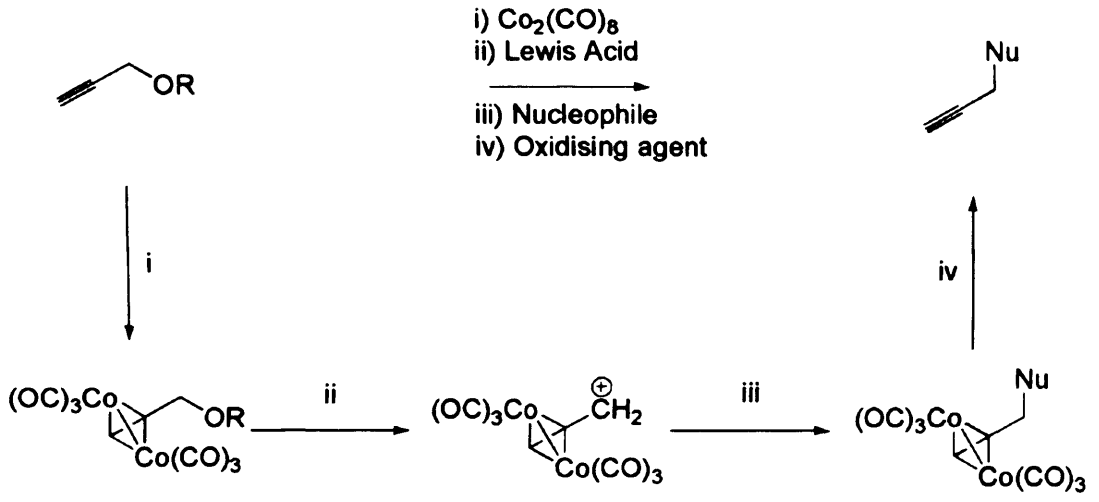

Scheme 4.4. The Nicholas reaction.

The dicobaltcarbonyl species first acts to protect the alkyne by coordination, forming the organodicobaltcarbonyl species and increasing the reactivity of the carbon α to the acetylene. A propargylic cation,[a] stabilised by the dicobaltohexacarbonyl complex of the triple bond, is formed by addition of a Lewis acid. This propargylic cation will then easily react with a variety of nucleophiles to form the corresponding derivative. The protective dicobaltcarbonyl group is then removed by addition of an oxidising agent. Due to the bulk of the protecting group, the reactions proceed with high regio- and stereo- selectivity.

4.1.4. Molecular Catalysts for Dechlorination.

The chemical inertness of organohalides, once their major advantage in industry, has now become their shortcoming when it comes to their destruction. The extreme conditions, previously discussed in **Section 1.2.1**, such as high temperature incineration,

[a] Cation α to an alkyne.

required for their destruction has lead to investigation of methods utilising milder conditions. To date there are no cost effective ambient chemical methods for their destruction. Research is currently being undertaken into the dehalogenation of these priority organic pollutants, with attention focused on the use of reduced metal complexes for the catalytic destruction of organohalides.

In 1995 Liu and Schwartz[11] reported the first catalytic molecular based system for dechlorination of chlorinated aromatic hydrocarbons. They reported that titanocene dichloride (Cp_2TiCl_2; Cp = η-C_5H_5) could be used as a catalyst for the dechlorination of PCBs, producing biphenyl as the only organic product after 24 hrs and at the relatively low (compared to the 300 °C required for incineration) temperature of 125 °C. It was also shown that this system would be catalytically active at 95 °C towards chlorinated benzenes, although only for the removal of one chloride.[12] Knowles and co-workers demonstrated that this approach could in principle be applied to contaminated soils, although there were major catalyst/soil compatibility issues to be overcome.[13]

Hor *et al* reported the use of $PdCl_2$(dppf) (dppf = 1,19- bis(diphenylphosphino) ferrocene) as a catalyst at 67 °C under inert conditions, finding that total conversion of the hexa-, penta- and tetrachlorobenzene starting materials to less chlorinated analogues occurred within 200 hours, though no benzene is observed. When the catalysis was attempted on PCBs, little dechlorination was observed even after four days reflux, with only one chloride removed.[14] Kagan's reagent (SmI_2) has been used extensively as a tool in organic synthesis as a species for reductive dehalogenation of organohalides.[15] When investigated as an alternative catalyst for dechlorination, it was found to be relatively efficient at dechlorinating PCBs at ambient temperatures, yielding only mono- or dichlorinated biphenyl, after only 1 hour. However, the process requires 1.7 equivalents of SmI_2, and is most effective when used with hexamethylphosphoramide (HMPA), which is highly toxic. Nevertheless, this process is carried out under mild conditions, i.e. ambient temperature and inert atmosphere, and has been shown to dechlorinate contaminated soil samples, and is tolerant to 5 % moisture. McNeill and Peterson[16] reported that $(PPh_3)_3RhCl$, with Et_3SiH as a reducing agent, at 35 °C is able to completely dehalogenate vinylhalides in 50 minutes at 8 mol %.

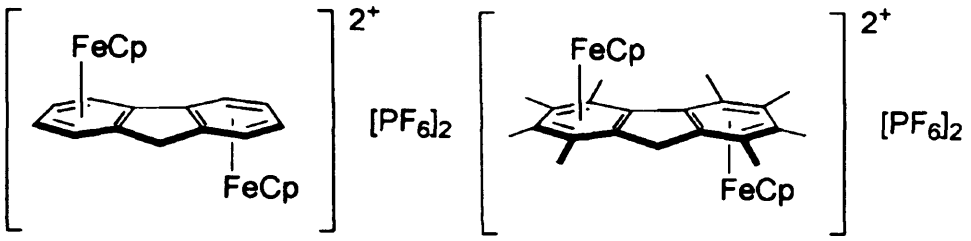

Figure 4.3. O' Hare's di-iron Fluorene catalysts; $[(FeCp)_2FluH]^{2+}[PF_6]_2$ and $[(FeCp)_2Flu^*H]^{2+}[PF_6]_2$.

O' Hare et al[17] presented di-iron complexes of fluorene (η^6-$C_{13}H_{10}$) and fluorene* (η^6-$C_{13}Me_9H$), portrayed in **Figure 4.3**, at 5 mol % catalyst loading, as agents for the dechlorination of PCBs at 125 °C. The reactions were undertaken in the dark, as iron arene complexes are somewhat light sensitive. It was found that after 24 hours, no PCB starting material was observed, with 39 % and 49 % conversion to biphenyl respectively. Whittlesey *et al*[18] reported that ruthenium N-heterocyclic carbenes, such as that shown in **Figure 4.4**, could act as catalytic defluorinating agents at 10 mol %, with the reaction occurring at 70 °C for 20 hours, with 70 % of the C_6F_6 starting material defluorinated to give $C_6F_4H_2$.

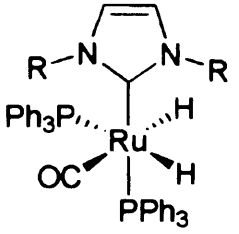

Figure 4.4. Whittlesey's Ruthenium NHC catalyst. R = 2,6-diisopropylphenyl.

Disadvantages are notable in many of these documented systems: few of the reported catalytic systems are effective at room temperature, with most requiring elevated temperatures, and so needing a high energy input. Moreover, a number of methods cannot be regarded as truly catalytic since the "catalyst" is employed in stoichiometric or even in excess amounts, making it effectively a reagent. Other shortcomings include complicated quenching procedures, harsh conditions such as high pressure, catalysts which are difficult to prepare, or the need to use multiphase systems.

4.2. Design of Bridged Cobaloximes.

Whilst there are numerous examples in the literature of simple cobaloximes bearing axial pyridine ligands, there are few examples of multinuclear cobaloximes containing different organocobalt centres. Hence, the aim of the work described in this chapter is to investigate a series of novel cobaloxime based complexes, initially with an alkyne group present, and then to bridge it with dicobaltcarbonyl species.

4.2.1. Target Structure.

This chapter will describe a series of compounds comprised of a cobaloxime and substituted pyridine species bearing an alkyne group. These will act as precursors for the bridged complexes, where the alkyne is bridged by a dicobaltcarbonyl cluster, which act as the secondary metal centre. The target is shown in **Figure 4.5**.

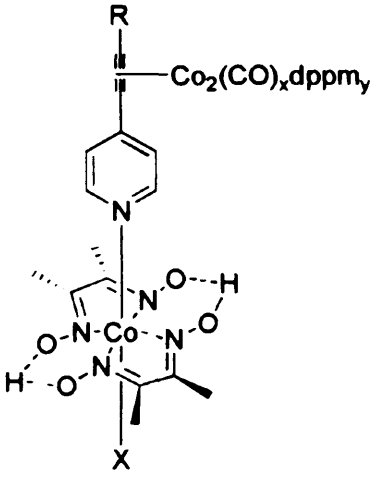

Figure 4.5. Target Cobaloxime.

Having shown in **Chapter 3** the ease with which pyridine species can coordinate to a cobaloxime, it follows that the first step towards the incorporation of the secondary metal centre should be into the pyridine molecule. A substituted ethynylpyridine can be made via the Sonogashira coupling between a substituted alkyne and a halogenated pyridine. The ethynyl bond of the ligand can act as our secondary binding site, and the addition of a dicobaltcarbonyl cluster across this would yield the desired multimetallic cobaloxime. The R-group on the alkyne can be varied to observe the effects of electron

donating or withdrawing groups on the redox potential of the dicobalt cluster. This strategy of attaching the redox centre *via* the axial *N* ligand to cobaloximes should not significantly affect the reactivity of the systems, as the nature of the axial *N* ligand has been shown to have only minor influence in cobalamin reactivity.[19] Based upon the considerations affecting the current literature of molecular dechlorination agents, detailed in **section 4.1.4**, this cobaloxime-based system is hoped to react at room temperature, with short reaction times and under aerobic conditions.

4.2.2. Retrosynthetic Analysis.

The proposed catalysts were based around a conventional cobaloxime structure with equatorial DMGH ligands supplemented by an axial pyridine. For ease of synthesis the additional metal centres were incorporated into the axial pyridine ligand. For the cobaloxime depicted in **Scheme 4.5**, two options were considered for the incorporation of the alkyne group into the axial ligand. Option A shows the Sonogashira coupling between a free alkyne and [XCo(DMGH)$_2$(4-bromopyr)]. Alternatively, option B, scheme shows the coordination of the preformed alkynylpyridine, synthesised via a Sonogashira coupling, to the cobaloxime.

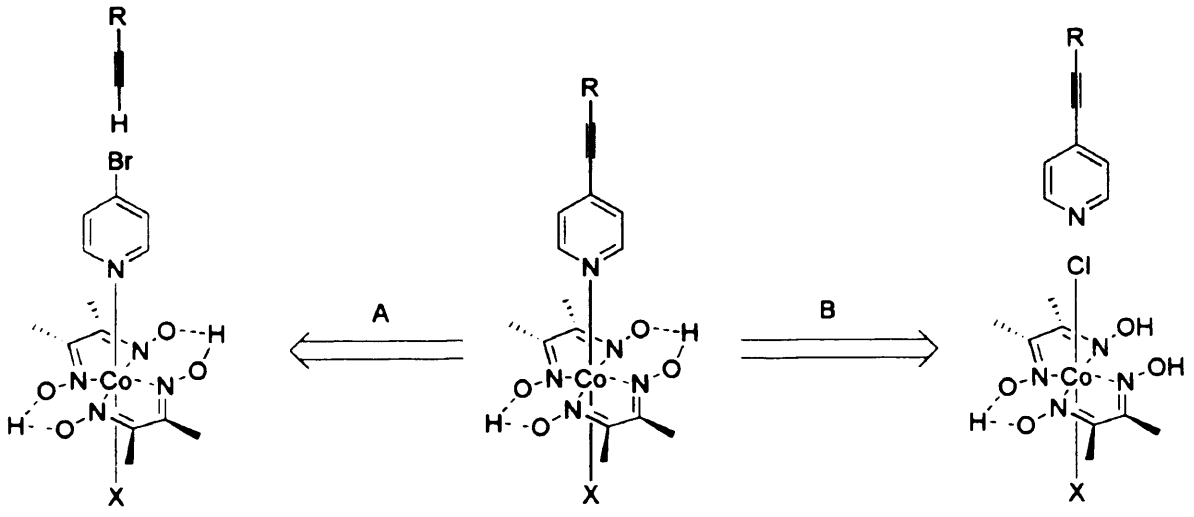

Scheme 4.5. The precursors for the Sonogashira coupling reactions.

For the multimetallic cobaloximes, there were also two options considered for the bridging, shown in **Scheme 4.6**. Option C shows the bridging of the $[XCo(DMGH)_2(R\text{-alkyne-pyr})]$, whereas option D represents the coordination of the bridged alkynylpyridine to the cobaloxime.

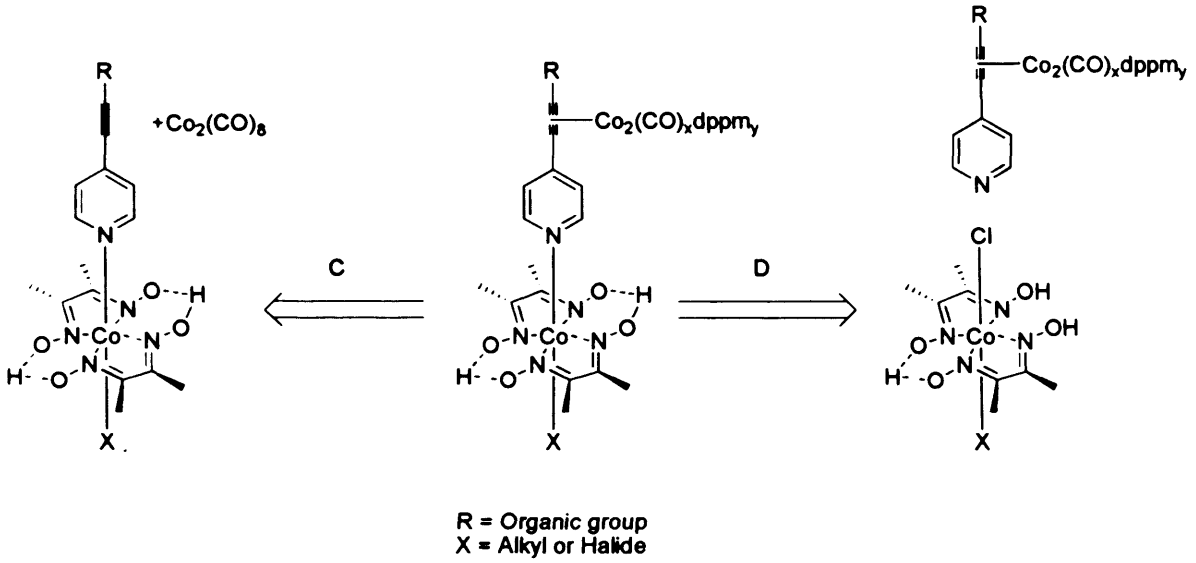

Scheme 4.6. The methods for incorporating the secondary metal centre.

The chosen alkynes and the 4-bromopyridine required for the coupling are commercially available; the pyridine is available as the hydrochloride salt, as is dicobaltoctacarbonyl. $[Co_2(\mu\text{-dppm})(CO)_6]$ and $[Cl_2Co(DMGH)(DMGH_2)]$ are literature preparations, whilst the coordination of pyridines has been discussed in **Chapter 3**.

4.3. Results and Discussion.

4.3.1. Synthesis, Physical and Structural Properties.

4.3.1.1. Synthesis of the Alkynylpyridine Cobaloxime Precursors.

Option A was chosen for the first approach towards the alkynylpyridine cobaloximes, where the Sonogashira coupling was undertaken on the 4-bromopyridine coordinated to the cobalt. The addition of 4-bromopyridine to a suspension of $[Cl_2Co(DMGH)(DMGH_2)]$ in dichloromethane in the presence of sodium bicarbonate afforded the desired $[ClCo(DMGH)_2(4\text{-bromopyr})]$, **4.1**; ethylation of which gave $[EtCo(DMGH)_2(4\text{-bromopyr})]$, **4.2**, both in good yields, 95 % and 93 % respectively, using the same approaches recorded in **Section 3.2.1**.

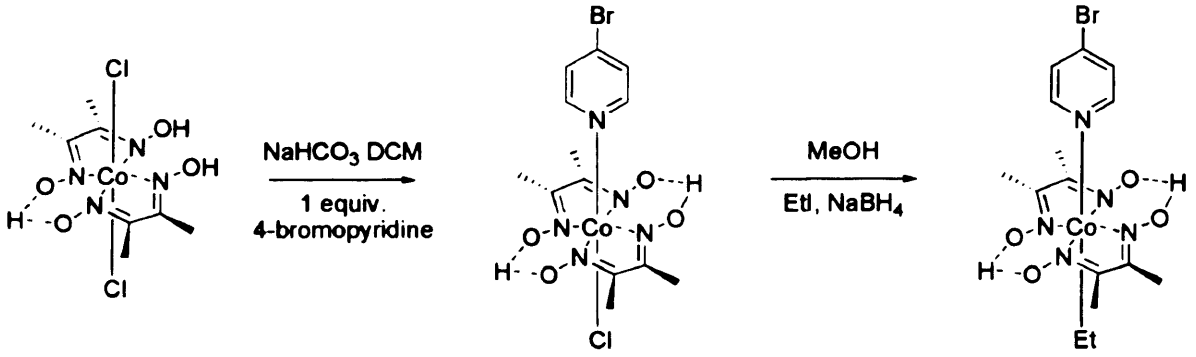

4.1 **4.2**

Scheme 4.7. Synthesis of Sonogashira coupling precursors.

The alkyne species chosen for the Sonogashira coupling were 2-methylbut-3-yn-2-ol and phenylacetylene. Varying the alkyl group of the alkyne bond may affect the chemistry of both the alkyne bond itself and the dicobalt cluster of the resultant bridged species, and hence the catalytic ability. Attempts at the Sonogashira couplings between these alkynes and the preformed complexes shown in **Scheme 4.8**, however, led to complicated product mixtures, which, by ^{1}H-NMR, showed the presence of vinyl groups in both cases, presumably derived from the reduction of the alkynes.

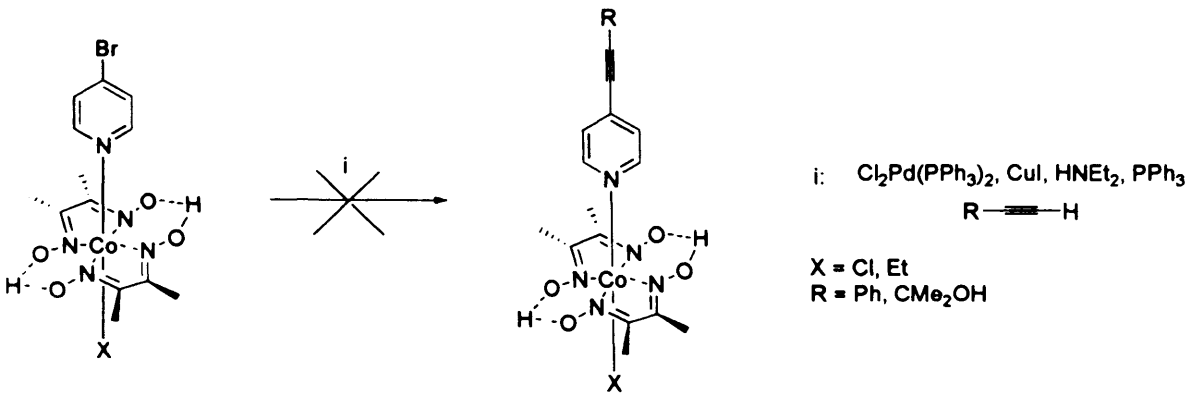

Scheme 4.8. Unsuccessful Sonogashira couplings.

This left option B as the only route to alkynylpyridine cobaloximes, with the Sonogashira couplings performed on the uncoordinated 4-bromopyridine salt. Both the 2-methylbut-3-yn-2ol and phenylacetylene were coupled to the 4-bromopyridine salt with ease, using palladium dichloride bistriphenylphosphine and copper iodide acting as the co-catalyst in the diethylamine solvent. ^{1}H-NMR and ^{13}C-NMR spectroscopic studies confirmed the synthesis of 2-methyl-4-(pyridin-4-yl)but-3-yn-2-ol (doublets at 8.45 ppm, 7.17 ppm, and a singlet at 1.57 ppm) and 4-(2-phenylethynyl)pyridine (doublet at 8.58 ppm and multiplets between 7.5–7.6 ppm and 7.2–7.4 ppm) were successful, in accordance with the literature.[20,21]

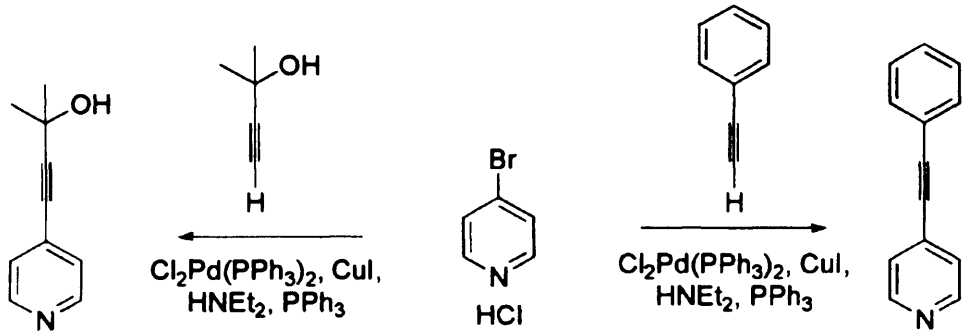

Scheme 4.9. Sonogashira coupled alkynylpyridines.

Coordination of these alkynylpyridines to the preformed $[Cl_2Co(DMGH)(DMGH_2)]$ was achieved by treating the suspension of the alkynylpyridine and the cobaloxime in dichloromethane with sodium carbonate, as shown in **Scheme 4.9**, to give the desired alkynylpyridylcobaloximes. The base has two roles in this reaction; to remove the hydrochloric acid from the reaction and to deprotonate the DMGH, which provides the reactive five-coordinate monochlorocobaloxime intermediate. The coordination of these

alkynylpyridines to this unsaturated cobaloxime proceeded with ease, as the reaction occurs with stirring at room temperature, giving [ClCo(DMGH)$_2$(2-methyl-4-(pyridin-4-yl)but-3-yn-2-ol)], **4.3**, and [ClCo(DMGH)$_2$(4-(2-phenyl ethynyl)pyridine)], **4.4**, in good yields, 91 % and 93 % respectively.

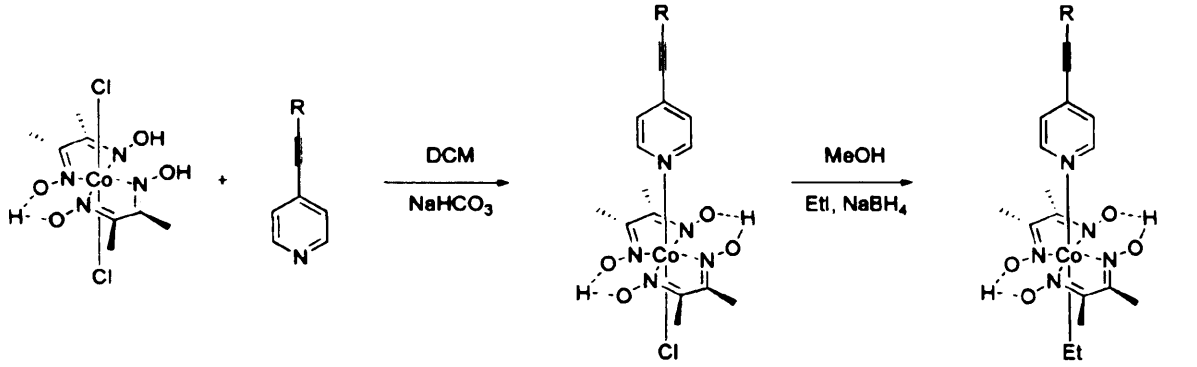

Scheme 4.10. Coordination followed by ethylation of alkynylpyridylcobaloximes.

With the alkynylpyridyl chlorocobaloximes synthesised, the stability of these complexes (particularly the acetylene bond) towards the standard reaction conditions required for dechlorination, was examined, as the acetylene bond may be susceptible to the reductive conditions. Using the standard alkylation techniques described in **Section 3.2.1** for the ethylation of pyridyl chlorocobaloximes, the ethylated derivatives of the alkynylpyridyl chlorocobaloximes synthesised previously. Reaction of a brown methanolic solution of both iodoethane and the alkynylpyridyl chloro cobaloximes, **4.3** and **4.4**, with sodium borohydride, gave the characteristic blue-green Co(I) intermediates, which, due to the presence of iodoethane, reformed the typically brown cobaloximes of [EtCo(DMGH)$_2$(2-methyl-4-(pyridin-4-yl)but-3-yn-2-ol)], **4.5**, and [EtCo(DMGH)$_2$ (4-(2-phenyl ethynyl)pyridine)], **4.6**, in good yields, 95 % and 93 % respectively. A one-pot synthesis of the **4.6** was also attempted, the conditions shown in **Scheme 4.11**, but the yield obtained, 68 %, was less than that achieved from the reaction in individual steps. Ethylation of the cobaloximes was confirmed by the presence of the resonance of the ethyl triplet at 0.40 ppm, and IR confirmed that the acetylene bond was still present, and had not been reduced by the reaction conditions.

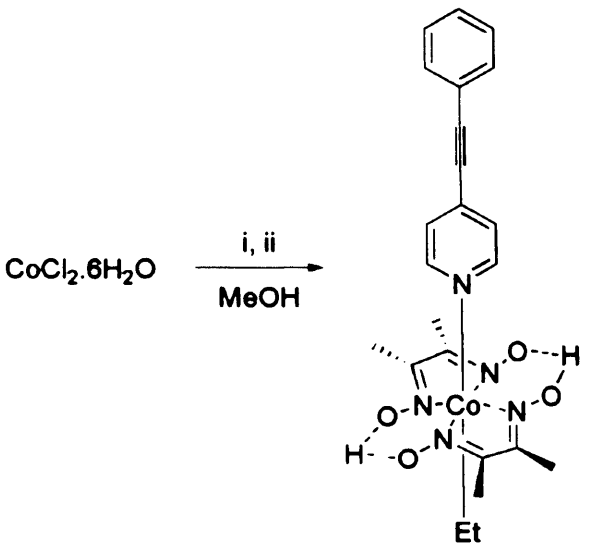

i: 2 DMGH, 4-(2-phenylethynyl)pyridine, NaOH (50 %).

ii: EtI, NaBH4, 0 °C. 68 %.

Scheme 4.11. One pot synthesis of **4.6**.

Data in **Table 4.1** shows the effect of coordination of the alkynyl pyridines to cobaloximes on the ν(C≡C) band. Replacement of the CMe_2OH group with a phenyl groups, results in a shift of the ν(C≡C) band to a lower frequency, hence a weakening of the bond. This can be rationalised by the resonance effects of the phenyl group, which results in the delocalisation of the alkyne electrons into the phenyl ring, and, consequentially, the alkyne bond becomes partially double bond in character. Whereas the electron donating methyl groups negate the electron withdrawing effects of the hydroxy group of the CMe_2OH species, hence there is little change in the electron density in the alkyne bond, and a higher frequency stretch is observed than the phenyl acetylene species.

Complex	Wavenumber/cm^{-1} ν(C-C)
2-methyl-4-(pyridin-4-yl)but-3-yn-2-ol	2230
4.3	2234
4.5	2233
4-(2-phenyl ethynyl)pyridine	2212
4.4	2217
4.6	2219

Table 4.1. The alkyne stretches of alkynylpyridylcobaloximes.

Upon coordination of the free pyridyl acetylene, there is a noticeable shift in the stretches of the alkyne bands to a higher frequency. This result is unexpected, as the coordination of an alkyne species to an electro-positive cobaloxime was expected to result in the weakening of the alkyne bond and a shift of the band to a lower frequency. Due to the electron withdrawing effect of the cobaloxime centre, the electrons of the alkyne bond would be "pulled" through the conjugated π system, leaving the alkyne bond as a partial double bond, and a lower stretching frequency is observed. However, a shift of the bands to a higher frequency implies slight strengthening of the bond. Upon substitution of the chloro group for the ethyl group, little change is observed in the stretching frequencies of the alkyne bond, hence the group *trans* to the pyridyl group has little effect on the electron density and so the strength of the alkyne bond.

^{1}H-NMR spectroscopic studies showed a shift in the *ortho-* pyridine protons to a lower frequency upon coordination to the chlorocobaloximes from 8.45 to 8.20 ppm. Ethylation was confirmed by the observation of a triplet resonance at around 0.4 ppm, which is in accordance with the ethylation results of **Chapter 3**. Upon ethylation, the *ortho-* pyridine peaks shift back to a higher frequency from 8.20 ppm to 8.55 ppm. The resonances attributed to the methyl groups of the equatorial DMGH ligand shifted from 2.41 to 2.14 ppm, upon ethylation. This factor can be attributed to the change in electron density on the cobalt centre transmitted through the π-electron system of the DMGH macrocycle. The ethyl group can be considered electron donating and the chloride as electron withdrawing, resulting in the DMGH methyl groups becoming more shielded and a lower frequency resonance observed following ethylation.

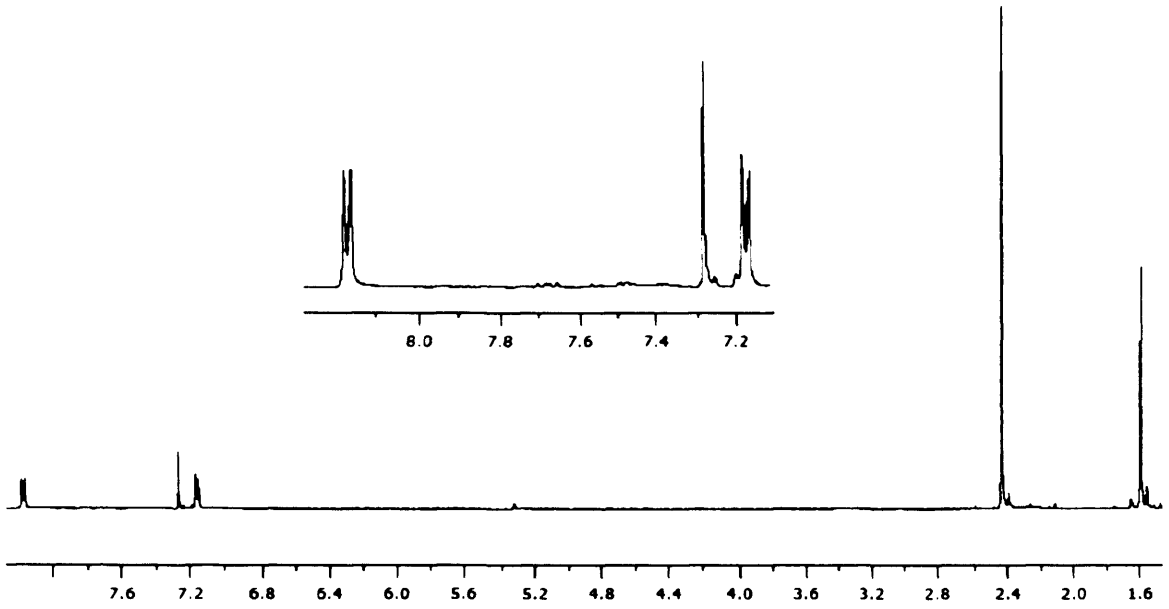

8.19 (2H, dd), 7.17 (2H, dd), 2.41, (12H, s), 1.59 (6H, s)

Figure 4.6. ^{1}H-NMR spectrum of **4.3**, recorded at 400 MHz in $CDCl_3$.

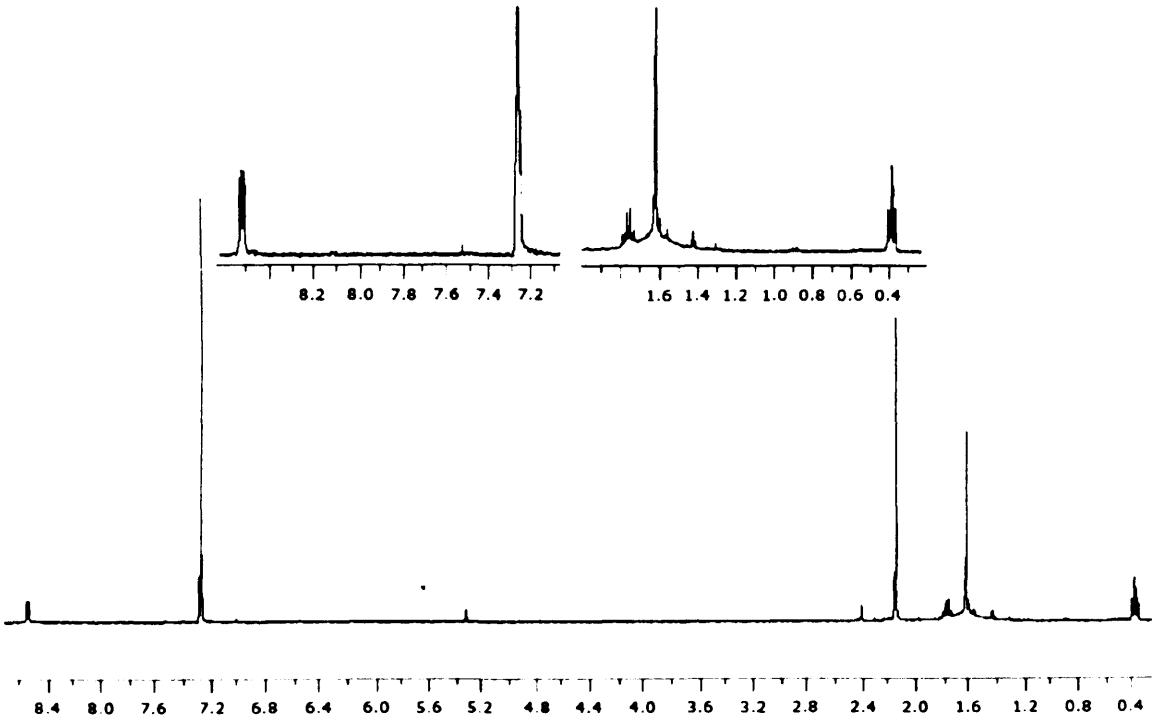

8.55 (2H, dd), 7.27 (2H, dd), 2.14, (12H, s), 1.75, (2H, q), 1.61 (6H, s), 0.36 (3H, t,).

Figure 4.7. ^{1}H-NMR spectrum of **4.5**, recorded at 400 MHz in $CDCl_3$.

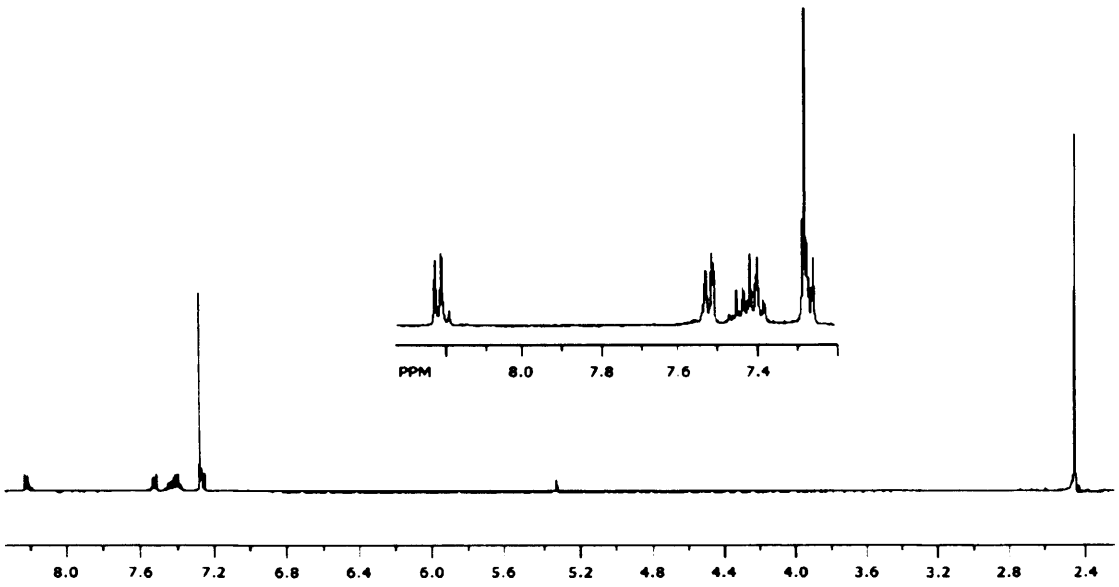

8.22 (2H, dd), 7.52 (2H, dd), 7.36-7.46 (3H, m), 7.27 (2H, dd), 2.43 (12H, s)

Figure 4.8. ^{1}H-NMR spectrum of **4.4**, recorded at 400 MHz in $CDCl_3$.

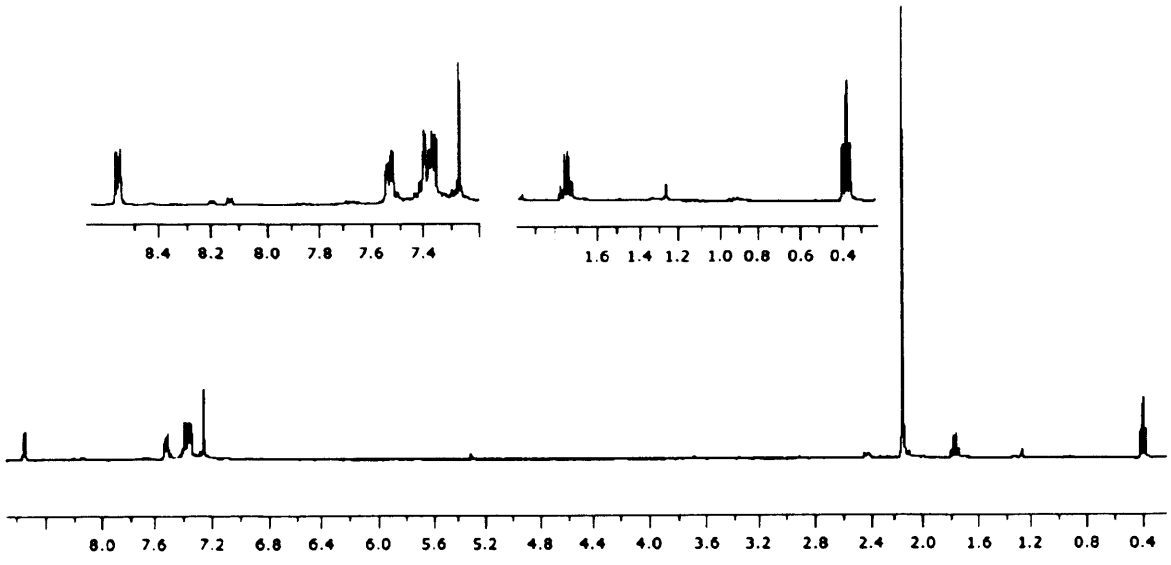

8.58 (2 H, dd), 7.55 (2 H, d), 7.37-7.41 (5H, m), 2.15 (12H, s), 1.76 (2H, q), 0.38 (3H, t,).

Figure 4.9. ^{1}H-NMR spectrum of **4.6**, recorded at 400 MHz in $CDCl_3$.

4.3.1.2 Synthesis of Dicobalt Bridged Cobaloximes.

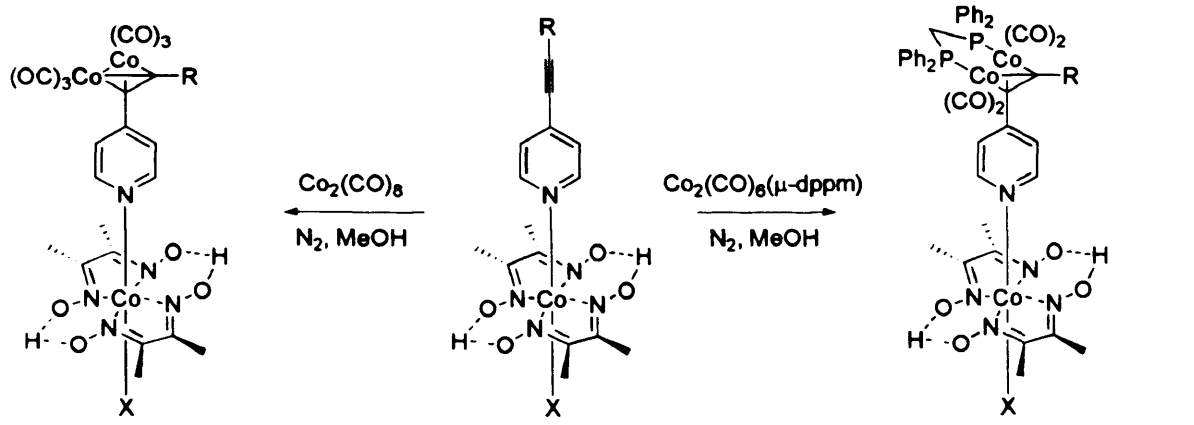

X = Cl, R = $C(Me)_2OH$ (**4.7**)
X = Cl, R = Ph (**4.8**)
X = Et, R = $C(Me)_2OH$ (**4.9**)
X = Et, R = Ph (**4.10**)

X = Cl, R = $C(Me)_2OH$ (**4.3**)
X = Cl, R = Ph (**4.4**)
X = Et, R = $C(Me)_2OH$ (**4.5**)
X = Et, R = Ph (**4.6**)

X = Cl, R = $C(Me)_2OH$ (**4.11**)
X = Cl, R = Ph (**4.12**)
X = Et, R = $C(Me)_2OH$ (**4.13**)
X = Et, R = Ph (**4.14**)

Scheme 4.12. Synthesis of dicobaltcarbonyl bridged cobaloximes.

Finally, in order to achieve cleavage of the Co-C bond, thus potentially allowing higher turn over in catalysis, dicobaltcarbonyl clusters, hoped to act as electron donors to the catalytically active cobalt centre, were incorporated into the cobaloximes. After careful analysis of the two synthetic routes, it was decided that the best route to incorporate the dicobalt carbonyl cluster into the cobaloxime was to synthesise the cobaloxime alkyne complex, and then to bridge it with the dicobaltcarbonyl clusters. The coordination of the preformed dicobaltcarbonyl pyridine ligand to $[Cl_2Co(DMGH_2)(DMGH)]$ requires basic conditions, as the dicobaltcarbonyl clusters were expected to be susceptible to the nucleophilic attack, hence, the method chosen limits the exposure of the pyridyl ligand to harsh conditions.

Under dry, inert conditions, methanolic solutions of alkynylcobaloximes were each reacted with both dicobaltoctacarbonyl and with dicobalthexacarbonyl diphenylphosphinomethane, $[Co(CO)_6(dppm)]$, to give the dicobalthexacarbonyl- and dicobalttetracarbonyl(dppm)- alkyne complexes **4.7** – **4.14**, respectively. In each case the reactions were followed by TLC analysis, with the formation of the cobalt carbonyl complex being indicated by the appearance of a dark red spot running higher than the parent alkyne. Recrystallisation from methanol afforded the pure compounds as red complexes.

The identities of the products were confirmed by the disappearance of the alkyne stretches (2230, 2215 cm^{-1}) and appearance of the characteristic terminal metal carbonyl stretching frequencies observed in the typical positions for $Co_2(CO)_6$ alkyne complexes (2020-2100 cm^{-1}) and $Co_2(CO)_4$(dppm) alkyne complexes (2030-1960 cm^{-1}) as shown in **Table 4.2**. In all cases, the IR spectrum revealed three ν(C≡O) bands for both the $Co_2(CO)_6$ alkyne and $Co_2(CO)_4$(dppm) alkyne complexes.

Complex	Wavenumber/cm^{-1} ν(C-O)
$Co_2(CO)_8$	2068, 2040, 2021
4.7	2082, 2062, 2022
4.8	2092, 2060, 2029
4.9	2095, 2059, 2042
4.10	2094, 2059, 2030
$Co_2(CO)_6$(μ-dppm)	2047, 2012, 1998
4.11	2011, 1991, 1961
4.12	2029, 2007, 1977
4.13	2032, 2002, 1976
4.14	2021, 1995, 1968

Table 4.2. The carbonyl stretches of alkynylpyridylcobaloximes.

Due to the fluxional nature of the dicobalt carbonyls, the ^{1}H-NMR spectra appeared broadened. Interestingly, the complexes derived from the addition of the dicobalt carbonyl fragment to the chloro-cobaloximes appeared to be paramagnetic from the ^{1}H-NMR in which the peaks were broad and shifted by comparison to the parent alkyne. This observation could indicate a delocalisation of electron density from the Co(0) centres of the cobalt carbonyl cluster, which has recently been proposed to be of a singlet diradical nature,[22] to the Co(III) cobaloxime nucleus. Unfortunately, the low long-term stability of these species so far has prevented a full study of this phenomenon.

Figure 4.13. Paramagnetic ^{1}H-NMR spectrum of **4.8**, recorded at 400 MHz in $CDCl_3$.

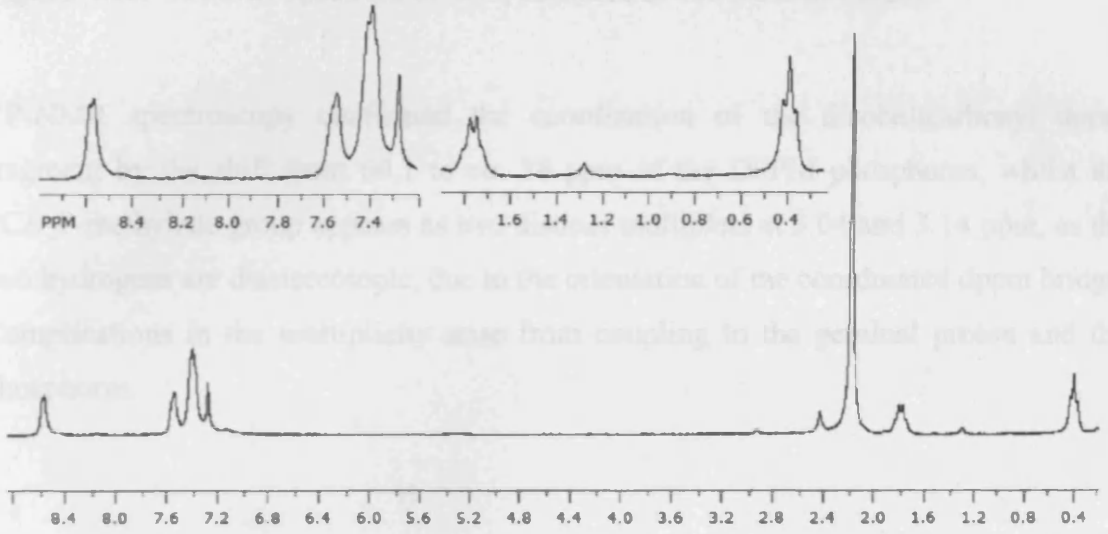

Figure 4.14. ^{1}H-NMR spectrum of **4.10**, recorded at 400 MHz in $CDCl_3$.

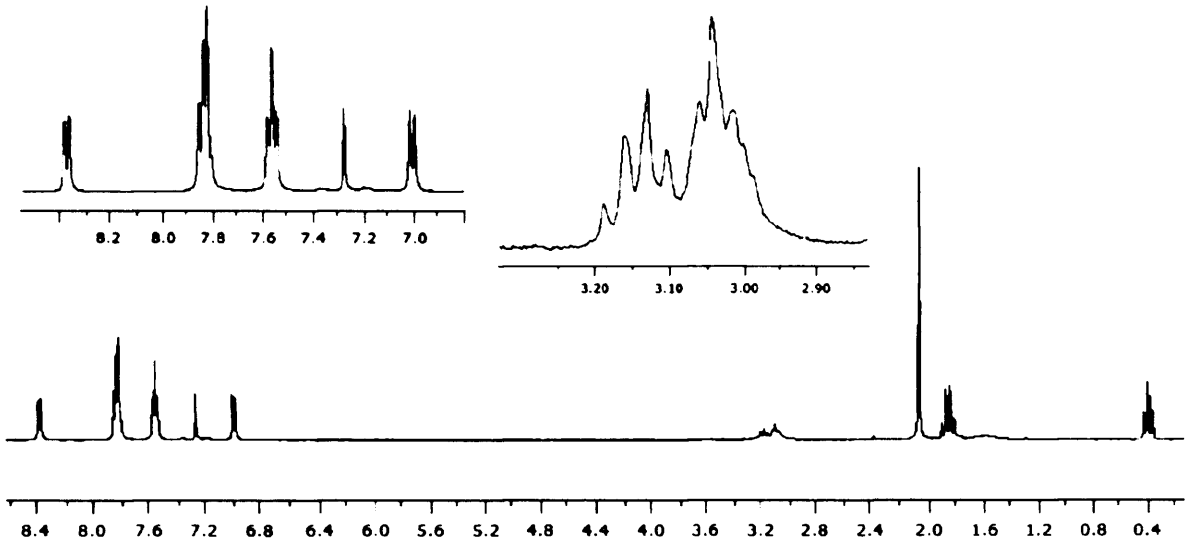

Figure 4.15. ^{1}H-NMR spectrum of **4.14**, recorded at 400 MHz in $CDCl_3$.

^{31}P-NMR spectroscopy confirmed the coordination of the dicobaltcarbonyl dppm fragment by the shift from 60.1 to *ca.* 38 ppm of the DPPM phosphorus, whilst the PCH_2P methylene group appears as two distinct multiplets at 3.04 and 3.14 ppm, as the two hydrogens are diastereotopic, due to the orientation of the coordinated dppm bridge. Complications in the multiplicity arise from coupling to the geminal proton and the phosphorus.

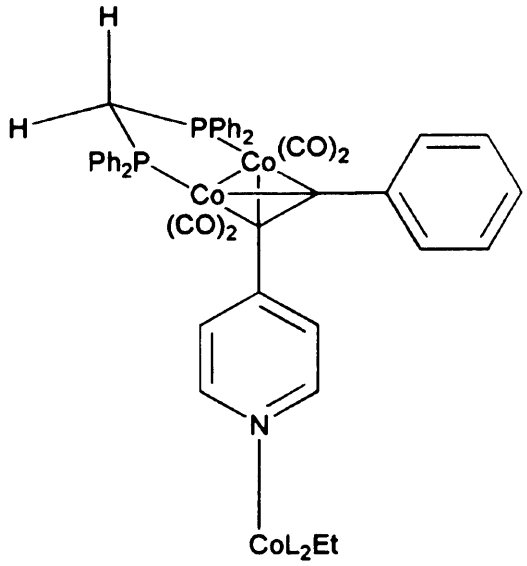

Figure 4.16. Diastereotopic hydrogens in the dppm backbone.

The stability of the dicobaltcarbonyl cobaloximes was investigated by leaving methanolic solutions of dicobalthexacarbonyl and dicobaltcarbonyl(dppm) bridged cobaloximes open to air for two weeks, after which a ^{1}H-NMR was recorded. The dicobalthexacarbonyl complex was found to decompose to an insoluble, black solid, believed to be cobalt particles, and a brown organic soluble compound, which upon analysis was found to be the alkynyl cobaloxime starting material. However, the dicobaltcarbonyl(dppm) bridged cobaloxime showed no black shiny solid, and the ^{1}H-NMR showed that no decomposition of the cobaloxime had occurred. Hence, the cobaloximes with a dppm backbone are more stable to air than the dicobalthexacarbonyl complexes.

4.3.2. Discussion of Crystal Structures.

Single crystals of complexes **4.3** and **4.4** were grown by slow evaporation of a saturated chloroform solution of the compound. Crystallographic refinement data are given in **Table 4.3**. The perspective ORTEP drawing of the studied complexes, **4.3** and **4.4**, with atomic numbering is shown in **Figures 4.17** and **4.18.**

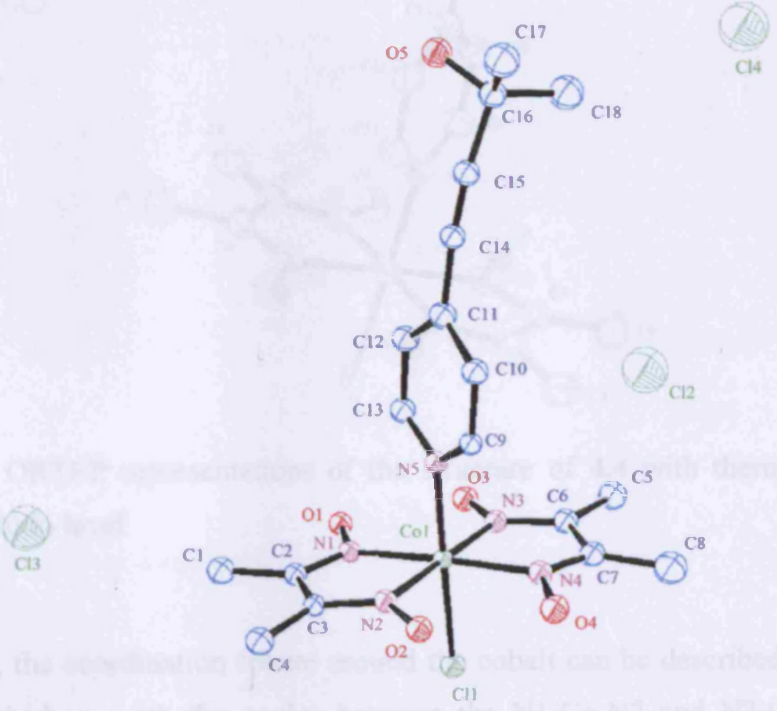

Figure 4.17. ORTEP representations of the structure of **4.3** with thermal ellipsoids drawn at the 50 % level.

In each case, the two dimethylglyoxime ligands form the equatorial plane, with the hydrogens of the hydroxy groups completing the macrocycle via two hydrogen bonds. The final two apical coordination sites are completed with the chloride moiety and the substituted pyridine species. The chlorides Cl2, Cl3 and Cl4 of **4.3** are fragments of disordered chloroform solvent molecules. Selected bond lengths and angles for **4.3** and **4.4** are given in **Tables 4.4** and **4.5** respectively. The Co-N (DMGH), Co-N (pyridine) and Co-Cl bond distances are close to those reported for analogous cobaloxime structures $[ClCo(DMGH)_2Pyr]$.[23] Upon comparison of complexes **4.3** and **4.4** the bond lengths were found to be essentially identical.

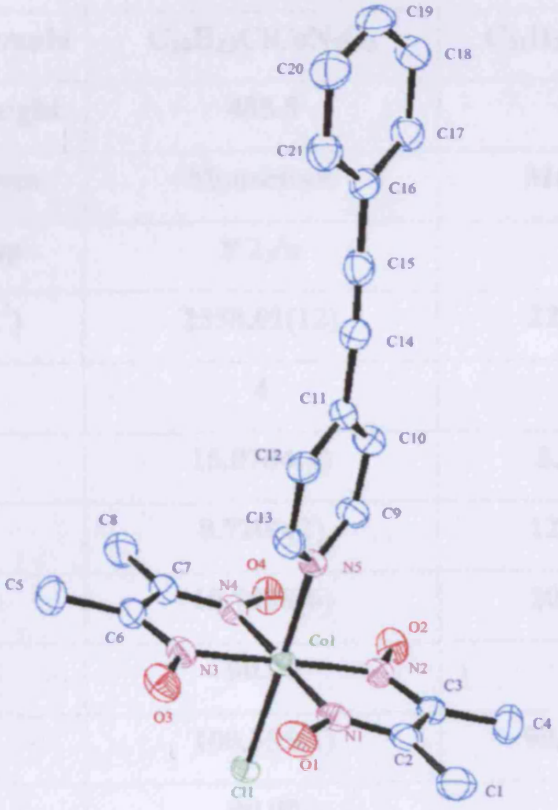

Figure 4.18. ORTEP representations of the structure of **4.4** with thermal ellipsoids drawn at the 50 % level.

In both cases, the coordination sphere around the cobalt can be described as a slightly distorted octahedron, with the angles between the N1-Co-N2 and N3-Co-N4 of the DMGH ligand approximately 80° and the angle between the DMGH ligands themselves, N1-Co-N3 and N2-Co-N4, was found to be closer to 100°, due to ring strain

of the planar Co-DMGH metallocycle. A slight distortion between the apical and the equatorial ligands is also observed, with the angle between the chloride and the DMGH ligands ranging from 87.7(2) to 89.48(18) and the angle between the pyridine and the DMGH ligands ranging from 89.7(3) to 91.9(3). This indicates that the DMGH equatorial ligands are bent away from the pyridine ligand, towards the chloride and is attributed to geometric constraints of the cell packing. In each case, the pyridine ring is observed to lie between the DMGH ligands so as to minimise the steric repulsion between the ortho- hydrogens and the DMGH atoms.

	4.3	**4.4**
Empirical Formula	$C_{18}H_{25}ClCoN_5O_5$	$C_{21}H_{23}ClCoN_5O_4$
Molecular weight	**485.5**	**503.5**
Crystal system	**Monoclinic**	**Monoclinic**
Space group	**P 2_1/n**	**P 2_1/c**
Volume (Å^3)	**2558.01(12)**	**2225.54(9)**
Z	**4**	**4**
a (Å)	**15.0784(4)**	**8.7740(2)**
b (Å)	**8.7200(2)**	**12.3980(3)**
c (Å)	**19.7898(6)**	**20.7280(5)**
α (°)	**90.00**	**90.00**
β (°)	**100.555(1)**	**99.2400(10)**
γ (°)	**90.00**	**90.00**

Table 4.3. Collection and refinement data for complexes **4.3** and **4.4**.

The alkyne group of the substituted pyridine deviates from the ideal linear geometry, as shown in **Figure 4.19**, with the Pyr-C≡C angle of 172.8(8)° and 179.82(4)°, and with the C≡C-C angle of 173.6(8)° and 174.97(3)° instead of the expected 180 ° for **4.3** and **4.4**

respectively. This originates from the packing within the unit cell. **Figure 4.20** shows the unit cells of both complexes, and it can be observed that the π systems of the 4-(2-phenylethynyl)pyridine ligand are distorted towards each other, presumably due to π stacking. However, the more bulky CMe_2OH group is held in close proximity to a DMGH ligand, which forces the 2-methyl-4-(pyridin-4-yl)but-3-yn-2-ol ligand to bend away from the cobaloxime centre.

Co-N1	1.894(6)	**N5-Co-N2**	91.7(2)
Co-N2	1.896(6)	**N5-Co-N3**	91.6(3)
Co-N3	1.903(6)	**N5-Co-N4**	89.7(3)
Co-N4	1.896(6)	**Cl-Co-N1**	88.80(19)
Co-N5	1.967(6)	**Cl-Co-N2**	89.48(18)
Co-Cl1	2.235(2)	**Cl-Co-N3**	87.7(2)
C≡C	1.170(10)	**Cl-Co-N4**	89.2(2)
N1-Co-N2	81.4(3)	**N5-Co-Cl**	178.73(18)
N3-Co-N4	80.9(3)	**N1-Co-N4**	176.5(3)
N1-Co-N3	99.3(3)	**N2-Co-N3**	178.4(3)
N2-Co-N4	98.3(3)	**Pyr-C≡C**	172.8(8)
N5-Co-N1	91.9(3)	**C≡C-C**	173.6(8)

Table 4.4. Selected bond length (Å) and angles (deg) for complex **4.3**.

Co-N1	1.895(2)	**N5-Co-N2**	91.62(10)
Co-N2	1.890(2)	**N5-Co-N3**	89.96(9)
Co-N3	1.892(2)	**N5-Co-N4**	89.39(10)
Co-N4	1.883(2)	**Cl-Co-N1**	89.21(7)
Co-N5	1.970(2)	**Cl-Co-N2**	88.89(7)
Co-Cl1	2.2424(7)	**Cl-Co-N3**	89.30(7)
C≡C	1.173(4)	**Cl-Co-N4**	90.11(7)
N1-Co-N2	80.69(10)	**N5-Co-Cl**	179.15()
N3-Co-N4	99.12(11)	**N1-Co-N4**	178.74(10)
N1-Co-N3	81.62(10)	**N2-Co-N3**	178.49(10)
N2-Co-N4	98.54(10)	**Pyr-C≡C**	179.82(4)
N5-Co-N1	91.54(9)	**C≡C-C**	174.97(3)

Table 4.5. Selected bond length (Å) and angles (deg) for complex **4.4**.

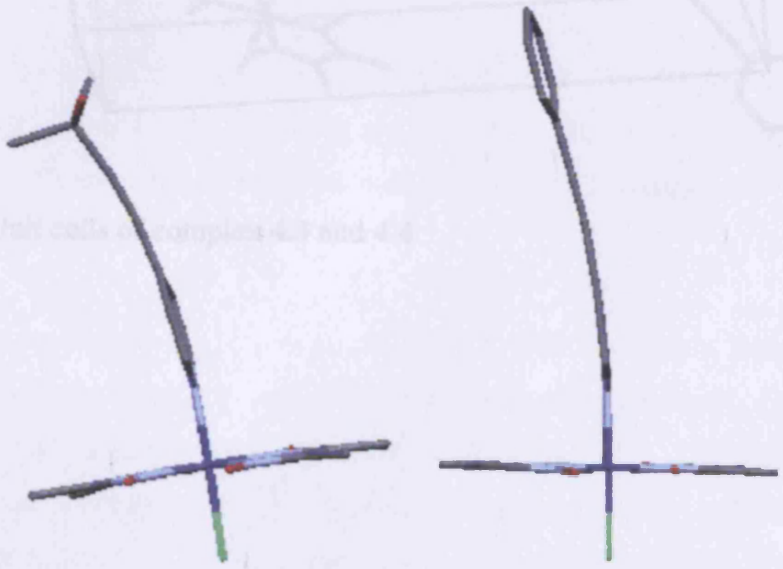

Figure 4.19. The distortion in pyridine substituent in complexes **4.3** and **4.4**.

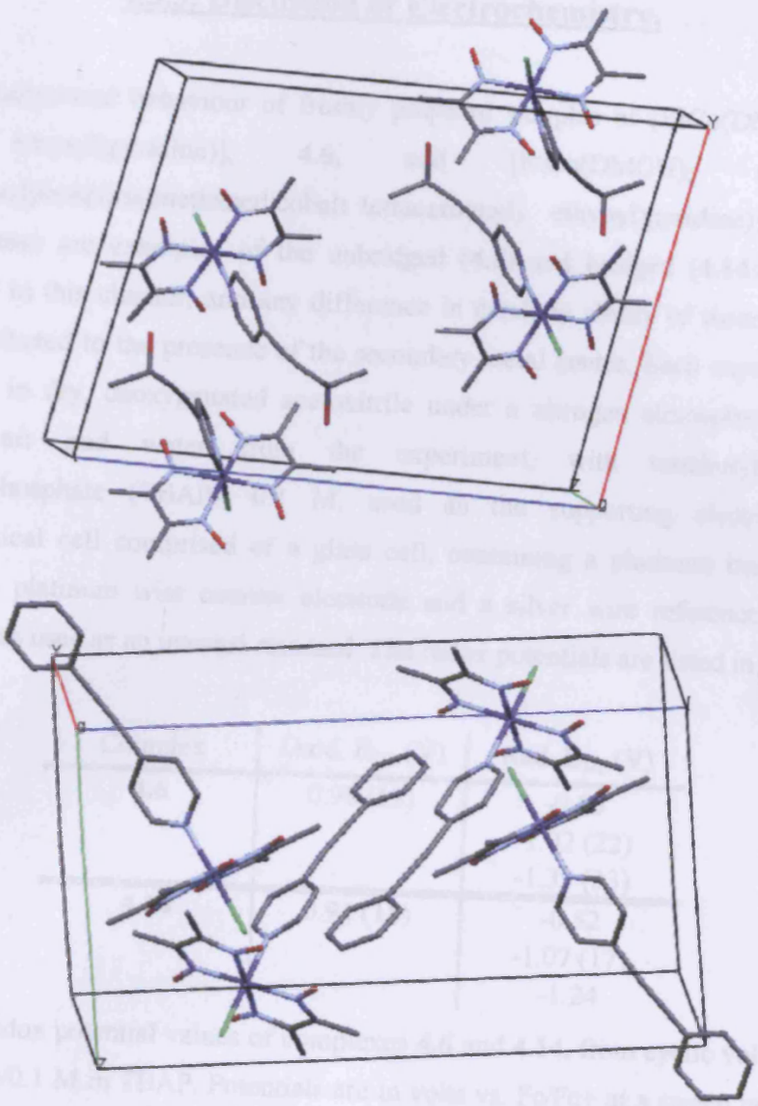

Figure 4.20. Unit cells of complex **4.3** and **4.4**.

4.3.3. Discussion of Electrochemistry.

The electrochemical behaviour of freshly prepared samples of [EtCo(DMGH)$_2$(4-(2-phenyl ethynyl)pyridine)], **4.6,** and [EtCo(DMGH)$_2$ (4-(2-phenyl μ^2(μ^2diphenylphosphinomethanedicobalt tetracarbonyl) ethynyl)pyridine)], **4.14**, was studied. These are examples of the unbridged (**4.6**) and bridged (**4.14**) complexes synthesised in this chapter, and any difference in catalytic ability of these complexes may be attributed to the presence of the secondary metal centre. Each experiment was carried out in dry, deoxygenated acetonitrile under a nitrogen atmosphere, so as to eliminate air and water from the experiment, with tetrabutylammonium hexafluorophosphate (TBAP), 0.1 M, used as the supporting electrolyte. The electrochemical cell comprised of a glass cell, containing a platinum bead working electrode, a platinum wire counter electrode and a silver wire reference electrode. Ferrocene was used as an internal standard. The redox potentials are listed in **Table 4.6**.

Complex	Oxid. $E_{1/2}$ (V)	Red. $E_{1/2}$ (V)
4.6	0.98 (13)	-0.50
		-1.02 (22)
		-1.39 (33)
4.14	0.94 (18)	-0.52
		-1.07 (17)
		-1.24

Table 4.6. Redox potential values of complexes **4.6** and **4.14**, from cyclic voltammetry in acetonitrile/0.1 M in TBAP. Potentials are in volts vs. Fc/Fc+ at a sweep rate of 200 mVs^{-1}. The difference between cathodic and anodic peak potentials (mV) is given in parentheses.

The complexes studied show a reversible oxidation at 0.94 and 0.98 V, corresponding to a Co(III)/Co(IV) metal centre oxidation. The dicobalttetracarbonyl dppm bridged species, **4.14**, exhibits two further oxidations; at 1.05 and 1.23 V. The first oxidation is reversible and the second irreversible. In each reduction cycle, there are three reduction potentials present. There is little change in those observed around -0.50 and -1.05 V upon comparison of **4.6** and **4.14**, with **4.6** exhibiting a more positive oxidation value than **4.14** by 0.02 V and 0.05 V respectively. However, upon comparison of the third

potential, there is a 0.15 V shift to a more positive value upon bridging complex **4.6** with the dicobalt fragment to give **4.14**, from -1.39 to -1.24 V. This indicates that there is more electron density on the cobalt centre of **4.14** than that of **4.6**, making it more difficult to reduce it, but the extra electron density provides more for the electron transfer to PCE in the first step of catalysis.

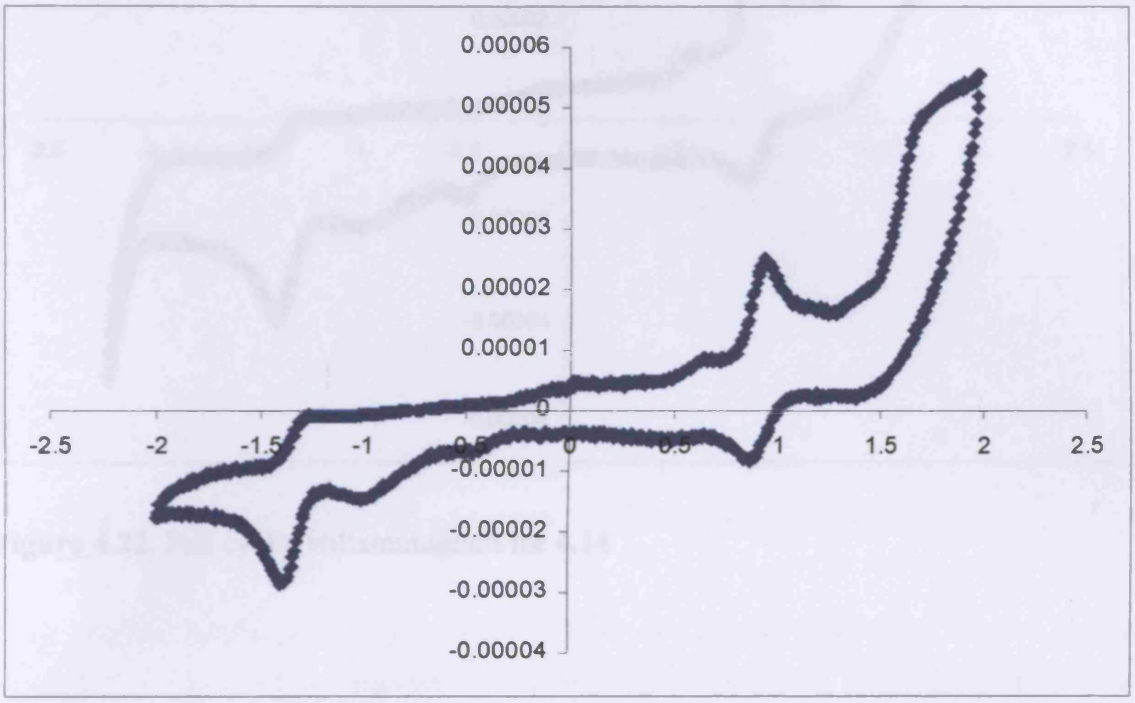

Figure 4.21. Full cyclic voltammogram for **4.6**.

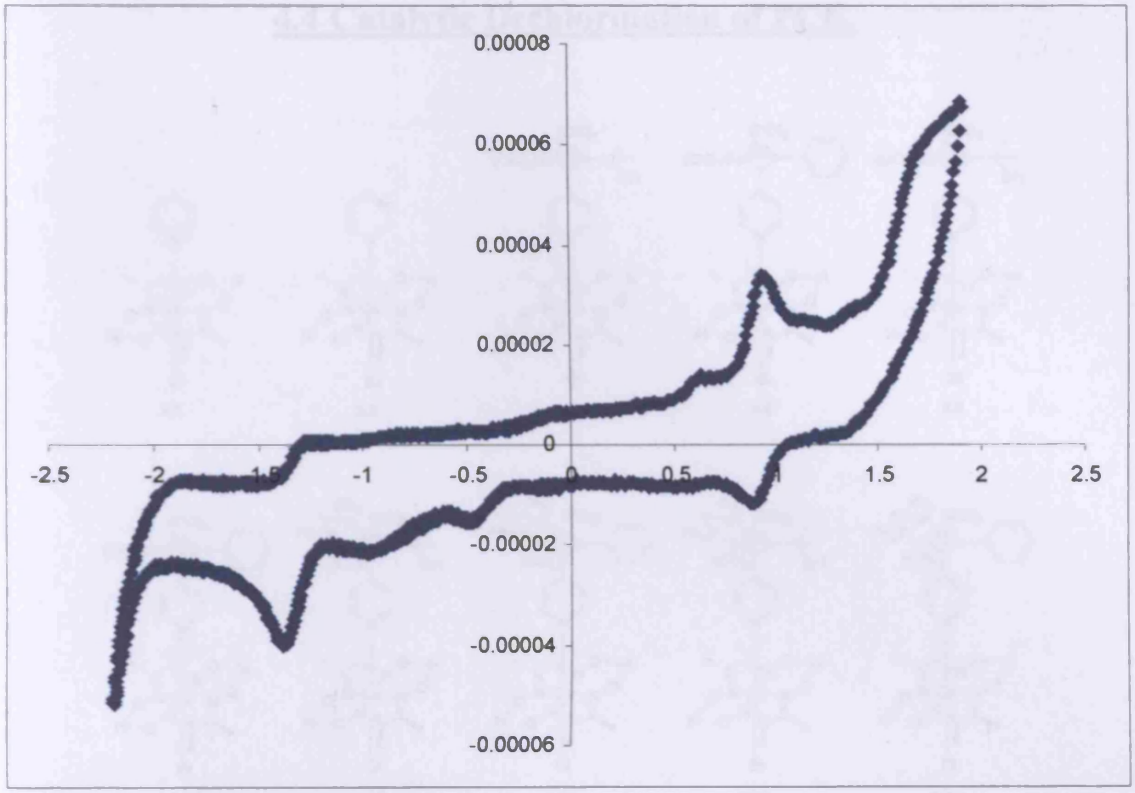

Figure 4.22. Full cyclic voltammogram for **4.14**.

4.4 Catalytic Dechlorination of PCE.

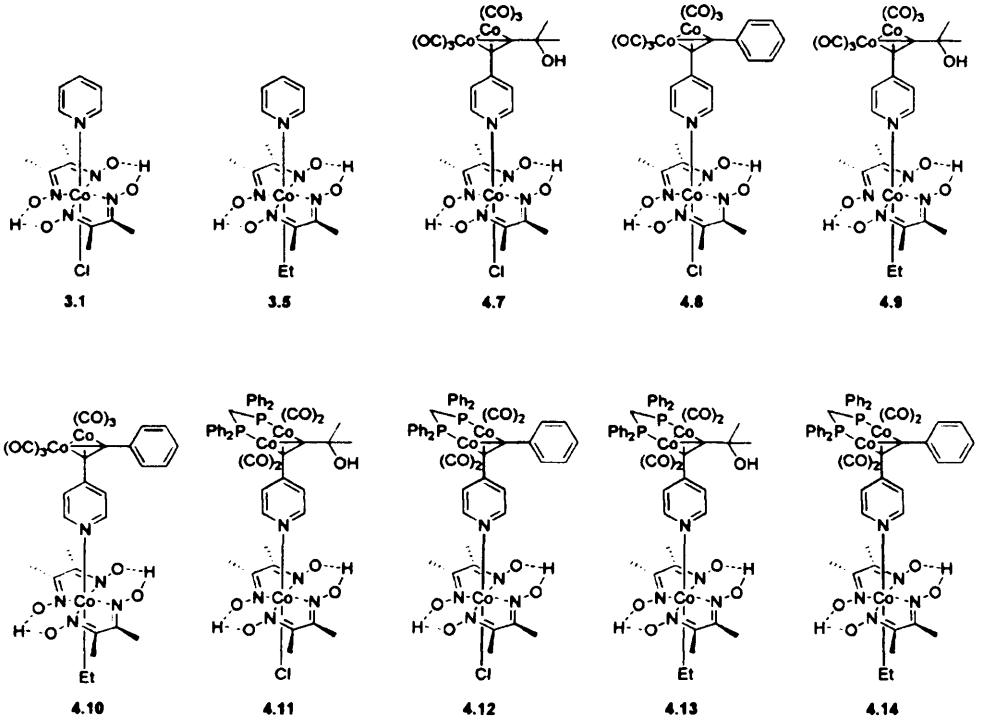

Figure 4.23. Cobaloximes prepared for catalytic dechlorination of PCE.

With freshly synthesised multimetallic cobalt complexes, shown in **Figure 4.23**, available, a series of experiments were undertaken to probe their effectiveness as catalysts in the dechlorination of PCE, where a 10 fold excess of PCE was treated with each of the proposed catalysts in methanolic solution and sodium borohydride as the sacrificial reducing agent. The loss of PCE and the production of TCE were monitored by gas chromatography against an internal standard of anisole and the reactions carried out in a sealed tube to prevent volatilisation of the products. A blank experiment with no cobalt species present validated the procedure by confirming that no loss of PCE or production of TCE was observed, indicating that the anisole and the sodium borohydride are not directly involved in the dechlorination of PCE or TCE. The results of the catalysis screening are summarised in **Table 4.7**.

Catalyst	Equiv. of PCE consumed	Equiv. of TCE recovered	Equiv. of DCE recovered	Equiv. further reduced
None	0	0	0	0
$[Cl_2Co(DMGH)(DMGH_2)]$	1.3	0.8	0	0.3
$Co_2(CO)_8$	1.1	0.2	0.3	0.8
$Co_2(CO)_6(dppm)$	1.1	0.1	0.8	0.9
3.1	3.8	1.9	0.9	0.5
3.5	3.2	2.3	0.5	0.2
4.7	4.5	1.0	0.2	3
4.8	4.5	0.6	3	3.6
4.11	3.8	1.6	3.6	1.4
4.12	4.7	1.4	1.4	2.2
4.9	7.3	0.9	2.2	5
4.10	7.9	1.4	5	5.2
4.13	7.6	0.4	5.2	6.4
4.14	8.2	1.0	6.4	6.9

Table 4.7. Catalytic dechlorination of PCE results. Reaction conditions: 1 mmol of catalyst, 10 mmol of PCE, 1 mmol of anisole, as the internal standard in methanol, 5 ml. 3 mmol of sodium hydroxide and 2 mmol of sodium borohydride in 1 ml of water added. Sample run through celite and silica, and submitted for GC and GC-MS analysis.

While $[Cl_2Co(DMGH)(DMGH_2)]$ appeared to act as a near stoichiometric reagent (1.3 equivs. of PCE consumed) the observation that a significant quantity of TCE (0.8 equivs.) was produced implies that for this species the inefficient catalysis is not a function of irreversible formation of an organometallic species. However, as it is possible in this case that a cobalt dihydrocarbyl species may be formed (although no discrete organometallic products were isolated from this reaction) it is difficult to draw conclusions about the comparison of this reaction with that of pyridyl cobaloximes or B_{12} itself. The free $Co_2(CO)_8$ and $Co_2(CO)_6(dppm)$ also react stoichiometrically with the PCE, only dechlorinating one equivalent of perchloroethene. However, this is reduced further, presumably due to the fact that there are two cobalt atoms present, adding weight to the premise that multimetallic species are better dechlorination catalysts. It is useful to remember that, as discussed in **Chapter 3**, the first step of dechlorination of PCE is believed to proceed via a one electron transfer from the Co(I) cobaloxime to the chlorinated olefin, whilst subsequent reduction proceeds via organocobalt species. It has

been postulated that the enhancement in catalytic ability is due to the incorporation of the secondary metal centre, which aids the electron transfer from the cobaloxime to the trichloroethynyl radical in the final step of making TCE.

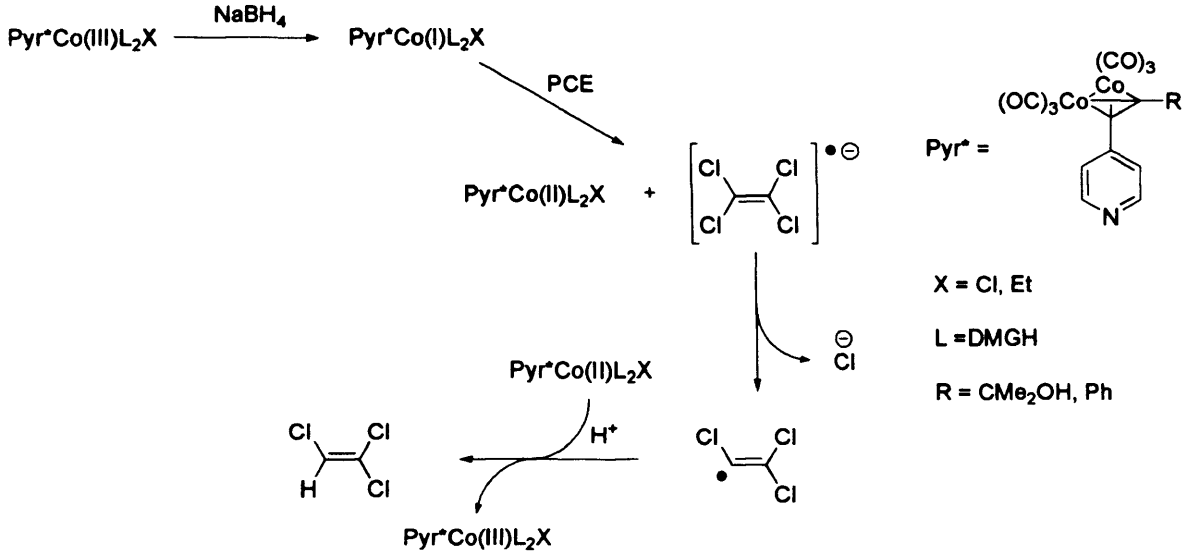

Scheme 4.13. First step of dechlorination catalysis.

Some catalytic activity was observed with simple pyridyl cobaloximes **3.1** and **3.5**. The level of PCE loss observed with pyridyl cobaloximes was higher, with between 3 and 4 equivalents of PCE consumed in each case, and significant levels of TCE observed, indicating that one dominant reaction is the mono-dechlorination, in which no organometallic is thought to be involved and that the further reactions are very limited. These low turnovers are compatible with a model in which a stable vinyl cobalt species is only slowly degraded and thus limits turnover. The low turnover numbers are thought to be a result of eventual catalyst degradation, as after the standard reaction time is completed, addition of further borohydride did not lead to further dechlorination, indicating that the catalytically active species had decomposed.

However, all of the complexes incorporating dicobalt carbonyl species showed a much greater degree of dechlorination, with the TCE formation being much less pronounced, possibly indicating that a different mechanistic pathway dominated, or that subsequent reductions occur very fast. The proposed function of the secondary metal centre was to provide a route for facile re-reduction of the active cobalt centre and allow cleavage of Co-C bonds, which should then give the possibility of further dechlorination reactions.

If, as discussed in **Section 3.1.1**, the first dechlorination step is indeed a simple electron transfer, and it is only subsequent dechlorinations which involve the formation of organocobalts, then it may be that the simple cobaloximes could represent catalysts for the formation of TCE, which are then deactivated by formation of organocobalts, and are never catalysts at all for subsequent dechlorinations. Alternatively, the multimetallic species could be catalysts for both the electron transfer first dechlorination and for subsequent steps. The mechanism by which the borohydride reduction is mediated by the cobalt cluster is unclear, but the effect is undoubtedly real.

The degree of PCE consumption was also larger for all of these multimetallic species, although there was no increase in PCE consumption associated with the phosphine-bridged species, which had been intended to confer greater stability on the catalysts and thus allow for further turnover. This suggests that the mechanism of catalyst deactivation does not involve degradation of the cobalt carbonyl cluster, but instead some other process. It was clear, however, from the results obtained that the alkylated species were the most effective catalysts with 7-8 equivalents of PCE being consumed per catalyst, and very little TCE produced (full dechlorination involves four turnovers of catalyst per molecule of PCE). In order to eliminate the possibility that a different mechanism was operating in which the dicobalt carbonyl species are responsible for the dechlorination, catalytic runs were performed in which each of these species were tested as catalysts without cobaloximes. However in no case was any significant degree of catalytic activity observed, although all were stoichiometric dechlorinaters.

GC-MS confirmed that in the multimetallic systems, the stepwise dechlorination of PCE proceeds via dichloroethene down to vinyl chloride, which was not detected in the mononuclear cobaloximes. In all cases, no chloroacetylene or acteylene was observed as by-products from the reaction. This could indicate an alternative mechanism for the dechlorination of DCE and VC, than is presented in the literature and discussed in **Chapter 3**, is taking place, or that, along with ethylene, it could not be detected due to the parameters of the GC-MS. The catalytic cycle demonstrated in **Scheme 4.14** shows how the incorporation of the secondary metal centre, and its ability to transfer electrons to and from the catalytically active cobaloxime centre, could facilitate the cleavage of the Co-C bond. It has yet to be determined whether the organocobalt species obtained

from the loss of the final chloride, shown below, is the final product of the catalysis cycle, or if cleavage of the Co-C bond occurs to yield the free ethylene, due to a strong trans influence of the dicobaltcarbonyl bridged pyridine, as any ethylene afforded is too volatile to be detected using this current procedure.

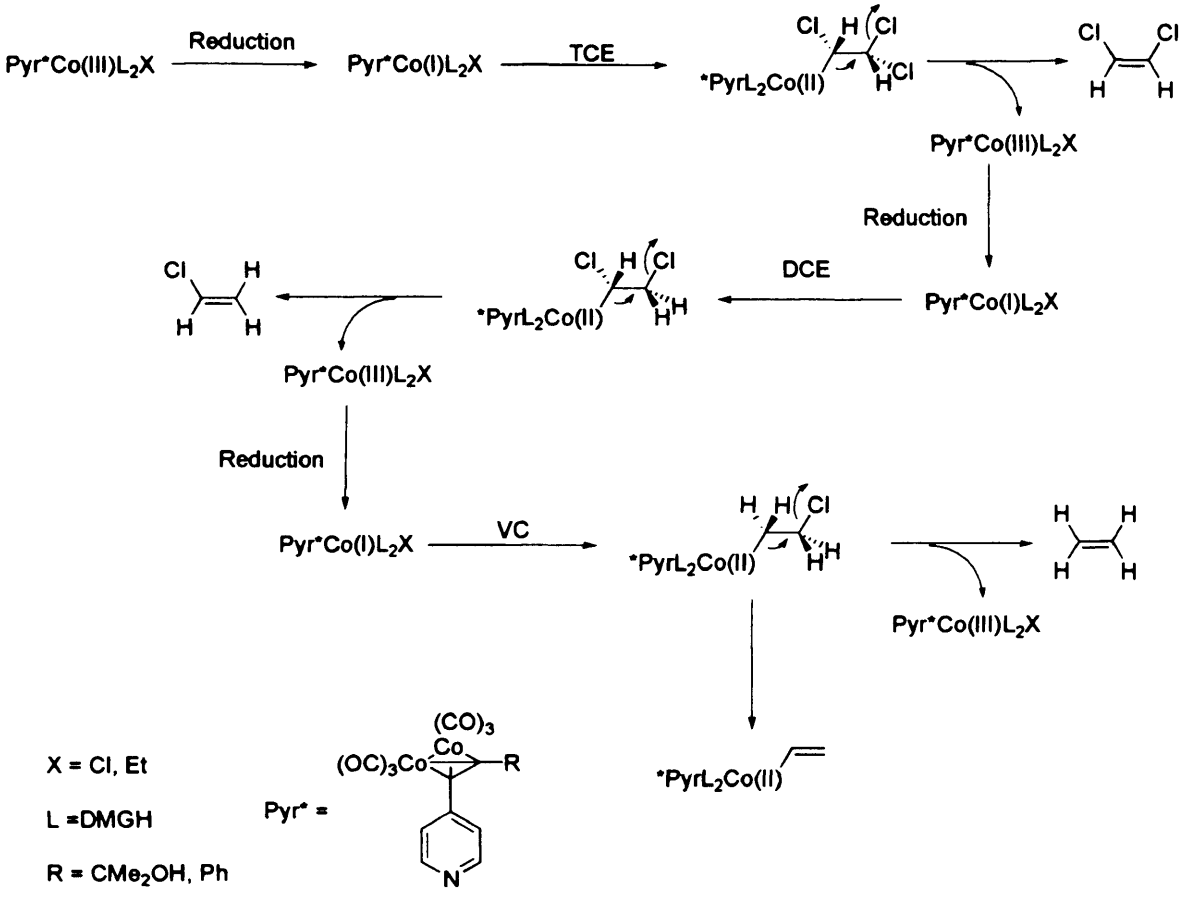

Scheme 4.14. Possible mechanism for the reduction of TCE to ethylene, without the formation of chloroacetylene or acetylene.

These results show that a degree of catalytic activity, albeit moderate, is achieved with the combination of cobaloximes and dicobalt carbonyl species, and provide *prima facie* support for the proposal that incorporation of secondary redox-active centres into cobaloximes allows for the reductive cleavage of the vinyl cobalt species. However, it is not immediately apparent why the alkyl cobaloximes should be such superior pre-catalysts to the chloro analogues, as evidence for the loss of both the axial ligands was provided by crossover reactions of **Chapter 3**, and should have little influence on the catalytic ability, as they are likely to be spectator ions in the catalysis cycle.

The most active catalysts **4.13** and **4.14** were tested for higher activity by reducing the catalyst loading to 1 mol %, and it was found that 7 % and 8 % of PCE had been dechlorinated respectively, though there was a decrease in the amount of TCE reduced further. This suggests that 8 equivalents is the maximum reactivity of the catalysts. Addition of further borohydride led to only a small amount of further dechlorination of PCE and TCE, indicating that the catalytic species had become inactive. Since there is little change in the amount of PCE consumed, it can be rationalised that after the first series of reactions, an organometallic intermediate is formed- which prevents further dechlorination. This organocobalt species is resistant to reduction, even when a second dose of sodium borohydride is added. This is in accordance with the findings of van der Donk, who observed ethenecobaloximes upon reduction of vinylchloride (**Chapter 3**).

Catalyst	Equiv. of PCE in	Equiv. of PCE consumed	Equiv. of TCE recovered	Equiv. further reduced	Estimated TON
4.13	10[a]	7.6	0.4	7.2	14.8
4.14	10[a]	8.2	1.0	7.2	15.4
4.13	10[b]	7.7	0.4	7.3	15.0
4.14	10[b]	8.4	0.7	7.7	16.1
4.13	100[c]	7.3	3.3	4.0	11.3
4.14	100[c]	8.1	3.2	4.9	13.0

Table 4.8. [a]Conditions: 1 mmol of catalyst, 10 mmol of PCE, 1 mmol of anisole, as the internal standard in methanol 5 ml. 3 mmol of sodium hydroxide and 2 mmol of sodium borohydride in 1 ml of water added. [b]Conditions: 1 mmol of catalyst, 10 mmol of PCE, 1 mmol of anisole, as the internal standard in methanol 5 ml. 3 mmol of sodium hydroxide and 2 mmol of sodium borohydride in 1 ml of water added, with a second dose added 30 minutes after the first addition. [c]Conditions: 1 mmol of catalyst, 100 mmol of PCE, 1 mmol of anisole, as the internal standard in methanol 5 ml. 3 mmol of sodium hydroxide and 2 mmol of sodium borohydride in 1 ml of water added.

Calculating a turnover number for these catalysts is difficult, since the number of cycles completed until the catalyst ceases to work depends on the degree of chlorination of remaining molecules. However, it can be estimated that the addition of the number of PCE equivalents reduced plus the number of TCE and DCE equivalents further reduced

would give a comparative turnover number, and this data is recorded in **Table 4.9**. These numbers are not perfect, as they do not include the turnover from VC to any ethylene produced.

Catalyst	Estimated TON
None	0.0
$[Cl_2Co(DMGH)(DMGH_2)]$	1.8
$Co_2(CO)_8$	2.0
$Co_2(CO)_6(dppm)$	2.1
3.1	5.7
3.5	4.1
4.7	8.0
4.8	8.4
4.11	6.0
4.12	8.0
4.9	13.7
4.1	14.4
4.13	14.8
4.14	15.4

Table 4.9. Estimated turnover numbers.

4.5. Conclusions.

A series of cobaloximes were synthesised and characterised, bearing an alkyne bond for the means of bridging this with a dicobaltcarbonyl fragment. The dicobaltcarbonyl-bridged species, where the ligand *trans-* to the multimetallic ligand is a chloride appeared to be paramagnetic, whereas those *trans-* to an ethyl group appeared diamagnetic. When the catalytic ability of these complexes was investigated, the pyridyl cobaloximes of **Chapter 3** were shown to react catalytically with PCE, with 50 and 70 % of which underwent only one reaction to TCE, with the rest carrying on to give DCE. No conversion to VC was observed with these cobaloximes. The multimetallic cobaloximes were observed to dechlorinate more of the PCE (between 3.8 and 8.2 equivalents) but the greatest enhancement in catalytic ability came in the second step of the catalysis- in most cases, 80 % of the TCE is reduced further to DCE and VC. This coincided with incorporation of dppm fragments into ethylcobaloximes.

In conclusion, the dicobaltcarbonyl-bridged cobaloximes synthesised in this chapter, are rare examples of molecular organotransition metal compounds that are able to catalytically reductively dechlorinate PCE stepwise to VC via TCE and DCE. More remarkably, these dechlorination reactions are undertaken at standard temperature and pressure under aerobic conditions. The ethylated diphenylphosphinomethane bridged cobaloximes were shown to be the most active catalysts, dechlorinating 7.5 and 8.5 equivalents of PCE reduced, with upwards of 90 % being reduced to DCE and further.

4.6. Experimental.

[ClCo(DMGH)$_2$(4-Bromopyr)] 4.1[24]

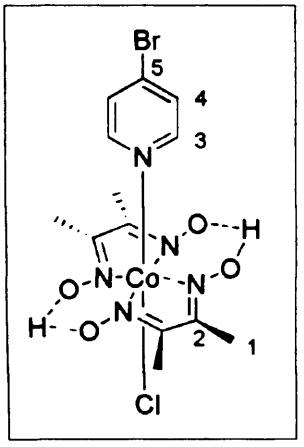

To a suspension of [Cl_2Co(DMGH)($DMGH_2$)] (2.5 g, 6.93 mmol) in dichloromethane (10 ml) was added 4-bromopyridine hydrochloride (1.35 g, 6.93 mmol) and sodium bicarbonate (10ml) sequentially. The mixture was stirred at room temperature for 2 hours and the resultant brown solution was diluted with dichloromethane (20 ml) and washed with water (2 x 20 ml). The organic fractions were combined, dried over Na_2SO_4, filtered and evaporated to dryness, yielding [ClCo(DMGH)$_2$(4-Bromopyr)] as a brown solid (3.16 g, 95 %). δH ($CDCl_3$) (ppm) 8.10 (2 H, dd, *J* = 6.9, 1.1 Hz, C*H* (3) Pyr), 7.41 (2 H, dd, *J* = 6.9, 1.1 Hz, C*H* (4) Pyr), 2.43 (12 H, s, CH_3 (1) DMGH). δC ($CDCl_3$) (ppm) 152.8 (C (3) Pyr), 151.4 (C (2) DMGH), 137.4 (C (5) Pyr), 129.3 (C (4) Pyr), 13.2 (C (1) DMGH). *m/z* (ESI) 504.1 $[MNa]^+$. HRMS (ESI) calculated $[MH]^+$ = 481.9637; measured $[MH]^+$ = 481.9651.

[EtCo(DMGH)$_2$(4-Bromopyr)] 4.2

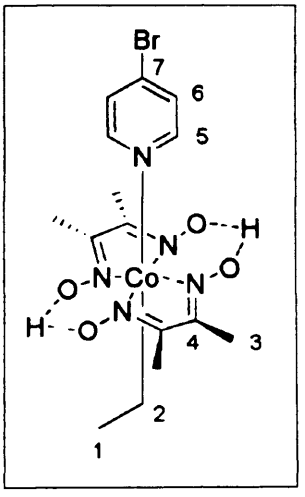

To a solution of [ClCo(DMGH)$_2$(4-Bromopyr)] (2.5 g, 5.18 mmol) and iodoethane (0.46 ml, 5.75 mmol) in MeOH (20 ml) was added $NaBH_4$ (0.23 g, 5.75 mmol). The mixture was stirred for 30 minutes at room temperature, when the solvent was removed under vacuum, and the crude solid was dissolved in dichloromethane (10 ml) and washed with distilled water (2 x 10 ml). The organic fractions were combined, dried over Na_2SO_4, filtered and evaporated to dryness, yielding [EtCo(DMGH)$_2$ (4-Bromopyr)] as a brown solid (2.29 g, 93 %). δH ($CDCl_3$) (ppm) 8.43 (2 H, dd, *J* = 5.3, 1.2 Hz, C*H* (5) Pyr), 7.49 (2 H, dd, *J* = 5.3, 1.3 Hz, C*H* (6) Pyr), 2.14 (12 H, s, CH_3 (3) DMGH), 1.75 (2 H, q, *J* = 7.7 Hz, CH_2 (2) Co-CH_2-CH_3), 0.35 (3 H, t, *J* = 7.6 Hz, CH_3 (1) Co-CH_2-CH_3). δC ($CDCl_3$) (ppm) 150.7 (C (7) Pyr), 149.3 (C (4) DMGH), 141.5, (C (7) Pyr), 129.3 (C (6) Pyr), 40.5 (C (2) CH_2 Co-CH_2-

CH_3), 13.3 (C (3) DMGH), 12.0 (C (1) CH_3 Co-CH_2-CH_3). *m/z* (ESI) 477.2 $[MH]^+$ HRMS (ESI) calculated $[MH]^+$ = 476.0344; measured $[MH]^+$ = 476.0361.

[ClCo(DMGH)$_2$(2-methyl-4-(pyridin-4-yl)but-3-yn-2-ol)] 4.3

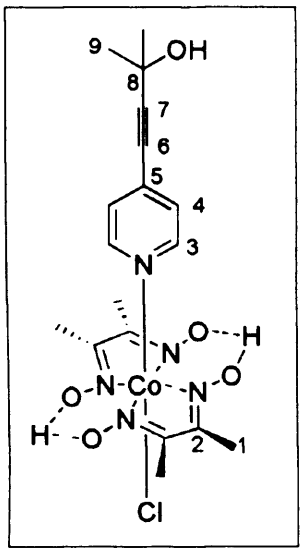

To a stirred suspension of $[Cl_2Co(DMGH)(DMGH_2)]$ (1 g, 2.77 mmol) and 2-methyl-4-(pyridin-4-yl)but-3-yn-2-ol (0.45 g, 2.77 mmol) in dichloromethane (15 ml) was added $NaHCO_3$ (15 ml). The reaction was allowed to stir for 1 hour at which point the solution was diluted further with dichloromethane (20 ml) and washed with water (2 x 20 ml). The organic fractions were combined, dried, filtered and evaporated to dryness, yielding [ClCo(DMGH)$_2$(2-methyl-4-(pyridin-4-yl)but-3-yn-2-ol)] as a brown solid (1.22 g, 91 %). δH ($CDCl_3$) (ppm) 8.19 (2 H, dd, *J* = 6.8 Hz, 1.2Hz, C*H* (3) Pyr), 7.17 (2 H, dd, *J* = 6.7 Hz, 1.1 Hz C*H* (4) Pyr), 2.41, (12 H, s, CH_3 (1) DMGH), 1.59 (6 H, s, CH_3 (9) CMe_2OH). δC ($CDCl_3$) (ppm) 151.7 (*C* (2) DMGH), 149.4 (*C* (3) Pyr), 133.9 (*C* (5) Pyr), 126.6 (*C* (4) Pyr), 103.3 (*C* (7) Pyr-C≡*C*), 83.1 (*C* (6) Pyr-*C*≡C), 64.5 (C (8) *C*Me_2OH), 30.1 (C (9) C(*C*H_3)$_2$OH), 12.1 (*C* (1) DMGH). ν (C≡C) 2234.1. *m/z* (ESI) $[MH]^+$ 486.3 and $[ML_2]^+$ 611.1. HRMS (ESI) calculated $[MH]^+$ = 486.0949; measured $[MH]^+$ = 486.0932. HRMS (ESI) calculated $[ML_2]^+$ = 611.2028; measured $[ML_2]^+$ = 611.2029. X-ray: $C_{18}H_{25}ClCoN_5O_5$, *M* = 485.81, 0.2 × 0.2 × 0.2 mm^3, monoclinic, space group $P2_1/n$ (No. 14), *a* = 15.0784(4), *b* = 8.7200(2), *c* = 19.7898(6) Å, *β* = 100.5550(10)°, *V* = 2558.01(12) Å^3, *Z* = 4, D_c = 1.261 g/cm^3, F_{000} = 1008, MoKα radiation, λ = 0.71073 Å, *T* = 173(2)K, $2\theta_{max}$ = 55.0°, 20875 reflections collected, 5828 unique (R_{int} = 0.1322). Final *GooF* = 1.937, *R1* = 0.1207, *wR2* = 0.3249, *R* indices based on 3946 reflections with I >2sigma(I) (refinement on F^2), 144 parameters, 0 restraints. Lp and absorption corrections applied, μ = 0.809 mm^{-1}.

[EtCo(DMGH)$_2$(2-methyl-4-(pyridin-4-yl)but-3-yn-2-ol)] 4.5

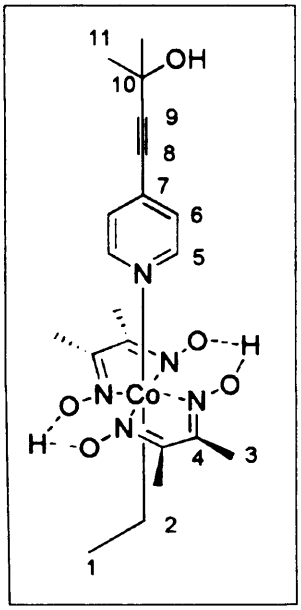

To a solution of [ClCo(DMGH)$_2$(2-methyl-4-(pyridin-4-yl)but-3-yn-2-ol)] (1 g, 2.06 mmol) and iodoethane (0.169 ml, 2.06 mmol) in MeOH (10 ml) was added $NaBH_4$ (90 mg, 2.25 mmol). The reaction was left to stir for 30 minutes, when the solvent was removed under vacuum, and the crude solid was dissolved in dichloromethane (10 ml) and washed with water (2 x 10 ml). The organic fractions were combined, dried over Na_2SO_4, filtered and evaporated to dryness, yielding [EtCo(DMGH)$_2$(2-methyl-4-(pyridin-4-yl)but-3-yn-2-ol)] as a brown solid (0.937 g, 95 %). δH ($CDCl_3$) (ppm) 8.55 (2 H, dd, *J* = 5.3 Hz, 1.4, C*H* (5) Pyr), 7.27 (2 H, dd, *J* = 6.5 Hz, 1.5 Hz, C*H* (6) Pyr), 2.14, (12 H, s, CH_3 (3) DMGH), 1.75, (2 H, q, *J* = 7.7 Hz, CH_2 (2) Co-CH_2-CH$_3$), 1.61 (6 H, s, CH_3 (11) CMe$_2$OH), 0.36 (3 H, t, *J* = 7.6 Hz, CH_3 (1) Co-CH$_2$-CH_3). δC ($CDCl_3$) (ppm) 153.6 (*C* (4) DMGH), 148.7 (*C* (5) Pyr), 135.1 (*C* (7) Pyr), 126.1 (*C* (6) Pyr), 104.8 (*C* (9) Pyr-C≡*C*), 78.3 (*C* (8) Pyr-*C*≡C), 65.9 (*C* (10) *C*Me$_2$OH), 41.0 (C (2) Co-*C*H$_2$-CH$_3$), 30.1 (C (11) C(*C*H$_3$)$_2$OH), 14.9 (C (1) Co-CH$_2$-*C*H$_3$) 12.2 (*C* (3) DMGH),. ν (C≡C) 2233.2. *m/z* (ESI) 480.1 $[MH]^+$. HRMS (ESI) calculated $[MH]^+$ = 480.1652; measured $[MH]^+$ = 480.1650.

[ClCo(DMGH)$_2$(4-(2-phenyl ethynyl)pyridine)] 4.4

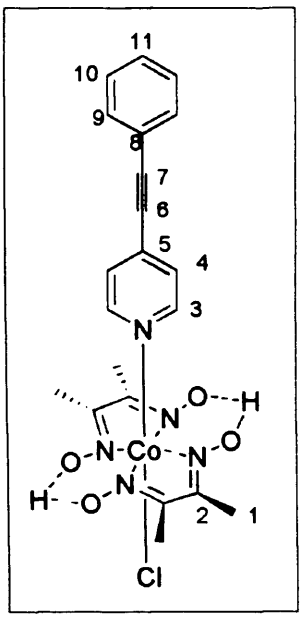

To a stirred suspension of [Cl_2Co(DMGH)($DMGH_2$)] (1 g, 2.77 mmol) and 4-(2-phenylethynyl)pyridine (0.33 mg, 2.77 mmol) in dichloromethane (10 ml) was added $NaHCO_3$ (5 ml). The reaction was allowed to stir for 1 hour at which point the solution was diluted further with dichloromethane (20 ml) and washed with water (2 x 20 ml). The organic fractions were combined, dried over Na_2SO_4, filtered and evaporated to dryness, yielding [ClCo(DMGH)$_2$(4-(2-phenyl ethynyl)pyridine)] as a brown solid (1.28 g, 93 %). δH ($CDCl_3$) (ppm) 8.22 (2 H, dd, *J* = 6.6 Hz, 1.4 Hz, C*H* (3) Pyr), 7.52 (2 H, dd, *J* = 6.7 Hz, 1.4 Hz, C*H* (10) Ph), 7.36-7.46 (3 H, m, C*H* (9,11) Ph), 7.27 (2 H, dd, *J* = 6.7 Hz, 1.4 Hz, C*H* (4) Pyr), 2.43 (12 H, s, CH_3 (1) DMGH). δC ($CDCl_3$) (ppm) 151.6 (*C* (2) DMGH), 149.5 (*C* (3) Pyr), 134.1 (*C* (5) Pyr), 131.1 (*C* (9) Ph), 129.2 (*C* (10) Ph), 127.7 (*C* (11) Ph), 126.3 (*C* (4) Pyr), 119.7 (*C* (8) Ph), 98.4 (*C* (7) Pyr-C≡*C*), 83.9 (*C* (6) Pyr-*C*≡C), 12.1 (*C* (1) DMGH). ν (C≡C) 2216.8. *m/z* (ESI) 504.0 $[MH]^+$ and 647.1 $[M\ L_2]^+$. HRMS (ESI) calculated $[M]^+$ = 504.0771; measured $[M]^+$ = 504.0827. HRMS (ESI) calculated $[ML_2]^+$ =; 647.1817 measured $[M\ L_2]^+$ = 647.1821. X-ray: $C_{21}H_{23}ClCoN_5O_4$, M = 503.82, 0.20 × 0.20 × 0.20 mm^3, monoclinic, space group $P2_1/c$ (No. 14), a = 8.7740(2), b = 12.3980(3), c = 20.7280(5) Å, β = 99.2400(10)°, V = 2225.54(9) Å^3, Z = 4, D_c = 1.504 g/cm^3, F_{000} = 1040, MoKα radiation, λ = 0.71073 Å, T = 150(2)K, $2\theta_{max}$ = 55.0°, 15099 reflections collected, 5058 unique (R_{int} = 0.0836). Final *GooF* = 1.038, *R1* = 0.0476, *wR2* = 0.1055, *R* indices based on 3413 reflections with I >2sigma(I) (refinement on F^2), 295 parameters, 0 restraints. Lp and absorption corrections applied, μ = 0.930 mm^{-1}.

[EtCo(DMGH)$_2$(4-(2-phenyl ethynyl)pyridine)] 4.6

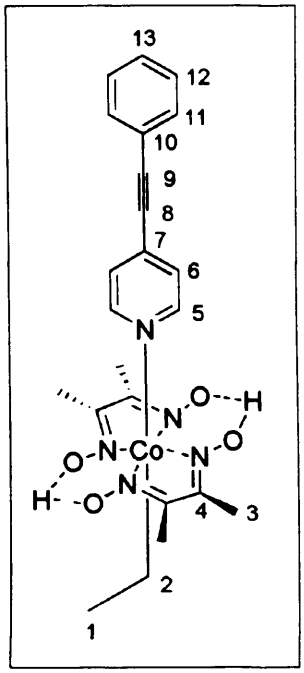

To a solution of [ClCo(DMGH)$_2$(4-(2-phenyl ethynyl)pyridine)] (1 g, 1.99 mmol) and iodoethane (0.18 ml, 2.2 mmol) in MeOH (5 ml) was added $NaBH_4$ (80 mg, 2 mmol). The reaction was left to stir for 30 minutes, when the mixture was diluted with dichloromethane (10 ml) and wash with water (2 x 10 ml). The organic fractions were combined, dried over Na_2SO_4, filtered and evaporated to dryness, yielding [EtCo(DMGH)$_2$(4-(2-phenyl ethynyl)pyridine)] as a brown solid (0.92 g, 93 %). δH ($CDCl_3$) (ppm) 8.58 (2 H, dd, *J* = 6.4 Hz, 1.4 Hz, C*H* (5) Pyr), 7.55 (2 H, d, *J* = 6.3 Hz, C*H* (12) Ph), 7.37-7.41 (5 H, m, C*H* (11, 13) Ph, C*H* (6) Pyr,), 2.15 (12 H, s, C*H* (3) Pyr), 1.76 (2 H, q, *J* = 7.6 Hz, CH_2 (5) Co-CH_2-CH_3), 0.38 (3 H, t, *J* = 7.6 Hz, CH_3 (5) Co-CH_2-CH_3). δC ($CDCl_3$) (ppm) 153.7 (*C* (4) DMGH), 149.5 (*C* (5) Pyr), 133.2 (*C* (7) Pyr), 132.0 (*C* (12) Ph), 128.6 (*C* (11) Ph), 127.7 (*C* (13) Ph), 126.3 (*C* (6) Pyr) 121.5 (*C* (10) Ph), 96.7 (*C* (9) Pyr-C≡*C*), 85.8 (*C* (8) Pyr-*C*≡C), 42.0 (C (2) CH_2 Co-CH_2-CH_3), 15.9 (C (1) CH_3 Co-CH_2-CH_3), 13.2 (C (3) CH_3 DMGH). ν (C≡C) 2218.7. *m/z* (ESI) $[MH]^+$ 498.1. HRMS (ESI) calculated $[M]^+$ = 498.1552; measured $[M]^+$ = 498.1549.

[EtCo(DMGH)$_2$(4-(2-phenyl ethynyl)pyridine)] 4.6 Method 2

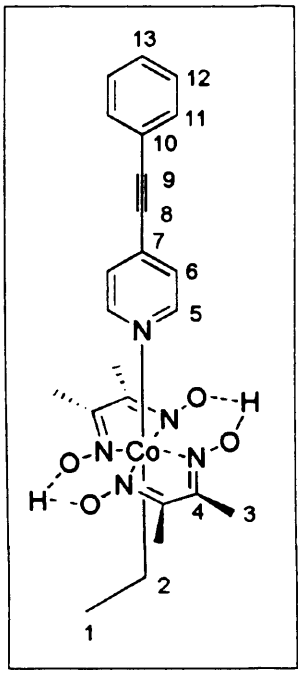

Under an atmosphere of nitrogen, cobalt(II) chloride hexahydrate (550mg, 2.30mmol), dimethylglyoxime (530 mg, 4.53 mmol), aqueous sodium hydroxide (50 %, 0.3 ml, 8.36 mmol) and 4-(2-phenylethynyl)pyridine (420 mg, 2.35 mmol) were added to stirred, de-gassed methanol (20 ml). The reaction was then cooled to 0 ^{O}C in an ice bath at which point, $NaBH_4$ (123 mg, 2.6 mmol) was added, turning the reaction mixture brown. The reaction was left to stir for ten minutes, when ethyl iodide (0.19 ml, 2.40 mmol), and the reaction was left to stir, and followed to completion by TLC (EtOAc:MeOH 9:1). The reaction mixture was pumped down, and the residue dissolved in dichloromethane (20 ml), and washed with distilled water (3 x 20 ml), dried over Na_2SO_4, and filtered. The organic fraction was then dried *in vacuo* to yield the title compound as a brown solid (783 mg, 68 %). δH ($CDCl_3$) (ppm) 8.58 (2 H, dd, *J* = 6.4 Hz, 1.4 Hz, C*H* (5) Pyr), 7.55 (2 H, d, *J* = 6.3 Hz, C*H* (12) Ph), 7.37-7.41 (5 H, m, C*H* (11, 13) Ph, C*H* (6) Pyr,), 2.15 (12 H, s, C*H* (3) Pyr), 1.76 (2 H, q, *J* = 7.6 Hz, CH_2 (5) Co-CH_2-CH_3), 0.38 (3 H, t, *J* = 7.6 Hz, CH_3 (5) Co-CH_2-CH_3). δC ($CDCl_3$) (ppm) 153.7 (*C* (4) DMGH), 149.5 (*C* (5) Pyr), 133.2 (*C* (7) Pyr), 132.0 (*C* (12) Ph), 128.6 (*C* (11) Ph), 127.7 (*C* (13) Ph), 126.3 (*C* (6) Pyr) 121.5 (*C* (10) Ph), 96.7 (*C* (9) Pyr-C≡*C*), 85.8 (*C* (8) Pyr-*C*≡C), 42.0 (C (2) CH_2 Co-*C*H_2-CH_3), 15.9 (C (1) CH_3 Co-CH_2-*C*H_3), 13.2 (C (3) CH_3 DMGH). ν (C≡C) 2218.7. *m/z* (ESI) $[MH]^+$ 498.1. HRMS (ESI) calculated $[M]^+$ = 498.1552; measured $[M]^+$ = 498.1549.

[ClCo(DMGH)$_2$(μ^2(dicobalthexacarbonyl)2-methyl-4-(pyridin-4-yl)but-3-yn-2-ol)] 4.7

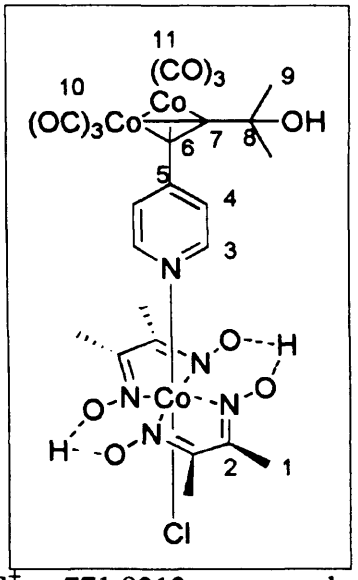

Under a nitrogen atmosphere, a solution of [ClCo(DMGH)$_2$(2-methyl-4-(pyridin-4-yl)but-3-yn-2-ol)] (0.5 g, 1.03 mmol) in dried, de-gassed dichloromethane (10 ml) was prepared, to which, dicobaltoctacabonyl (0.39 g, 1.13 mmol) was added. The solution was allowed to stir for 3 hours, and followed by TLC (petroleum ether:diethyl ether 1:1). Upon completion, the reaction mixture was put onto silica, and chromatography was carried out, with an eluent of petroleum ether: diethyl ether 1:1, yielding the title complex as a red solid. (0.492 g, 62 %) ν (C≡O) 2081.8, 2061.8, 2021.0 *m/z* (ESI) 771.9 $[MH]^+$. HRMS (ESI) calculated $[MH]^+$ = 771.9313; measured $[MH]^+$ = 771.9320.

[EtCo(DMGH)$_2$(μ^2(dicobalthexacarbonyl)2-methyl-4-(pyridin-4-yl)but-3-yn-2-ol)] 4.9

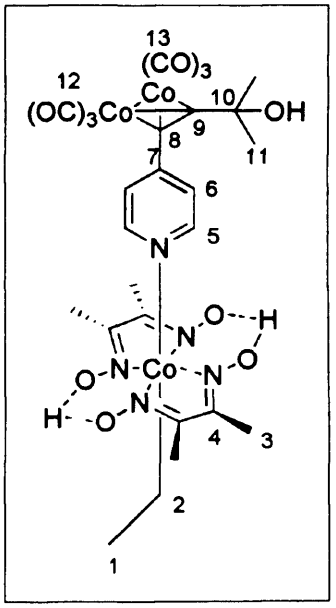

Under a nitrogen atmosphere, a solution of [EtCo(DMGH)$_2$(2-methyl-4-(pyridin-4-yl)but-3-yn-2-ol)] (0.5 g, 1.04 mmol) in dried, de-gassed dichloromethane (10 ml) was prepared, to which, dicobaltoctacabonyl (0.39 g, 1.15 mmol) was added. The solution was allowed to stir for 3 hours, and followed by TLC (petroleum ether:diethyl ether 1:1). Upon completion, the reaction mixture was put onto silica, and chromatography was carried out, with an eluent of petroleum ether:diethyl ether 1:1, yielding the title complex as a red solid. (0.52 g, 65 %) δH ($CDCl_3$) (ppm) 8.47 (2 H, broad d, *J* = 6.5 Hz, C*H* (5) Pyr), 7.45, (2 H, broad d, *J* = 6.4 Hz, C*H*(6) Pyr), 2.20, (12 H, s, CH_3 (3) DMGH), 1.76 (2 H, q, J = 7.6 Hz, CH_2 (2) Co-CH_2-CH_3), 1.68 (6 H, s, CH_3 (11) CMe_2OH), 0.38 (3 H, broad t, *J* = 7.6 Hz, CH_3 (1) Co-CH_2-CH_3) δC ($CDCl_3$) (ppm) 152.3 (*C* (4) DMGH), 147.2 (*C* (5) Pyr), 134.9 (*C* (7) Pyr), 126.0 (*C* (6) Pyr), 103.2 (*C*

(9) Pyr-C≡*C*), 79.4 (*C* (8) Pyr-*C*≡C), 65.5 (*C* (10) *C*Me$_2$OH), 41.2 (C (2) Co-*C*H$_2$-CH$_3$), 30.1 (C (11) C(*C*H$_3$)$_2$OH), 14.8 (C (1) Co-CH$_2$-*C*H$_3$) 12.5 (*C* (3) DMGH). ν(C≡O) 2095.3, 2058.6, 2042.3. *m/z* (ESI) 766.2 $[MH]^+$, 788.2 $[MNa]^+$. HRMS (ESI) calculated $[MH]^+$ = 766.0016; measured $[MH]^+$ = 766.0039.

[ClCo(DMGH)$_2$(μ^2(μ^2diphenylphosphinomethanedicobalttetracarbonyl))2-methyl-4-(pyridin-4-yl)but-3-yn-2-ol)] 4.11

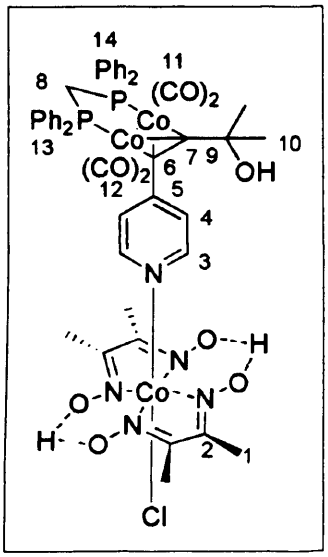

Under a nitrogen atmosphere, a solution of [ClCo(DMGH)$_2$(2-methyl-4-(pyridin-4-yl)but-3-yn-2-ol)] (0.5 g, 1.03 mmol) in dried, de-gassed dichloromethane (10 ml) was prepared, to which, μ^2diphenylphosphinomethanedicobalthexacarbonyl (0.759 g, 1.13 mmol) was added. The solution was allowed to stir for 3 hours, and followed by TLC (petroleum ethe r: diethyl ether 1:1). Upon completion, the reaction mixture was put onto silica, and chromatography was carried out, with an eluent of petroleum ether:diethyl ether 1:1, yielding the title complex as a red solid. (0.66 g, 58 %) δP (ppm) 33.4 ν (C≡O) 2011.5, 1990.7, 1960.6 *m/z* (ESI) 1100.0 $[MH]^+$. HRMS (ESI) calculated $[MH]^+$ = 1100.0612; measured $[MH]^+$ = 1100.0618.

[EtCo(DMGH)$_2$(μ^2(μ^2diphenylphosphinomethanedicobalttetracarbonyl))2-methyl-4-(pyridin-4-yl)but-3-yn-2-ol)] 4.13

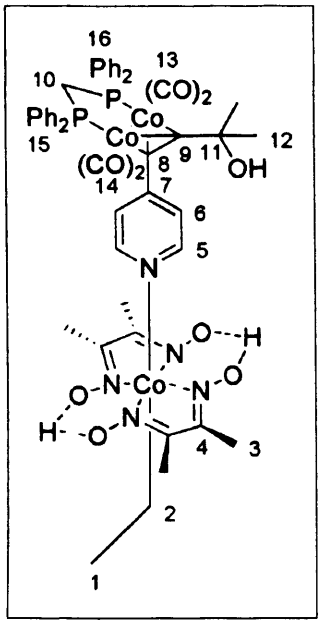

Under a nitrogen atmosphere, a solution of [EtCo(DMGH)$_2$(2-methyl-4-(pyridin-4-yl)but-3-yn-2-ol)] (ethyl)cobaloxime (0.5 g, 1.04 mmol) in dried, de-gassed dichloromethane (10 ml) was prepared, to which, dicobaltoctacabonyl (0.77 g, 1.15 mmol) was added. The solution was allowed to stir for 3 hours, and followed by TLC (petroleum ether:diethyl ether 1:1). Upon completion, the reaction mixture was put onto silica, and chromatography was carried out, with an eluent of petroleum ether:diethyl ether 1:1, yielding the title complex as a red solid. (0.72 g, 61 %) δH ($CDCl_3$) (ppm) 8.38 (2 H, broad d, J = 7.6 Hz, C*H* (5) Pyr), 7.82-7.88 (m, Ph (15, 16)), 7.55 (2 H, broad d, J = 7.5 Hz, C*H* (6) Pyr), 7.02 (m, Ph (15, 16)), 3.12 (m, 1H, PC*H*$_2$P, (10)), 3.04 (m, 1H, PC*H*$_2$P, (10)), 2.22, (12 H, s, C*H*$_3$ (3) DMGH), 1.85 (2 H, broad q, J = 6.9 Hz, C*H*$_2$ (2) Co-C*H*$_2$-CH$_3$), 1.72 (6 H, s, C*H*$_3$ (11) CMe$_2$OH), 0.40 (3 H, broad t, J = 7.0 Hz, 3 H, broad t, J = 7.6 Hz, C*H*$_3$ (1) Co-CH$_2$-C*H*$_3$). δC ($CDCl_3$) (ppm) 153.6 (*C* (4) DMGH), 148.7 (*C* (5) Pyr), 135.1 (*C* (7) Pyr), 132.0 (Ph), 128.3 (Ph), 127.5 (Ph), 126.1 (*C* (6) Pyr), 122.5 (Ph), 104.8 (*C* (9) Pyr-C≡*C*), 78.3 (*C* (8) Pyr-*C*≡C), 65.9 (*C* (11) *C*Me$_2$OH), 41.0 (C (2) Co-*C*H$_2$-CH$_3$), 36.6 (C (10) t, J_{CP} = 21 Hz, P*C*H$_2$P), 30.1 (C (12) C(*C*H$_3$)$_2$OH), 14.9 (C (1) Co-CH$_2$-*C*H$_3$) 12.2 (*C* (3) DMGH). δP (ppm) 37.1 ν (C≡O) 2031.6, 2001.5, 1975.6 *m/z* (ESI) 1094.1 $[MH]^+$. HRMS (ESI) calculated $[MH]^+$ = 1094.1315; measured $[MH]^+$ = 1094.1323.

[ClCo(DMGH)$_2$(4-(2-phenyl (μ^2(dicobalthexacarbonyl) ethynyl))pyridine)] 4.8

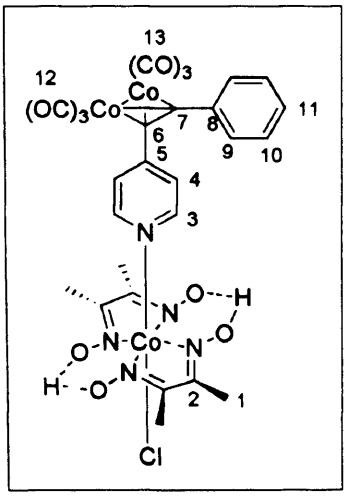

Under a nitrogen atmosphere, a solution of [ClCo(DMGH)$_2$(4-(2-phenylethynyl)pyridine)] (0.50 g, 0.99 mmol) in dried, degassed dichloromethane was prepared, to which, dicobaltoctacabonyl (0.37 g, 1.09 mmol) was added. The solution was allowed to stir for 3 hours, and followed by TLC (petroleum ether:diethyl ether 1:1). Upon completion, the reaction mixture was put onto silica, and chromatography was carried out, with an eluent of petroleum ether:diethyl ether 1:1, yielding the title complex as a red solid. (0.45 g, 58 %)
ν (C≡O) 2092.3, 2059.6, 2028.8 *m/z* (ESI) 799.0 $[MH]^+$. HRMS (ESI) calculated $[MH]^+$ = 789.9208; measured $[MH]^+$ = 789.9213.

[EtCo(DMGH)$_2$(4-(2-phenyl μ^2(dicobalthexacarbonyl) ethynyl)pyridine)] 4.10

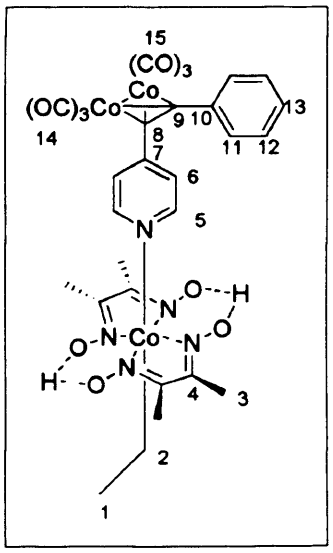

Under a nitrogen atmosphere, a solution of [EtCo(DMGH)$_2$(4-(2-phenylethynyl)pyridine)] (0.50 g, 1.01 mmol) in dried, degassed dichloromethane was prepared, to which, dicobaltoctacabonyl (0.38 g, 1.11 mmol) was added. The solution was allowed to stir for 3 hours, and followed by TLC (petroleum ether:diethyl ether 1:1). Upon completion, the reaction mixture was put onto silica, and chromatography was carried out, with an eluent of petroleum ether:diethyl ether 1:1, yielding the title complex as a red solid (0.47 g, 57 %). δH ($CDCl_3$) (ppm) 8.58 (2 H, broad d, J = 4.5 Hz, C*H* (5) Pyr), 7.50-7.58 (2 H, broad m, C*H* (12) Ph), 7.35-7.40 (7 H, broad m, C*H* (6) Pyr, C*H* (11, 13) Ph), 2.15 (12 H, broad s, CH_3 (3) DMGH), 1.77 (2 H, broad q, J = 6.9 Hz, CH_2 (2) Co-CH_2-CH_3), 0.38 (3 H, broad t, J = 7.0 Hz, CH_3 (1) Co-CH_2-CH_3), δC ($CDCl_3$) (ppm) 149.5 (*C* (4) DMGH), 148.9 (*C* (5) Pyr), 131.8 (*C* (7) Pyr), 129.5 (*C* (12) Ph), 128.4 (*C* (11) Ph), 127.8 (*C* (13) Ph), 126.8 (*C* (6) Pyr), 121.3 (*C* (10) Ph), 95.2 (*C* (9) Pyr-C≡*C*), 85.0 (*C* (8) Pyr-*C*≡C), 42.0 (C (2) CH_2 Co-CH_2-CH_3), 15.8 (C (1) CH_3 Co-CH_2-CH_3),

13.2 (C (3) CH_3 DMGH). ν (C≡O) 2094.3, 2058.6, 2029.7. *m/z* (ESI) 783.9 $[MH]^+$. HRMS (ESI) calculated $[MH]^+$ = 783.9910; measured $[MH]^+$ = 783.9923.

[ClCo(DMGH)2 (4-(2-phenyl μ2(μ2diphenylphosphinomethanedicobalt tetracarbonyl) ethynyl)pyridine)] 4.12

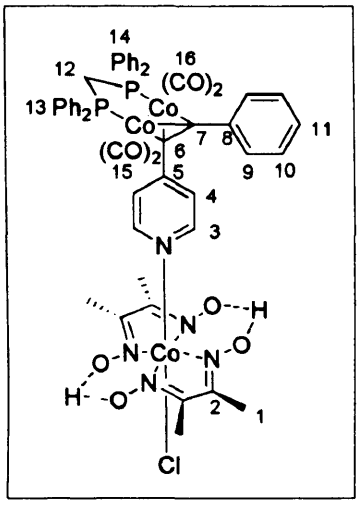

Under a nitrogen atmosphere, a solution of [ClCo(DMGH)$_2$(4-(2-phenyl ethynyl)pyridine)] (0.50 g, 0.99 mmol) in dried, de-gassed dichloromethane was prepared, to which, μ^2diphenylphosphinomethanedicobalthexacarbonyl (0.73 g, 1.09 mmol) was added. The solution was allowed to stir for 3 hours, and followed by TLC (petroleum ether:diethyl ether 1:1). Upon completion, the reaction mixture was put onto silica, and chromatography was carried out, with an eluent of petroleum ether:diethyl ether 1:1, yielding the title complex as a red solid. (0.71 g, 64 %) δP (ppm) 36.0. ν (C≡O) 2029.4, 2006.8, 1977.1. *m/z* (ESI) 1118.1 $[MH]^+$. HRMS (ESI) calculated $[MH]^+$ = 1118.0506; measured $[MH]^+$ = 1118.0511.

[EtCo(DMGH)$_2$ (4-(2-phenyl μ^2(μ^{2}diphenylphosphinomethanedicobalt tetracarbonyl) ethynyl)pyridine)] 4.14

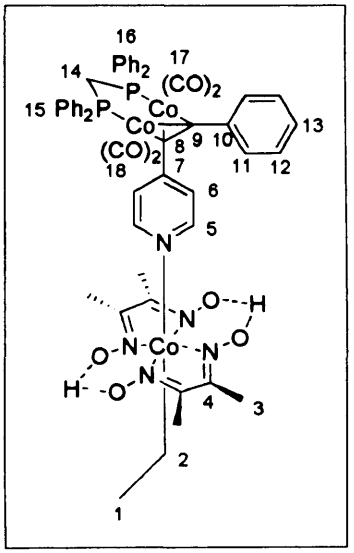

Under a nitrogen atmosphere, a solution of [EtCo(DMGH)$_2$(4-(2-phenylethynyl)pyridine)] (0.50 g, 1.01 mmol) in dried, de-gassed dichloromethane was prepared, to which, μ^2diphenylphosphinomethanedicobalthexacarbonyl (0.74 g, 1.11 mmol) was added. The solution was allowed to stir for 3 hours, and followed by TLC (petroleum ether:diethyl ether 1:1). Upon completion, the reaction mixture was put onto silica, and chromatography was carried out, with an eluent of petroleum ether:diethyl ether 1:1, yielding the title complex as a red solid. (0.69 g, 62 %) δH ($CDCl_3$) (ppm) 8.39 (2 H, broad d, *J* = 7.8 Hz, C*H* (5) Pyr), 7.70-7.87 (25 H, m, Ph (11-13 15, 16)), 7.56 (2 H, broad d, *J*

= 7.5 Hz, C*H* (6) Pyr), 3.13 (1 H, m, PC*H*$_2$P (10)), 3.04 (1 H, m, PC*H*$_2$P (10)), 2.05 (12 H, s, DMGH, (3)), 1.77 (2 H, broad q, J = 6.9 Hz, C*H*$_2$ (2) Co-C*H*$_2$-CH$_3$) 0.38 (3H, broad t, J = 7.0 Hz, C*H*$_3$ (1) Co-CH$_2$-C*H*$_3$), δC ($CDCl_3$) (ppm). 153.7 (*C* (4) DMGH), 149.5 (*C* (5) Pyr), 133.2 (*C* (7) Pyr), 132.0 (Ph), 128.6 (Ph), 128.4 (Ph), 127.7 (Ph), 127.2 (Ph), 126.3 (*C* (6) Pyr), 122.7 (Ph), 121.5 (Ph), 96.7 (*C* (9) Pyr-C≡*C*), 85.8 (*C* (8) Pyr-*C*≡C), 42.0 (C (2) *C*H$_2$ Co-*C*H$_2$-CH$_3$), 36.6 (C (14) t, J_{CP} = 21 Hz, P*C*H$_2$P), 15.9 (C (1) *C*H$_3$ Co-CH$_2$-*C*H$_3$), 13.2 (C (3) CH$_3$ DMGH). δP (ppm) 37.3. ν (C≡O) 2021.0, 1995.0, 1968.0 *m/z* (ESI) 1112.2 $[MH]^+$. HRMS (ESI) calculated $[MH]^+$ = 1112.1209; measured $[MH]^+$ = 1112.1214.

General protocol for catalytic dechlorination.

A solution of the catalyst (0.1 mmol), anisole (0.1 mmol) and perchloroethylene (1 mmol) in methanol (5 ml) was prepared and a solution of sodium borohydride (0.2 mmol) and sodium hydroxide (0.3 mmol) in water (1 ml) was added. The mixture was sealed and allowed to stir for one hour at which point, 1 ml of the solution was taken, filtered through a plug of celite and silica to remove inorganics and submitted for GC analysis.

4.7. References.

1 J. C. Klotz, C. L. Nivert, *J. Organomet. Chem.* **1973**, 52, 387.

2 J. Zakrzewski, C. Giannotti, *J. Organomet. Chem.* **1990**, 358, c23.

3 M. P. Coogan, L. S. Stanton and T. Walther, *J. Organomet. Chem* **2003**, 677, 125.

4 L. Zhao, B. H. Northrop, P. J. Stang, *J. Am. Chem. Soc.* **2008**, 130, 11886.

5 R. L. Cordiner, D. Corcoran, D. S. Yufit, A. E. Goeta, J. A. K. Howard P. J. Low, *Dalton Trans*, **2003**, 3541.

6 L. Hore, C. J. McAdam, J. L. Kerr, N. W. Duffy, B. H. Robinson, J. Simpson *Organometallics*, **2000**, 19, 5039.

7 C. J. McAdam, N. W. Duffy, B. H. Robinson, J. Simpson, *Organometallics* **1996**, 15, 3935.

8 G. G. Sumner, H. P. Klug, L. E. Alexander *Acta Cryst.* **1964**, 17, 6, 732.

9 M. J. S. Dewar, *Bull. Soc. Chim. Fr.* 18 **1951** C71; J. Chatt, L.A. Duncanson, *J. Chem. Soc.* **1953**, 2939

10 D. L. Thorn, R. Hoffman, *Inorg Chem.* **1976**, 17, 126

11 Y. Liu, J. Schwartz, C. Cullen. *Environ. Sci. Technol.* **1995**, 29, 836.

12 Y. Liu, J. Schwartz, *Tetrahedron*, **1995** 51, 4471.

13 M. A. Wright, C. J. Knowles, J. Stratford, S. A. Jackman G. K. Robinson, *International Biodeteriation & Biodegradation.* **1996**, 6147.

14 L. Lassova , H. K. Lee, and T. S. A. Hor, *J. Organomet. Chem.* **1998**, 63, 3538.

15 S. A. Jackman, C. J. Knowles, G. K. Robinson, *Chemosphere.* **1999**, 38, 1889.

16 A. A. Peterson and K. McNeill, *Organometallics.* **2006**, 25, 4938.

17 A. E. D. Fletcher, J. Moss, A. R. Cowley, D. O'Hare, *Chem. Comm.* **2007**, 2971.

18 S. P. Reade, M. F. Mahon, M. K. Whittlesey. *J. Am. Chem. Soc.* **2009**, 131, 1847.

19 K. P. Jensen and U. Ryde, *J. Mol. Struct., Theo. Chem*, **2002**, 585, 239.

20 L. Yu, J. S. Lindsey *J. Organomet. Chem.* **2001**, 66, 7402.

21 J. D. Lewis, J. N. Moore, *Dalton Trans.* **2004**, 1376.

22 J. A. Platts, G. J. S. Evans, M. P. Coogan, J. Overgaard, *Inorg. Chem.* **2007**, 46, 6291.

23 B.D. Gupta, K. Qanungo, T. Barclay, W. Cordes, *J. Organomet. Chem*, **1998**, 560, 155.

24 J.M. Rubin-Preminger, U. Englert, *Inorg. Chim. Acta*, **2009**, 362, 1135.

Chapter 5.

Bipyridyl and Pyrazine Bridged Dicobaloximes.

5.0 Compound List.

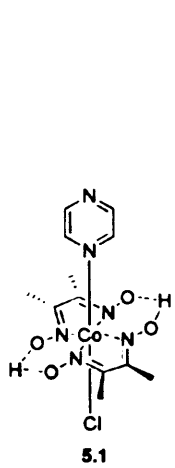
5.1

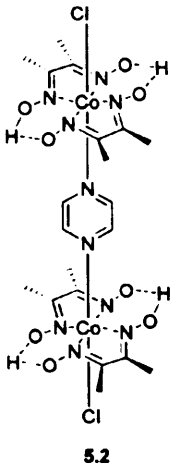
5.2

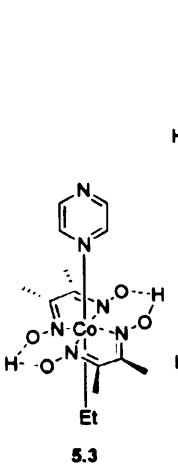
5.3

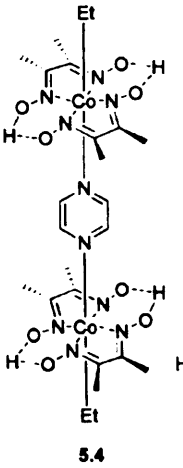
5.4

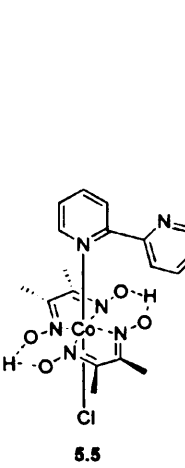
5.5

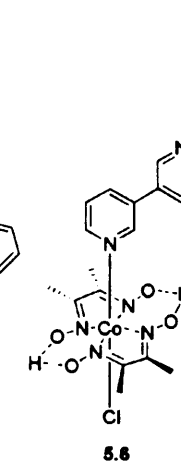
5.6

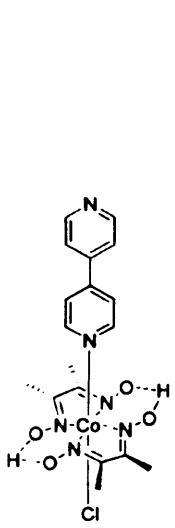
5.7

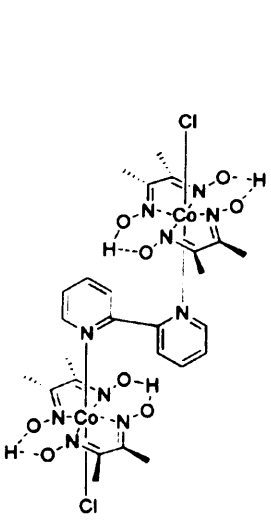
5.8

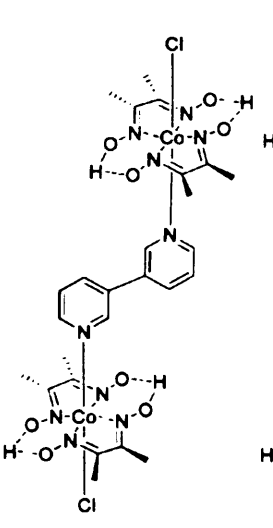
5.9

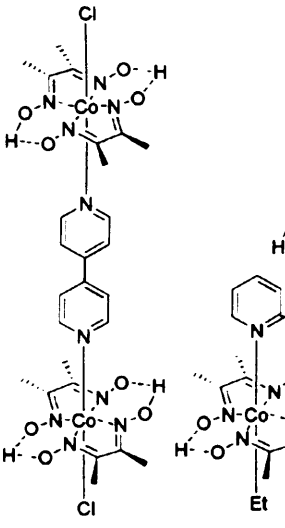
5.10

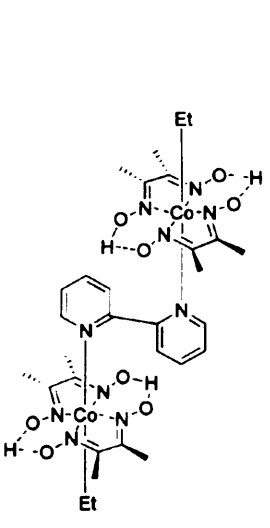
5.11

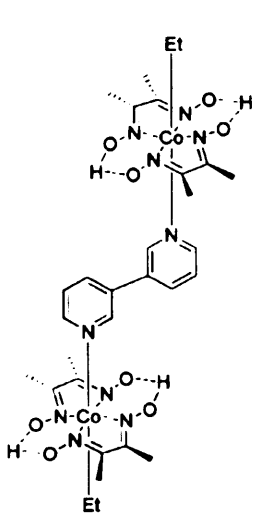
5.12

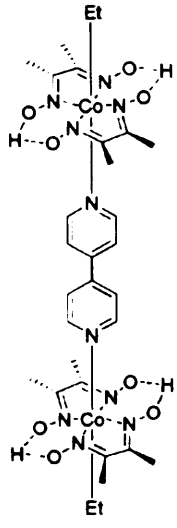
5.13

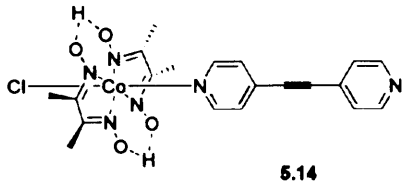
5.14

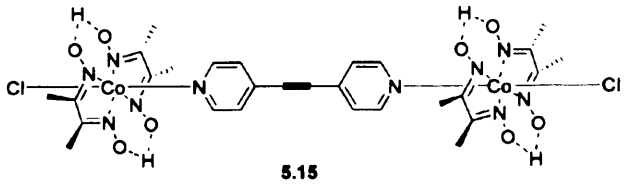
5.15

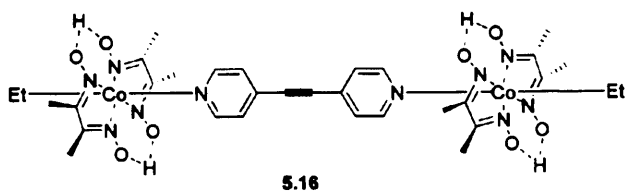
5.16

5.1. Introduction.

5.1.1. Current Synthetic Routes Towards Dinuclear Cobaloximes.

Considerable research has been undertaken into the formation and cleavage of metal-carbon σ-bonds in organometallic complexes, with free radicals believed to be involved in this cleavage process, particularly if there is homolytic cleavage of the bond.[1] Examples of such bond cleavage include the photolysis, thermolysis and electrolysis reactions of vitamin B_{12}.[2] Few examples of organobridged dicobaloximes with two reactive cobalt-carbon bonds exist, such as the biphenyl, xylyl and alkyl bridged dicobaloximes exhibited in **Figure 5.1**, and they have been proposed as models for the bonding of hydrocarbons at metal surfaces,[3] as they are considered to be "latent alkanediyl radicals".[4]

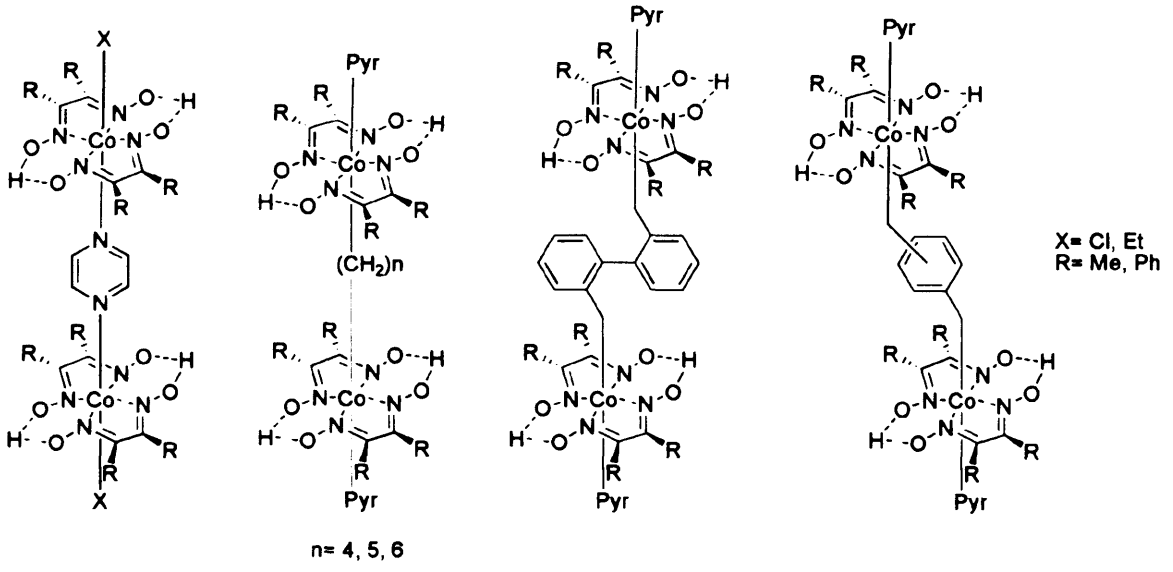

Figure 5.1. Pyrazine, polymethylene, biphenyl and xylene linked cobaloximes.

In the 1960s, Smith *et al.*[5] prepared a series of dinuclear polymethylene-bridged vitamin B_{12} complexes. Schrauzer[6] continued this concept, and synthesised the first example of a μ-polymethylene bridged dicobaloxime and characterised the organic products from the photolysis of these complexes by chromatography. Moss[7] systematically studied the preparation of organobridged dicobaloximes from $Br(CH_2)_nBr$, where n = 4-8, whilst Chen *et al* studied the photolysis and thermal decomposition of these μ-polymethylene dicobaloximes.[8] Gupta[9] reported the synthesis of biphenyl and xylyl bridged

dicobaloximes, studying the influences of the bridging ligands on the other ligands present in these dicobaloximes. These complexes are of interest as ligand-bridged homo- and hetero-nuclear complexes play an important role in efforts to understand inner-sphere electron-transfer reactions.[10]

In addition to these, dicobaloximes have also been reported with bridging ambidentate ligands. These include dicobaloximes bridged by cyano, thiocyanato and carbonyl ligands,[11,12] and dicobaloximes bridged by nitrogen heterocycles, such as bipyridine and pyrazine. [13] The earliest example of the use of ligands with two coordination sites as a bridge between cobaloxime systems dates back to the work of Gaus[14] who, in 1974, synthesised a cyano-bridged dicobaloxime species. These dicobaloximes were synthesised by reaction of an aquacobaloxime with cyanocobaloxime, where the nitrogen of the cyanocobaloxime displaced the labile water ligand of the aquacobaloxime, as shown in **Scheme 5.1**.

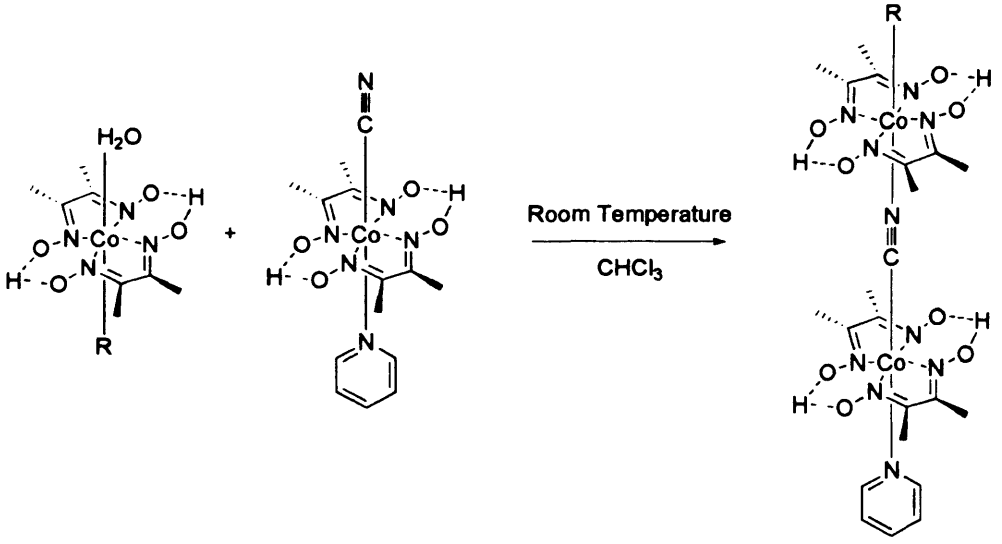

Scheme 5.1. Synthesis of cyano-bridged dicobaloxime, from the aquacobaloxime.[11]

In addition to the synthetic route shown in **Scheme 5.1**, there are three further routes reported in the literature. Dehydration of two equivalents of the aquacobaloxime *in vacuo* at high temperatures yields the dimer $[RCo(DMGH)_2]_2$. The reaction of this dimer with a bidentate ligand, such as diphos[a] or para-dithiane, under inert conditions yielded the bridged dicobaloxime depicted in **Scheme 5.2**. The final reported method,

[a] Bis(diphenylphosphino)ethane.

portrayed in **Scheme 5.3**, utilises the high nucleophilicity of Co(II) cobaloximes, by the reaction of cobaloximes with a dihaloalkane, via oxidative alkylation of the cobaloxime.[15] An alternative disproportionation method has also been reported for the synthesis of the polymethylene bridged cobaloximes,[16] however, yields of the bridged dicobaloxime species are lower than those reported in the oxidative alkylation method.

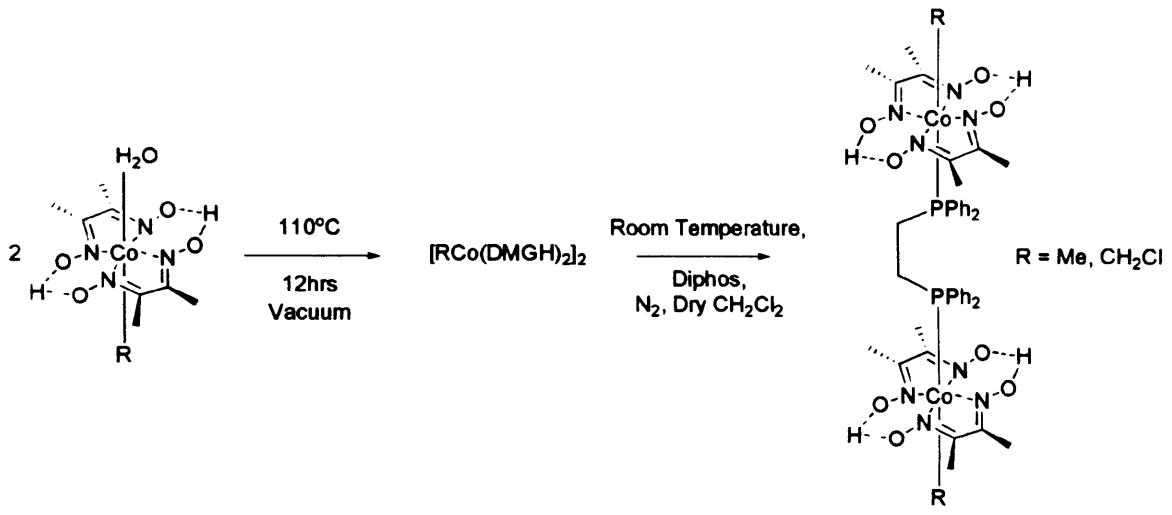

Scheme 5.2. Two step synthesis of a diphos-bridged dicobaloxime, via dehydration to a dicobaloxime dimer.[13]

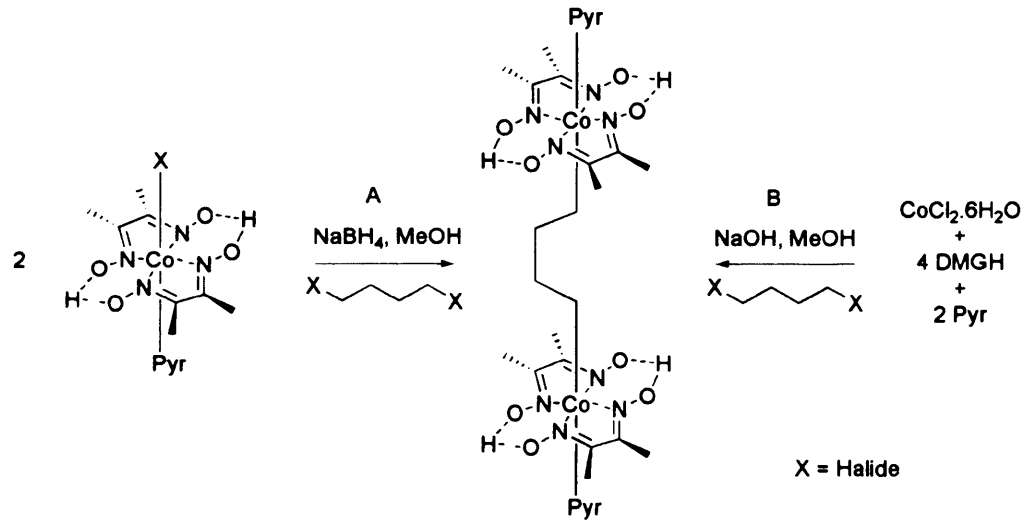

Scheme 5.3. Polymethylene bridged dicobaloxime, via oxidative alkylation (A),[15] or disproportionation (B).[16]

Whilst the synthetic routes shown afford the desired dicobaloxime in decent yields, *ca.* 60 % for the aqua substitution reaction,[11] between 70 and 90 % for the dimer dehydration[13] and, at its most optimal, 93 % for the oxidative alkylation,[9] each has

negative aspects associated with it. The dehydration step of the reaction depicted in **Scheme 5.2** requires temperatures greater than 110 °C for longer than 12 hours, and has been described as "long and tedious", whereas the reaction of $[RCo(DMGH)_2(H_2O)]$ with a near stoichiometric amount of pyrazine via the substitution of the water ligand to give the pyrazine bridged dicobaloxime $[R(DMGH)_2Co]_2$-μ-(Pyz), was found to be a more viable alternative.[20] Gupta *et al* refined reaction conditions for the oxidative alkylation, but were unable to get a consistently good yield for the dicobaloximes, with yields varying from 2 % to 93 %.[9] This was attributed to longer reaction times favouring the dicobaloxime and shorter reaction times favouring the monocobaloximes. Mixtures of both mono- and dicobaloximes were observed in all reactions, necessitating column chromatography to separate the two.

5.1.2. The Chemistry of Dimeric Cobaloximes.

In the late 1990s Gupta and co-workers carried out an extensive study of a range of organobridged dinuclear cobaloximes, using numerous ligands as bridges between the cobaloximes, including biphenyls, pyrazine and alkyl chains, shown in **Figure 5.1**. They were particularly interested in the effects of the bridging ligands on the geometries of the cobalt centre and the chemical effects on the *cis* and *trans* ligands. Since two cobaloximes are present, they were also interested in the electrochemistry of these species. These systems have gone on to help further understanding of the electronic interactions in more complicated multimetallic species.

These organo-bridged cobaloximes exhibit two inherently labile cobalt-sp^3 carbon bonds, the cleavage of which makes these complexes catalysts for a variety of reactions.[17] The reactivity of the Co-C bond is due to a combination of features including the steric and electronic properties of the oxime alkyl group, the electronic properties of the bridging unit and the chemical properties of the ligand *trans* to the bridging unit. Bulky alkyl groups on the oxime, flexible bridging units between the cobaloximes and a bulky, electron donating group *trans* to the bridging unit can weaken the cobalt-carbon bond, by addition of electrons to the anti-bonding orbitals of the Co-C bond. As a consequence, the biphenyl and pyrazine complexes were found to be the most stable, due to a combination of steric interactions between the bridging ligands and steric bulk of the glyoxime ligands. These biphenyl derivatives give rise to *axial*

chirality-atropisomerism, due to bulky groups present in the ortho position hindering the rotation between cobalt centres.[18]

Gupta *et al* synthesised a series of dicobaloximes bridged by organic species including xylene, alkyl chains and substituted biphenyls,[9,15,16] to study the spectroscopic effects of the incorporation of a second cobaloxime into a first. Particular interest was given to the *cis* and *trans* effects of the bridging, equatorial and apical ligands on each other, and whether the previously observed spectroscopic trends of monocobaloximes could be extended to dicobaloximes. The extent of the Co-C bond rotation was also studied. Both the mono- and dicobaloximes were observed in each oxidative alkylation reaction, with the combined yields in biphenyl synthesis ranged from 70-80 %, whilst the polymethylene yields ranged from 49-93 % and the xylyl were *ca.* 50 %. In all cases, some decomposition was observed when the dicobaloxime was left in solution, even under an inert atmosphere.

The Co-CH_2 resonances of the meta- and para- xylene bridged dicobaloximes appear as a singlet, with the meta- substituted species resonating at a lower frequency than the para- substituted species, due to electronic effects of the cobaloxime. The resonances of the biphenyl and ortho- xylene bridged dicobaloximes appeared as a diastereotopic doublet of doublets. Variable temperature ^{1}H-NMR showed that the rotation of the Co-C bonds between the cobaloxime and the biphenyl or ortho-xylyl groups is restricted by the bridging ligand itself, and as a result, the CH_2 becomes diastereotopic, as shown by the doublet of doublets and a geminal coupling observed in ^{1}H-NMR, hence the occurrence of *axial chirality-atropisomerism*. The pyridine resonances were found to shift between the diphenylglyoxime (DPGH) and the DMGH dicobaloximes, as did the Co-CH_2, due to the electron withdrawing effects of the alkyl group of the oxime ligands. DPGH was found to exert the greatest effect, followed by glyoxime (GH) and cyclohexanedioneglyoxime (CHGH), with DMGH exerting the smallest *cis* effect on the pyridine and Co-CH_2 protons.

Cyclic voltammetry studies on the organo-bridged dicobaloximes were undertaken to observe the effects of the bridging xylene groups on the redox potentials of the two metal centres. In the reduction half, the xylyl bridged species shows a single step two electron reduction between -1.30 V and -1.41 V corresponding to the Co(III) to Co(I)

reduction. From this, Gupta deduced that both metal centres undergo reduction at the same potential. On moving from para- to ortho- and meta- substituted, a 0.1 V shift towards a more positive potential was observed, indicating there is more electron density on the Co atoms in para-substituted xylyl dicobaloximes than in the meta- or ortho-substituted xylyl dicobaloximes, implying that the para-substituted xylyl bridged dicobaloxime is the more electron donating. Oxidation was found to be irreversible for the biphenyl bridged and ortho-xylyl bridged dicobaloximes, but reversible for meta-xylyl and para-xylyl bridged dicobaloximes. To date, no electrochemistry has been undertaken on the polymethylene species.

Bridging nitrogen heterocyclic based ligands have been used extensively for the synthesis of a variety of one-, two-, and three-dimensional organic-inorganic polymeric network structures, in which the two nitrogens are joined by a metal center, as well as for pure organic networks.[19,20] A series of pyrazine-linked cobaloximes, of the type $[XCo(DRGH)_2]_2$-μ-(pyz), depicted in **Figure 5.1** have been synthesised by Gupta *et al* with a view to understanding their electrochemisty and the extent of the influence of the oxime ligands on the cobalt coordinated species,[15,16] using the dehydration and aqua methods stated previously, though the dehydration method was found to be less reliable, and the aqua route gave 60-70 % yields. The variation in the N-Co-C bond properties has been described in terms of *trans* influence of the axial base as well as the steric and electronic properties of the alkyl groups. The pyrazine-bridged cobaloximes were synthesised directly from the aquacobaloxime complexes, as shown in **Scheme 5.4**.

$$2\ RCoL_2(H_2O) + Pyz \rightarrow RCoL_2\text{-}Pyz\text{-}CoL_2R$$

Scheme 5.4. Synthesis of pyrazine linked cobaloximes. R = Me, Cl, L = DPGH or DMGH.

Upon comparison between the ^{1}H-NMR spectra of the pyrazine-bridged DPGH and DMGH cobaloximes, the resonances associated with the pyrazine and Co bound methyl protons were observed to be consistently down field in the DPGH compared to the DMGH. This has been attributed to the influence of varying the alkyl groups of the equatorial ligand. This is in contrast with earlier findings of simple pyridylcobaloximes, where the pyridine protons experienced less *cis* influence than the Co bound alkyl protons. The comparable *cis* influence on the α-proton and the pyrazine protons is due

to the fact that there are two metallocycles affecting the pyrazine. X-ray crystallography revealed that the two cobaloximes were staggered so as to minimise the steric repulsion between the alkyl groups of the oxime ligands. CV studies showed two irreversible waves in the reduction half at -0.97 V and -1.37 V corresponding to the Co(III)/Co(II) and Co(II)/Co(I) reductions, and the oxidation half showed only one reversible wave at + 0.94 V of Co(IV)/Co(III), with both the cobalt centres behaving similarly.

5.1.3. Target Structures.

Having shown that the catalytic properties associated with the cobaloximes are enhanced in those bearing a secondary dicobalt centre, the idea arose of synthesising a series of dimeric cobaloximes, with one to act as the active catalytic centre, and the other to act as the redox active centre. Initially, the synthetic methods used in **Chapter 3** were applied the synthesis of a series of pyrazine-based cobaloximes, which, though the complexes are already known, the catalytic dehalogenation properties of these dicobaloximes has yet to be studied. Following on from this, extension of the pyrazine to a bipyridyl species affords the opportunity to synthesise a series of novel dicobaloximes, with the secondary cobaloxime in the ortho- meta- and para- positions of the pyridine to study whether these directing effects will influence the electronic communication between the two cobalt centres, and hence catalysis. The fact there is free rotation between the pyridines may affect the electronic communication, as the orbital overlap is not expected to be as great as in the pyrazine-bridged species. To overcome this, the incorporation of a triple bond between the pyridines will also be attempted, so as to increase conjugation of the π–electron system and aid electron transfer between the cobaloximes, and afford an opportunity to incorporate a dicobalt carbonyl fragment.

5.2. Results and Discussion.

5.2.1. Synthesis, Physical and Structural Properties.

5.2.1.1. Pyrazine Bridged Dicobaloximes.

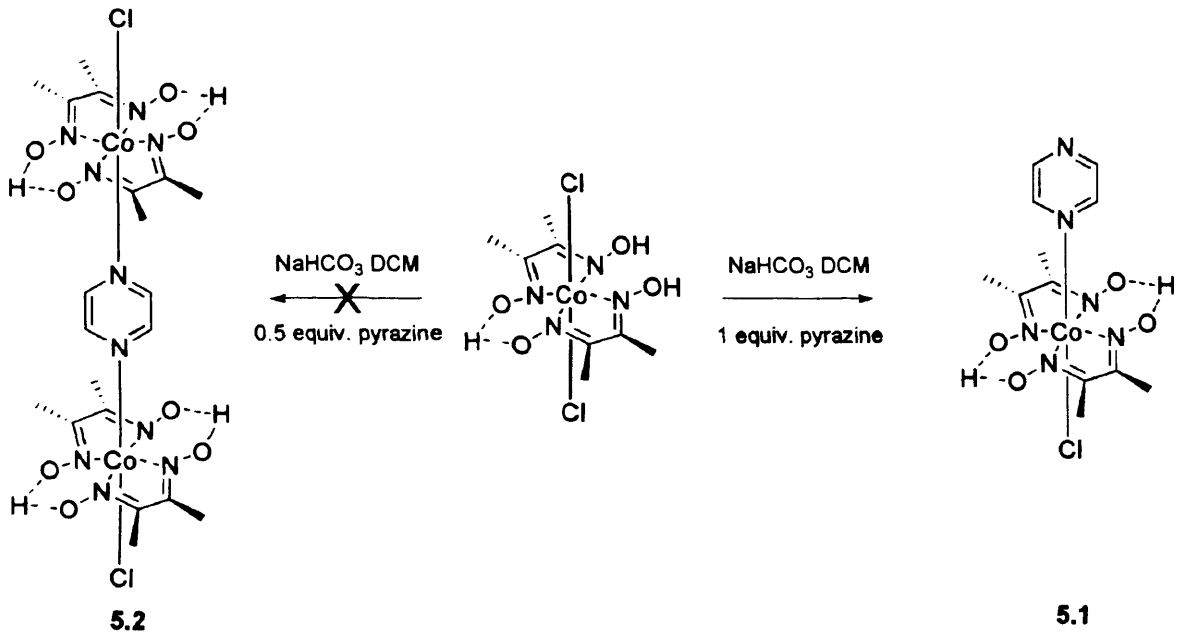

Scheme 5.5. Synthesis of pyrazine bridged cobaloximes.

Employing the procedure used previously in **Chapters 3** and **4** for the coordination of nitrogen heterocyclic ligands to cobaloximes, attempts were made at synthesising μ-pyrazine bridged dicobaloximes, **Scheme 5.5**. On sequential addition of 0.5 equivalents of pyrazine and excess sodium bicarbonate to a suspension of $[Cl_2Co(DMGH)(DMGH_2)]$ in dichloromethane, only the mono-coordinated species $[ClCo(DMGH)_2(pyz)]$, **5.1**, was observed, as characterised by the presence of two broad resonances at 8.52 ppm and 8.31 ppm in the ^{1}H-NMR spectra, depicted in **Figure 5.2**. The two broad resonances correspond to the inequivalent pyrazine hydrogens, resulting from the coordination of only one of the pyrazine nitrogens to a cobaloxime, making the pyrazine ligand unsymmetrical. The resonance at 8.31 ppm is attributed to the protons in closest proximity to the cobaloxime, where the ring currents of the macrocycle have the greatest affect in shifting the resonances to a lower frequency than the resonance at 8.59 ppm for uncoordinated pyrazine hydrogens.

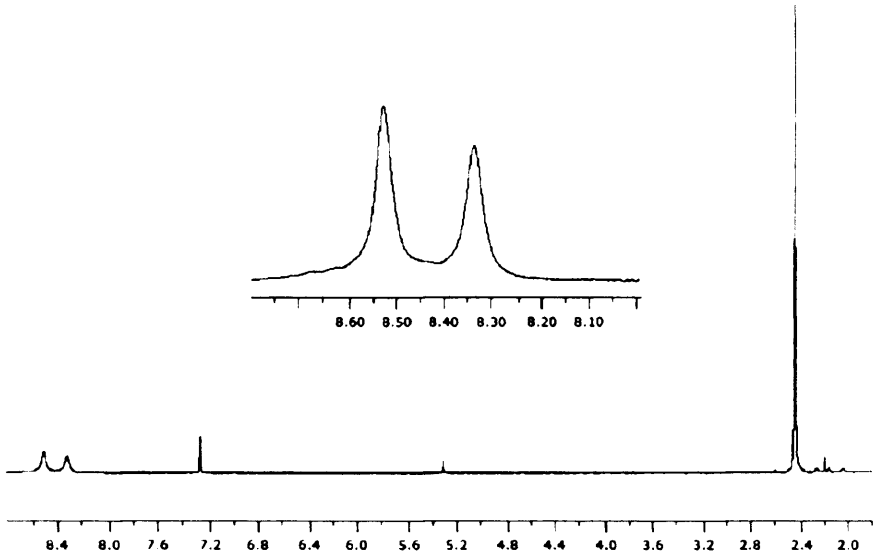

Figure 5.2. ^{1}H-NMR spectra of [Cl(DMGH)$_2$Co(Pyz)] **5.1**, recorded at 400 MHz in $CDCl_3$.

On addition of a range of bases, including sodium bicarbonate and Hűnigs base, to a three phase system of [ClCo(DMGH)$_2$(Pyz)] and [Cl$_2$Co(DMGH)(DMGH$_2$)] in dichloromethane, and increasing the ratio of [Cl$_2$Co(DMGH)(DMGH$_2$)] to pyrazine to 5:1, no dicobaloxime [Cl(DMGH)$_2$Co]$_2$-μ-(Pyz), **5.2**, was observed. This may be due to the lone pair of electrons on the uncoordinated pyrazino nitrogen being less available for coordination, a feature attributed to electron withdrawing effects of the chlorocobaloxime centre.

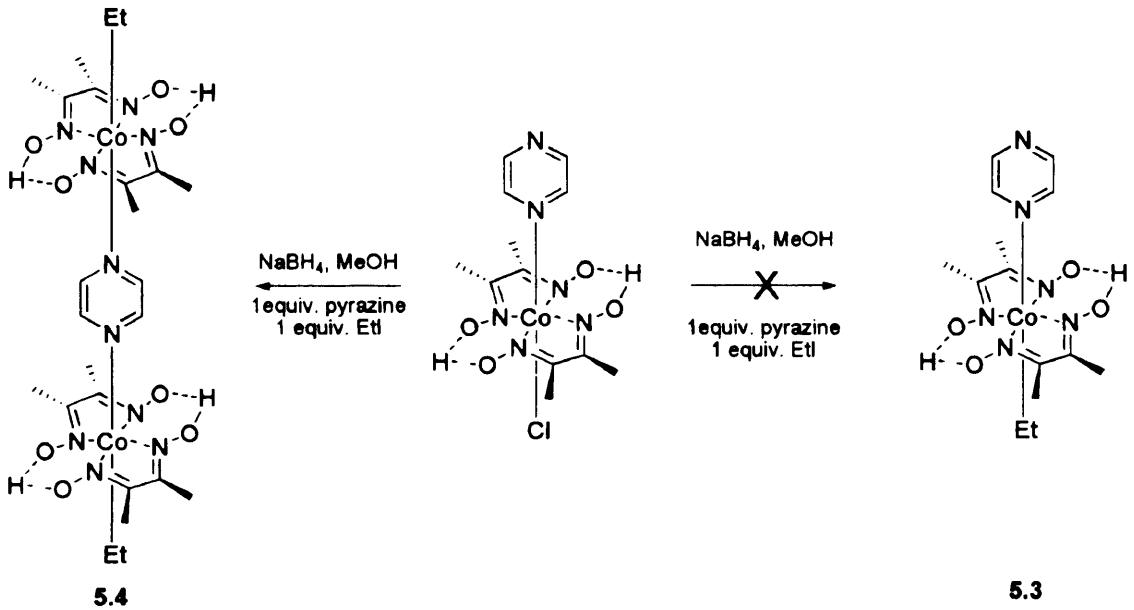

Scheme 5.6. Ethylation of [ClCo(DMGH)$_2$(pyz)] **5.1**.

Conversely, when an attempt was made to synthesise the monocoordinated ethylated analogue [EtCo(DMGH)$_2$(pyz)], **5.3**, via ethylation of [ClCo(DMGH)$_2$(pyz)], the resonances attributed to the pyrazine hydrogens were observed as a sharp singlet resonance at 8.44 ppm, **Figure 5.3**, indicating a symmetrical complex, where all four of the pyrazino hydrogens are now equivalent. The resonance is shifted upfield of the proton resonances of uncoordinated pyrazine, which are observed at 8.59 ppm, due to the ring current exerted on the pyrazine by the two cobaloxime systems. Hence the ethylation of the [ClCo(DMGH)$_2$(pyz)] afforded the dicobaloxime [Et(DMGH)$_2$Co]$_2$-μ-(pyz), **5.4**, as opposed to the expected mono-nuclear [EtCo(DMGH)$_2$(pyz)] **5.3**. The ethyl group is considered to be electron donating and so will push electrons towards the π-system of the equatorial ligand, resulting in more shielding of the pyrazine hydrogens and so the resonance is observed at a lower frequency. Ethylation of [ClCo(DMGH)$_2$(pyz)] was then attempted at a series of ratios, however, in all cases, the dicobaloxime species was observed.

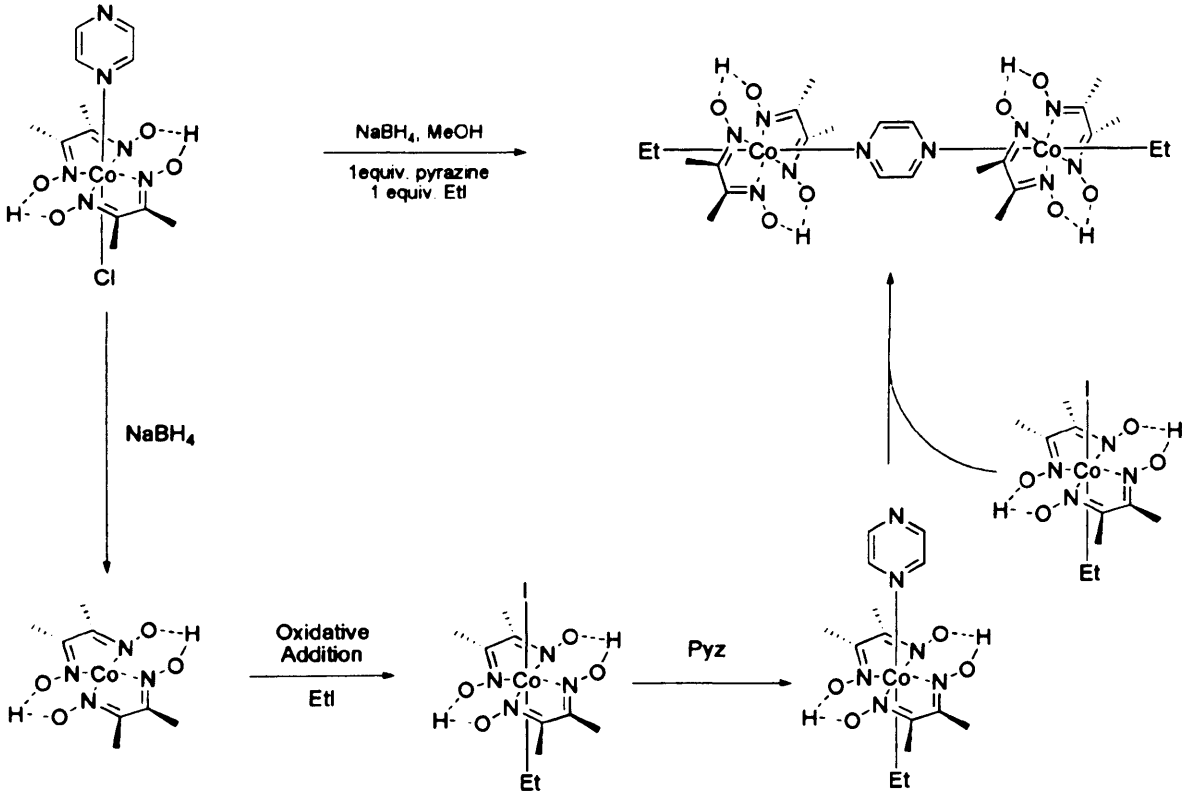

Scheme 5.7. Proposed mechanism for formation of [Et(DMGH)$_2$Co]$_2$-μ-(pyz) **5.4**.

The first step of the ethylation reaction involves the reduction of the [ClCo(DMGH)$_2$(pyz)] to give the 16-electron, four-coordinate cobaloxime intermediate.

This intermediate undergoes oxidative addition of the iodoethane to yield the five-coordinate ethyl cobaloxime intermediate, which is followed by the coordination of pyrazine, yielding [EtCo(DMGH)$_2$(pyz)] **5.3**. Both these reaction intermediates appear to be transient species, as they are not observed in ^{1}H-NMR spectroscopy. As a result of exchange of the electron-withdrawing chloride for the electron-donating ethyl moiety, the lone pair are more available for coordination, and coordinate to a five-coordinate ethyl cobaloxime species, resulting in the formation of the dicobaloximes [Et(DMGH)$_2$Co]$_2$-μ-(pyz), **5.4**.

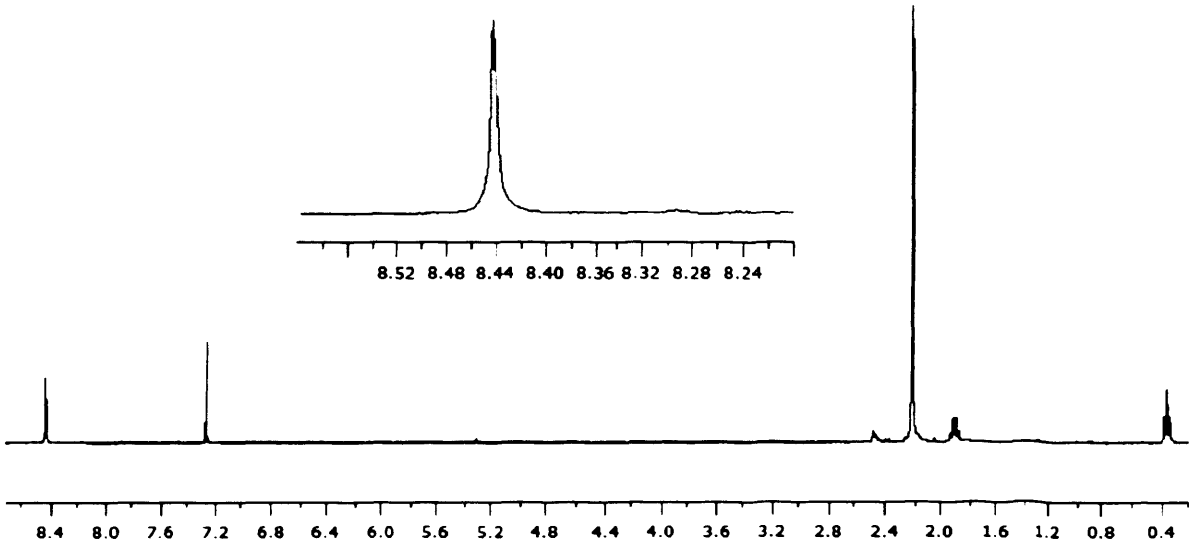

Figure 5.3. ^{1}H-NMR spectra of [Et(DMGH)$_2$Co]$_2$-μ-(Pyz) **5.4**, recorded at 400 MHz in $CDCl_3$.

The yield achieved from the ethylation to give the ethylated dicobaloxime was 88 %, greater than the 60-70 % quoted by Gupta from the dehydration of [EtCo(DMGH)$_2$(H$_2$O)] in the presence of pyrazine.[21] The chlorinated dicobaloxime [Cl(DMGH)$_2$Co]$_2$-μ-(pyz) species was then prepared by addition of a solution of [ClCo(DMGH)$_2$(H$_2$O)] to a solution of pyrazine according to the method described by Gupta[22] for catalyst screening. In all cases, there was no need for purification by column chromatography.

5.2.1.2 Bipyridyl Bridged Dicobaloximes.

Herlinger[13] described a series of dicobaloximes bridged by 4,4'-bipyridine, $[R(DMGH)_2Co]_2$-μ-(4,4'-bipy) (where R = Me or CH_2Cl), by the dehydration method described in **Scheme 5.2**.[23] Expansion of the pyrazine-bridged species to a series of bipyridyl-bridged dicobaloximes affords the opportunity to study how a secondary cobaloxime in the *ortho-*, *meta-* and *para-* positions of a pyridine affects the catalytic ability. Bipyridine is a strong candidate for the bridging ligand. 2,2'-bipyridine and 4,4'-bipyridine are commercially available, whereas 3,3'-bipyridine was synthesised from 3-bromopyridine, following the procedure shown in **Scheme 5.8**.

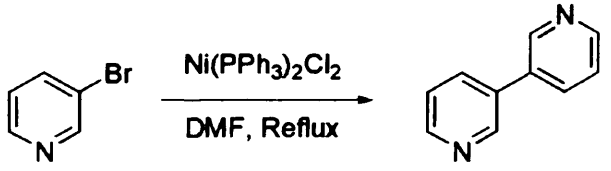

Scheme 5.8. Synthesis of 3,3'-bipyridine.

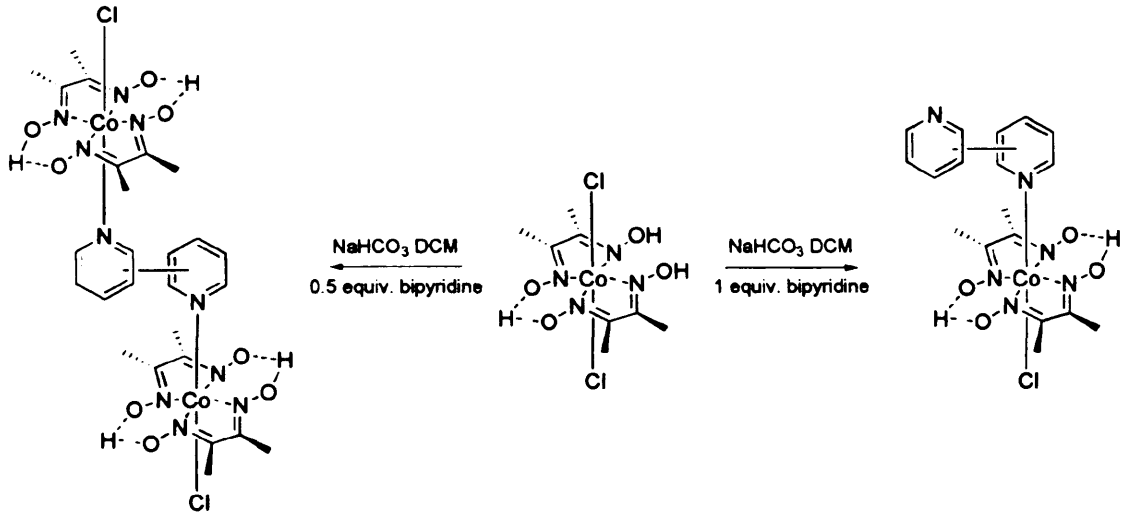

[Cl(DMGH)2Co]$_2$-μ-(2,2'-bipy) (**5.8**)
[Cl(DMGH)2Co]$_2$-μ-(3,3'-bipy) (**5.9**)
[Cl(DMGH)2Co]$_2$-μ-(4,4'-bipy) (**5.10**)

[ClCo(DMGH)$_2$(2,2'-bipy)] (**5.5**)
[ClCo(DMGH)$_2$(3,3'-bipy)] (**5.6**)
[ClCo(DMGH)$_2$(4,4'-bipy)] (**5.7**)

Scheme 5.9. Synthesis of bipyridine bridged dicobaloximes.

The bipyridyl bridged dicobaloximes were prepared by addition of sodium bicarbonate to a suspension of the bipyridyl species and $[Cl_2Co(DMGH)(DMGH_2)]$, depicted in **Scheme 5.9**. Addition of one equivalent of bipyridine to $[Cl_2Co(DMGH)(DMGH_2)]$ will yield the monocobaloxime $[ClCo(DMGH)_2(bipy)]$, whilst addition of 0.5

equivalents of bipyridine will yield the desired bipyridine-bridged dicobaloxime $[Cl(DMGH)_2Co]_2$-μ-(bipy). The results of these reactions are summarised in **Table 5.1.**

Bipyridine	Ratio (Bipy : Cob)	Expected Product	Yield
2,2'-Bipyridine	1:1	$[ClCo(DMGH)_2$(2,2'-bipy)] (**5.5**)	0%
2,2'-Bipyridine	1:2	$[Cl(DMGH)_2Co]_2$-μ-(2,2'-bipy) (**5.8**)	0%
3,3'-Bipyridine	1:1	$[ClCo(DMGH)_2$(3,3'-bipy)] (**5.6**)	78%
3,3'-Bipyridine	1:2	$[Cl(DMGH)_2Co]_2$-μ-(3,3'-bipy) (**5.9**)	0%[a]
4,4'-Bipyridine	1:1	$[ClCo(DMGH)_2$(4,4'-bipy)] (**5.7**)	87%
4,4'-Bipyridine	1:2	$[Cl(DMGH)_2Co]_2$-μ-(4,4'-bipy) (**5.10**)	89%

[a]The reaction yielded $[ClCo(DMGH)_2$ 3,3'-bipy] as the product.

Table 5.1. The results of the coordination.

No reaction was observed between $[Cl_2Co(DMGH)(DMGH_2)]$ and 2,2'-bipyridine, presumably due to the steric repulsion between 2,2'-bipyridine and the DMGH ligands upon addition. The non-coordinating ring is held approximately at a 60 ^{O} angle to the apical position, consequently the approach of the bipyridine to the cobalt is hindered by the equatorial DMGH.

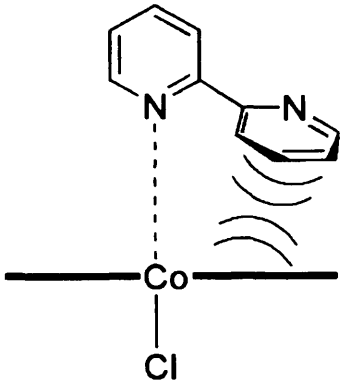

Figure 5.4. The coordination of 2,2'-bipyridine is prevented by the pyridine in the *ortho-* position.

Addition of 3,3-bipyridine to the cobaloxime in both 1:1 and 1:2 ratios yielded the mononuclear species $[ClCo(DMGH)_2$(3,3'-bipy)], **5.6**. Analysis of the aromatic region of the ^{1}H-NMR, **Figure 5.5**, showed the presence of eight resonances attributed to the

3,3-bipyridine species. The peaks at 8.86, 8.67, 7.90 and 7.43 ppm are ascribed to the uncoordinated pyridine ring, with little influence on the ring from the coordination of the cobaloxime and little shift from the resonance of the free 3,3'-bipyridine. The four resonances of the coordinated pyridine are observed at a lower frequency, 8.72, 8.30, 7.80 and 7.38 ppm, due to coordination to the cobaloxime.

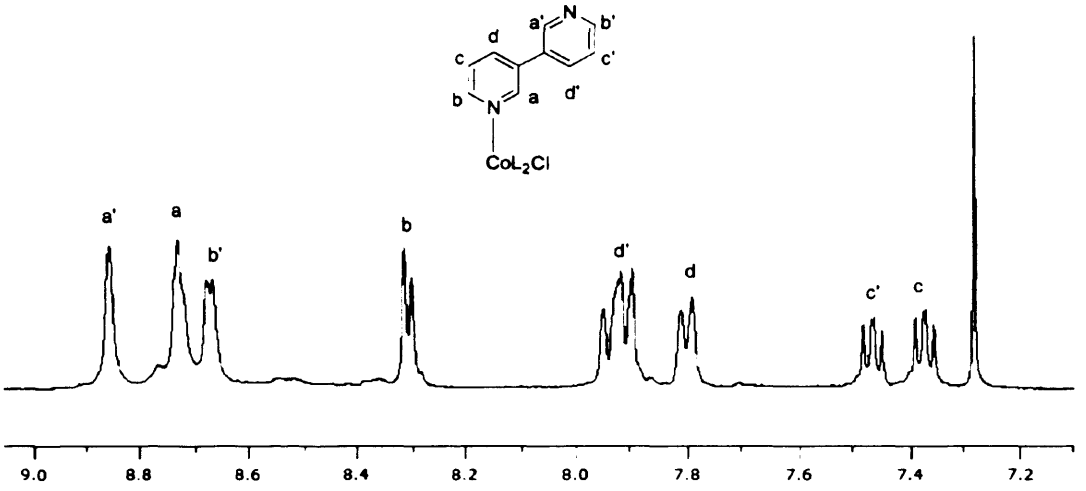

Figure 5.5. Aromatic region of ^{1}H-NMR of [ClCo(DMGH)$_2$(3,3'-bipy)] **5.6**, recorded at 400 MHz in $CDCl_3$.

From the representation of [ClCo(DMGH)$_2$(3,3'-bipy)] depicted in **Figure 5.5**, it was expected that the coordination of a second cobaloxime to yield the dinuclear [Cl(DMGH)$_2$Co]$_2$-μ-(3,3'-bipy) species would proceed with ease, as there is no apparent steric hindrance - the postulated reason preventing the synthesis of [ClCo(DMGH)$_2$(2,2'-bipy)]. Hence, the factor which prevents the coordination of a second cobaloxime to [ClCo(DMGH)$_2$(3,3'-bipy)] is likely to be electronic based, e.g. the lone pair of the uncoordinated pyridine of [ClCo(DMGH)$_2$(3,3'-bipy)] being less available for coordination. The delocalisation, demonstrated in **Scheme 5.10**, of the π-system electrons onto the coordinated pyridine ring could account for this.

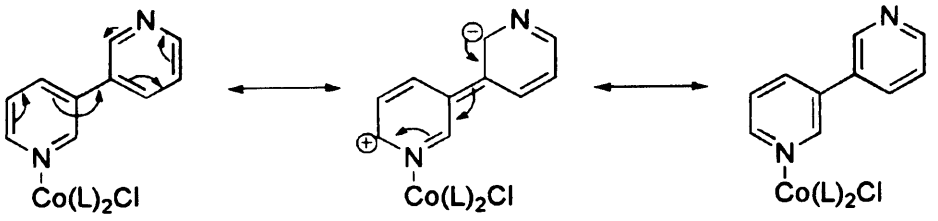

Scheme 5.10. Resonance forms leading to non-coordination of a second cobaloxime.

The addition of 4,4-bipyridine to cobaloxime in a 1:1 ratio yielded the mononuclear species $[ClCo(DMGH)_2(4,4'\text{-bipy})]$, **5.7**. Analysis of the ^{1}H-NMR aromatic region showed the presence of four resonances attributed to the unsymmetrical bipyridine. The resonances at 8.77 and 7.67 ppm correspond to the uncoordinated pyridine ring, and show little shift from the proton resonances of unligated 4,4'-bipyridine (8.77 and 7.57 ppm). The coordinated pyridine resonances are observed at 8.40 and 7.45 ppm and are observed at a lower frequency than observed in unligated 4,4'-bipyridine, again due to the coordination to the cobaloxime.

Reaction of $[Cl_2Co(DMGH)(DMGH_2)]$ with 4,4'-bipyridine in a 2:1 ratio yielded the dicobaloxime $[Cl(DMGH)_2Co]_2$-μ-(4,4'-bipy), **5.8**. This was confirmed by the observation of two resonances in the ^{1}H-NMR spectra, at 8.42 and 7.35 ppm, demonstrating that the two pyridine rings are now equivalent and hence the presence of a dicobaloxime species. The bipyridine resonances are shifted to a lower frequency compared to 4,4'-bipyridine, due to the ring currents of the cobaloxime rings.

The reaction of $[Cl_2Co(DMGH)(DMGH_2)]$ with $[ClCo(DMGH)_2(4,4'\text{-bipy})]$ in the presence of base, also afforded the dinuclear $[Cl(DMGH)_2Co]_2$-μ-(4,4'-bipy) species. This is in contrast with the analogous reaction on $[ClCo(DMGH)_2(Pyz)]$, where no reaction was observed. This unreactivity of the pyrazine cobaloxime was attributed to the lone pair of electrons of the uncoordinated pyrazino nitrogen being unavailable for coordination- a feature attributed to electron withdrawing effects of the chlorocobaloxime centre. It would appear that this factor is negated in the 4,4'-bipyridine bridged system where the orbital overlap is less in the 4,4'-bipyridine than in pyrazine, implying less electronic communication between the cobaloximes bridged by bipyridine than pyrazine.

The ethylation of $[Cl(DMGH)_2Co]_2$-μ-(4,4'-bipy) gave the dicobaloxime $[Et(DMGH)_2Co]_2$-μ-(4,4'-bipy), **5.13**, in good yield (95 %) with the resonances attributed to the bipyridine protons observed at 8.72 and 7.49 ppm, a higher frequency than those of $[Cl(DMGH)_2Co]_2$-μ-(4,4'-bipy). Upon ethylation of the monocobaloximes $[ClCo(DMGH)_2(3,3'\text{-bipy})]$ and $[ClCo(DMGH)_2(4,4'\text{-bipy})]$, the ethylated dicobaloximes $[Et(DMGH)_2Co]_2$-μ-(3,3'-bipy), **5.12**, and $[Et(DMGH)_2Co]_2$-μ-(4,4'-

bipy) were confirmed by the observation of the distinctive triplet resonances around 0.40 ppm. The dicobaloximes were characterised by the pyridine resonances coalescing into four and two peaks respectively at 8.81, 8.63, 7.86 and 7.39 ppm for $[Et(DMGH)_2Co]_2$-μ-(3,3'-bipy), and 8.72 and 7.49 ppm for $[Et(DMGH)_2Co]_2$-μ-(4,4'-bipy). This is in accordance with the ethylation of the monocobaloxime $[ClCo(DMGH)_2(pyz)]$, detailed in **Section 5.2.1.1**, where the mechanism of formation of the ethylated dicobaloximes has been discussed.

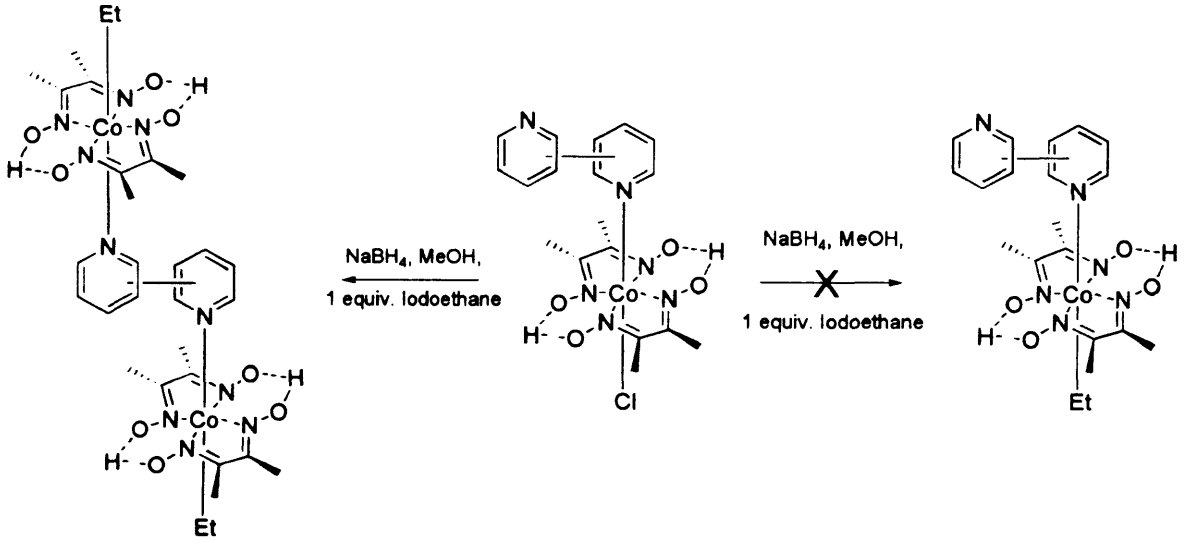

[Et(DMGH)2Co]$_2$-μ-(2,2'-bipy) **(5.11)**
[Et(DMGH)2Co]$_2$-μ-(3,3'-bipy) **(5.12)**
[Et(DMGH)2Co]$_2$-μ-(4,4'-bipy) **(5.13)**

Scheme 5.11. Ethylation of $[ClCo(DMGH)_2(bipy)]$.

Although the chlorinated dicobaloxime **5.9** could not be synthesised by addition of $[Cl_2Co(DMGH)(DMGH_2)]$ to $[ClCo(DMGH)_2(3,3'\text{-bipy})]$, the analogous compound, **5.12,** was synthesised by ethylation of $[ClCo(DMGH)_2(3,3'\text{-bipy})]$. It has been postulated that the difference in reactivity of these cobaloximes is due to the difference in electron affinity of the ethyl and chloride moieties *trans* to the bipyridine. This results in the lone pair of the uncoordinated pyridine becoming more available for coordination to a second cobaloxime in the ethylated species, as the chloride is deemed electron withdrawing and the ethyl moiety electron donating. This affects the degree of electron delocalisation in the 3,3'-bipyridine species and hence the availability of the lone pair.

5.2.1.3. Bis pyridyl acetylene bridged dicobaloximes.

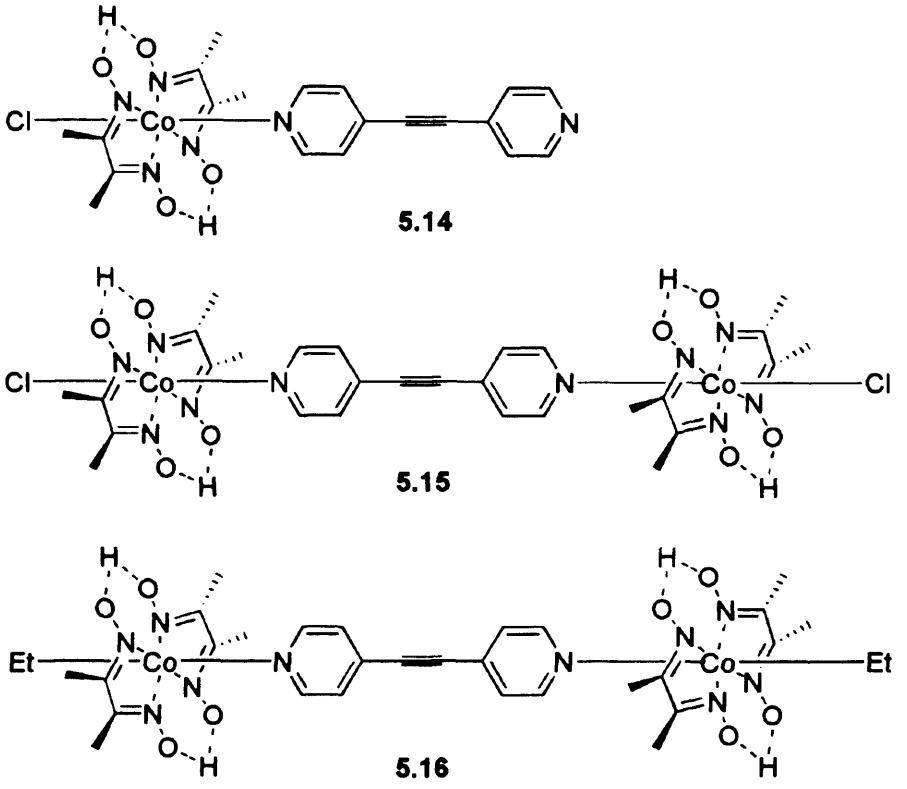

Figure 5.6. Bis(4-pyridyl)acetylene bridged dicobaloximes.

The free rotation between the two pyridine rings of 4,4'-bipyridine results in little conjugation of the π-system when the two rings are orthogonal to each other. Expansion of the π-system of the bridging ligand can be used to improve electronic communication between the cobaloximes. This may be achieved by inserting an alkyne bond between the two pyridine rings, a ligand such as bis(4-pyridyl)acetylene (BPA). This resultant extended π-system increases the orbital overlap and hence the conjugation between the two rings and reduces the degree of rotation around the pyridine-pyridine plane, yielding a more rigid electronic species. The complexes shown in **Figure 5.6** were prepared in order to examine the influence of inserting an alkyne bond between the pyridine rings. Resonance forms of bis(4-pyridyl)acetylene results in partial double bonds forming between the pyridine rings, increasing the conjugation, and therefore electronic communication, between the two pyridine rings. Bond order of single bonds increases, whilst the bond order of the triple bond decreases, as a result of electrons moving into anti-bonding orbitals.

Scheme 5.12. Resonance forms of the BPA ligand, demonstrating the conjugation between the two pyridine rings.

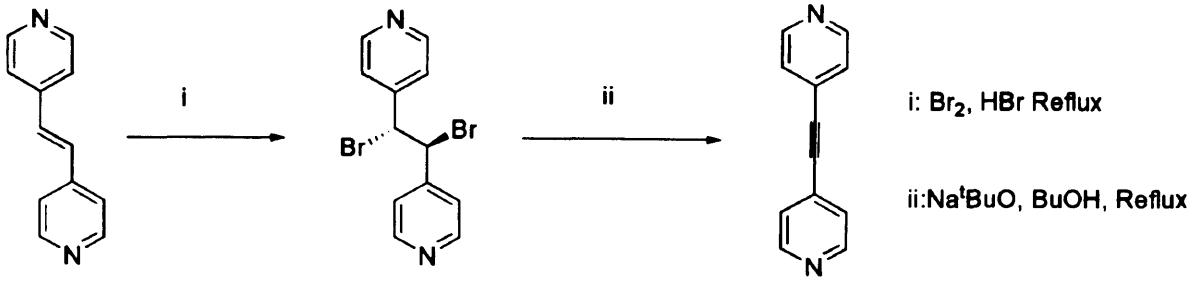

Scheme 5.13. Synthesis of bis(4-pyridyl)acetylene.

Bis(4-pyridyl)acetylene was synthesised by reaction of *trans*-1,2-bis(4-pyridyl)ethylene with bromine, and the resultant 1,2-dibromo-1,2-bis(4-pyridyl)ethane was then de-brominated with NaO^tBu to give bis(4-pyridyl)acetylene, following the method reported in the literature, **Scheme 5.13**.[24] Addition of sodium bicarbonate to a three-phase equimolar mixture of the bis(4-pyridyl)acetylene and $[Cl_2Co(DMGH)(DMGH_2)]$ yielded the mononuclear $[ClCo(DMGH)_2(BPA)]$, **5.14**, characterised by four resonances in the aromatic region at 8.67, 8.29. 7.37, 7.31 ppm. In a 1:2 ratio, the dinuclear $[Cl(DMGH)_2Co]_2$-μ-(BPA), **5.15**, species was achieved, with resonances observed at 8.33 and 7.31 ppm. In all cases, the resonances show a shift from those attributed to uncoordinated bis(4-pyridyl) acetylene which are observed at 8.60 and 7.35 ppm. Ethylation of $[ClCo(DMGH)_2(BPA)]$, and $[Cl(DMGH)_2Co]_2$-μ-(BPA) each gave the ethylated dicobaloximes $[Et(DMGH)_2Co]_2$-μ-(BPA), **5.16**, characterised by the triplet resonance observed at 0.38 ppm, and two resonances at 8.51 and 7.32 ppm in the aromatic region.

5.2.1.4. Heterometallic Cobaloximes.

A long-term goal of this project was to design and carry out chemical reactions with the minimum amount of solvents and reagents. One possible way of cutting down on reagents is to initiate reactions with light. The coordination of luminescent Re centres to the free nitrogen heterocycles of **5.1**, **5.6**, **5.7** and **5.14** would afford the opportunity to

photochemically initiate the catalytic cycle. The substitution of the acetonitrile ligand of $[Re(bipy)(CO)_3(MeCN)][PF_6]$ for the uncoordinated nitrogen heterocycle of compounds **5.1**, **5.6**, **5.7** and **5.14** was attempted by refluxing in acetonitrile, **Scheme 5.14**, whilst the halide abstraction of $[Re(bipy)(CO)_3Cl]$ by heating with the relevant cobaloximes and $AgBF_4$ in toluene, with precautions to eliminate light, **Scheme 5.15,** was hoped to yield the desired heteronuclear species, but these reactions were unsuccessful, presumably due to the low availability of the lone pair, as discussed earlier in this chapter.[25]

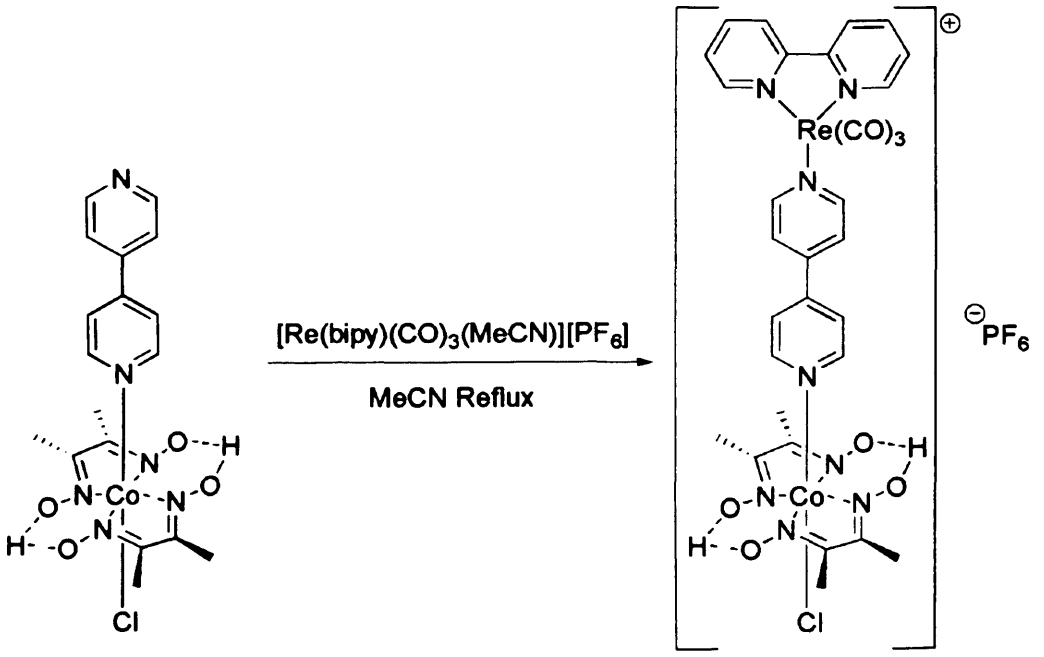

Scheme 5.14. Attempted coordination of $[Re(bipy)(CO)_3]^+$ by substitution of the acetonitrile ligand.

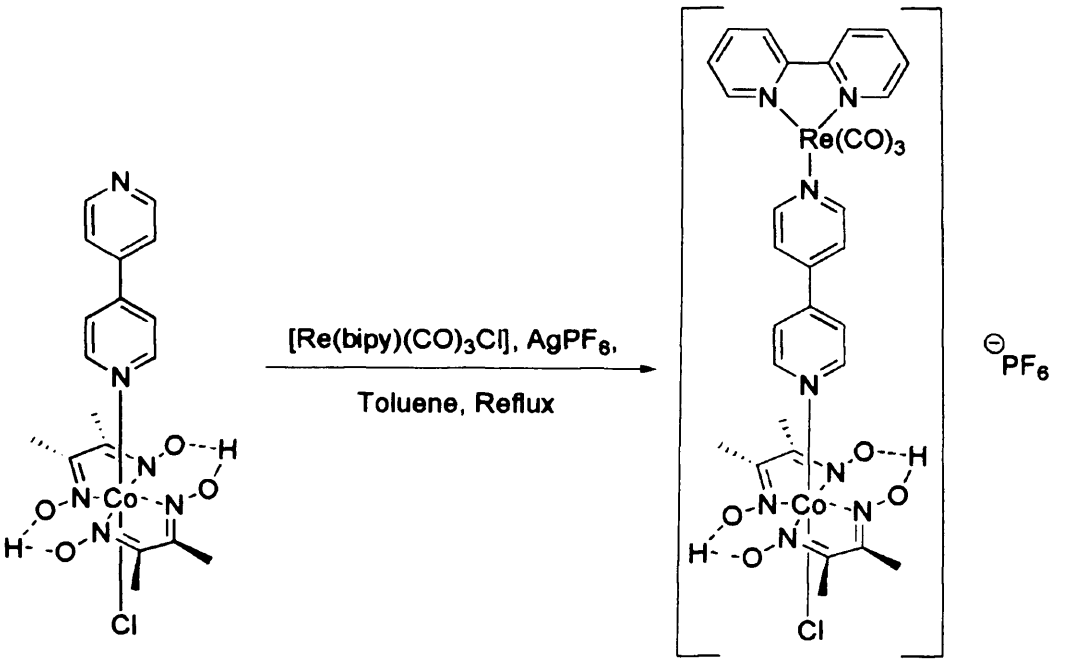

Scheme 5.15. Attempted coordination of $[Re(bipy)(CO)_3]^+$ by abstraction of the chloride ligand.

Alternatively, coordinating a bifunctional ligand, such as 4-ethynylpyridine, to the rhenium centre could afford a metalloligand, which could then coordinate to $[Cl_2Co(DMGH)(DMGH_2)]$. 4-ethynylpyridine was prepared from the addition of NaOH to 2-methyl-4-(pyridin-4-yl)but-3-yn-2-ol or 4-(2-(trimethylsilyl)ethynyl)pyridine, as depicted in **Scheme 5.16**. Both reactions, however, were troubled by low yields arising from sublimation of the product at low pressures and dimerisation of the product after only a short period of time. Hence the 4-ethynylpyridine was prepared on the day of use and kept in the dark at low temperatures.

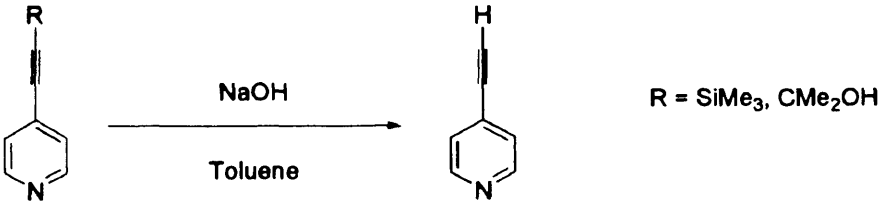

Scheme 5.16. Synthesis of 4-ethynylpyridine.[26]

Freshly prepared 4-ethynylpyridine was added to a series of known rhenium complexes, of the type $[Re(L)(CO)_3Cl]$,[25] where L = 2,2'-bipyridine, 1,10-phenanthroline and 1,10-phenanthroline-5,6-dione, with an excess of metal hexafluorophosphate salt, such as $NaPF_6$, $TlPF_6$ or $AgPF_6$, as depicted in **Scheme 5.17**. It was believed that this metal

salt would aid the coordination of the 4-ethynylpyridine to the rhenium centre. However, despite best efforts to exclude light, moisture and air from the reaction, the 4-ethynylpyridine dimerised, as characterised by the disappearance of the alkyne proton resonance at 3.25 ppm and the appearance of the alkene proton resonance at 5.20 ppm. Attempts at coupling the commercially available 4-ethynylpyridine.HCl salt, but again, only rhenium starting material and the dimer were observed.

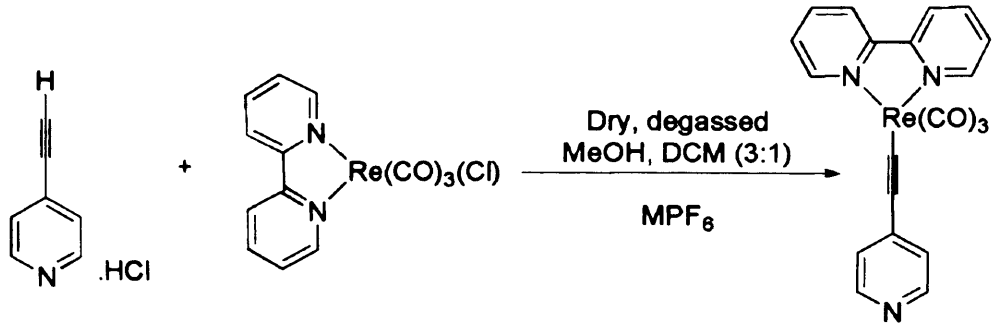

Scheme 5.17. Towards a Co-Re heterometallic complex with a 4-ethynylpyridine spacer.[27]

5.3. Catalytic Dechlorination of PCE.

The activity of these nitrogen-heterocycle bridged dicobaloximes towards dechlorination catalysis was tested in a manner similar to that described in Chapter 4, thus allowing a direct comparison between the two schematics of multimetallic cobaloximes. The results of the catalysis are shown in **Table 5.2**.

Catalyst	Equiv. of PCE consumed	Equiv. of TCE recovered	Equiv. further reduced	Estimated T.O.N.
3.1	3.8	1.9	1.9	5.7
3.5	3.2	2.3	0.9	4.1
5.1	4.1	0.7	3.4	7.5
5.2	4.5	0.8	3.7	8.2
5.12	4.0	0.8	3.2	7.2
5.13	4.3	0.7	3.6	7.9
5.14	5.0	0.5	4.5	9.5
5.15	4.2	0.6	3.6	7.8
5.16	4.4	0.5	3.9	8.3

Table 5.2. Catalytic dechlorination of PCE results. Reaction conditions: 1 mmol of catalyst, 10 mmol of PCE, 1 mmol of anisole, as the internal standard in methanol, 5 ml.

3 mmol of sodium hydroxide and 2 mmol of sodium borohydride in 1 ml of water added. Sample run through celite and silica, and submitted for GC and GC-MS analysis.

Each dicobaloxime tested showed a small enhancement over the simple pyridylcobaloximes [$R(DMGH)_2Co(Pyr)$] for PCE dechlorinated, but the main improvement over the pyridyl cobaloximes **3.1** and **3.5**, was observed when studying the amount of TCE recovered, with between 83 and 90 % of the TCE yielded from the first reduction step being reduced further. As there are two cobaloximes present, the enhanced catalytic activity could be attributed to the presence of these two cobaloximes acting independently. If there was no electronic communication between the two cobaloximes, i.e. they are isolated, then it would be expected that the catalytic ability of the two cobaloximes would be the sum of the two individual cobaloximes. However, the marked increase in the dechlorination of TCE implies that there is communication between the two centres in that one is reduced initially, and allows the second to act as the catalyst. The presence of this second cobaloxime could facilitate the cleavage of the Co-C bond, allowing greater turnover of catalyst.

The most effective catalyst was found to be the pyrazine bridged $[Cl(DMGH)_2Co]_2$-μ-(pyz) species, followed by the bis-(4-pyridyl) acetylene $[Cl(DMGH)_2Co]_2$-μ-(BPA) species, and the least active were the $[Cl(DMGH)_2Co]_2$-μ-(3,3'-bipy) species. The superior catalytic ability attributed to the bis-(4-pyridyl) acetylene and the pyrazine bridged dicobaloximes is due to the extra orbital overlap of these species over the bipyridine, which has free rotation between the two pyridine rings, allowing for better electron transfer between the two cobaloxime centres. There is a slight enhancement of catalytic ability of the 4,4'-bipyridyl bridged dicobaloximes over the 3,3'-bipyridyl bridged dicobaloximes, so the changing from the meta- to the para- subsitiuted results in a marginal increase in catalytic ability, possibly due to directing effects of moving the position of the second cobaloxime.

Once again, GC-MS analysis showed the presence of dichloroethylene and vinylchloride. It is important to note that, although the catalytic ability is enhanced over the pyridyl cobaloximes, the dicobaloxime catalysts are not as effective as the dicobaltcarbonyl alkyne bridged cobaloximes of **Chapter 4**. The electrochemistry of the

pyrazine bridged dicobaloximes was studied in **Section 5.2.1.**, where the reduction half of the cyclic voltamogramm showed two reduction potentials at -0.97 and -1.37 V. The electrochemistry of the dicobaltcarbonyl bridged cobaloxime, **4.14**, was discussed in **Section 4.3.3.**, where three reduction potentials, at -0.52, -1.07, -1.24 V, were recorded. That there is a 0.13 V shift to a more positive oxidation value could account for the enhancement of catalytic ability in the dicobaltcarbonyl bridged species over the pyrazine bridged cobaloximes.

5.4. Towards Cobalt Complexes with an Equatorial Secondary Metal Centre.

Chapter 4 demonstrated how the incorporation of secondary metal centres into cobaloximes enhances the catalytic ability towards reductive dechlorination of PCE, whilst the work undertaken in **Chapter 3** showed that both the axial ligands are lost upon reduction from Co(III) to Co(I). It follows that the loss followed by re-association of the axial ligand containing the redox active centre could have an affect on catalytic ability and turnover frequencies. This section investigates the issues arising from this, by attempting to synthesise a series of cobaloximes where the equatorial ligands have been designed to contain secondary metal centres to see whether secondary metals centres in the equatorial plane is an viable alternative.

5.4.1. Alkyne glyoximes.

Gupta *et al*, synthesised a range of cobaloxime species with varied glyoxime ligands, including DMGH, DPGH, GH and CHGH, forming the equatorial plane.[9,15,16] The first target molecule, shown in **Figure 5.7**, was an extension of these glyoxime ligands, containing an alkyne group, which could be bridged by a dicobaltcarbonyl fragment.

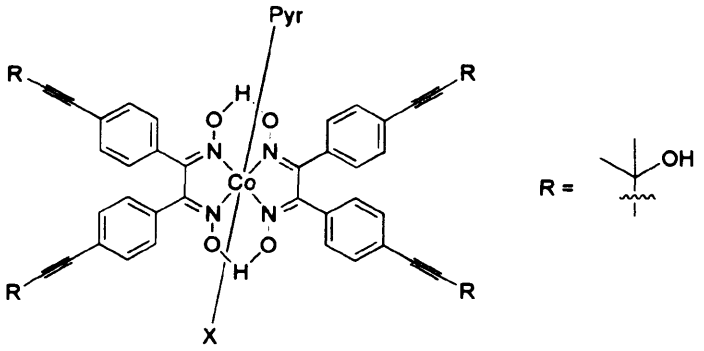

Figure 5.7. Proposed cobaloxime with equatorial ligands for bridging with dicobaltcarbonyl fragments.

The functionalisation of diphenylglyoxime would give a ligand containing an alkyne spacer necessary for bridging. Retrosynthetic analysis, shown in **Scheme 5.18**, of the alkyne glyoxime ligand, 1,2-bis(4-(3-hydroxy-3-methylbut-1-ynyl)phenyl)ethane-1,2-dioxime, showed that there are two possible routes for synthesising the ligand, which only differ in the order of the reactions. The full disconnection to the substituted benzaldehyde was avoided, as the diketone, 2-bis(4-bromophenyl)ethane-1,2-dione, was commercially available.

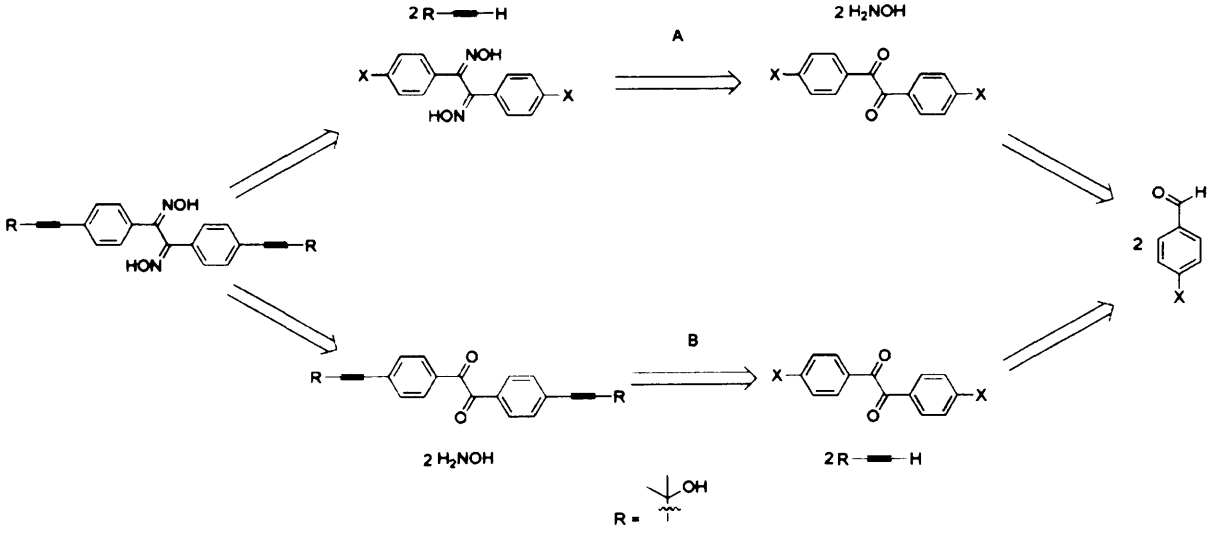

Scheme 5.18. Disconnection of 1,2-bis(4-(3-hydroxy-3-methylbut-1-ynyl)phenyl) ethane-1,2-dioxime.

Option A undergoes the conversion of the diketone 4,4'-dibromobenzil to 1,2-bis(4-bromophenyl)ethane-1,2-dione dioxime, followed by a Sonogashira coupling to give the

desired product. Option B first undergoes the Sonogashira coupling on 4,4'-dibromobenzil and then the conversion to the target dioxime.

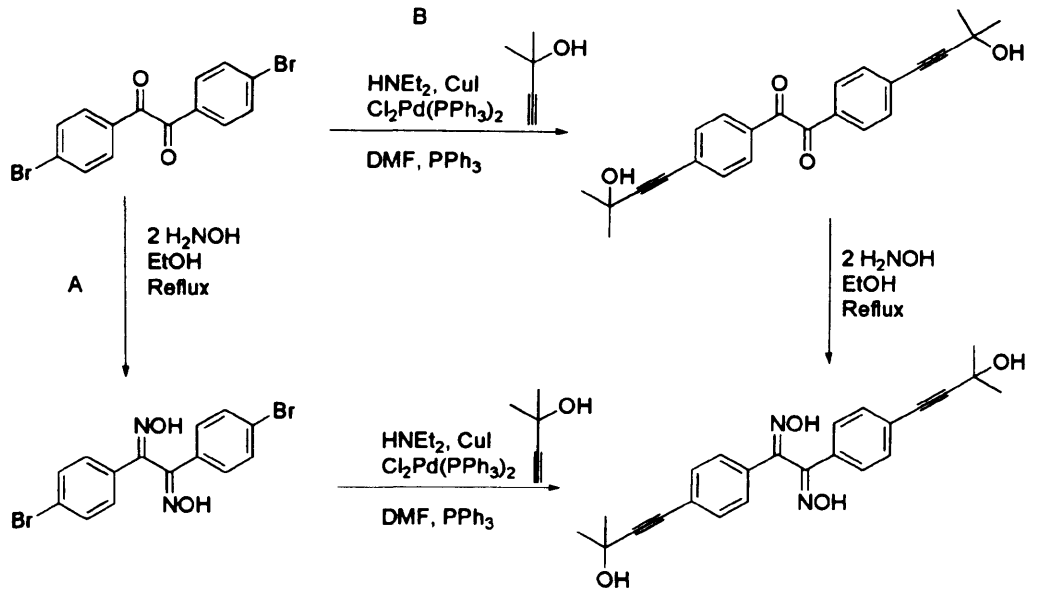

Scheme 5.19. Strategy for alkyne glyoxime synthesis.

Initially, route A was undertaken to convert the diketone to the glyoxime, and then attempt the coupling. The conversion to the glyoxime by reaction in ethanol with hydroxylamine hydrochloride was undertaken and the glyoxime product was characterised by the shift of the phenyl peaks to 7.98 and 7.73 ppm. However, when the Sonogashira coupling was carried out on this species, no alkyne glyoxime was observed, as undertaking the Sonogashira coupling in the presence of oxime groups is believed to be prevented by the oxime binding to the palladium catalyst, rendering the catalyst ineffective.

Alternatively, route B, where the Sonogashira coupling was followed by conversion to the oxime. The coupling of the diketone 1,2-bis(4-bromophenyl)ethane-1,2-dione with the alkyne 2-methylbut-3-yn-2-ol yielded 1,2-bis(4-(3-hydroxy-3-methylbut-1-ynyl)phenyl)ethane-1,2-dione in good yield and was characterised by the presence of the resonances at 7.92, 7.55, 1.65 ppm. However, the subsequent reaction of the diketone with hydroxylamine to give the alkyne glyoxime yielded thick oil, with no C≡C band observed in the IR spectra, presumably due to the polymerisation of the alkyne group at the high temperatures required for conversion to the glyoxime.

5.4.2. Bifunctional Phenanthroline Imines as Ligands for Multimetallic Complexes.

An alternative option is to synthesise an ambidentate ligand, shown in **Figure 5.8**, with two coordination sites, one for cobalt and one for a redox active metal, to give a possible candidate for catalysis.[28]

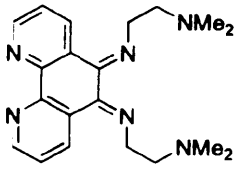

Figure 5.8. (E)-N1-((E)-6-(2-(dimethylamino)ethylimino)-1,10-phenanthrolin-5(6H)-ylidene)-N2,N2-dimethylethane-1,2-diamine.

Condensation of unsym-dimethyl-ethylenediamine with 1,10-phenathroline-4,5-dione was achieved by adding the diamine dropwise to a methanolic solution of 1,10-phenathroline-4,5-dione and a catalytic amount of acetic acid. The reaction was left to stir at 60 ^{O}C for 30 mins, at which point the insoluble matter was filtered off, and the solvent removed *in vacuo* to yield (E)-N1-((E)-6-(2- (dimethylamino)ethylimino) -1,10-phenanthrolin- 5(6H)-ylidene)- N2, N2-dimethylethane-1,2-diamine as a brown powder, which proved to very extremely hygroscopic. The alternative route of adding unsym-dimethyl-ethylenediamine to [ReBr(1,10-phenathroline-4,5-dione)$(CO)_3$] yielded a red solid, which was also extremely hygroscopic. Addition of $CoCl_2$ and $[Co(NH_3)_6]Cl_3$ to this, yielded no multimetallic product.

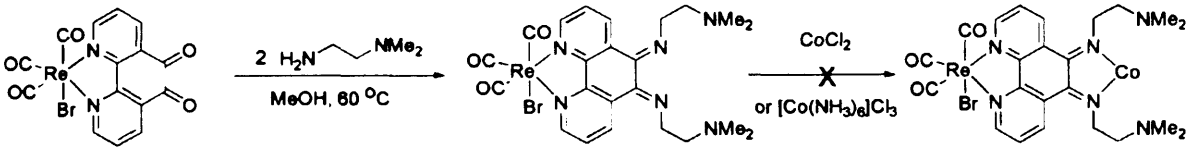

Scheme 5.20. Attempted synthesis of multimetallic Re-Co species.

5.5. Conclusions.

As an alternative route to nitrogen heterocyclic bridged dicobaloximes, the addition of the nitrogen heterocycle to $[Cl_2Co(DMGH)(DMGH_2)]$ in the presence of a base is a good method, with higher yields and a simpler work up, although $[ClCo(DMGH)_2]_2$-μ-pyz and $[ClCo(DMGH)_2]_2$-μ-3,3'-bipy could not be made by this method. It is interesting to note that upon ethylation of the monomeric cobaloximes, the dicobaloxime is yielded, as opposed to the expected ethylated monomer.

Each dicobaloxime was subjected to catalyst screening, and an enhancement over the pyridylcobaloximes was observed, with the dicobaloximes found to reduce between four and five equivalents of PCE to TCE. Furthermore, nearly all of the TCE is reduced further and the turnover numbers approximately 8. Though further proof for the incorporation of secondary metal centres enhances dechlorination, the results gained are not as good as those achieved by the dicobaltcarbonyl bridged cobaloximes of **Chapter 4**.

5.6. Experimental.

[ClCo(DMGH)$_2$Pyz] 5.1

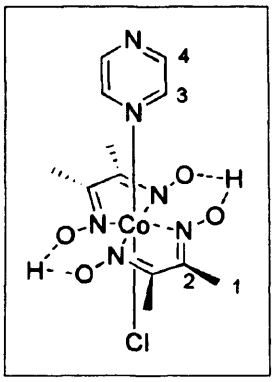

To a suspension of [Cl_2Co(DMGH)($DMGH_2$)] (2.5 g, 6.9 mmol) in dichloromethane (10 ml) was added pyrazine (0.609 g, 7.6 mmol) and sodium bicarbonate (10 ml) sequentially. The mixture was stirred at room temperature for 2 hours and the resultant brown solution was diluted further with dichloromethane (20 ml) and washed with water (2 x 20 ml). The organic fractions were combined, dried over sodium sulfate, filtered and evaporated to dryness, yielding [ClCo(DMGH)$_2$(Pyz)] as a brown solid. (2.58 g, 92 % yield), δH ($CDCl_3$) (ppm) 8.52 (2 H, br, C*H* (4) Pyz), 8.31 (2 H, br, C*H* (3) Pyz), 2.43 (12 H, s, CH_3 (1) DMGH) δC ($CDCl_3$) (ppm) 151.5 (*C* (2) DMGH), 146.2 (*C* (4), Pyz), 145.3 (*C* (3), Pyz), 12.3 (CH_3 (1) DMGH), *m/z* (ESI) $[MH]^+$ = 405.0 HRMS (ESI) calculated $[MH]^+$ = 405.0488; measured $[MH]^+$ = 405.0492.

[ClCo(DMGH)$_2$]$_2$-μ-pyz 5.4

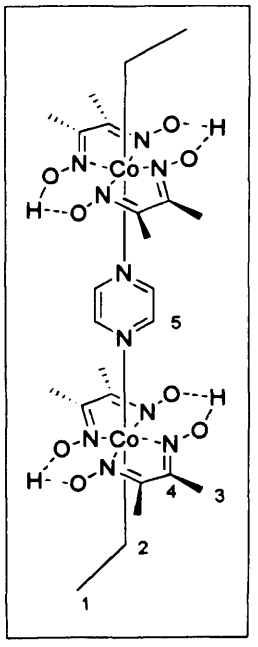

To a solution of [ClCo(DMGH)$_2$(Pyz)] (1 g, 1.4 mmol) and iodoethane (0.12 ml, 1.5 mmol, 1.1 equivs.) in methanol (20 ml) was added sodium borohydride (0.165 g, 4.1 mmol, 3 equivs.). The reaction was left to stir for 30 minutes, when the solvent was removed *in vacuo*, and the crude solid was dissolved in dichloromethane (10 ml) and washed with distilled water (2 x 10 ml). The organic fractions were combined, dried over sodium sulfate, filtered and evaporated to dryness, yielding [EtCo(DMGH)$_2$]$_2$-μ-(pyz) as a brown solid. (0.43 g, 88 % yield), δH ($CDCl_3$) (ppm) 8.44 (4 H, s, C*H* (5) Pyz), 2.19 (24 H, s, CH_3 (3) DMGH), 1.89 (2 H, q, J = 7.5 Hz, CH_2 (2) Co-CH_2-CH_3) 0.33 (3 H, t, J = 7.5 Hz, CH_3 (1) Co-CH_2-CH_3) δC ($CDCl_3$) (ppm) 150.9 (*C* 42) DMGH), 146.7 (*C*H (5) Pyz), 38.2 (*C* (2) Co-CH_2-CH_3), 15.2 (*C* (1) Co-CH_2-CH_3), 12.4 (*C* (3) DMGH). *m/z* (ESI) 717.2 $[MH]^+$ HRMS (ESI) calculated $[MH]^+$ = 717.1929; measured $[MH]^+$ = 717.1925.

[ClCo(DMGH)$_2$(3,3'-bipy)] 5.6

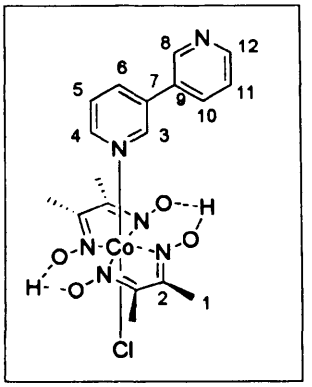

To a suspension of [Cl_2Co(DMGH)(DMGH$_2$)] (1 g, 2.8 mmol) in dichloromethane (10 ml) was added 3,3'-bipyridine (0.475 g, 3.0 mmol, 1.1 equivs.) and sodium bicarbonate (10 ml) sequentially. The mixture was stirred at room temperature for 2 hours and the resultant brown solution was diluted further with dichloromethane (20 ml) and washed with water (2 x 20 ml). The organic fractions were combined, dried over sodium sulfate, filtered and evaporated to dryness, yielding [ClCo(DMGH)$_2$(3,3'-bipy)] as a brown solid. (1.05 g, 78 % yield) δH ($CDCl_3$) (ppm) 8.86 (1 H, s, C*H* (8) Bipy), 8.72 (1 H, s, C*H* (3) Bipy), 8.67 (1 H, d, *J* = 4.1 Hz, C*H* (12) Bipy), 8.30 (1 H, d, *J* = 4.0 Hz, C*H* (4) Bipy), 7.90 (1 H, d, *J* = 7.7 Hz, C*H* (10) Bipy), 7.80 (1 H, d, *J* = 5.3 Hz, C*H* (6) Bipy), 7.43 (1 H, dt, C*H* (11) Bipy), 7.38 (1 H, dt, C*H* (5) Bipy), 2.35 (12 H, s, CH_3 (1), DMGH). δC ($CDCl_3$) (ppm) 150.2 (*C* (2) DMGH), 149.1 (*C* (8) Pyr), 148.0 (*C* (12) Pyr), 147.2 (*C* (3) Pyr), 146.3 (*C* (4) Pyr), 134.1 (*C* (10) Pyr), 133.2 (*C* (9) Pyr), 132.6 (*C* (6) Pyr), 131.9 (*C* (7) Pyr), 124.0 (*C* (11) Pyr), 123.5 (*C* (5) Pyr), 12.0 (*C* (1) DMGH). *m z* (ESI) 481.0 $[MH]^+$ HRMS (ESI) calculated $[MH]^+$ = 481.0801; measured $[MH]^+$ = 481.0807.

[EtCo(DMGH)$_2$]$_2$-μ-(3,3'-bipy) 5.12

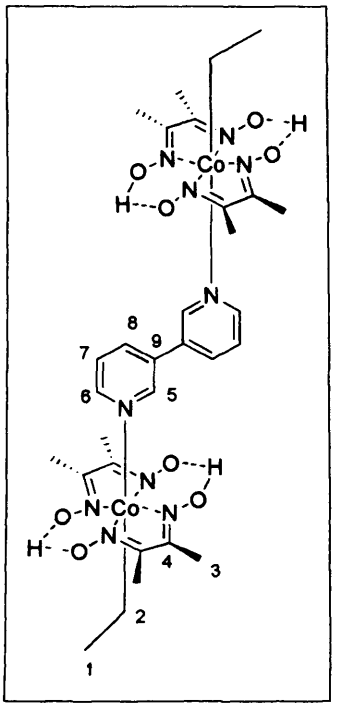

To a suspension of [ClCo(DMGH)$_2$(3,3'-bipy)] (0.5 g, 1.0 mmol) in methanol (5 ml) was added iodoethane (0.17 ml, 2.2 mmol, 2.1 equivs.) and sodium borohydride (0.120 g, 3.0 mmol, 3 equivs.) were added sequentially. The mixture was allowed to stir for two hours, after which, the solvent was removed *in vacuo*, and the crude brown solid was dissolved in dichloromethane (20 ml) and washed with water (2 x 20 ml). The organic fractions were combined, dried over sodium sulfate, filtered and evaporated to dryness, yielding the [EtCo(DMGH)$_2$]$_2$-μ-(3,3'-bipy) as a brown solid. (0.29 g, 73 % yield), δH ($CDCl_3$) (ppm) 8.86 (2H, s, C*H* (3) Bipy), 8.63 (2 H, d, J = 4.1 Hz, C*H* (6) Bipy), 7.96 (2 H, d, J = 7.7 Hz, C*H* (8) Bipy), 7.39 (2 H, dt, C*H* (7) Bipy), 2.42 (12 H, s, CH_3 (3), DMGH). 1.77 (2 H, q, J = 7.6 Hz, CH_2 (2), Co-CH_2-CH_3), 0.41 (3 H, t, J = 7.6 Hz, CH_3 (1), Co-CH_2-CH_3) δC ($CDCl_3$) (ppm) 151.7 (*C* (4) DMGH), 147.1 (*C* (5) Pyr), 146.0 (*C* (6) Pyr), 133.1 (*C* (8) Pyr), 125.2 (*C* (7) Pyr), 122.9 (*C* (9) Pyr), 40.8 (*C* (2) Co-CH_2-CH_3), 16.1 (*C* (1) Co-CH_2-CH_3), 12.0 (*C* (3) DMGH). *m/z* (ESI) 793.2 $[MH]^+$. HRMS (ESI) calculated $[MH]^+$ = 793.2242; measured $[MH]^+$ = 793.2248.

[ClCo(DMGH)$_2$(4,4'-bipy)] 5.7

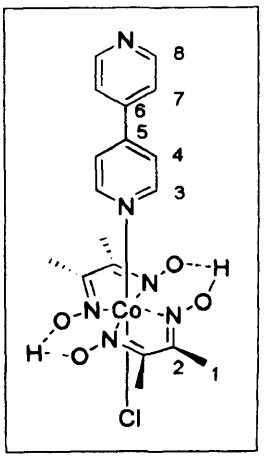

To a suspension of [Cl_2Co(DMGH)(DMGH$_2$)] (2.5 g, 6.9 mmol) in dichloromethane (10 ml) was added 4,4'-bipyridine (1.19 g, 7.6 mmol, 1.1 mmol) and sodium bicarbonate (10 ml) sequentially. The mixture was stirred at room temperature for 2 hours and the resultant brown solution was diluted further with dichloromethane (20 ml) and washed with water (2 x 20 ml). The organic fractions were combined, dried over sodium sulfate, filtered and evaporated to dryness, yielding [ClCo(DMGH)$_2$(4,4'-bipy)] as a brown solid. (2.9 g, 87 % yield), δH ($CDCl_3$) (ppm) 8.77 (2 H, d, J = 6.2 Hz, C*H* (8) Bipy), 8.40 (2 H, d, J = 6.9 Hz, C*H* (3) Bipy), 7.67 (2 H, d, J = 6.9 Hz, C*H* (7) Bipy), 7.45 (2 H, d, J = 6.2

Hz, C*H* (4) Bipy), 2.44 (12 H, s, CH_3 (1) DMGH), δC ($CDCl_3$) (ppm) 151.3 (*C* (2) DMGH), 150.9 (*C* (8) Pyr), 148.1 (*C* (3) Pyr), 127.8 (*C* (7) Pyr), 126.5 (*C* (4) Pyr), 125.3 (*C* (6) Pyr), 123.7 (*C* (5) Pyr), 11.9 (*C* (1) DMGH). *m/z* (ESI) 481.0 $[MH]^+$. HRMS (ESI) calculated $[MH]^+$ = 481.0801; measured $[MH]^+$ = 481.0805.

[ClCo(DMGH)$_2$]$_2$-μ-(4,4'-bipy) 5.8

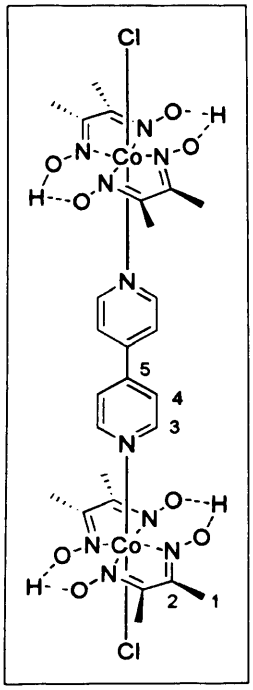

To a suspension of [Cl_2Co(DMGH)(DMGH$_2$)] (1 g, 2.8 mmol) in dichloromethane (10 ml) was added 4,4'-bipyridine (0.22 g, 1.4 mmol, 0.5 equiv.) and sodium bicarbonate (10 ml) sequentially. The mixture was stirred at room temperature for 2 hours and the resultant brown solution was diluted further with dichloromethane (20 ml) and washed with water (2 x 20 ml). The organic fractions were combined, dried over sodium sulfate, filtered and evaporated to dryness, yielding [ClCo(DMGH)$_2$]$_2$-μ-(4,4'-bipy) as a brown solid. (1 g, 89 % yield), δH ($CDCl_3$) (ppm) 8.42 (2 H, d, *J* = 6.6 Hz, C*H* (3) Pyr), 7.35 (2 H, d, *J* = 6.6 Hz, C*H* (4) Pyr), 2.41 (24 H, s, CH_3 (1) DMGH), δC ($CDCl_3$) (ppm) 150.2 (*C* (2) DMGH), 147.2 (*C* (3) Pyr), 125.2 (*C* (4) Pyr), 123.1 (*C* (5) Pyr), 12.0 (*C* (1) DMGH). *m/z* (ESI) 805.0 $[MH]^+$. HRMS (ESI) calculated $[MH]^+$ = 805.0837; measured $[MH]^+$ = 805.0841.

[ClCo(DMGH)$_2$]$_2$-μ-(4,4'-bipy) – method 2. 5.8

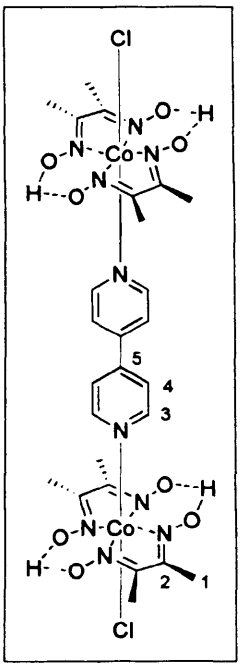

To a suspension of [Cl_2Co(DMGH)(DMGH$_2$)] (1.0 g, 2.8 mmol) in dichloromethane (10 ml) was added [ClCo(DMGH)$_2$-μ-(4,4'-bipy)] (1.48 g, 3.46 mmol, 1 equiv.) and sodium bicarbonate (10 ml) sequentially. The mixture was stirred at room temperature for 2 hours and the resultant brown solution was diluted further with dichloromethane (20 ml) and washed with water (2 x 20 ml). The organic fractions were combined, dried over sodium sulfate, filtered and evaporated to dryness, yielding [ClCo(DMGH)$_2$]$_2$-μ-(4,4'-bipy) as a brown solid. (1.74 g, 77 % yield), δH ($CDCl_3$) (ppm) 8.42 (2 H, d, *J* = 6.6 Hz, C*H* (3) Pyr), 7.35 (2 H, d, *J* = 6.6 Hz, C*H* (4) Pyr), 2.41 (24 H, s, CH_3 (1) DMGH), δC ($CDCl_3$) (ppm) 150.2 (*C* (2) DMGH), 147.2 (*C* (3) Pyr), 125.2 (*C* (4) Pyr), 123.1 (*C* (5) Pyr), 12.0 (*C* (1) DMGH). *m z* (ESI) 805.0 $[MH]^+$. HRMS (ESI) calculated $[MH]^+$ = 805.0837; measured $[MH]^+$ = 805.0841.

[EtCo(DMGH)$_2$]$_2$-μ-(4,4'-bipy) 5.13

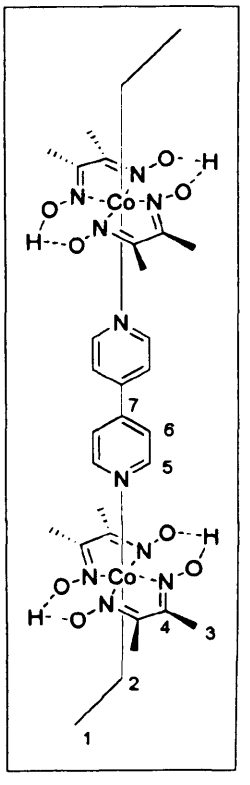

To a solution of [ClCo(DMGH)$_2$]$_2$-μ-(4,4'-bipy) (0.5 g, 0.6 mmol) and iodoethane (0.10 ml, 1.3 mmol, 2.1 equivs.) in methanol (5 ml) was added sodium borohydride (0.03 g, 0.8 mmol). The reaction was left to stir for 30 minutes, when the solvent was removed in vacuo, and the crude solid was dissolved in dichloromethane (10 ml) and washed with distilled water (2 x 10 ml). The organic fractions were combined, dried over sodium sulfate, filtered and evaporated to dryness, yielding [EtCo(DMGH)$_2$]$_2$-μ-(4,4'-bipy) as a brown solid. (0.45 g, 95 % yield), δH ($CDCl_3$) (ppm) 8.72 (2 H, d, *J* = 6.6 Hz, C*H* (5) Pyr), 7.49 (2 H, d, *J* = 6.6 Hz, C*H* (6) Pyr), 2.38, (24 H, s, CH_3 (3) DMGH), 1.74 (2 H, q, *J* = 7.6 Hz. CH_2 (2), Co-CH_2-CH_3), 0.37 (3 H, t, *J* = 7.6 Hz, CH_3 (1), Co-CH_2-CH_3). δC ($CDCl_3$) (ppm) 150.3 (*C* (4) DMGH), 148.0 (*C* (5) Pyr), 124.7 (*C* (6) Pyr), 122.6 (*C* (7) Pyr), 40.8 (*C* (2) Co-*C*H_2-CH_3), 16.1 (*C* (1) Co-CH_2-*C*H_3), 12.0 (*C* (3) DMGH). *m/z* (ESI) 793.1

$[MH]^+$. HRMS (ESI) calculated $[MH]^+$ = 793.2242; measured $[MH]^+$ =793.2246.

[EtCo(DMGH)$_2$]$_2$-μ-(4,4'-bipy) – method 2. 5.13

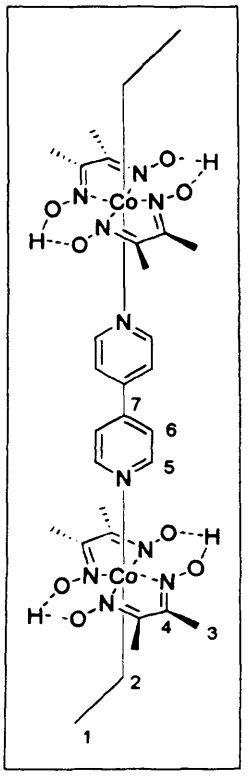

To a solution of [ClCo(DMGH)$_2$(4,4'-bipy)] (0.5 g, 1.0 mmol) and iodoethane (0.08 ml, 1.0 mmol, 1.0 equivs.) in methanol (5 ml) was added sodium borohydride (0.04 g, 1.0 mmol). The reaction was left to stir for 30 minutes, when the solvent was removed in vacuo, and the crude solid was dissolved in dichloromethane (10 ml) and washed with distilled water (2 x 10 ml). The organic fractions were combined, dried over sodium sulfate, filtered and evaporated to dryness, yielding [EtCo(DMGH)$_2$]$_2$-μ-(4,4'-bipy) as a brown solid. (0.38 g, 93 % yield), δH ($CDCl_3$) (ppm) 8.72 (2 H, d, *J* = 6.6 Hz, C*H* (5) Pyr), 7.49 (2 H, d, *J* = 6.6 Hz, C*H* (6) Pyr), 2.38, (24 H, s, CH_3 (3) DMGH), 1.74 (2 H, q, *J* = 7.6 Hz. CH_2 (2), Co-CH_2-CH$_3$), 0.37 (3 H, t, *J* = 7.6 Hz, CH_3 (1), Co-CH$_2$-CH_3). δC ($CDCl_3$) (ppm) 150.3 (*C* (4) DMGH), 148.0 (*C* (5) Pyr), 124.7 (*C* (6) Pyr), 122.6 (*C* (7) Pyr), 40.8 (*C* (2) Co-*C*H$_2$-CH$_3$), 16.1 (*C* (1) Co-CH$_2$-*C*H$_3$), 12.0 (*C* (3) DMGH). *m/z* (ESI) 793.1 $[MH]^+$. HRMS (ESI) calculated $[MH]^+$ = 793.2242; measured $[MH]^+$ =793.2246.

[ClCo(DMGH)$_2$(BPA)] 5.14

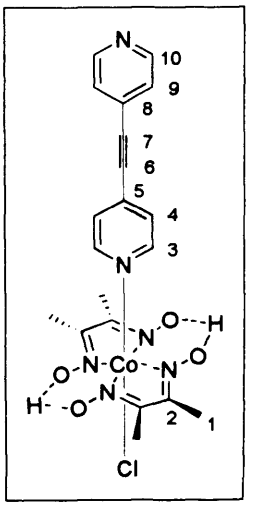

To a suspension of [Cl$_2$Co(DMGH)(DMGH$_2$)] (1.0 g, 2.8 mmol) in dichloromethane (10 ml) was added bis(4-pyridyl)acetylene (0.55 g, 3.0 mmol) and sodium bicarbonate (10 ml) sequentially. The mixture was stirred at room temperature for 2 hours and the resultant brown solution was diluted further with dichloromethane (20 ml) and washed with water (2 x 20 ml). The organic fractions were combined, dried over sodium sulfate, filtered and evaporated to dryness, yielding [ClCo(DMGH)$_2$(BPA)] as a brown solid. (1.2 g, 85 % yield), δH ($CDCl_3$) (ppm) 8.67 (2 H, d, *J* = 5.5 Hz, C*H* (10) Pyr)), 8.29 (2 H, d, *J* = 6.4 Hz, C*H* (3) Pyr)). 7.37 (2 H, d, *J* = 5.5 Hz, C*H* (9) Pyr)), 7.31 (2 H, d, *J* = 6.4 Hz, C*H* (4) Pyr)), 2.43 (12 H, s, CH_3 (1) DMGH). δC ($CDCl_3$) (ppm) 154.5 (*C* (10) Pyr),

153.5 (*C* (3) Pyr), 152.6, (*C* (8) Pyr), 151.9, (*C* (5) Pyr), 128.2 (*C* (4) Pyr), 127.2 (*C* (9) Pyr), 127.3 (*C* (2) DMGH), 88.6 (*C* (7) Co-Pyr-*C*≡C), 87.6 (*C* (6) Co-Pyr-C≡*C*), 12.3 (*C*H_3 (1) DMGH). *m/z* (ESI) 505.1 $[MH]^+$. HRMS (ESI) calculated $[MH]^+$ = 505.0801; measured $[MH]^+$ = 505.0803.

[ClCo(DMGH)$_2$]$_2$-μ-(BPA) 5.15

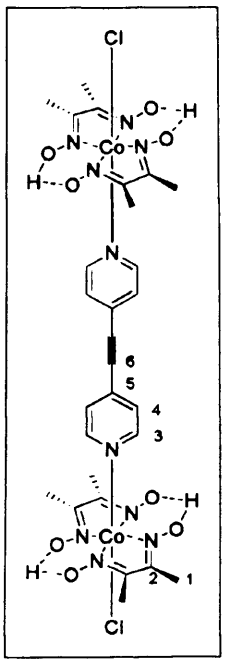

To a suspension of [Cl_2Co(DMGH)(DMGH$_2$)] (1.0 g, 2.8 mmol) in dichloromethane (10 ml) was added bis(4-pyridyl)acetylene (0.25 g, 1.4 mmol, 0.5 equivs.) and sodium bicarbonate (10 ml) sequentially. The mixture was stirred at room temperature for 2 hours and the resultant brown solution was diluted further with dichloromethane (20 ml) and washed with water (2 x 20 ml). The organic fractions were combined, dried over sodium sulfate, filtered and evaporated to dryness, yielding [ClCo(DMGH)$_2$]$_2$-μ-(BPA) as a brown solid. (0.96 g, 81% yield), δH ($CDCl_3$) (ppm) 8.33 (4 H, d, *J* = 6.8 Hz, C*H* (3) Pyr), 7.31 (2 H, d, *J* = 6.8 Hz, C*H* (4) Pyr), 2.41 (24 H, s, CH_3 (1) DMGH). δC ($CDCl_3$) (ppm) 153.5 (*C* (3) Pyr), 151.9, (*C* (2) DMGH), 128.2 (*C* (4) Pyr), 127.6 (*C* (5) Pyr), 87.6 (*C* (6) Pyr-*C*≡C), 12.8 (*C*H_3 (1) DMGH). *m/z* (ESI) 844.1 $[MH]^+$. HRMS (ESI) calculated $[MH]^+$ = 844.1072; measured $[MH]^+$ = 844.1076.

[EtCo(DMGH)$_2$]$_2$-μ-(BPA) 5.16

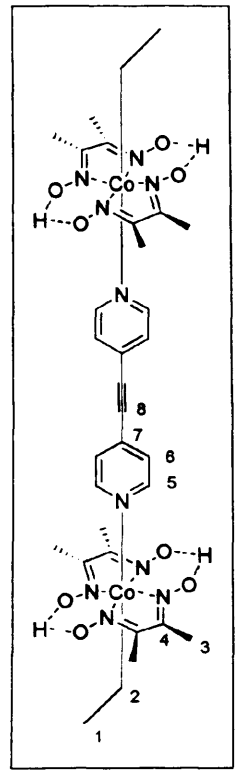

To a solution of [ClCo(DMGH)$_2$]$_2$-μ-(BPA) (1.0 g, 1.2 mmol) and iodoethane (0.20 ml, 2.5 mmol, 2.1 equivs.) in methanol (20 ml) was added sodium borohydride (0.1 g, 2.5 mmol, 2 equivs.). The reaction was left to stir for 30 minutes, when the solvent was removed *in vacuo*, and the crude solid was dissolved in dichloromethane (10 ml) and washed with distilled water (2 x 10 ml). The organic fractions were combined, dried over sodium sulfate, filtered and evaporated to dryness, yielding [EtCo(DMGH)$_2$]$_2$-μ-(BPA) as a brown solid. (0.86 g, 86 % yield), δH ($CDCl_3$) (ppm) 8.51 (4 H, d, J = 6.0 Hz C*H* (5) Pyr) 7.32 (4 H, d, J = 6.0 Hz, C*H* (6) Pyr) 2.41 (24 H, s, CH_3 (3) DMGH), 1.58 (4 H, t, J = 7.6 Hz, CH_2 (2), Co-CH_2-CH_3), 0.35 (6 H, q, J = 7.6 Hz, CH_3 (1), Co-CH_2-CH_3). δC ($CDCl_3$) (ppm) 151.6 (*C* (4) DMGH), 148.9, (*C* (5) Pyr), 129.2 (*C* (6) Pyr), 125.6 (*C* (7) DMGH), 89.6 (*C* (8) Pyr-*C*≡C), 40.8 (*C* (2) Co-*C*H_2-CH_3), 16.1 (*C* (1) Co-CH_2-*C*H_3), 12.3 (*C*H_3 (3) DMGH). *m/z* (ESI) 832.2 $[MH]^+$.HRMS (ESI) calculated $[MH]^+$ = 832.2477; measured $[MH]^+$ = 832.2482.

1,2-bis(4-bromophenyl)ethane-1,2-dione dioxime[29]

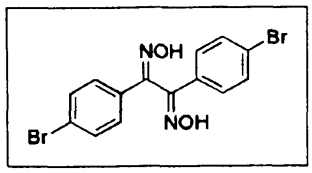

4,4'-dibromobenzil (1 g, 2.72 mmol) and hydroxylamine (415 mg, 5.97 mmol, 2.2 equivs.) were dissolved in ethanol (50 ml) to this solution, sodium hydroxide (239 mg, 5.98 mmol, 2.2 equivs.) was added, and refluxed for 4 hours. The reaction mixture was cooled, diluted with water (100 ml) and the product was precipitated with dilute sulfuric acid (20 ml). The white solid was filtered off, and washed with ethanol (100 ml) and diethyl ether (100 ml) sequentially, to give the title compound as a white powder (1.064 g, 98 %). δH ($CDCl_3$) ppm 7.98 (4 H, d, J = 8.6 Hz) 7.73 (4 H, d, J = 8.7 Hz).

1,2-bis(4-(3-hydroxy-3-methylbut-1-ynyl)phenyl)ethane-1,2-dione

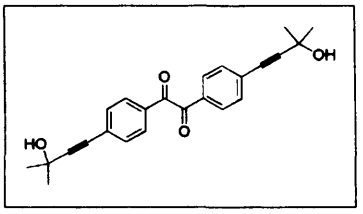

To a stirred suspension of 4,4'-dibromobenzil (1 g, 2.72 mmol) and 2-methylbut-3-yn-2-ol (0.58 ml, 5.98 mmol, 2.2 equivs.) in diethylamine (15 ml) was added bis-(triphenylphosphine) palladium dichloride (190 mg, 2.7×10^{-1} mmol) and copper iodide (44 mg, 2.7×10^{-1} mmol), and the mixture was stirred for 18 hours. The diethylamine was removed *in vacuo*, and the residue dissolved in dichloromethane (20 ml) and washed successively with water (2 x 10 ml) and brine (2 x 10 ml). The organic fractions were then dried over Na_2SO_4, filtered and evaporated to dryness, yielding 1,2-bis(4-(3-hydroxy-3-methylbut-1-ynyl)phenyl)ethane-1,2-dione as a brown crystalline solid (0.968 g, 95 %). δH ($CDCl_3$) ppm 7.92 (4 H, d, J = 8.4 Hz), 7.55 (4 H, d, J = 8.4 Hz), 1.65 (12 H, s)

1,2-bis(4-(3-hydroxy-3-methylbut-1-ynyl)phenyl)ethane-1,2-dioxime-Method 1

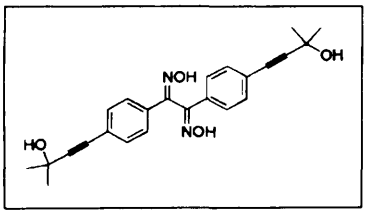

1,2-bis(4-(3-hydroxy-3-methylbut-1-ynyl)phenyl)ethane-1,2-dione (250 mg, 0.67 mmol) and hydroxylamine (102 mg, 1.47 mmol, 2.2 equivs.) were dissolved in ethanol (10 ml) to this solution, sodium hydroxide (59 mg, 1.47 mmol, 2.2 equivs.) was added, and refluxed for 4 hours. The reaction mixture was cooled, diluted with water (100 ml) and the product was precipitated with dilute sulfuric acid. No product observed.

1,2-bis(4-(3-hydroxy-3-methylbut-1-ynyl)phenyl)ethane-1,2-dioxime-Method 2

To a stirred suspension of 1,2-bis(4-bromophenyl)ethane-1,2-dione dioxime (250 mg, 0.68 mmol) and 2-methylbut-3-yn-2-ol (0.13 ml, 1.38 mmol, 2.2 equivs.) in diethylamine (5 ml) was added bis-(triphenylphosphine) palladium dichloride (44 mg, 6.3×10^{-2} mmol) and copper iodide (10 mg, 6.2×10^{-2} mmol), and the mixture was stirred for 18 hours. The diethylamine was removed *in vacuo*, and the residue dissolved in dichloromethane (20 ml) and washed successively with brine (2 x 10 ml). No product observed.

(E)-N1-((E)-6-(2-(dimethylamino)ethylimino)-1,10-phenanthrolin-5(6H)-ylidene)-N2,N2-dimethylethane-1,2-diamine[28]

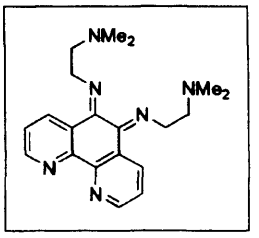

To a solution of 1,10-phenathroline-4,5-dione (0.5 g, 2.3 mmol) in warm methanol (5 ml) was added *unsymm*-ethylene dimethyldiamine (0.3 µl, 23 mmol, 10 equiv.) dropwise over 10 mins and left to stir at 60 °C for 2 hours. The resultant orange solution was filtered and the solvent removed *in vacuo*, to give the compound as a brown crystalline solid. δH ($CDCl_3$) ppm, 8.99 (2 H, dd, J = 1.7, 0.3 Hz), 8.60 (2 H, dd, J = 1.7, 0.3 Hz), 7.73 (2 H, dq, J = 1.7, 0.2 Hz), 4.71 (6 H, t, J = 6.9 Hz), 2.90 (6 H, t, J = 6.8 Hz), 2.37 (12 H, s,).

General Procedure for coordination of *fac*-[Re(CO)$_3$Br(L)]to 4-ethynylpyridine.

All reactions were carried out under N_2 with precautions taken to avoid light, using standard Schlenk techniques under inert atmosphere. All solvents used in synthesis of the metallo ligands were taken from a MB SPS-800 solvent purification system. *fac*-[Re $(CO)_3$Br (L)] species were prepared according to literature methods.

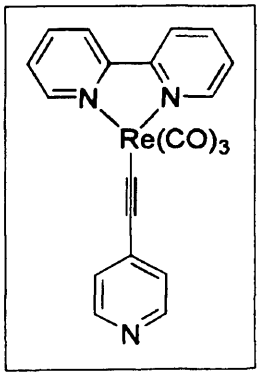

A mixture of *fac*-[Re(CO)$_3$Br(L)] (0.1 mmol) sodium hexafluorophosphate (0.15 mmol) and 4-ethynylpyridine hydrochloride (0.2 mmol) in ethanol/dichloromethane (5 ml, 1:3) was stirred at room temperature under nitrogen and in the dark for three hours. The solvent was removed *in vacuo* and the dark green residue was dissolved in acetone, with the insoluble solid filtered off to give the starting material as a yellow.

5.7. Overall Conclusions and Future Work.

A series of multimetallic cobaloximes have been synthesised, with a view to acting as pre-catalysts for the reductive dechlorination of toxic chlorinated olefins. **Chapter 4** described the synthesis and analysis of cobaloximes with a dicobaltcarbonyl cluster situated in an axial ligand, whilst **Chapter 5** described the synthesis and analysis of a series of dinuclear cobaloximes. All of these cobaloximes were then subjected to reductive conditions in the presence of perchloroethylene, and the resultant mixture was analysed to find the degree of dechlorination. All multimetallic cobaloximes were found to reductively dechlorinate PCE to TCE, DCE and VC, thought the experiment was too insensitive to determine whether the any PCE was completely dechlorinated to give ethene or ethane. Further modification of the analytical process would help determine whether any PCE was completely dechlorinated, a long term goal of this project, as VC is more volatile and toxic than the starting material PCE.

The dicobaltcarbonyl cobaloximes were observed to dechlorinate up to 8.2 equivalents of the initial dose of PCE, but the greatest enhancement in catalytic ability over the simple pyridyl cobaloximes presented in **Chapter 3**, came in the second step of the catalysis- in most cases, 80 % of the TCE is reduced further to DCE and VC. The best catalyst was found to be those with dppm fragments incorporated into ethylcobaloximes. However, these bridged cobaloximes were found to be air and moisture sensitive, which undoubtedly had a negative effect on the long-term catalytic ability of these species. The alternative dicobaloximes were found to be more stable to air and moisture, but were found to be less catlytic than the dicobaltcarbonyl bridged cobaloximes. These dicobaltcarbonyl-bridged cobaloximes and dicobaloximes described in this work are rare examples of molecular organotransition metal compounds that are able to catalytically reductively dechlorinate PCE stepwise to VC via TCE and DCE. More remarkably, these dechlorination reactions are undertaken at standard temperature and pressure under aerobic conditions, an advantage over the molecular dechlorination catalysts described in **Section 4.1.4**. Further multimetallic cobaloximes need to be synthesised and studied to find how small changes to the systems will have an effect on the stability of these complexes, and on the catalytic ability.

More surprisingly, the results of the ligand exchange experiments of **Chapter 3** showed that upon reduction of the cobaloximes from Co(III) to Co(I), both the axial ligands are lost, leaving the cobaloxime as a four-coordinate species. This process of the axial ligands continually dissociating and re-coordinating was expected have a major bearing on the catalysis; as the secondary metal centre believed to facilitate the reaction is situated in the axial ligand.

As a result of the work in **Chapter 3**, the final sections of **Chapter 5** described the attempts at: incorporating the secondary metal centre into the equatorial plane, though with little success, and incorporating metals other than cobalt into the cobaloximes. Cobaloximes with a Re(I)(bipy) or Ru(II)(bipy) moiety were favoured as both are luminescent, offering an opportunity to photochemically initiate the dechlorination with light as opposed to laboratory reducing agents. Further experiments are needed to achieve this goal. The reactions of $[RCo(DMGH)_2(4,4'\text{-bipy})]$ with $[Re(bipy)(CO)_3(MeCN)][PF_6]$ or $[Re(bipy)(CO)_3Cl]$ are possible, but the reactions need to be carried out under inert dry conditions, whilst the synthesis of the $[Re(bipy)(CO)_3(4\text{-ethynylpyridine})]$ fragment, though described in the literature, didn't work in our hands, again inert reaction conditions are needed. This metallo ligand would prove very interesting in the role of a photochemical moiety for the initiation of the dechlorination process.

5.8. References.

1 B. P. Branchaud, M. S. Meier, M. N. Malekzadeh, *J. Org. Chem.* **1987**, 52, 212.

2 L. Randaccio, L. G. Marzelli, *Chem. Soc. Revs.* **1989**, 18, 225.

3 J. R. Moss, *J. Organomet.. Chem*, **1982**, 231, 229.

4 B. Krautler, T. Derer, P. Liu, W. Muhlecker, M. Puchberger, K. Gruber, C. Kratky, *Angew. Chem. Int. Ed. Engl.* 1995, 34, 84.

5 E. L. Smith, L. Mervyn, P.W. Muggleton, A.W. Johnson, N. Shaw, Ann. NY Acad. Sci. 112 (1964) 565

6 G. N. Schrauzer, R. J. Windgassen, *J. Am. Chem. Soc.* **1966**, 88, 3738.

7 K. P. Finch, J. R. Moss, *J. Organomet. Chem.* **1988**, 346, 253.

8 H. Chen, X. Zhang, Y. Li, Y. Mei, *J. Organomet.. Chem.* **2006**, 691, 659.

9 B.D. Gupta, K. Qanungo, *J. Organomet.. Chem.* **1997**, 534, 213.

10 A. Haim, *Act. Chem. Res.* **1975**, 8, 264.

11 P. L. Gaus and A. L. Crumbliss, *Inorg. Chem.* **1976**, 15, 2080.

12 N. E. Schore, C. Ilenda, R. G. Bergman, *J. Am. Chem. Soc.* 1976, 98, 7436.

13 A. Herlinger, W. Ramakrishna, *Polyhedron*, **1985**, 4, 551.

14 P. L. Gaus, *Inorg. Nucl. Chem. Letters,* **1974**, 10, 485.

15 B. D. Gupta, K. Qanungo, *J. Organomet.. Chem.* **1997**, 534, 213.

16 B. D. Gupta, V. Vijaikanth, V. Singh, *Organometallics.* **2004**, 23, 2069.

17 (a) Johnson, M. D. *Acc. Chem. Res.* **1983**, *16*, 343. (b) Walton, J. C. *Acc. Chem. Res.* **1998**, *31*, 99. (c) Tada, M. *Rev. Hetero. Chem.* **1999**, *20*, 97. (d) Welker, M. E. *Curr. Org. Chem.* **2001**, *5*, 785.

18 M. M. Harris, C. K. Ling, *J. Chem. Soc.* **1964**, 1825.

19 P. J. Hagrman, D. Hagrman, J. Zubieta, *Angew. Chem., Int. Ed.* **1999**, 38, 2638.

20 S. R. Batten, R. Robson, *Angew. Chem., Int. Ed.* **1998**, 37, 1460.

21 B. D. Gupta, K. Qanungo, *J. Organomet.. Chem.* **1998**, 557, 243.

22 B. D. Gupta, D. Mandal, *Eur. J. Inorg. Chem.* **2006**, 4086.

23 A.W. Herlinger, T.L. Brown, *J. Am. Chem. Soc.* **1972**, 94, 388.

24 B. J. Coe, J. L. Harries, J. A. Harris, B. S. Brunschwig, S. J. Coles, M. E. Light, M. B. Hursthouse. *Dalton Trans.* **2004**, 2935.

25 D. J. Stufkens, A. Vlcek, *Coord. Chem. Revs.* **1998**, 177, 127.

26 (a) A. S. Kalgutkar, N. Castagnoli, *J. Med. Chem.* **1992**, 35, 4165; (b) J. A. Whiteford, C. V. Lu, P. J. Stang, *J. Am. Chem. Soc.* **1997**, 119, 2524; (c) C. Richardson, C. A. Reed, *J. Org. Chem.* **2007**, 72, 4750; (d) J. Suffert, R. Ziessel, *Tet. Lett.* **1991**, 32, 757; (e) R. Ziessel, *J. Org. Chem.* **1996**, 61, 6535; (f) S. Grunder, R. Huber, V. Horhoiu, M. Teresa-Gonzalez, C. Schonenberger, M. Calame, M. Mayor, *J. Org. Chem.* **2007**, 72, 8337.

27 (a) V. Wing-Wah Yam, K. Man-Chung Wong, S. Hung-Fai Chong, V. Chor-Yue Lau, S. Chan-Fung Lam, L. Zhang, Kung-Kai Cheung, *J. Organomet.. Chem.* **2003**, 670 205; (b) Q. Ge, T. S. A. Hor, *Dalton Trans.*, **2008**, 2929; (c) V. Wing-Wah Yam, *Chem. Commun.*, **2001**, 789; (d) B. J. Liddle, S. V. Lindeman, D. L. Reger, J. R. Gardinier *Inorg Chem*, **2007**, 46, 21, 8484.

28 K.R. Rupesh, S. Deepalatha, M. Krishnaveni, R. Venkatesan, S. Jayachandran, *Eur. J. Med. Chem.* **2006**, 41, 1494.

29 G. C. Tron, F. Pagliai, E. Del Grosso, A. A. Genazzari, G. Sorba, *J. Med. Chem.* **2005**, 48, 3260.